Development of Human Silent Information Regulator 1 Modulators for Treatment of Cancer and Metabolic Disorders

THESIS

Submitted in partial fulfillment
of the requirements for the degree of
DOCTOR OF PHILOSOPHY

by

M. MALLIKA
(2010PHXF013H)

Under the Supervision of
Dr. D. SRIRAM

BIRLA INSTITUTE OF TECHNOLOGY AND SCIENCE

PILANI (RAJASTHAN) INDIA

2013

BIRLA INSTITUTE OF TECHNOLOGY AND SCIENCE

PILANI (RAJASTHAN)

<u>CERTIFICATE</u>

This is to certify that the thesis entitled "**Development of human silent information regulator 1 modulators for treatment of cancer and metabolic disorders** and submitted by **M. Mallika** ID.No**:2010PHXF013H** for award of Ph.D. Degree of the Institute embodies original work done by her under my supervision.

Signature in full of the Supervisor_____

Name in capital Block letters **: D. SRIRAM**

Designation   **: Associate Professor**

Date:

ACKNOWLEDGEMENT

Any attempt to list the people and opportunities with which my life has been richly blessed would be like trying to count the stars in the heavens.

*It's a great pleasure and immense satisfaction in expressing my deep gratitude towards my research supervisor, **Dr. D. Sriram**, Associate Professor, Department of Pharmacy, BITS, Pilani-Hyderabad campus, for his dexterous guidance, suggestions and support which he bestowed to me. Mere acknowledging with words is inadequate to express my gratitude to him. He was always an inspiration to me in research. The work environment given to me under him, the experiences gained from him and his creative working culture are treasured and will be remembered throughout my life.*

*I deeply acknowledge and heartfelt thanks to **Dr. P. Yogeeswari**, Associate Professor, Department of Pharmacy, BITS, Pilani-Hyderabad campus, for her valuable suggestions, guidance and precious time which she offered me throughout my research.*

*I am grateful to **Prof. Bijendra Nath Jain**, Vice-Chancellor (BITS) and Director **Prof. V.S.Rao** (Hyderabad campus), for allowing me to carry out my doctoral research work in the institute.*

*I am thankful to **S.K.Verma** Dean, Academic Research Division, BITS-Pilani, for his co-operation and encouragement at every stage of this research work.*

*I would like to express my gratitude to **Dr. V.Vamsi Krishna**, Head of the department, Pharmacy, for providing me with all the necessary laboratory facilities and for having helped me at various stages of my research work.*

I sincerely acknowledge the help rendered by Dr. Punna Rao Ravi, Dr. Sajeli Begum, Dr. Palash Mandal, faculty at the BITS-Pilani, Hyderabad campus.

I would like to begin by dedicating this piece of work to **my parents and in-laws**, whose dreams had come to life with me getting the highest degree in education. I owe my doctorate degree to my parents and in-laws who kept with their continuous care, support and encouragement my morale high. Thanks are due if I don't dedicate this thesis to my sister and brother-in-law, and family, whose constant and continuous support, love and affection made me reach this height.

Lastly, and above all, I would like to thank the God Almighty; for all that he has given to me.

Date: M. Mallika

ABSTRACT

Silent **I**nformation **R**egulators or **sirtuins** are class III NAD^+-dependent proteins which possess either histone deacetylase or mono-ribosyltransferase activity found in organisms ranging from bacteria to humans. These are important for many cellular metabolisms including gene silencing, regulation of p53, cell cycle regulation, life span extension, cancer, diabetes, obesity, etc. Among all seven human sirtuins, SIRT1 is well studied, having more than a dozen substrates, known to have protective role against oxidative stress and DNA damage and plays a predominant role in metabolism.

In the present study, a diverse set of series of molecules viz. Acridinedione (ACD), Benzthiazolyl-2-thiosemicarbazone (B2TS) as SIRT1 inhibitors and Spiro-piperidine-4-one (SP), Pyrido[2,3-d]pyrimidine (PP), 1-(isonicotinamido)azetidine-2,4-dicarboxamides (AZD) as SIRT1 activators were identified by virtual screening of *in house* database against catalytic core and allosteric site of SIRT1. Further to develop a significant SAR, various derivatives of ACD, B2TS, SP, PP, and AZD were designed, synthesized and characterized. Upon fluorescence based cell-free deacetylation SIRT1 assay, compound **4d** (ACD series), **BH1** and **BH13** (B2TS series) showed significant inhibition with an IC_{50} of 10.13±0.08 μM, 46.27±0.7 μM and 15.3±0.8 μM respectively and **H3** (SP series), **B9** (PP series) and **6A11** (AZD series) showed significant 2-3 fold increase in deacetylase activity of SIRT1 at 10 μM, 5 μM and 5 μM concentrations respectively.

MTT assay of SIRT1 inhibitors (ACD and B2TS series) on various cancer (K562, MDA-MB231, LNCaP and PC3) cell lines yielded that compound **4d** (ACD series) induced apoptosis

in MDA-MB 231 cells with an IC_{50} of 0.25 µM and compound **BH1** and **BH13** induced apoptosis in LNCaP cells with an IC_{50} of 4.09±0.02 µM and 5.07±1.25 µM respectively. Further mechanistic studies of active compounds revealed down regulation of SIRT1 and upregulation of caspase 3 and acetylated p53K382 protein levels. Moreover, **BH1** and **BH13** reduced the testosterone -induced hyperplasia at 10 mg/kg body weight in a rat model with decrease in the SIRT1 and PSA transcript levels.

Adipogenesis assay of SIRT1 activators (SP, PP and AZD series) on 3T3-L1 cells was carried out and all the compounds showed significant inhibition of adipogenesis and triglyceride accumulation. RT-PCR studies revealed the up regulation of SIRT1 followed by decrease in the adipogenic markers PPARγ, C/EBPα along with FAS, E2F1, Leptin and LPL. Compounds **H3** and **B9** showed significant modulation in weight gain and lipid profile of high fat diet-induced obese mice at 30 mg/kg body weight.

TABLE OF CONTENTS

LIST OF TABLES

LIST OF FIGURES

ABBREVIATIONS

μg	:	Microgram
μM	:	Micromolar
AA	:	Amino acid
AMV-RT	:	Avian Myeloblastosis Virus- Reverse Transcriptase
ABCA1	:	ATP binding cassette transporter A1
AROS	:	Active regulator of sirt1
ATP	:	Adenosine triphosphate
BCL11A	:	B-cell lymphoma/leukemia 11A
BESTO	:	B-cell-specific SIRT1-overexpressing
C/EBPα	:	CCAAT/enhancer binding protein α
Chk2	:	Checkpoint kinase 2
CPT	:	Carnitine palmitoyl transferase
CR	:	Caloric restriction
CREB	:	Cyclic AMP response element binding protein
CRTC2	:	CREB regulated transcription coactivator 2
CTIP2/BCL11B	:	B-cell lymphoma/leukemia 11B
DBC1	:	Deleted in breast cancer
E2F1	:	Transcription factor
FAS	:	Fatty acid synthase
FBPase	:	Fructose-1, 6- bisphosphatase
FDA	:	Food and drug administration
FOXO	:	Fork head box protein o
G6Pase	:	Glucose 6 phosphatase enzymes
GADD	:	Growth arrest and DNA-damage-inducible
GLUT2	:	Glucose transporter 2
HAT	:	Histone acetyl transferases
HDAC	:	Histone deacetylases
HDL	:	High density lipoproteins
Hes1	:	Hairy and enhancer of split-1
Hey2	:	Hairy/enhancer-of-split related with YRPW motif protein 2

HFD	:	High fat diet
HIC1	:	Hypermethylated in cancer 1
HMGR	:	Hydroxy methyl glutaryl-CoA reductase
HNFα	:	Hepatocyte nuclear factor-α
HPLC	:	High performance liquid chromatography
IBMX	:	Isobutylmethylxanthine
InsR	:	Insulin receptor
IRS-2	:	Insulin receptor substrate-2
LDL	:	Low density lipoproteins
LKB1	:	Liver kinase B1
LPL	:	Lipoprotein lipase
LXR	:	Liver X receptor
MafA	:	Mast cell function-associated antigen
MAFbx	:	Muscle atrophy F-box
MAR	:	Mating-type regulator 1
MCAD	:	Malonyl-CoA decarboxylase
MEF	:	Myocyte enhancing factor
MEF2C	:	Myocyte specific enhancer factor 2C
ml	:	Milliliter
MMP2	:	Matrix metalloproteinase-2
MnRF1	:	Muscle RING finger 1
mRNA	:	Messenger rna
MyoD	:	Transcription factor
NAMPT	:	Nicotinamide phopho ribosyl transferase
NF-κB	:	Nuclear factor kappa-light-chain-enhancer of activated B cells
OXPHOS	:	Oxidative phosphorylation
PCAF	:	P300/CBP associated factor
PDX1	:	Pancreatic and duodenal homeobox 1
PEPCK	:	Phosphoenolpyruvate carboxykinase
PGC1-α	:	Peroxisome proliferator activated receptor co-activator 1α
PIN	:	Prostatic intraepithelial neoplasia
PML	:	Promyelocytic leukemia
PPARγ	:	Peroxisome proliferator-activated receptor γ

PSA	:	Prostate specific antigen
PTP-1B	:	Protein tyrosine phosphatase 1B
RelA	:	Transcription factor p65
ROS	:	Reactive oxygen species
RP-HPLC	:	Reverse phase high performance liquid chromatography
RT	:	Room temperature
RT-PCR	:	Reverse transcriptase polymerase chain reaction
SAR	:	Structure activity relationship
SENP1	:	Sumo1/sentrin specific peptidase 1
siRNA	:	Small interfering RNA
SIRT1	:	Silent information regulator 1
SP	:	Standard precision
SREBP	:	Sterol regulatory element binding protein
STAT3	:	Signal transducer and activator of transcription-3
T2DM	:	Type ii diabetes mellitus
TG	:	Triglycerides
TNF-α	:	Tumor necrosis factor α
TORC2	:	Transducer of regulated CREB activity
Total-C	:	Total cholesterol
tR	:	Retention time
TRAMP	:	Transgenic adenocarcinoma of mouse prostate
UCP2	:	Uncoupling protein-2
VLDL	:	Very low density lipoproteins
XP	:	Extra precision

CHAPTER 1

INTRODUCTION

CHAPTER 1
INTRODUCTION

Cancer is a group of diseases characterized by uncontrolled growth and spread of abnormal cells. While cells in the body undergo a tightly regulated cycle of generation, division and death, cancer cells typically evade cell death and are capable of constant multiplication and expansion. They develop traits which are commonly identified as the hallmarks of cancer, namely, self-sufficiency in growth signals and insensitivity to growth-inhibitory signals, evasion of apoptosis, sustained replicative potential and angiogenesis as well as tissue invasion and metastasis [Hanahan D., *et al*., 2000]. Cancer is caused by both external (tobacco, infectious organisms, chemicals, and radiation) and internal factors (inherited mutations, hormones, immune conditions, and mutations that occur from metabolism). The earliest evidence of cancer was discovered in Egypt in 1600 B.C and it was described as a disease that had no cure. Hippocrates, a Greek physician known as the father of medicine used the terms carcinos and carcinoma to describe the appearance of cancer.

Cancer is the second leading cause of death in economically developed countries. According to the statistics obtained by the U.S National Cancer Institute, 1 in 2 men in the United States have a lifetime risk of developing cancer while this risk is 1 in 3 for women. Lung cancer has the highest mortality rate in both men and women followed by breast cancer in women and prostate cancer in men [Cancer facts & figures, 2012]. These statistics emphasize the need for continued development and progress in the field of cancer research. Century leading to the advanced understanding of anatomy and physiology did the origin and progression of cancer become clear. We now find ourselves in the fortunate position of understanding a portion of the

molecular mechanisms that regulate cancer initiation and progression. This knowledge has led to the development of modern cancer therapies that effectively treat many cancers. However, treatment options remain limited and deaths attributed to cancer are still a major cause of mortality throughout the world. To fully combat cancer, continued research into the molecular causes and novel therapies must be completed. A task which seems to become more tangible with each passing day as new technologies for this research becomes available.

1.1 Carcinogenesis:

Carcinogenesis can be defined as the creation or production of cancer. In most cases, cellular transformation is a result of activation of oncogenes or suppression of tumor suppressor genes. Cellular oncogenes, also called proto-oncogenes, are normal genes required for important functions in the cell. These genes however, can be transformed into oncogenes by retro-viruses resulting in abnormal cellular proliferation [Cooper G.M.,1982 ; Haber M., *et al.,* 1985]. On the other hand, tumor suppressor genes or anti-oncogenes limit cellular transformation. These genes encode proteins that inhibit cell cycle progression, promote DNA damage repair and bring about cell death in the event of mutations or stress [Comings D.E., 1973; Sherr C.J., 2004]. Knudson's 'two-hit hypothesis' holds true for most tumor suppressor genes wherein two mutational events are required for carcinogenesis. Both alleles of the tumor suppressor gene are required to be lost, mutated or inactivated for manifestation of cancer [Knudson A.G., 1971]. Carcinogenesis is a multistage process that develops through three phases: Initiation, promotion and progression [Pitot H.C., *et al*., 1991]. Initiation involves an irreversible change in the cell which is generally an insult to the DNA of the cell. Chemicals such as aromatic hydrocarbons, radiation (ionizing and ultraviolet) or biological agents such as retroviruses can act as carcinogens to initiate cancer. These carcinogens can cause multiple mutations in the DNA of the cells such that the DNA

repair machinery is impaired. As a result, cell cycle checkpoints are deregulated and the cell divides and proliferates despite the mutations. Tumor Promotion involves the proliferation and expansion of the mutant and genetically unstable cell and accumulation of further mutations with each round of cell division such that the resulting population of cells is capable of surviving in normally unsuitable cellular environments [Cahill D.P., *et al*., 1999]. The Progression step comprises of tumor cells that have attained malignant properties, invasiveness and metastatic capabilities. Of note is the fact that mutations that occur during the process of carcinogenesis do not just involve the genetic alteration (deletion, translocation, point mutation, duplication or amplification) of oncogenes or tumor suppressor genes, but can also be epigenetic changes such as modifications of gene promoters byacetylation/ deacetylation or methylation/demethylation [Feinberg A.P., *et al.,* 2002; Feinberg A.P., *et al.*, 2004]. These causal factors may act together or in sequence to initiate or promote the development of cancer. Ten or more years often pass between exposure to external factors and detectable cancer.

1.1.1 Epigenetics:

Epigenetics is the study of reversible heritable changes in gene function, expression that occur without a change in nucleotide sequence of the DNA [Jaenisch R., *et al.*, 2003]; therefore, gene function is not only determined by the DNA code but also by epigenetic phenomena. Transient environmental influences during development can cause permanent changes in epigenetic gene regulation, and accumulating evidence links epigenetic dysregulation to human disease [Waterland R.A., *et al.*, 2004]. In eukaryotes, over the past fifteen years, it has been shown that gene expression can be regulated by the proteins called histones which are of small molecular weight and alkaline in nature, helps in packing genomic DNA into the nucleus and also by enzymes that modify both histones and the DNA [Mai A., *et al*., 2005; Fire A., *et al*.,

1998]. The two main mechanisms in the epigenetic regulation of gene expression involve DNA methylation and histone modifications. The study of these mechanisms is important since the change of gene expression is implicated in numerous human disorders and diseases, including obesity, diabetes, cancer and developmental abnormalities etc. [Feinberg A.P., 2001].

1.1.2 Histones and Chromatin structure:

Histones were discovered by Albrecht Kossel in 1884. The word "histone" comes from the German word of "Histon", of uncertain origin and perhaps from Greek word histanai or histos. Until the early 1990s, histones were known just as packing material for nuclear DNA. The regulatory functions of histones were discovered during the early 1990s. It is now known that histones are small basic architectural proteins of 102-135 amino acids that package the genomic DNA of eukaryotic organism into chromatin which is a dynamic macromolecular complex [Malik H.S., *et al*., 2003].

The basic repeating units of chromatin, the 2 nucleosome, is composed of two super helical turns of DNA containing approximately 146 base pairs which wrap around an octamer of the four core histones H2A, H2B, H3, and H4 with the addition of linker DNA and histone H1(**Fig.1.1**). H1 determines the level of DNA condensation [Grant P.A., 2001].
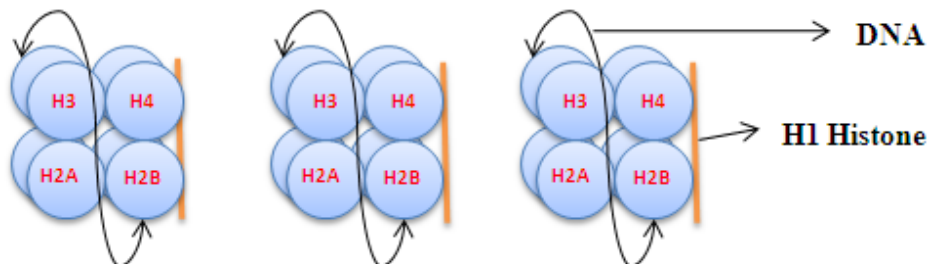
Fig.1.1: Structure of histones core.

These highly conserved histone proteins play an important role in determining the structure and function of chromatin which can be dynamically changed. Chromatin condensation provides an extensive barrier to the nuclear machinery that drives processes such as replication, transcription, or DNA repair; while chromatin decondensation facilitates those processes (**Fig. 1.2**). Each core histone protein has two domains: a histone fold domain or globular domain, which is involved in histone-histone interactions as well as in wrapping DNA in nucleosomes; and a more flexible and charged amino terminal 'tail' domain of 25-40 residues [Grant P.A., 2001]. The tail lies on the outside of the nucleosome where it can interact with other regulatory proteins and DNA. The basic N-terminal tails of the core histones are subject to various post-translational modifications. The functional effects of tail modifications are dependent on the specific amino acids that are modified. The selected amino acid residues of the core histones (H3-H4)2 tetramer are modified by acetylation (AC), methylation (Me), and phosphorylation (P); and H2A-H2B dimers are modified by acetylation; phosphorylation, ubiquitination (Ub), Multiubiquitination and ADP-ribosylation. These post translational modifications are cell and tissue specific. The function of these modifications is the focus of attention due to the possibility that the nucleosome, with its modified tail domains, is not only a packer of DNA but also a carrier of epigenetic information that indicates both how genes are expressed as well as how their expression patterns are maintained from one cell generation to the next. Of three such modifications, acetylation and deacetylation have generated the most interest. Also acetylation was the first modification that had been reported to have correlation with gene activity [Allfrey V.G., *et al.*, 1964].
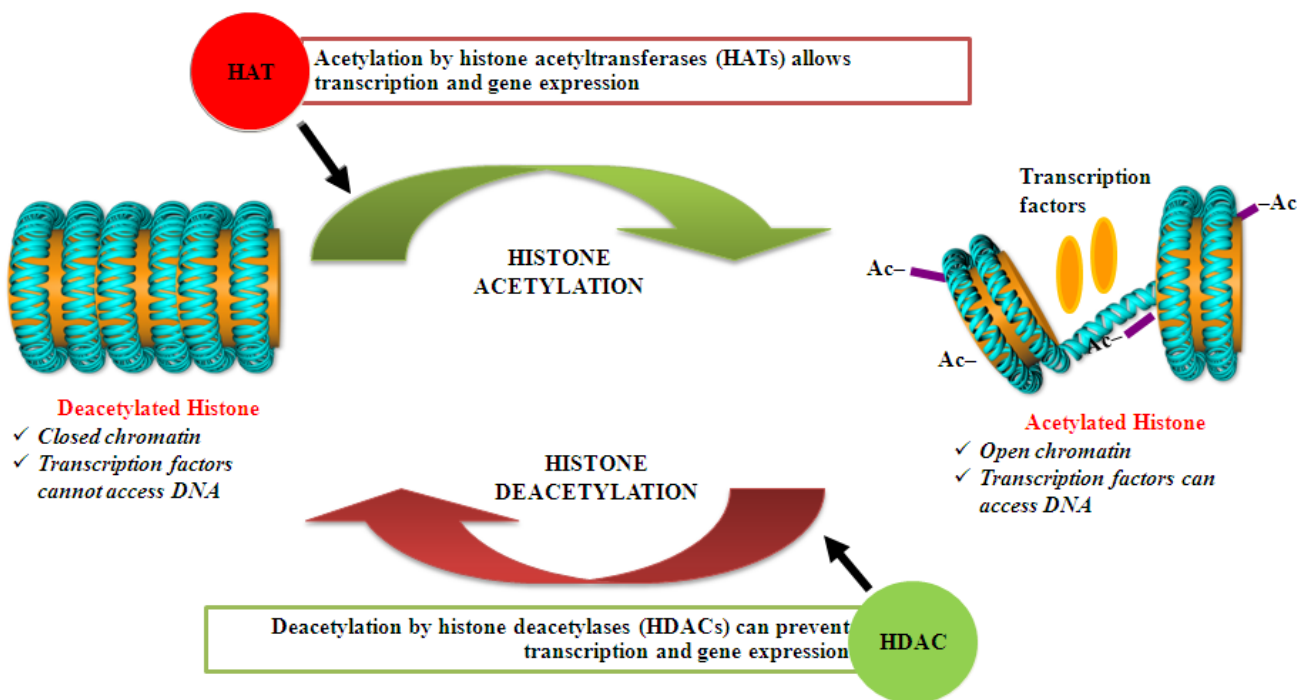
Ac: acetyl group

Fig.1.2: Modulation in chromatin structure facilitated by HAT and HDAC enzymes.

1.1.3 Therapy of Cancer:

Cancer is treated with surgery, radiation, chemotherapy, hormone therapy, biological therapy, and targeted therapy. Considering the complexity of cancer, it is of utmost importance to investigate the genes that are involved in its manifestation and the molecular mechanisms which explain their deregulation. Mapping and characterizing epigenomic changes will transform our understanding of pathology and enhance our ability to diagnose and treat cancer. Epigenetic alterations are easier to reverse than mutations affecting the genetic code. Two inhibitors of DNA methyltransferases, azacytidine and deoxyazacytidine, have already been approved by the FDA (Food and Drug Administration) as effective drugs for treatment of patients with myelodysplastic syndromes. An inhibitor of histone deacetylases, vorinostat

(suberoylanilidehydroxamic acid), is approved for the treatment of cutaneous T-cell lymphoma. Other epigenetic drugs targeting histone modifying enzymes or DNA methylation are in clinical trials or development [Tadokoro Y., *et al.*, 2007]. Detailed understanding of chromatin dysregulation will undoubtedly be translated into new and more effective ways of cancer treatment. Recently CHR-3996 has been completed phase I clinical trials and approved for the treatment of solid tumors [ClinicalTrials.gov.ID:NCT00697879]. FR901228 under phase II clinical trials has been used for treatment of B-cell non-Hodgkin's lymphoma [ClinicalTrials.gov.ID:NCT00383565]. ITF2357 with Mechlorethamine was completed phase I and II clinical trials for Relapsed/Refractory Hodgkin's Lymphoma [ClinicalTrials.gov.ID:NCT00792467]. LBH589 [ClinicalTrials.gov.ID:NCT00686218] and 4SC-202 [ClinicalTrials.gov.ID:NCT01344707] has been recruited for phase I clinical trials for Leukemia and Advanced Hematologic Malignancies respectively. Panobinostat (LBH589) recruited for phase II trials in treatment of metastatic gastric cancers. JNJ-2641585, HDAC inhibitor in combination with VELCADE and Dexamethasone is under phase I trials in multiple myeloma condition [ClinicalTrials.gov.ID:NCT01464112]. MS-275 also completed phase I trials in solid tumors and lymphomas [ClinicalTrials.gov.ID:NCT00020579].

1.2 Obesity:

Obesity has reached epidemic proportions worldwide. Obesity leads to several co-morbidities, such as diabetes, dyslipidemia, hypertension, sleep apnea, osteoarthritis, stroke, congestive heart failure, deep vein thrombosis and pulmonary embolism [Haslam D.W., *et al.*, 2005].Compelling human epidemiologic and animal model data indicate that during critical periods of prenatal and postnatal mammalian development, nutrition and other environmental stimuli influence developmental pathways and thereby induce permanent changes in metabolism

and chronic disease susceptibility. The biologic mechanisms underlying such 'metabolic imprinting' are poorly understood, but epigenetic mechanisms are likely involved [Waterland R.A., *et al*., 1999]. The worldwide increase in the prevalence of obesity in recent decades has occurred too rapidly to be explained completely by genetic variation, suggesting the involvement of epigenetic mechanisms. Indeed, data from animal models and humans demonstrate that epigenetic dysregulation can cause obesity [Waterland R.A., *et al*., 2005].

1.2.1 Epigenetics in obesity:

The major epigenetic processes related to obesity are DNA methylation, histone modification and lysine acetylation. To date, most studies on the effect of early-life nutrition on the epigenetic regulation of genes have focused on DNA methylation. Recently KA Lillycrop *et al.,* in his review explained genes [Lillycrop K.A., *et al*., 2011] involved in metabolic, vascular or endocrine function whose methylation status is altered by changes in diet either during prenatal or early postnatal life and cause risk of obesity in future. DNA methylation involves DNA methyltransferase catalyzing the covalent addition of a methyl group from S-adenosylmethionine to the 5' carbon of the nucleotide cytosine forming 5-methylcytosine. Upon donating the methyl group S-adenosylmethionine converts to S-adenosyl homocysteine. DNA methylation is associated with transcriptional suppression. Another epigenetic modulation, Lysine acetylation has been implicated as both a post-transcriptional and post-translational process in modulating immunological and metabolic pathways and may therefore be important in maintaining energy homeostasis [Norvell A., *et al*., 2010]. Lysine acetylation involves transfer of an acetyl group from acetyl CoA to the ε-amino group on the target lysine [Shakespear M.R., *et al*., 2011; Weinert B.T., *et al*., 2011; Choudhary C., *et al*., 2009]. Control of lysine acetylation has been studied as a therapeutic target in a wide variety of diseased states, including

cardiovascular dysfunction, obesity and many forms of cancer [Halili M.A., *et al*., 2009; McKinsey T.A., 2011; Bush E.W., *et al*., 2009; Librizzi M., *et al*., 2012]**.** A better understanding of the roles of HDAC enzymes in immunology and metabolism could help directs HDAC modulator development towards dual modulation of metabolic and immune systems, thereby realizing effective treatments for metabolic disease.

1.2.2 Current drug therapy:

Currently only few drugs are available in market for treatment of obesity. Till date there are only two FDA approved anti-obesity drugs available in the market [Chaput J.P., *et al*., 2007]. Orlistat and Sibutramine, both of which have many side effects like increased blood pressure, dry mouth, constipation, headache, and insomnia [De Simone G., *et al*., 2008; Karamadoukis L., *et al*., 2009; Slovacek L., *et al*., 2008]. Also cofounded by diminishing response in long term treatment [Fernstrom J.D., *et al*., 2008; Li Z., *et al*., 2005]. Rimonabant (Acomplia) is a recently developed anti-obesity medication. It is cannabinoid (CB1) receptor antagonist that acts centrally on the brain thus decreasing appetite. It may also act peripherally by increasing thermogenesis and therefore increasing energy expenditure [Akbas F., *et al*., 2009]. Rimonabant is withdrawn from market for treatment of obesity as it is associated with increased risk of psychiatric adverse events, including suicidality.

Moreover, most of the new anti-obesity drug development continues to focus on either central or peripheral acting inhibitors of food intake and would likely encounter the above problems [Cooke D., *et al*., 2006]. Recently, Lorcaserin, a selective 5-HT$_{2C}$ receptor agonist was approved on June 28, 2012 for obesity with other co-morbidities and it has completed phase 3 clinical trials by arena pharmaceuticals [ClinicalTrials.gov.ID:NCT00603902]. Due to the undesirable side-effects associated with the currently available anti-obesity medications and

limited efficacy, much attention has been focused on developing drugs that directly modulate energy metabolism without affecting the central nervous system. Several natural compounds and their respective components (curcumin, berberine, and resveratrol) are well recognized for their potential to exert anti-obesity activity with limited or no side effects. These natural compounds ameliorate obesity by distinct mechanisms like decrease in lipid absorption, decrease in energy intake, increased energy expenditure, decreased pre-adipocyte differentiation and proliferation, decreased lipogenesis and increased lipolysis [Yun J.W., 2010].

Alternatively, it has been hypothesized that combinations of drugs may be more effective by targeting multiple pathways and possibly inhibiting feedback pathways that prevent most monotherapies from producing sustained large amounts of weight loss. This was evidenced by the success of the combination of phentermine and fenfluramine or dexfenfluramine, popularly referred to phen-fen, in producing significant weight loss but fenfluramine and dexfenfluramine were pulled from the market due to safety fears regarding a potential link to heart valve damage. The damage was found to be a result of activity of fenfluramine and dexfenfluramine at the 5-HT2B serotonin receptor in heart valves. Newer combinations of SSRIs (Selective serotonin reuptake inhibitors) and phentermine, known as phenpro, have been used with equal efficiency as fenphen with no known heart valve damage due to lack of activity at this particular serotonin receptor due to SSRIs. There has been a recent resurgence in combination therapy clinical development with the development of 3 combinations: Qnexa (topiramate + phentermine), Empatic (bupropion + zonisamide) and Contrave (bupropion + naltrexone).

CHAPTER 2

LITERATURE

REVIEW

CHAPTER 2
LITERATURE REVIEW

2.1 Histone deacetylases (HDACs):

Reversible acetylation modification of both histone and non-histone proteins at lysine residues is catalyzed by the opposing activities of *histone acetyltransferases* (HATs) and *histone deacetylases* (HDACs) (**Fig.1.2**). Protein acetylation regulates a wide variety of cellular functions, including the recognition of DNA by proteins, protein-protein interactions, and protein stability. HATs and HDACs are classified into many families that are often conserved from yeast to humans [Marmorstein R., *et al.*, 2001; Thiagalingam S., *et al.*, 2003; Legube G., *et al.*, 2003]. HDACs are grouped as class I (HDAC1, 2, 3 and 8), class II (HDAC4, 5, 6, 7, 9 & 10), class III (SIRT1-7) and class IV (HDAC11) based on their homology to yeast transcriptional repressors (Fig.2.1).

Class I and II HDACs have significant similarity between their catalytic domains and are homologous to yeast Rpd3p [Taunton J., *et al.*, 1996] and Hda1p [Fischle W., *et al.*, 1999] deacetylases respectively. The class III HDACs, also called *Sirtuins*, is homologous to the yeast transcriptional repressor Sir2p and has no sequence similarity to class I and II HDACs. Cellular localization, substrates and functions of histone deacetylases has been shown in **Table 1**.
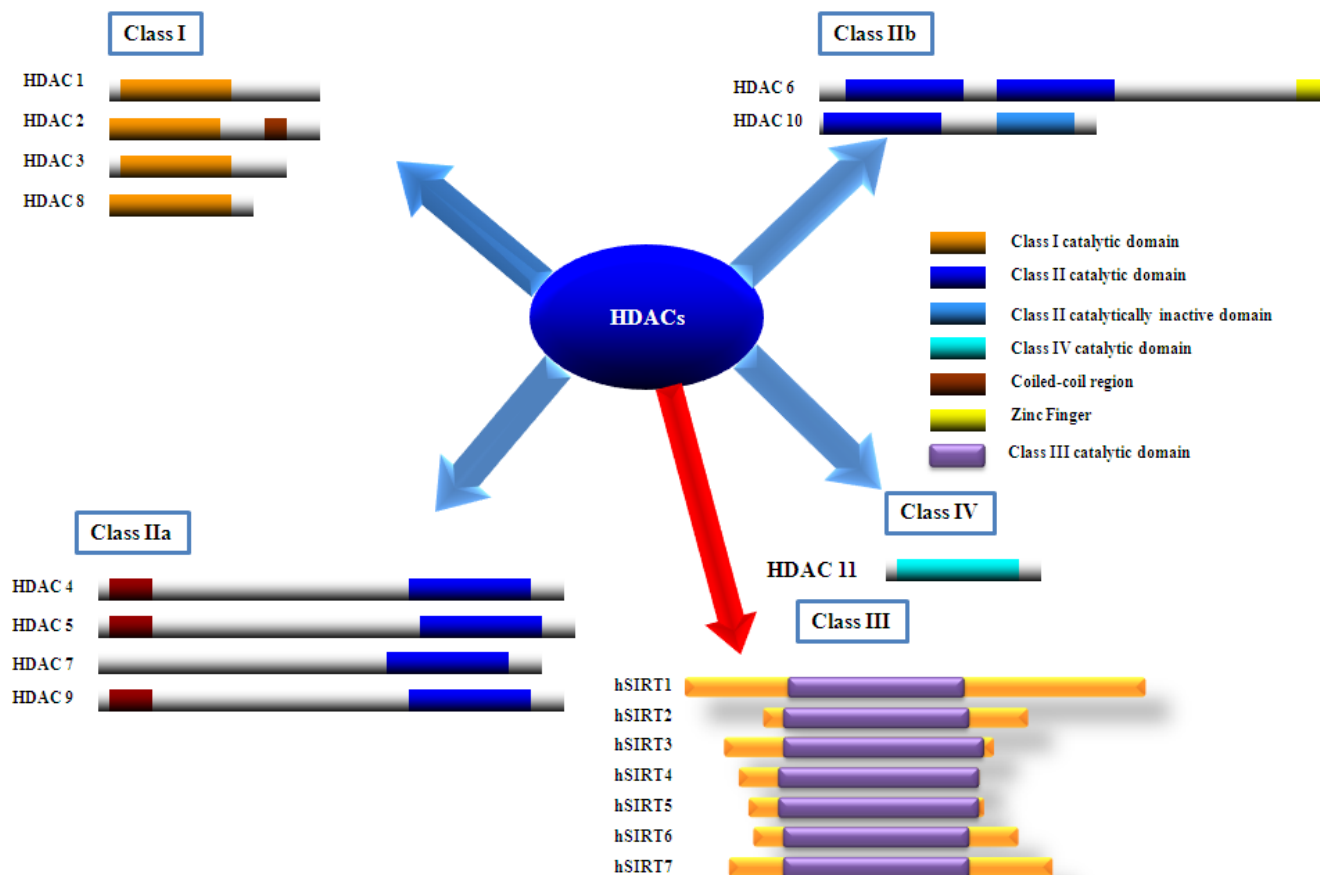
Fig.2.1: Classification of HDACs with their conserved domains.

Table 1: Histone deacetylases: Location, biological function, activity and interacting substrates.

	Member	Location	Biological Function	Activity	Substrates
Class I	HDAC1	Nucleus	cell survival and proliferation	Deacetylase	Histones,MEF2,GATA, YY1,NFk-B,DNMT1-SHP,ATM,MyoD,p53, AR,BRCA1,MECP2,pRb
	HDAC2	Nucleus	Insulin resistance; cell proliferation	Deacetylase	Histones,GATA2,HOP, NFk-B,BRCA1,MECP2,pRb,IRS-1
	HDAC3	Nucleus	cell survival and proliferation	Deacetylase	Histones,HDAC4,5,7,9, SHP, GATA1, NFk-B,pRb
	HDAC8	Nucleus	Cell Proliferation	Deacetylase	HSP70
Class IIA	HDAC4	Nucleus/ Cytoplasm	Regulation of skeletogenesis and glucogenesis	Deacetylase	Histones,SRF,RunX2,p53,p21,GATA,FOXO, HIF-1α,SUV39H1,Hp1, HADC3,MEF2,CaM,14-3-3.
	HDAC5	Nucleus/ Cytoplasm	Cardiovascular growth and function: cardiac myocytes and endothelial cell function; Gluconeogenesis	Deacetylase	Histones,HDAC3,YY1, MEF2,RunX2,CaM,14-3-3
	HDAC7	Nucleus/ Cytoplasm	Thymocyte differentiation, endothelial function-gluconeogenesis	Deacetylase	Histones,HDAC3,, MEF2,RunX2,CaM,14-3-3,PM1,HIF-1α
	HDAC9	Nucleus/ Cytoplasm	Thymocyte differentiation; cardiovascular growth and function	Deacetylase	Histones, HDAC3, MEF2, CaM, 14-3-3.

Cont...

Class IIB	HDAC6	Mostly Cytoplasm	Cell motility-control of cytoskeletal dynamics	Deacetylase	Cortactin,HSP90,HDAC11,SHP,PP1,RunX2,LcoR
	HDAC10	Mostly Cytoplasm	Homologous recombination	Deacetylase	LcoR,PP1
Class III	SIRT1	Nucleus/ Cytoplasm	Aging, redox control-cell survival, autoimmune system regulation, Metabolism Inflammation	Deacetylase	Histones, p53,p73,p300,NF-kB,FOXO,PTEN,NICD,MEF2,HIFs,SREBP-1c,β-catenin,PGC1α,Per2,Ku70,XPA,SMAD7,Cortactin,Ku70,IRS-2,APE1,PCAF,TIP60,PPARγ,ER-α,,AR,LXR
	SIRT2	Cytoplasm	Cell cycle, Tumorigenesis	Deacetylase/ mono-ADP-ribosyl transferase	Histones, α-tubulin
	SIRT3	Nucleus/ Mitochondria	Metabolism	Deacetylase/ mono-ADP-ribosyl transferase	Histones,Ku70,IDH2,HMGCS2,GDH,AceCS,SdhA,SOD2,LCAD
	SIRT4	Mitochondria	Insulin secretion	Mono-ADP-ribosyl transferase	GDH
	SIRT5	Mitochondria	Ammonia detoxification	Deacetylase	Cytochrome C,CPS1
	SIRT6	Nucleus	DNA repair, metabolism, telomere maintenance.	Mono-ADP-ribosyl transferase/ Deacetylase	Histones H3,TNF-α
	SIRT7	Nucleolus	rDNA transcription	Unknown	p53
Class IV	HDAC11	Nucleus/ Cytoplasm			Histones, HDAC6

2.2 Sirtuins:

In the past decade, a novel class of regulators called the 'Silent Information Regulator 2 (SIR2) family or Sirtuins, have been implicated in regulating aging and lifespan in many organisms. Initially discovered in yeast, Sirtuins are a family of proteins with protein deacetylase and ADP-ribosyltransferase activity [Blander G., *et al*., 2004; Imai S., *et al*., 2000; Liszt G., *et al*., 2005]. The name 'Sirtuins' was first given to the family of these proteins by Roy Frye in 1991 who identified five of the human SIR2 homologues, SIRT1-5. The first sirtuin gene was discovered in *Saccharomyces cerevisiae* more than two decades ago by Klar and colleagues [Klar A.J., *et al*., 1979]. The founding member of the Sirtuin family of proteins, the yeast SIR2 (Sir2p), was originally known as MAR1, for mating-type regulator 1. It was discovered by observing a spontaneous mutation that caused sterility due to loss of silencing at the mating-type loci HMR and HML. Later on, a series of mutations resulting in sterile phenotypes were co-discovered by Jasper Rine, who named the set of four genes, homologues of SIR2 (HST), responsible for this trait, as Silent Information Regulator (SIR) 1-4 [Ivy J.M., *et al*., 1985; Shore D., *et al*., 1984]. Subsequently, SIR2 homologues were found in bacteria, worms, flies, plants and mammals, suggesting that the Sirtuin family genes are ancient and evolutionarily conserved.

More than a decade after the discovery of the SIR2 gene, two different groups [Aparicio O.M., *et al*., 1991; Gottlieb S., *et al*., 1989], demonstrated that the SIR2 gene from the Sirtuin family, is required to suppress rDNA recombination and silencing at telomeric DNA. Subsequently it was shown that the gene silencing at mating-type loci and telomeres, is associated with hypo-acetylated histone proteins at the N-terminal lysine residues [Braunstein M., *et al*., 1993]. After the initial discovery that sirtuins metabolize NAD^+ and possess ADP-ribosyltransferase activity, it was soon established that the enzymatic activity of yeast SIR2

protein was essential for gene silencing [Frye R.A., *et al*., 2000; Tanny J.C., *et al*., 1999]. The first identified protein substrates of the yeast SIR2 (Sir2p) were histones [Blander G., *et al*., 2004]. Initially it was thought that ADP-ribosylation of histones by SIR2 interferes with histone acetylation, leading to hyper-acetylation and loss of silencing in SIR2 mutants. However, soon it was shown that SIR2 deacetylated histones and this activity was absolutely dependent on NAD^+ [Landry J., *et al*., 2000]. The NAD^+ dependent deacetylase activity was later described for numerous other sirtuins, including bacterial CobB, archeabacterial SIR2-AF (*Archaeoglobus fulgidus*) and human SIRT1-3 and 5 [Smith J.S., *et al*., 2000]. Sirtuins were thus categorized as class III histone deacetylase (HDAC-III). While class I and II histone deacetylases use zinc as a co-factor [Hernick M., *et al*., 2005], the sirtuins are NAD^+ dependent in that they consume one NAD^+ for removing each acetyl group from the protein substrate. Landry *et al*.,[Landry J., *et al*., 2000] elucidated the mechanism of SIR2 mediated deacetylation showing that the hydrolysis of every molecule of NAD^+ produces one molecule of nicotinamide and one molecule of OAADPr (2'3'-O-acetyl-ADP-ribose), as shown in **Fig.2.2.**

OAADPr formed as a byproduct of NAD^+ dependent deacetylation reaction acts as a secondary messenger for sirtuin triggered signaling pathways. The absolute requirement of NAD^+ for sirtuin catalysis suggests that sirtuins may have evolved as sensors of cellular energy and redox states coupled to the metabolic status of the cell. Increasing evidence support that sirtuins are indeed adapted to interact with changes in NAD^+ involving metabolic pathways, manifested by changes in the concentration of NAD^+, NADH and/or nicotinamide [Denu J.M., 2003; Guarente L., 2000; Leibiger I.B., *et al*., 2006; Lin S.J., *et al*., 2000; Lin S.J., *et al*., 2004; Lin, S.J., *et al*., 2002; Revollo J.R., *et al*., 2004; Sauve A.A., *et al*., 2003]. Nicotinamide, and the

reduced dinucleotide, NADH, are inhibitors of sirtuins. Unlike class I and II HDACs, sirtuins are not affected by Trichostatin A (TSA).
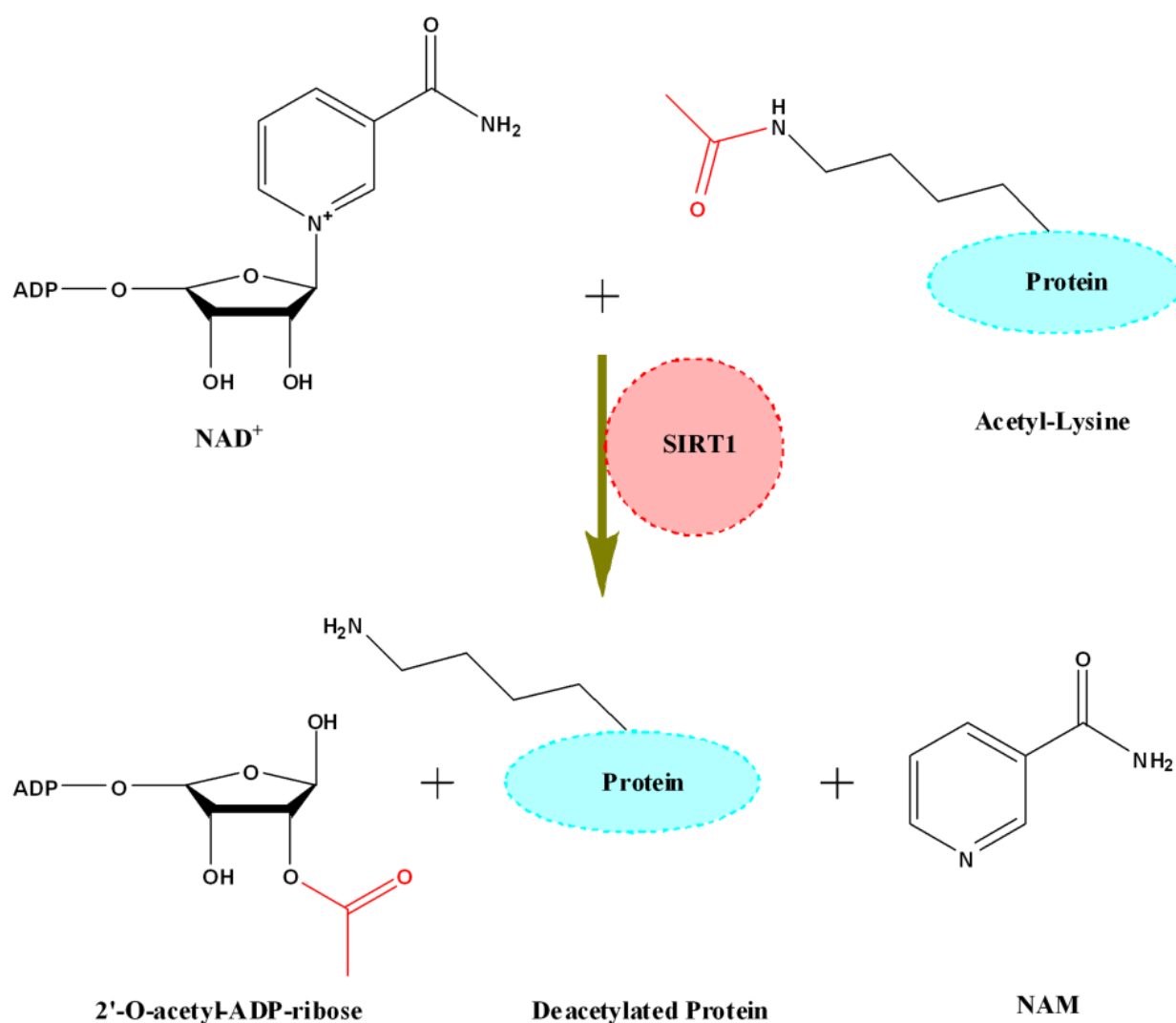
Fig.2.2: Biochemical Reaction of SIRT1-mediated deacetylation.

2.3 Mammalian Sirtuins:

The mammalian sirtuin family consists of seven sirtuins discovered in humans so far namely, SIRT1-7 [Frye R.A., 2000]. All of these have an NAD$^+$ dependent catalytic core domain, which may act preferentially as a NAD$^+$ dependent deacetylase (DAC) and/or mono-ADP-ribosyl transferase (ART). The N-terminal and C-terminal sequences that flank the catalytic core domain vary in length between the different sirtuins. The seven mammalian sirtuins (**Table 1**) also differ in their sub-cellular localization; SIRT1, SIRT6 and SIRT7 being predominately nuclear, SIRT2 cytoplasmic [Frye R.A., 1999; North B.J., *et al*., 2003] and SIRT3, SIRT4 and SIRT5 mostly described as mitochondrial. Although initially, SIRT1 was known to be a nuclear protein, more recently it has been found to shuttle between the nucleus and the cytoplasm, displaying some important cytoplasmic functions as well [Cohen H.Y., *et al*., 2004; Hallows W.C., *et al*., 2006; Moynihan K.A., *et al*., 2005; Tanno M., *et al*., 2007]. .

In the nucleus, a large fraction of SIRT1 is associated with euchromatin, whereas SIRT6 associates with the heterochromatin and SIRT7 localizes in the nucleous [Ford E., *et al*., 2006; Michishita E., *et al*., 2005]. Among the seven sirtuins, SIRT1 show robust deacetylase activity [Vaziri H., *et al*., 2001], SIRT5 has weak deacetyalse activity and SIRT2, 3and 6 possess both deacetylase as well as mono-ADP-ribosyl transferase activities [Shi T., *et al*., 2005]. On the other SIRT4 have only mono-ADP-ribosyl transferase activity [Haigis M.C., *et al*., 2006], and no significant activity has been found for SIRT7 yet. Like their diverse sub-cellular localization, the mammalian sirtuins are expressed differentially in organs, have multiple target substrates and affect a broad range of cellular functions**.** Of the seven mammalian sirtuins, SIRT1 is the most extensively studied, with more than a dozen known substrates and implicated roles in a wide range of cellular processes including cell survival and apoptotic pathways.

2.4 Structure of SIRT1:

The SIRT1 gene is located on chromosome 10q21 and encodes a 747 amino acid long protein. It consists of eight exons and the protein shuttle between the nucleus and cytoplasm..

The SIRT1 protein can be considered composed by four different regions: N-terminal domain, allosteric site, catalytic core and C-terminal domain. The catalytic domain of SIRT1 that spans from 244 to 498 amino acids is composed of a helical module, a zinc-binding module (**Fig. 2.3**) and allosteric region spans from 181–243 amnioacids. The AROS protein interacts directly with amino acids 114–217 in the SIRT1 protein to enhance deacetylation activity as measured by SIRT1-dependent p53 suppression [Kim E.J., *et al*., 2007]. The interface between the two sub-domains creates a large grove that consists of the active site where NAD^+ and the acetylated substrate bind [Huhtiniemi T., *et al*., 2006]. While the mechanism of deacetylation of substrate has been resolved, it has been reported that SIRT1 shows no substrate specificity in vitro. The amino acids proximal to the acetylated lysine do not show any consensus sequences among the SIRT1 substrates [Blander G., *et al*., 2005]. Sasaki *et al*. reported that SIRT1 protein consists of about 13 sites that can be potentially phosphorylated [Sasaki T., *et al*., 2008]. Numerous experimental data [Milne J.C., *et al*., 2007; Bemis J.E., *et al*., 2009; Vu C.B., *et al*., 2009] have shown the modulation of the catalytic activity of SIRT1 exerted through its allosteric effectors. Recently, Sharma *et al*., group reported studies that SIRT1 activators, SRT1460, SRT1720, SRT2183, and resveratrol interacts with SIRT1 at AROS binding domain with good affinity [Sharma A., *et al*., 2012].
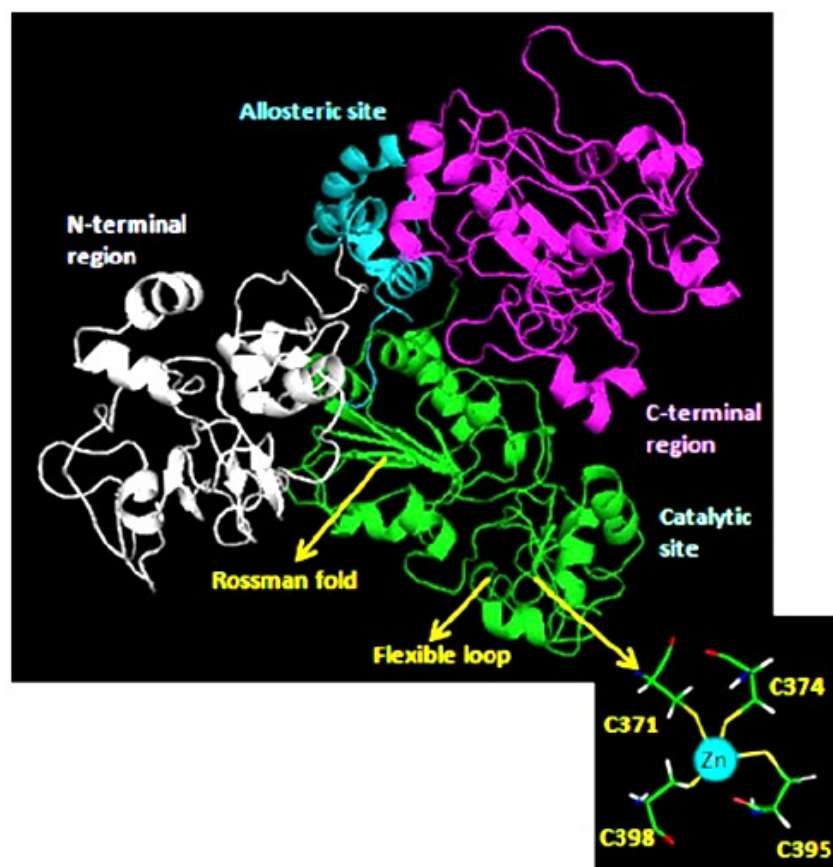
Fig.2.3: Model of human SIRT1. The different structural/functional regions are shown in different colors: in white the N-terminal region, in cyan the allosteric site, in green the catalytic core and in magenta the C-terminal region. The region of the zinc binding (down on the right) shows the four tetrahedrically coordinated cysteines [Photo source: Autiero I., *et al*., 2009].

2.5 Functions of SIRT1:

2.5.1 Regulation at transcriptional and translational levels:

It is important to know that SIRT1 can be regulated both at transcriptional and translational level. Repression of gene expression is associated with histone hypo-acetylation. Heterochromatin, which is the more tightly packed form of chromatin, is associated with hypo-acetylated histones. SIRT1, like the yeast SIR2, facilitates the formation of heterochromatin by

targeting and deacetylating various histone proteins. It deacetylates histone protein H1 at the lysine residues 9 and 26, H3 at 14 and H4 at 16. Apart from deacetylating histone proteins, SIRT1 plays a role in gene expression by targeting transcription factors. Several studies mainly in tissue culture systems have implicated SIRT1 in various cellular processes by means of its interaction with other proteins as shown in **Fig.2.4** downloaded from STRING 9.0 [Sringdb.org].

Proteins like p53 andHIC1 (Hypermethylated in cancer 1) can bind to the SIRT1 promoter region to repress its transcription, and inactivation of HIC1 could result in upregulation of SIRT1 [Chen W.Y., *et al.*, 2005], and those cells are tumor prone. RNA binding protein like HuR binds to the 3' UTR region (untranslated region) of SIRT1 mRNA for stabilizing its expression, whereas Chk2 (cell cycle checkpoint kinase 2) phsophorylates the HuR and represses the SIRT1 expression [Abdelmohsen K., *et al.*, 2007]. E2F1 (transcription factor) is another important apoptosis regulator which binds to SIRT1 promoter inducing its expression, but it is surprising to know that SIRT1 protein in turn binds to E2F1 and inhibits its expression [Wang C., *et al.*, 2006]. SIRT1 modulation can also occur at translational level through protein-protein interactions. AROS (active regulator of SIRT1) binds to the N-terminus of SIRT1 protein and increases its deacetylation function. Whereas DBC1 (Deleted in breast cancer) inhibits the SIRT1 activity by binding to the catalytic domain of SIRT1 [Zhao W., *et al.*, 2008].
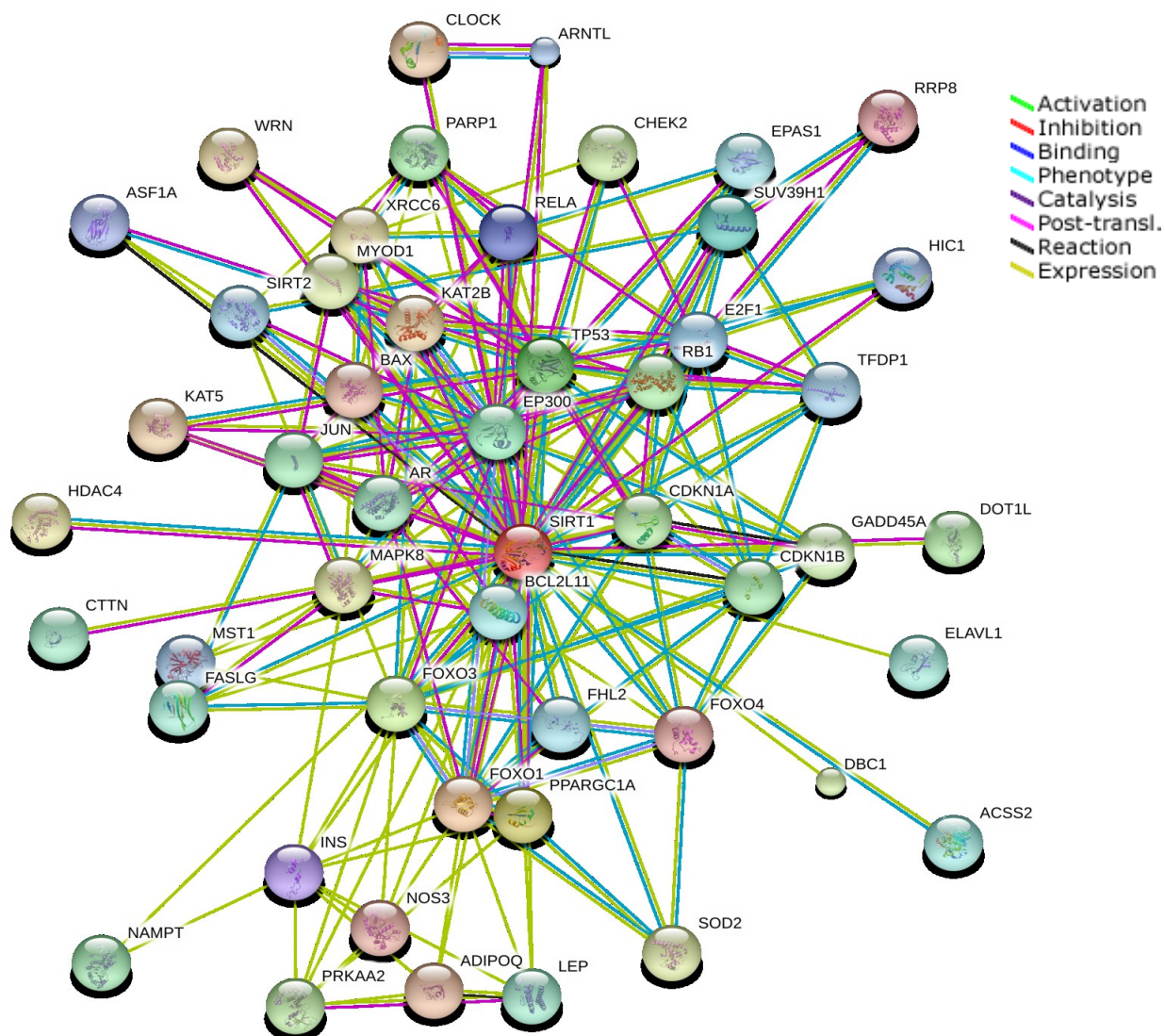
Fig.2.4: SIRT1 interacting proteins [Photo source: Sringdb.org].

Desumoylation of SIRT1 could also reduce its activity. For example, SENP1 desumoylates SIRT1 by binding to the C-terminus which results in repression of SIRT1 activity [Yang, Y., *et al*., 2007]. Manterio *et al*., in their recent review explained that phosphorylation also contributes in controlling the level and function of SIRT1 required for normal cell cycle progression and cell survival under stress conditions [Monteiro, J.P., *et al*., 2011] (**Fig.2.5**).

Although phosphorylation of SIRT1 has a role in cell proliferation and stress conditions, yet there is no profound study related to phosphorylation of SIRT1 which can lead to diabetes development. Whereas, phosphorylation of other proteins like PGC-1α in skeletal muscle by SIRT1 plays a role in alleviating T2DM.
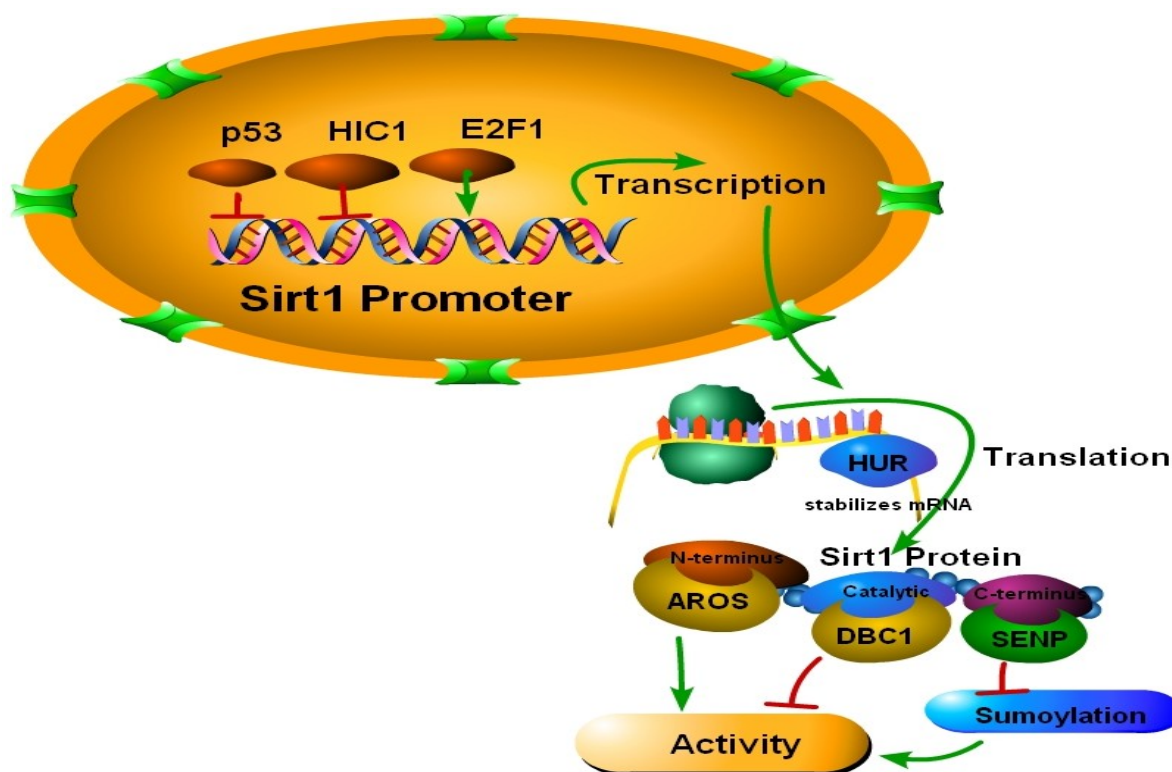
Fig.2.5: SIRT1 mediated transcriptional and translational regulation (Published in Journal of Experts opinion on therapeutic targets by our group [Pulla V.K., *et al*., 2012]).

2.5.2 Apoptosis and survival:

SIRT1 plays a role in apoptosis by targeting multiple proteins such as p53, p73, E2F, HIC1 and Ku70. SIRT1 binds the tumor suppressor p53 and deacetylates it at multiple lysine residues, thereby inhibiting p53 transactivation and suppressing apoptosis in response to oxidative stress and DNA damage [Luo J., *et al*., 2001]. SIRT1 also binds with HIC1

transcriptional repressor and mediates the bypass of apoptosis, potentially by promoting cell survival and tumorigenesis via p53. Since HIC1 can repress SIRT1 expression and p53 is able to transactivate HIC1 transcription, SIRT1, HIC1 and p53 are believed to act in a complex loop where HIC1 represses SIRT1, promoting p53 activity and apoptosis under stress. However, under conditions, where cells are to be recovered from DNA damage, p53 down-regulates HIC1, which induces SIRT1 transcription and promotes cell survival.

Another mechanism by which SIRT1 regulates apoptosis is by binding and deacetylating the DNA repair factor Ku70. Ku70 acts as an inhibitor of Bax mediated apoptosis. Deacetylated Ku70 complexes with the proapoptotic factor Bax, sequestering it away from mitochondria, thereby blocking it from triggering apoptosis in 293 cells in response to stress. SIRT1 also binds the cell proliferation and cell-cycle regulator, E2F1, and inhibits the apoptotic function of E2F1. On the other hand, E2F1 binds directly to the SIRT1 promoter and induces its transactivation, forming a negative feedback loop between SIRT1 and E2F1 functions. This mutual regulation of SIRT1 and E2F1 protects against DNA damage. p73 is yet another protein that SIRT1 targets to regulate apoptosis. Similar to p53, SIRT1 binds and deacetylates p73, thereby suppressing its transcriptional activity and inhibiting p73 mediated apoptosis in 293 cells [Dai J.M., *et al*., 2007].

2.5.3 Regulation of Oxidative Stress:

SIRT1 also plays a role in cell survival by regulating the Forkhead transcription factors (FOXOs). SIRT1 has been documented to deacetylate three out of the four known FOXO proteins, namely FOXO1, FOXO3a and FOXO4. SIRT1 affects FOXO3a in neurons and fibroblasts, reducing stress induced apoptosis and increasing expression of DNA repair and cell cycle checkpoint genes [Brunet, A., *et al*., 2004; Motta, M.C., *et al*., 2004]. SIRT1 also

deacetylates FOXO4 and rescues its repression under oxidative stress, thereby increasing expression of growth arrest and DNA repair protein, GADD45 (growth arrest and DNA-damage-inducible) [Kobayashi Y., *et al*., 2005; Van der Horst A., *et al*., 2004]. Acting through Foxo4, SIRT1 also suppresses the pro-apoptotic proteases caspase-3 and 7 only in transformed cells but not in normal cells [Ford J., *et al*., 2005]. Interestingly, caspase-9 and Bcl-xL regulate SIRT1 cleavage during apoptosis, shifting its localization from nucleus to cytoplasm [Ohsawa S., *et al*., 2006].

Furthermore, SIRT1 protects pancreatic β-cells against glucose induced cytotoxicity by acting through FOXO1 [Kitamura Y.I., *et al*., 2005]. In diabetic patients, chronically high plasma glucose causes cytotoxicity leading to β-cell degeneration. This is believed to be caused by increased mitochondrial oxidation rates, due to higher glucose levels, leading to increased ROS (reactive oxygen species) production. Under these conditions, SIRT1 is required in sustaining FOXO1-mediated transcription of MafA and NeuroD, which regulate expression of insulin gene2 to prevent apoptosis.

2.5.4 Cellular Senescence:

Cellular senescence is a state of permanent cell cycle arrest which is manifested by defined morphological changes. Senescence can be natural or induced by certain stimuli. SIRT1's role in regulating cellular senescence is conflicting. Under certain conditions, SIRT1 has been found to localize with PML (promyelocytic leukemia) in discrete nuclear structures called the nuclear bodies. PML proteins are believed to act as co-activator or co-repressor to various transcription factors affecting apoptotic signals. It is believed that SIRT1 rescues primary mouse embryonic fibroblasts from PML-mediated premature cellular senescence by inhibiting the pro-apoptotic factor p53 [Langley E., *et al*., 2002]. However, in other cases, SIRT1 has been

shown to promote cellular senescence, SIRT1 null MEFs show extended replicative potential and higher proliferation during chronic but sub lethal stress [Chua K.F., *et al*., 2005]. Interestingly, lower SIRT1 levels have been documented in dividing tissue of older mice, such as testis and thymus or in cells that have been serially passaged. However, this was not true for immortalized cells or post-mitotic organs [Sasaki T., *et al*., 2006]. Thus, although SIRT1's regulatory role in senescence is conflicting, SIRT1 mediated regulation of senescence may play a significant role with regard to tumorigenesis in the elderly and aging.

2.5.5 DNA repair:

A couple of reports have suggested a potential role of the mammalian sirtuins in DNA repair. Recently, Mostoslavsky *et al* showed that SIRT6 knockout mice exhibit impairment in base excision repair [Mostoslavsky R., *et al*., 2006]. While the mechanism by which SIRT6 regulates DNA repair is not clear, the various phenotypic defects found in SIRT6 knockout mice such as premature aging, abnormal spine curvature and metabolic defects have been attributed to defects in DNA repair. More recently, SIRT1 has also been implicated in DNA repair mechanism. Upon exposure to radiation, SIRT1 enhances DNA repair capacity and deacetylation of the repair protein Ku70. Over-expression of SIRT1 results in the increased repair of DNA strand breakages produced by radiation. On the other hand, repression of endogenous SIRT1 expression by SIRT1 siRNA decreases repair activity, indicating that SIRT1 can regulate DNA repair capacity of cells with DNA strand breaks [Jeong J., *et al*., 2007].

2.5.6 Role in Inflammation:

SIRT1 plays a role in inflammation by regulating a key regulator NF-κB. SIRT1 represses NF-κB activity possibly by multiple mechanisms. It has been shown that SIRT1 deacetylates the RelA/p65 subunit of NF-κB, thereby inhibiting its transactivation potential

[Yeung F., *et al*., 2004]. Consistent with this, it has been shown that cigarette smoke extracts can increase pro-inflammatory responses mediated by NF-κB by decreasing the interaction between SIRT1 and RelA/p65 resulting in increased acetylation and activation of NF-κB [Yang S.R., *et al*., 2007]. Interestingly, SIRT1 is expressed at higher levels in calorie restricted rodents which also show decreased inflammatory responses. Recently in a high-throughput screen, SIRT1 activating compounds were shown to have anti-inflammatory properties such as reduction of the pro-inflammatory cytokine TNF-α (tumor necrosis factor α) [Nayagam V.M., *et al*., 2006].

2.5.7 Cell development:

Many lines of evidence suggest a role of SIRT1 in development. Using a Sir2 knock out transgenic mice model, McBurney *et al*. showed that the protein SIRT1 is important for embrogenesis and gametogenesis. First, only half of the typically expected numbers of pups are born, and of those that are born, only 20% survive to adulthood. These mice showed developmental defects such as markedly smaller size as compared to their littermates, slower development, defects in eye morphogenesis and cardiac septation. Furthermore, the mice that survive to adulthood are sterile in both sexes, with males having lower sperm count and females failing to ovulate, potentially due to hormonal inefficiency [McBurney M.W., *et al*., 2003]. The developmental defects in SIRT1 mutant mice can be explained by SIRT1's regulation of the transcriptional repressors Hes1 and Hey2, which play a role in development [Takata T., *et al*., 2003]. Apart from this, SIRT1 is also known to regulate BCL11A and CTIP2, a mammalian and chicken protein respectively, which play a role in hematopoietic cell development and malignancies [Senawong T., *et al*., 2005]. Consistent with SIRT1's role in development, another report showed that SIRT1 is expressed at higher levels in the heart, brain, spinal cord and dorsal root ganglia of embryos [Sakamoto J., *et al*., 2004]. Another sirtuin member, SIRT2, has been

shown to interact with a homeobox transcription factor important for embryogenesis, HOXA10, indicating potential role for the other sirtuins in development [Bae N.S., *et al*., 2004].

2.5.8 Reproduction:

It has been documented that developing spermatocytes express higher levels of SIRT1 and deletion of the SIRT1 gene leads to severe sperm abnormality and sterility in mice [McBurney M.W., *et al*., 2003]. Thus SIRT1 potentially plays a role in the reproductive capacity of animals.

2.5.9 Muscular differentiation and maintenance:

SIRT1 regulates muscle differentiation and muscle mass maintenance by regulating multiple proteins. SIRT1 deacetylates and inhibits the transcription factor MyoD, a key player in muscle differentiation. On the other hand, SIRT1's activity is regulated by decreasing levels of NAD+ during muscle differentiation to alleviate SIRT1-mediated MyoD suppression [Fulco M., *et al*., 2003]. SIRT1 also deacetylates MEF2 (myocyte enhancing factor 2), another transcription factor that regulate muscle differentiation. Deacetylation of MEF2 by SIRT1 facilitates the HDAC4 mediated SUMO addition by E3 ligase on MEF2; thereby inhibiting MEF2 mediated transcription [Zhao X., *et al*., 2005]. Reduction in muscle mass is a common cause in diseases like muscular dystrophy, cancer and aging. Balanced turnover of protein is critical for muscle mass maintenance. Two proteins involved in proteosome mediated proteolysis are MnRF1 (for muscle RING finger 1) and MAFbx/atrogin-1 (for muscle atrophy F-box) [Glass D.J., *et al*., 2005]. These two proteins are transcriptionally regulated by NF-κB and FOXO pathways, which in turn are regulated by SIRT1. Thus, along with its regulation of MyoD, MEF2, NF-κB and Forkhead transcription factors, SIRT1 plays a broader role in controlling muscle mass maintenance during injury and aging.

2.6 SIRT1, cancer and controversies:

The earliest reports of SIRT1 as a non-histone deacetylase involved p53. It was shown that deacetylation of p53 by SIRT1 inhibited its transcriptional function and hence, SIRT1 was considered an oncogene [Smith J., *et al*., 2002].The role of SIRT1since then has been studied in detail and a number of SIRT1 functions have been brought to light. While some reports have deemed SIRT1 as an oncogene based on its function and expression pattern in tumors [Huffman D.M., *et al*., 2007; Stunkel W., *et al*., 2007], other reports have provided evidence for a tumor suppressive function of SIRT1 [Firestein R., *et al*., 2008; Wang R.H., *et al*., 2008]. The importance of p53 acetylation in its stabilization and transcriptional function has been questioned. While some researchers have shown that acetylation of p53 mediated by p300/CBP in response to DNA damage enhances sequence-specific DNA binding [Lill N.L., *et al*., 1997; Olsson A., *et al*., 2007; Sakaguchi K., *et al*., 1998], others have shown that enhancement of p53 function is independent of its acetylation status [Espinosa J.M., *et al*., 2001]. In light of the above conclusions, the significance of p53 acetylation is controversial and so is the functional effect of SIRT1-mediated p53 deacetylation. Besides p53, SIRT1 has been shown to regulate proteins that participate in various pro-apoptotic and anti-apoptotic pathways. To date the controversies regarding the exact role of SIRT1 in cancer have not been resolved and further research will be required to reach a conclusion. Stunkel *et al*., compared the levels of SIRT1 in various cancer cell lines with normal cells and found that SIRT1 was over expressed in almost all the cancer cell lines that were tested. When stained with anti-SIRT1 antibody, HeLa and SW620 cell lines exhibited cytoplasmic localization of SIRT1. Staining of a colon tumor microarray also revealed cytoplasmic localization of SIRT1 in the tumor as well as normal colon tissue. This result was unexpected since the nuclear localization of SIRT1 is a well-established fact and further

investigation of this expression pattern will reveal its significance. Another research group identified two nuclear import and two export sequences on SIRT1 protein and found that SIRT1 could shuttle between the nucleus and cytoplasm in C2C12 myoblast cells. SIRT1 was nuclear in undifferentiated C2C12 and localized to the cytoplasm upon differentiation. Nuclear SIRT1 was found to protect the cells against oxidative damage induced cell death but the function of cytoplasmic SIRT1 is yet to be determined. It was hypothesized that the cytoplasmic localization of SIRT1 is a mode of regulation such that removal of SIRT1 from the nucleus allows for acetylation and activation of certain nuclear substrates of SIRT1. To study the role of SIRT1 in cancer, Huffman *et al*., developed a prostate cancer mouse model called TRAMP (Transgenic adenocarcinoma of mouse prostate) [Huffman D.M., *et al*., 2007]. SIRT1 levels were found to be elevated in prostate adenocarcinomas in these mice. Simultaneously, HIC1 levels were down regulated leading the authors to suggest that lower levels of HIC1 expression were responsible for the observed increase in SIRT1. Levels of acetylated Lys9 on histone H3 were also reduced in these cancers. Upon staining prostate tumor biopsies, it was found that SIRT1 expression was high in the cancer cells as compared to the normal surrounding cells. Based on the association of elevated SIRT1 levels with advanced prostate cancer, the authors summarized that SIRT1functions as an oncogene and may serve as a potential target for prostate cancer therapy. However, this model does not provide conclusive evidence for SIRT1 as a cause of prostate cancer. It merely shows an association between high SIRT1 expression and prostate cancer. Recently, a research group generated a Sirt1 null mouse model to determine the role ofSIRT1 in tumorigenesis [Wang R.H., *et al*., 2008]. They discovered that cells obtained from SIRT1-/- embryos exhibited incomplete chromosome condensation and chromosome instability. These cells also demonstrated cell cycle abnormalities and impaired DNA damage repair as compared

to SIRT1+/+ cells. Furthermore, it was discovered that SIRT1+/-p53+/- mice were more prone to development of spontaneous tumors as compared to SIRT1+/- or p53+/- mice. These observations led the authors to suggest that SIRT1 may function as a tumor suppressor. They then analyzed a set of clinical tissues to study the levels of SIRT1expression in tumors and found that SIRT1 levels were lower than normal in glioblastoma, bladder carcinoma, prostate carcinoma and certain ovarian cancers. This expression pattern in the different tumors along with observations from the Sirt1 null mice led the authors to suggest that SIRT1 has a tumor suppressive function.

On the contrary to above, Lovaas *et al* reported that SIRT1 is an important regulator of MMP2 (matrix metalloproteinase-2) expression, activity, and prostate cancer cell invasion. Over expressed SIRT1 in advanced prostate cancer may play an important role in prostate cancer progression [Lovaas J. D., *et al*., 2012]. In the case of prostate cancer, Kuzmichev *et al* [Kuzmichev A., *et al*., 2005] demonstrated over expression of SIRT1 by immunohistochemical analysis. Huffman *et al* reported that SIRT1 expression in the *dorso-lateral* prostate was increased in mice with poorly differentiated adenocarcinomas compared with those with normal tissue and high grade PIN (prostatic intraepithelial neoplasia). They also showed that human prostate cancer cells had greater SIRT1 expression than uninvolved cells by analyzing prostate tumor biopsy samples. Based on these findings, enhanced expression of endogenous SIRT1 has been implicated in promoting tumorigenesis [Lim C.S., 2006].

2.7 Sirt1 and obesity-associated metabolic diseases:

Hepatic metabolic derangements are key components in the development of fatty liver, insulin resistance, and atherosclerosis. Sirt1 is an important regulator of energy homeostasis in response to nutrient availability. Energy homeostasis is regulated by three processes, which

include energy intake, storage and expenditure. During healthy homeostasis, abnormality in any processes would be counter balanced by other two processes. Insulin resistance is an inability to respond to insulin in circulating fluid, which is generally believed to be the important characteristic of T2DM (Type 2 diabetes mellitus). In recent years it was demonstrated that abnormality in energy expenditure could be the prime cause of insulin resistance.

Dependence of SIRT1 on NAD^+ levels infer that it acts as a key sensor for changes in metabolism. SIRT1 has a range of targets involved in regulating the metabolism at various tissues. The complexity of SIRT1 can be explained with an example, as it has been known that SIRT1 inhibits the activity of p300 (Acetyl transferase), expressed in a broad range of tissues and hence it has a role in regulating various genes.SIRT1 was also shown as modulator for two other acetyltransferases like PCAF (p300/CBP associated factor) and GCN5, where it forms a complex with MyoD (transcription factor). It is important to know that SIRT1 regulation on various targets like FOXO, PPARγ, PGC-1α and AMPK, which are related to many chronic diseases including T2DM. To demonstrate the importance of SIRT1 in treating metabolic disorders, we need to know its role in various signaling pathways like insulin receptor signaling, gluconeogenesis, fatty acid oxidation, obesity and caloric restriction. These details are discussed in forthcoming sections.

2.7.1 SIRT1 in hepatic glucose homeostasis:

The liver plays a central role in regulating key aspects of lipid and glucose homeostasis in response to nutritional and hormonal signals [Van den Berghe G., 1991]. In response to low nutrient conditions gluconeogenesis helps in the production of glucose, to supply necessary glucose to active tissues like brain and blood cells. In response to low nutrient conditions α-pancreatic cells release glucagon, which activates the translocation of TORC2 (Transducer of

regulated CREB activity) into the nucleus and activates the CREB (cyclic AMP response element binding protein), which helps in induction of PGC-1α. Later PGC-1α, after binding to the FOXO1 and HNFα (hepatocyte nuclear factor-α) inducts gluconeogenesis by activating the PEPCK (phosphoenolpyruvate carboxykinase) and G6Pase (Glucose 6 phosphatase enzymes) [Yoon J.C., *et al*., 2001; Puigserver P., *et al*., 2003; Rhee J., *et al*., 2003].

During caloric restriction (CR), various transcription factors like CREB, CRTC2 (CREB regulated transcription coactivator 2); FOXO1 and PGC-1α are activated by SIRT1 which increases glycogenolysis and gluconeogenesis enzymes like G6Pase, FBPase (fructose-1, 6-bisphosphatase) and PEPCK 24. Furthermore, SIRT1 also deacetylates and inactivates the STAT3 (signal transducer and activator of transcription-3), which is known to be a repressor of gluconeogenesis. It is interesting to know that reduction of SIRT1 expression in mice liver reduces the gluconeogenesis, resulting in mild hypoglycemia and increased expression of SIRT1 results in mild hyperglycemia. Similar studies in *in vivo* models of T2DM rats showed decreased expression of gluconeogenic enzymes when SIRT1 is inhibited by antisense oligonucleotides because of increased acetylation of STAT3, FOXO1 and PGC-1α.Anothersurprising and prominent finding is that prolonged starvation would result in decrease in the expression of gluconeogenesis genes because of deacetylation and ubiquitination of CRTC2. During nutrient deprivation, SIRT1 activation causes hepatic fatty acid oxidation along with TORC2 suppression [Purushotham A., *et al*., 2009; Feige J.N., *et al*., 2008]. SIRT1 acts through PGC-1α to activate PPARα transcription to induce fatty acid catabolic genes [Purushotham A., *et al*., 2009]. Thus prolonged fasting leads to increased deacetylation of PGC-1α by SIRT1 resulting in mitochondrial fatty acid oxidation in response to improved glucose homeostasis demands [Purushotham A., *et al*., 2009; Rodgers J.T., *et al*., 2005; Dominy J.E. Jr., *et al*., 2010]. In

contrast to the above findings during CR condition, SIRT1 liver specific knockout mice were found to initiate gluconeogenesis as similar to control animals, and showed upregulation of gluconeogenic genes like PEPCK, G6Pase andPGC-1α (**Fig.2.6**). This infers that SIRT1 does not have any control over gluconeogenesis during CR [Chen D., *et al*., 2008]. In extension to the above findings scientists have proved that SIRT1 improves the insulin sensitivity when fed with HFD (high fat diet).

2.7.2 SIRT1 in pancreatic β cells insulin secretion:

In the development of T2DM, pancreatic islet β-cell failure is a crucial pathological contributor. The molecular mechanisms and cellular pathways involved in this T2DM development have been extensively investigated [Kitamura Y.I., *et al*., 2005; Steppel J.H., *et al*., 2004]. Accumulation of triglycerides, excess intracellular fatty acids and cellular stress due to over nutrition are the general contributors leading to b-cell dysfunction as well as impaired insulin secretion. Recent investigations revealed UCP2 (uncoupling protein-2) as a key modulator of insulin secretion in pancreatic cells. Polymorphism of UCP2 promoter with higher expression of UCP2 leads to decreased insulin secretion at T2DM conditions.

Insulin is released by pancreatic-β cells following meal consumption. Glucose enters into the pancreatic-b cells through GLUT2 transporter and later undergoes oxidation to give ATP. The increase in the ATP results in closure of ATP/K^+ channels causing depolarization of membrane, and opening of voltage gated Ca^{2+} channels that results in the release of insulin. The role of SIRT1 in expressing insulin was best demonstrated in BESTO mice (β-cell-specific SIRT1-overexpressing), which improved insulin secretion in response to glucose whereas in the SIRT1 knock out animals it was found that there was significant decrease in the insulin secretion [Bordone L., *et al*., 2006]. It has been proposed that SIRT1 increased insulin levels by repressing

the action of UCP2, which prevents insulin release during food deprivation (**Fig.2.6**) [Bordone L., *et al*., 2006]. It is very much evident thatSIRT1 expression would be activated during high glucose meals and inhibited during starving conditions in pancreatic β-cells. This can be best explained that during overnight fasting there would be a significant decrease in the NAD^+ which in turn decreases the activity of SIRT1 [Bordone L., *et al*., 2005]. By deacetylating FOXO1, SIRT1 also promotes the activation and transcription of NeuroD and MAFA (mast cell function associated antigen), which preserve insulin secretion and promote β-cell survival [Kitamura Y.I., *et al*., 2005].

Transgenic mice studies under the control of rat insulin promoter revealed that SREBP-1c (sterol regulatory element binding protein) was over-expressed and involved in impaired insulin secretion and glucose intolerance [Yamashita T., *et al*., 2004; Takahashi A., *et al*., 2005]. Impaired insulin secretion due to over-expression of SREBP-1c was associated with the accumulation of triglycerides and increased gene expression of lipogenic genes in β-cells.SREBP-1c did not only lead to functional disturbances in mature β-cells but also interrupted β-cell differentiation and replication, resulting in loss of β-cell mass. Studies on RIP-SREBP-1c transgenic mice model revealed that impairment of β-cell function was mediated through suppression of IRS2 (insulin receptor substrate-2) and PDX1 (pancreas duodenum homeobox 1). It has been reported in rodents that SREBP-1c binds to the IRS2 promoter and suppresses it. Similar mechanism was also observed in hepatocytes (**Fig.2.6**) [Ide T., *et al*., 2004]. IRS2 is proven to promote β-cell growth and survival [Withers D.J., *et al*., 1998]. Therefore, suppression of IRS2 expression by SREBP-1c should contribute, at least in part, to β-cell glucolipotoxicity [Wang H., *et al*., 2005]. Hence in this context activating SIRT1 would be a

right option to combat T2DM as it results in suppression of SREBP-1c and eventual increase in the expression of IRS2, PDX1 and GLUT2.
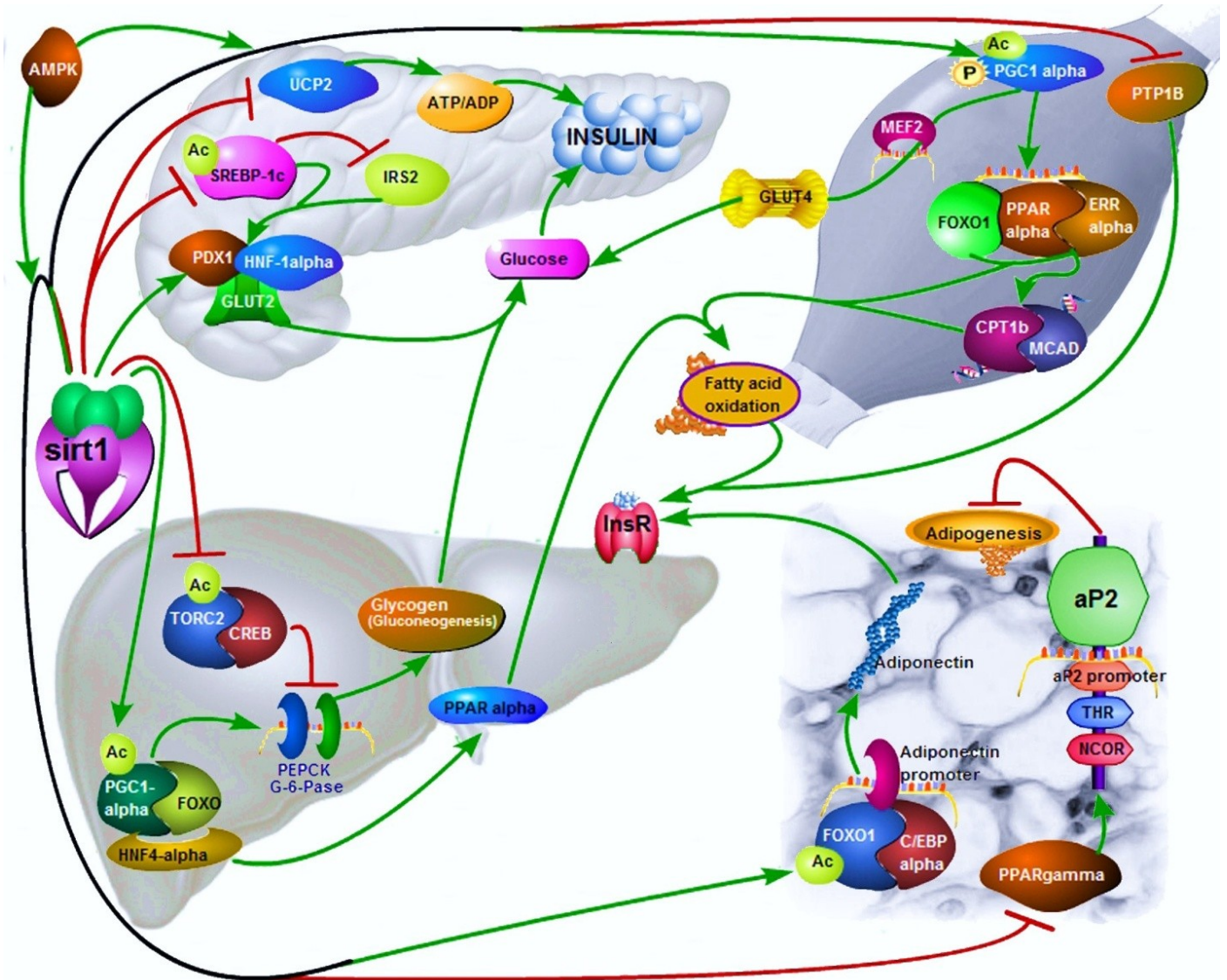
Fig.2.6: SIRT1 pathway within the tissues of liver, pancreas, skeletal muscle and adipose tissue (clock wise) in relation to T2DM. (Green arrows indicate activation, Red arrow indicates inhibition, and Black lines indicate mixed action from the same source). (Published in Journal of Experts opinion on therapeutic targets by our group [Pulla V.K., *et al.*, 2012]).

2.7.3 SIRT1 in skeletal muscle metabolic homeostasis:

Skeletal muscle is a key metabolic tissue in maintaining metabolic pathways to endorse energy and nutrient homeostasis. Nutrient deprivation and alteration in food availability triggers a whole rearrangement of glucose and lipid metabolism. Excessive accumulation of fatty acids and lipid metabolites in muscle causes lowered uptake of glucose, leading to complications of T2DM [Randle P.J., *et al.*, 1963; Furler S.M., *et al.*, 2001]. Activating fatty acid β-oxidation has been suggested to be a promising approach to alleviate muscle insulin resistance and to increase glucose uptake. *In vitro* and *in-vivo* studies demonstrated that activation of PGC-1α in skeletal muscles would be the right strategy to treat T2DM. For instance, exposure of L6 rat myotubes to high concentrations of fatty acid had decreased b-oxidation. On the other hand over-expression of PGC-1α in muscle increased the ratio of complete fatty acid β-oxidation [Koves T.R., *et al.*, 2005]. It has been known that PPAR receptors are one of the primary regulators of lipid metabolism. It is interesting to know that activation of PCG-1α results in activation of PPARα which further stimulates insulin sensitivity. PGC-1α is a common transcriptional co-activator for several transcriptional factors such as FOXO1, ERRα and PPARα that induces activation of a major regulatory metabolic enzyme called PDK4 (pyruvate dehydrogenase kinase-4) at the transcription level [Wende A.R., *et al.*, 2005]. To undergo mitochondrial oxidation of fatty acids PGC-1α also triggers OXPHOS (Oxidative phosphorylation) genes which are involved in the final step of electron transport chain and ATP synthesis in muscle cell [Wu Z., *et al.*, 1999]. In fact, mitochondrial OXPHOS targets are down regulated in human skeletal muscle of T2DM patients due to increased intramyocellular triglyceride accumulation [Mootha V.K., *et al.*, 2003; Patti M.E., *et al.*, 2003]. In addition, interaction of PGC-1α with PPARα and ERRα transcription factors results in induction of fatty acid oxidation genes such as CPT-1b

(Carnitinepalmitoyltransferase) and MCAD (Malonyl-CoA decarboxylase) (**Fig.2.6**) [Schreiber S.N., *et al*., 2004; Mootha V.K., *et al*., 2004]. Interestingly, several experimental reports identified that SIRT1 is the major deacetylase of PGC-1α that positively regulates mitochondrial fatty acid utilization genes. During starvation there would be an increase in the NAD^+ levels, which is correlated with increase in the PGC-1α deacetylation, suggesting an increase in the enzyme activity of SIRT1 [Gerhart-Hines Z., *et al*., 2007]. Thus, in skeletal muscles, SIRT1 activates PPARα through deacetylation of PGC-1α to induce transcription of fatty acid catabolic genes during nutrient deprivation [Pfluger P.T., *et al*., 2008]. From the above details we get to know the importance of PGC-1α in treating diabetes, and equally very important proteins which mediate its activity and their interregulation. Expression of PGC-1α and mitochondrial biogenesis had also been shown to be mediated by AMPK [Jager S., *et al*., 2007]. AMPK is another metabolic sensor that activates PGC-1α based on intracellular AMP/ATP ratio. According to Canto *et al*., AMPK activates PGC-1α via sirtuins [Canto C., *et al*., 2009]. Furthermore, AICAR, a direct activator of AMPK showed an increase in NAMPT (nicotinamide phophoribosyltransferase), which further helps in the activation of SIRT1 through increased synthesis of NAD^+ [Fulco M., *et al*., 2008]. Activation of AMPK by metformin had also shown to increase the PGC-1α, cytochrome-c and other oxidative enzymes [Suwa M., *et al*., 2006]. In diabetic patients, PGC-1α levels were found to be decreased in skeletal muscle, which further demonstrates the importance of PGC-1α [Canto C., *et al*., 2009]. It is interesting to know that AMPKs are in turn regulated by various kinases and deacetylases as well. Kinases like LKB1 (liver kinase B1) and calcium/calmodulin kinase-b activate AMPK by phsophorylating threonine residue at 172 positions. SIRT1 regulation on AMPK was demonstrated by Lan *et al*., when SIRT1 was over-expressed in embryonic kidney 293T cell line and there was a reduced

acetylation of LKB1 resulting in translocation from nucleus to cytoplasm which activated itself and the AMPK (**Fig.2.7**) [Lan F., *et al*., 2008]. The importance of SIRT1 *in vivo* was also explained by Hou *et al*., when resveratrol increased the activity of AMPK in mouse liver in the presence of SIRT1 and LKB1 [Hou X., *et al*., 2008]. Activation of AMPK was also found to increase insulin sensitivity through a greater level of GLUT4 translocation and glucose transport that triggers insulin release [Jessen N., *et al*., 2003; Fisher J.S., *et al*., 2002]. Moreover, PGC-1α appears to regulate GLUT4 transcription in conjunction with the transcription factor MEF2C (myocytespecific enhancer factor 2C) [Michael L.F., *et al*., 2001]. Here, AMPK activation increases GLUT4 gene expression through PGC-1α phosphorylation while MEF2 nuclear translocation leads to promotion of GLUT4 membrane translocation [Holmes B.F., *et al*., 2005]. Alleviating insulin resistance is also a key for the treatment of T2DM. Increased expression of PTP1B (protein tyrosine phosphatase 1B) is one another cause for insulin resistance in tissues like skeletal muscle and liver. Whereas, it is well displayed that decreased expression of PTP1B results in better responses to insulin stimulation. Moreover, current target SIRT1 represses PTP1B at both the mRNA and protein levels [Elchebly M., *et al*., 1999; Zinker B.A., *et al*., 2002]. Rise in the expression of PTP1B counteracts with SIRT1-mediated improved InsR (insulin receptor) phosphorylation and glucose uptake due to insulin stimulation (**Fig.2.6**). For instance, a SIRT1 activator resveratrol derived from natural source also repressed PTP1B both *in vitro* and *in vivo*, signifying that resveratrol has a positive effect on insulin sensitivity [Vaquero A., *et al*., 2004]. Furthermore, similar results were found in C2C12 myotubes where SIRT1 represses PTP1B transcription at the chromatin level. It has been already known that SIRT1 protein levels are increased in calorie-restricted animals [Howitz K.T., *et al*., 2003] and CR is considered to be an effective dietary intervention for enhancing insulin sensitivity [Barzilai N., *et*

al., 1998; Fontana L., *et al*., 2004]. Moreover, PTP1B protein levels were decreased by increasing levels of SIRT1 in liver of fasting mice indicating the possibility that SIRT1 negatively regulates PTP1B *in vivo* [Gu F., *et al*., 2003]; however, the entire mechanism involved was not fully elucidated.
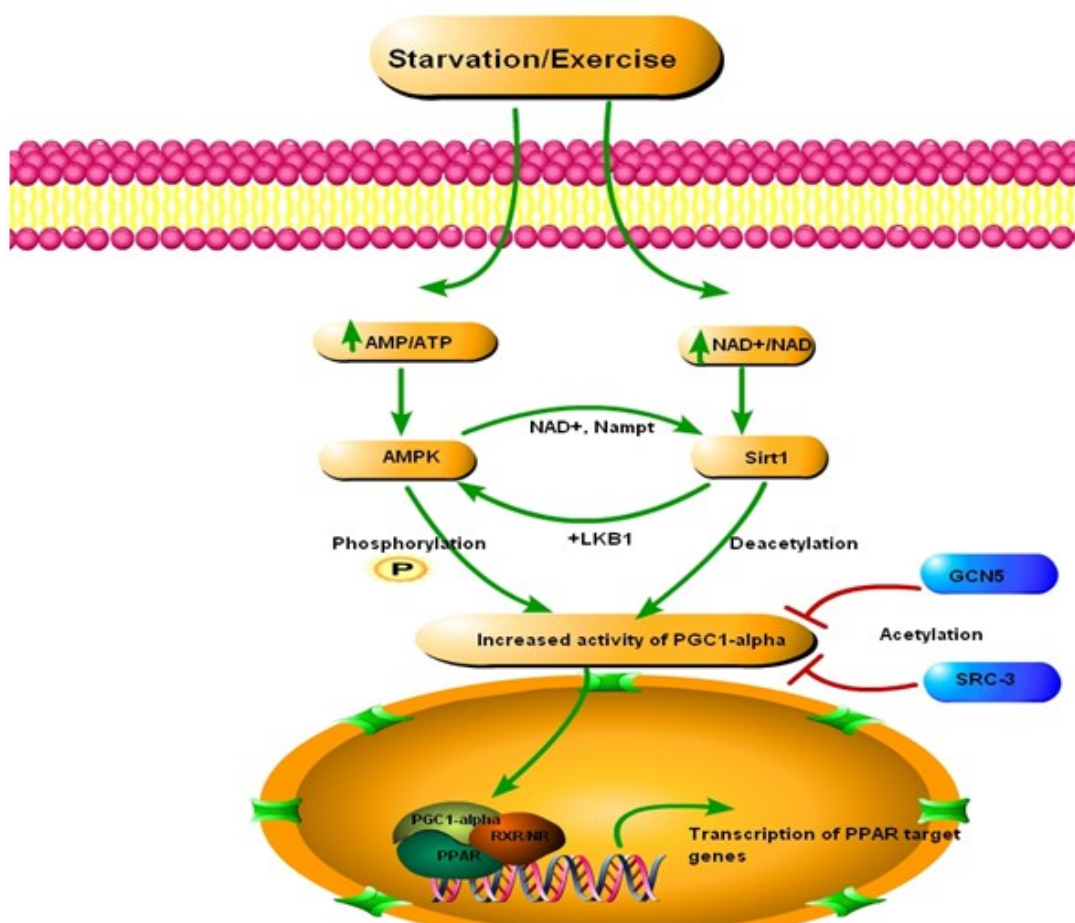
Fig.2.7: The relation between AMPK, SIRT1, PGC-1α and PPARγ upon starvation/exercise (Published in Journal of Experts opinion on therapeutic targets by our group [Pulla V.K., *et al*., 2012]).

2.7.4 SIRT1 in adipocyte energy homeostasis and insulin sensitization:

Adipose tissue, widely known as a storage compartment for fatty lipids also deals with functions such as innate immune response, endocrine functions, vascular remodeling and

synthesis of key modulators for insulin sensitivity and whole body energy homeostasis [Rajala M.W., *et al*., 2003]. An adipocyte-derived hormone also known as adiponectin plays a crucial role in aspects like energy metabolism, immunological responses and also in insulin sensitivity with compelling evidences [Berg A.H., *et al*., 2005; Kadowaki T., *et al*., 2005]. In general, in deprived nutritional conditions, SIRT1 mobilizes fat storage in adipocytes and increases adiponectin gene expression which sensitizes cells to respond to insulin and enhances fatty acid oxidation. Profoundly, SIRT1 enhances the coordinative interaction between two transcription factors FOXO1 and C/EBPα (CCAAT enhancer binding protein alpha) mediated adiponectin promoter activation followed by release of adiponectin (**Fig.2.6**).Moreover, decrease in FOXO1 and SIRT1 expression or impairments of FOXO1-C/EBPα transcription complex formation; contribute to the reduced adiponectin gene expression in T2DM and obesity [Qiao L., *et al*., 2006]. Furthermore, studies on differentiated 3T3-L1 adipocyte cells revealed a few obligatory attestations such as overexpression or knocking down of endogenous SIRT1 resulting in increased or decreased adiponectin gene expression respectively. Triglycerides are usually stored in adipose tissue, hence during starving conditions triglycerides from adipose tissue are mobilized to give free fatty acids, which later undergo b-oxidation and deliver energy. SIRT1 is also believed to suppress adipocyte differentiation and triglyceride accumulation in adipose tissue by suppressing the action of PPARγ (**Fig.2.6**). SIRT1 deacetylates and activates the LXR (liver X receptor), ABCA1 (ATP binding cassette transporter A1) and SREBP-1c. LXR enhances the cholesterol transport from peripheral tissue to blood through the expression of ABCA1 and later it mediates conversion of cholesterol to HDL (high density lipoprotein). The importance of SIRT1 was studied in liver knockout mice, which showed a significant decrease in the HDL cholesterol levels in both CR and HFD fed animals [Li X., *et al*., 2007]. When HFD fed mice

were treated with resveratrol and SRT1720 (agonist of SIRT1), they improved the physiology and metabolic function by reduction of lipogenesis. In addition to that, moderate overexpression of SIRT1 in whole body under the control of promoter resulted in complete protection of hepatic steatosis. It was also known that AMPK plays an important role in inhibiting the hepatic lipogenesis, and cholesterol synthesis by phosphorylation and inactivation of SREBP-1, fatty acid synthase and HMGR (hydroxymethylglutaryl-CoA reductase). As both AMPK and SIRT1 inhibit lipogenesis by targeting same proteins, it might be considered that they are components of the same pathway. Therefore, we can suggest that SIRT1 regulation in adipose tissue differentiation is a promising path for the optimization of treatment for T2DM and obesity.

2.8 Small molecule modulators of SIRT1:

The biological functions of SIRT1 have triggered interest in the development of SIRT1 activators and inhibitors. Sirtuin enzymes catalyze NAD^+ dependent protein/histone deacetylation, where the acetyl group from the lysine epsilon-amino group is transferred to the ADP-ribose moiety of NAD^+, producing nicotinamide and the novel metabolite O-acetyl-ADP-ribose. Soon enough it was shown that physiological concentrations of nicotinamide noncompetitively inhibit both SIR2 and SIRT1 in vitro. Furthermore, the degree of inhibition by nicotinamide ($IC_{50} < 50$ μM) was shown to be equal to or better than the most effective known synthetic inhibitors of this class of proteins. It was proposed that nicotinamide inhibits deacetylation by binding to a conserved pocket adjacent to NAD^+, thereby blocking NAD^+ hydrolysis [Bitterman K.J., *et al*., 2002]. Recently, it was demonstrated that nicotinamide inhibition is the result of nicotinamide intercepting an ADP-ribosyl-enzyme-acetyl peptide intermediate with regeneration of NAD^+ (transglycosidation) [Jackson M.D., *et al*., 2003].

Several small molecule inhibitors (**Fig.2.8**) of SIRT1 like EX-527 analogues [Napper A.D., *et al*., 2005], Splitomicin analogues [Bedalov A., *et al*., 2001; Posakony J., *et al*., 2004], Sirtinol analogue [Mai A., *et al*., 2005], Cambinol [Heltweg B., *et al*., 2006], 2-Anilinobenzamides [Suzuki T., *et al*., 2006], Aristoforin [Gey C., *et al*., 2007], Nicotinamide [Peck B., *et al*., 2010], ILS-JGB-1741 [Kalle A.M., *et al*., 2010], Aurone derivatives [Manjulatha K., *et al*., 2012] were reported for treatment of various cancers. SEN0014196 or EX-527 is an investigational drug not yet approved by the FDA. It is a SIRT1 Inhibitor, which is being studied as a potential treatment for Huntington's disease entered into phase 1b clinical trials to assess the safety, tolerability, and fed/fasted pharmacokinetics of repeated oral doses [ClinicalTrials.gov: ID NCT01485965].
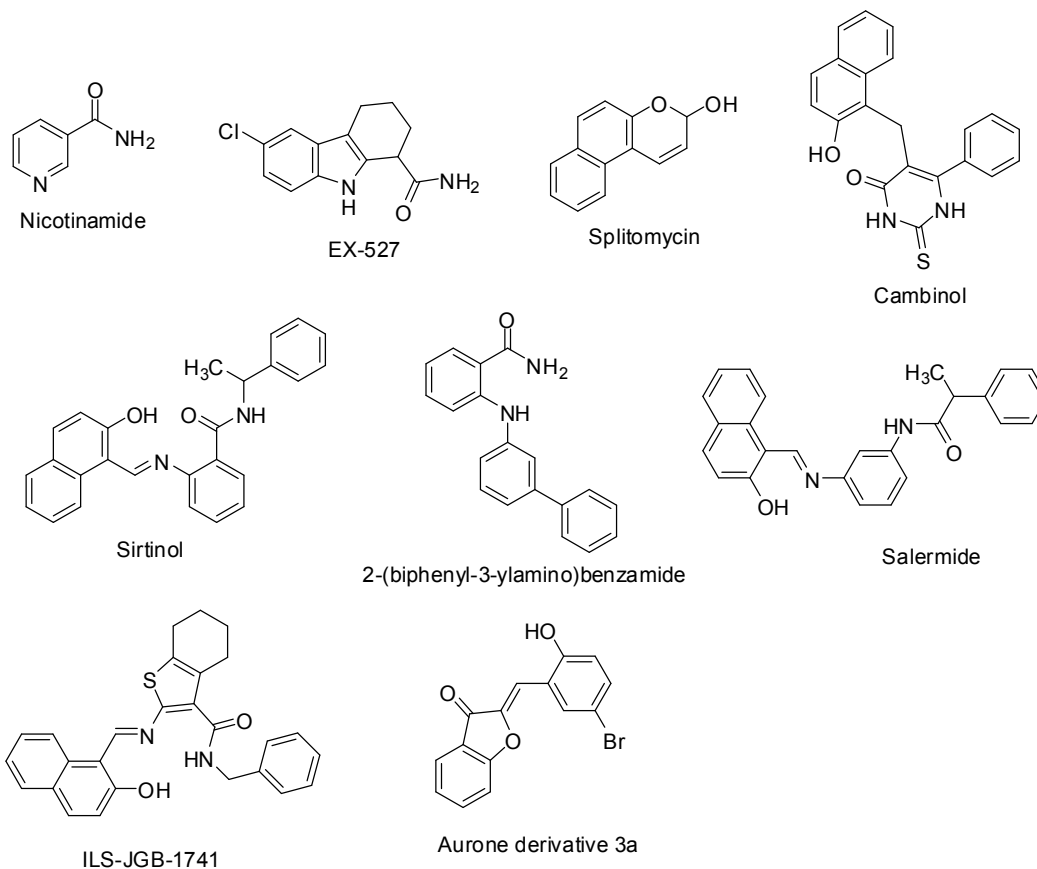
Fig.2.8: Known Small molecule inhibitors of SIRT1

Besides, Sirtris pharmaceuticals (now owned by GSK) and various other groups are competitively working on the development of small molecule SIRT1 activators. Majority of patents still disclose structures that are analogs of resveratrol and various plant polyphenols including butein, pinosylvin, fisetin, piceatannol and quercetin shown in **Fig.2.9**.
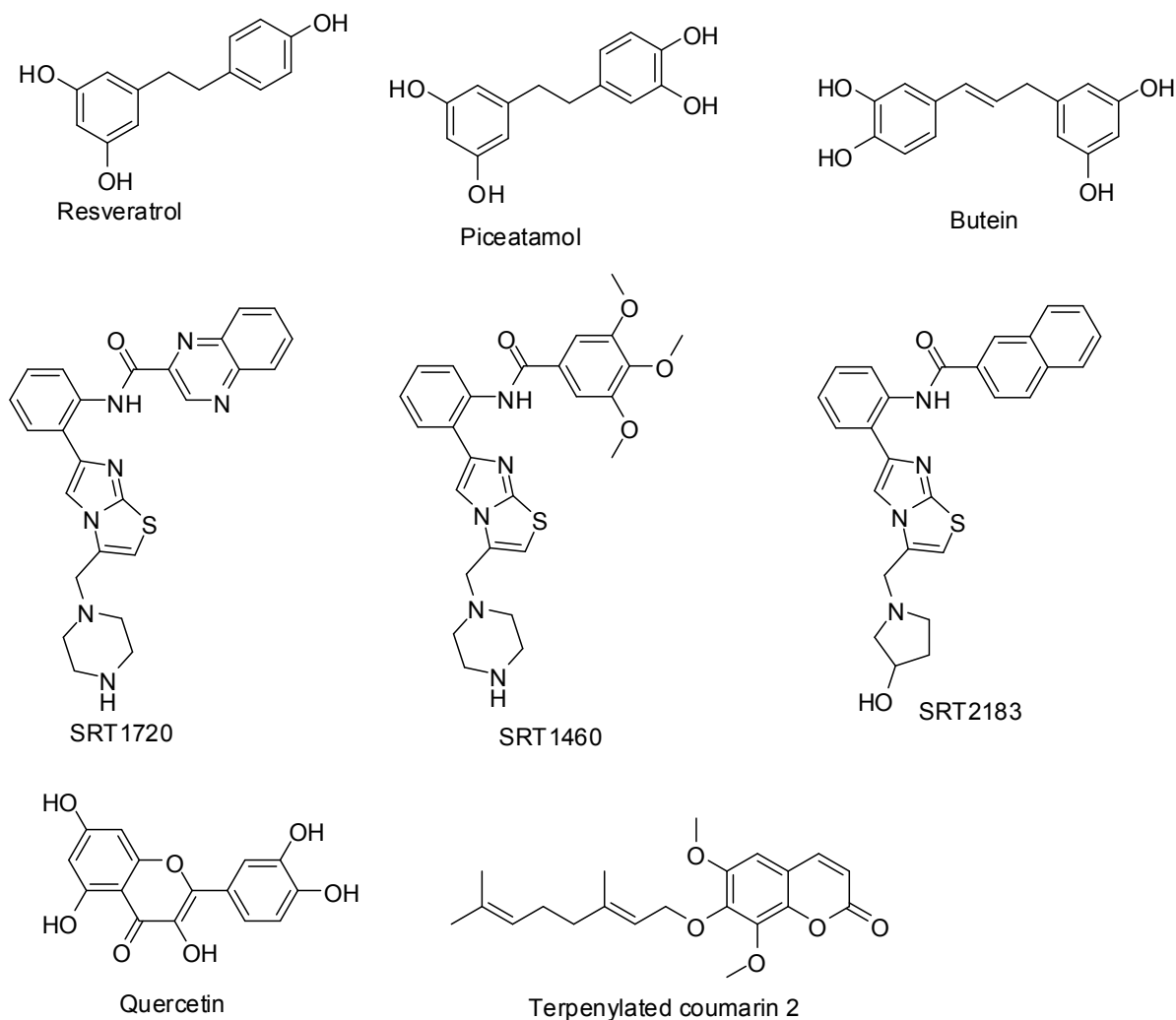
Fig.2.9: Known small molecule activators of SIRT1

Moreover, many upcoming companies are working and had filed so many patents but none of them got issued. Recently a number of Sirtris compounds, includingSRT1720, SRT2183 and SRT1460 were reported asSIRT1 activators but later Pacholec *et al*.,[Pacholec M.,*et al*.,

2010] demonstrated that these molecules interact with fluorophore of P53 substrate instead of direct activation of SIRT1. A major effort is focused on developing SIRT1 activators either from natural and synthetic resources. Recently, resveratrol from grape wine fruit has been identified as the most potent SIRT1 activator [Wood J.G., *et al*., 2004] but had poor bioavailability and fast metabolism, and its direct effect on the SIRT1enzyme is controversial [Guerrero R.F., *et al*., 2009]. Some patents disclose other commercially available SIRT1 activators like camptothecin but these are less potent compared to resveratrol. Resveratrol and other polyphenols contain various promiscuous activities along with SIRT1 activation, including antioxidant functionality but display poor pharmaceutical properties and thus have limited potential as drug candidates [Pillarisetti S., 2008]. Based on the structure of nicotinamide, Mai *et al*., prepared a series of 1, 4 dihydropyridine and their off-target activities were not reported [Mai A., *et al*., 2009].

Recently Sirtris pharmaceuticals had launched SRT501, an oral formulation of resveratrol, for the potential treatment of diabetes and obesity (currently in Phase II clinical trials). Furthermore, compoundsSRT-1460, SRT-1720 and SRT-2183 were identified by Sirtris as SIRT1 activators for the potential treatment of diabetes, aging and cancer. Blum *et al*. in his recent review clearly explained the various chemical classes of SIRT1 activators [Blum C.A., *et al*., 2011]. However, due to limited effect on human health span, SRT-1720 was withdrawn from clinical trials and thus promoted another candidate from the same series, SRT-2104 which was more suitable for human consumption and now it successfully completed Phase II clinical trials [ClinicalTrials.gov: ID NCT01018017] . In 2010, Boston University had performed a pilot study on SRT501 for the endothelial function in subjects with T2DM [ClinicalTrials.gov: ID NCT01038089]. Kaleida Health, recently recruited SRT501 for the treatment of T2DM and obesity into Phase III clinical trials after successful completion of Phase II trials

[ClinicalTrials.gov: ID NCT01158417]. Also University of Aarhus had recruited oral resveratrol formulation (SRT501) for investigation of potential metabolic effects in men with metabolic syndrome [ClinicalTrials.gov: ID NCT014112645]. SRT2379 has completed Phase I trials by Glaxo SmithKline [ClinicalTrials.gov: ID NCT01018628]. Furthermore, computer assisted drug designing of activators based on the structure of the protein is still ambiguous due to the lack of 3D crystal structure information of full length SIRT. Sugunadevi *et al.* in 2009 reported a four featured ligand based pharmacophore model for SIRT1 activators based on resveratrol, SRT1720, SRT2183, and SRT1460. In 2009 Autiero *et al.*, explained His 363, Asn 346, Ser 265, Gly 261 and Pro447 residues are to be important for catalytic role activity of SIRT1 [Autiero I., *et al.*, 2009].

CHAPTER 3

OBJECTIVES
AND
PLAN OF WORK

CHAPTER 3
OBJECTIVES AND PLAN OF WORK

3.1 Objectives:

As previously mentioned, cancer, obesity are major health problems affecting the global population both in developed and developing countries. The crucial role of SIRT1 in the regulation of the many cellular metabolisms including gene silencing, regulation of p53, cell cycle regulation, life span extension, lipid and glucose metabolism has indicated SIRT1 as potential targets for treating cancer and the metabolic disorders.

After thorough review of the literature, design of small molecule modulators (inhibitors/activators) of human SIRT1 considered as prime importance hence the below mentioned strategy has been followed.

I.   To discover new SIRT1 inhibitors and activators by

   A. Development of homology model of SIRT1 (catalytic and allosteric domain).

   B. High throughput virtual screening of *in house* database (~3000 molecules) against catalytic and allosteric domain of SIRT1.

II.   Synthesis of various analogues of SIRT1 inhibitors and activators based on virtual screening.

III. *In vitro* screening of synthesized molecules for SIRT1 modulation.

IV.   *In vitro* cell lines studies for anticancer and anti adipogenesis activity.

V.   *In vivo* pharmacological studies on disease induced animal models.

3.2 Plan of Work:

The plan of work was classified into the following categories

3.2.1 Development of homology model of hSIRT1:

```
┌─────────────────────────────────┐   ┌─────────────────────────────────┐
│  Catalytic domain (244-498)      │   │   Allosteric site (114-217)      │
└─────────────────────────────────┘   └─────────────────────────────────┘
                        ↓           ↓
                   ┌──────────────────┐
                   │     Blast P       │
                   └──────────────────┘
                             ↓
        ┌──────────────────────────────────────────────┐
        │ Selection of top hits based on identity and similarity │
        └──────────────────────────────────────────────┘
                             ↓
             ┌──────────────────────────────────┐
             │ Sequence alignment by using Clustal W │
             └──────────────────────────────────┘
                             ↓
          ┌──────────────────────────────────────┐
          │ Development of homology model using PRIME │
          └──────────────────────────────────────┘
                             ↓
        ┌──────────────────────────────────────────┐
        │ Validation of model by PROCHECK and PROSA │
        └──────────────────────────────────────────┘
                             ↓
     ┌────────────────────────────────────────────────┐
     │ Minimization of model to get lowest energy confirmation │
     └────────────────────────────────────────────────┘
                             ↓
 ┌────────────────────────────────────────────────────────────┐
 │ Validation of active site pocket using known inhibitors like  │
 │ sirtinol, suramin, Ex-527 and activator site by resveratrol,  │
 │ SRT1720, etc.                                                  │
 └────────────────────────────────────────────────────────────┘
                             ↓
      ┌────────────────────────────────────────────┐
      │ High throughput Virtual screening of In-house database │
      └────────────────────────────────────────────┘
                             ↓
                   ┌──────────────────┐
                   │    SP Docking     │
                   └──────────────────┘
                             ↓
                   ┌──────────────────┐
                   │    XP Docking     │
                   └──────────────────┘
                             ↓
  ┌──────────────────────────────────────────────────────────┐
  │ Selection of molecules based on Docking score, Hbond, Binding pattern │
  └──────────────────────────────────────────────────────────┘
```

3.2.2 Synthesis of various analogues.

3.2.3 *In vitro* SIRT1 assay using cayman direct fluorescent SIRT1 kit.

3.2.4 *In vitro* cytotoxicity studies on various cell lines like K562, MDA-MB231, PC3, LNCaP, 3T3-L1 and HEK293 cells.

3.2.5 Measurement of gene and protein levels of SIRT1 as well as various key regulators of cancer and metabolic disorders using RT-PCR and western blot analysis.

3.2.6 *In vivo* cancer and obesity studies.

CHAPTER 4

MATERIALS

AND

METHODS

CHAPTER 4
MATERIALS AND METHODS

4.1 Design of homology model of catalytic domain (244-498AA) and allosteric domain of human SIRT1 (114-217AA):

The three-dimensional model of catalytic site of human SIRT1 (Uniprot code: Q96EB6, region 244–498) was developed by comparative modeling strategy using the template structures of human SIRT2 (PDB code: 1J8F chain A) [Finnin M.S., *et al*., 2001], human SIRT5 (PDB code: 2NYR chain A) [Schuetz A., *et al*., 2007], human SIRT6 (PDB code: 3PKI chain A) [Pan P.W., *et al*., 2011] and human SIRT3 with acetyl-lysine AceCS2 peptide (PDB code: 3GLR chain A) [Jin L., *et al*., 2009] because the percentage of sequence identity between these proteins and human SIRT1 was equal to 46%, 28%, 23% and 41% respectively. Protein sequences were aligned with CLUSTALW 2.1 program [Thompson J.D., *et al*., 1994]. The PRIME program (Version 2.2.108) of Schrödinger suite 2010 was used to build consensus model [Jacobson M.P., *et al*., 2004] of catalytic site, we used the ProSA-web program to check the fitness of the sequences relative to the obtained structures and to assign a scoring function, and the PROCHECK program [Laskowski R.A., *et al*., 1993] to evaluate their stereo chemical and structural packing quality. Final model was minimized in order to get lowest energy confirmation using OPLS 2005 minimization program of Schrödinger. Possible active site pocket was identified by SITEMAP program (Version 2.4.109) of Schrödinger suite 2010 [Halgren T.A., *et al*., 2009]. Moreover, the three-dimensional model of allosteric site of human SIRT1 region 114-217 was performed using the template structure of a hexokinase from SulfolobusTokodaii by comparative modeling (PDB code: 2E2N) [Nishimasu H., *et al*., 2007]. As the sequence identity

between this SIRT1 region and the homologous template model was lower than 30% (i.e. 26%) we used a procedure strategy in agreement with the rules recently reviewed to improve the quality of the modeling results at low target-template sequence similarity [Dalton J.A., *et al*., 2007]. Active site pocket was identified by SITEMAP program and the known activators like resveratrol, SRT1720, SRT1284 etc were used to validate the active site pocket by considering the important amino acids reported by Sharma *et al*., group recently [Sharma A., *et al*., 2012].

Sequence of full length SIRT1:

>sp|Q96EB6|2-747

ADEAALALQPGGSPSAAGADREAASSPAGEPLRKRPRRDGPGLERSPGEPGGAAPEREV

PAAARGCPGAAAAALWREAEAEAAAAGGEQEAQATAAAGEGDNGPGLQGPSREPPLA

DNLYDEDDDDEGEEEEEAAAAAIGYRDNLLFGDEIITNGFHSCESDEEDRASHASSSDW

TPRPRIGPYTFVQQHLMIGTDPRTILKDLLPETIPPPELDDMTLWQIVINILSEPPKRKKRK

DINTIEDAVKLLQECKKIIVLTGAGVSVSCGIPDFRSRDGIYARLAVDFPDLPDPQAMFDI

EYFRKDPRPFFKFAKEIYPGQFQPSLCHKFIALSDKEGKLLRNYTQNIDTLEQVAGIQRIIQ

CHGSFATASCLICKYKVDCEAVRGDIFNQVVPRCPRCPADEPLAIMKPEIVFFGENLPEQ

FHRAMKYDKDEVDLLIVIGSSLKVRPVALIPSSIPHEVPQILINREPLPHLHFDVELLGDCD

VIINELCHRLGGEYAKLCCNPVKLSEITEKPPRTQKELAYLSELPPTPLHVSEDSSSPERTS

PPDSSVIVTLLDQAAKSNDDLDVSESKGCMEEKPQEVQTSRNVESIAEQMENPDLKNVG

SSTGEKNERTSVAGTVRKCWPNRVAKEQISRRLDGNQYLFLPPNRYIFHGAEVYSDSED

DVLSSSSCGSNSDSGTCQSPSLEEPMEDESEIE.

Sequence of allosteric site of SIRT1 (114-217AA):

PPLADNLYDEDDDDEGEEEEEAAAAAIGYRDNLLFGDEIITNGFHSCESDEEDRASHASS

SDWTPRPRIGPYTFVQQHLMIGTDPRTILKDLLPETIPPPELDD.

Sequence of catalytic core of SIRT1 (244-498AA):

EDAVKLLQECKKIIVLTGAGVSVSCGIPDFRSRDGIYARLAVDFPDLPDPQAMFDIEYFR

KDPRPFFKFAKEIYPGQFQPSLCHKFIALSDKEGKLLRNYTQNIDTLEQVAGIQRIIQ

CHGSFATASCLICKYKVDCEAVRGDIFNQVVPRCPRCPADEPLAIMKPEIVFFGENLPEQ

FHRAMKYDKDEVDLLIVIGSSLKVRPVALIPSSIPHEVPQILINREPLPHLHFDVELLGDCD

VIINELCHRLGGEYA.

Multiple sequence alignment of catalytic core

CLUSTAL 2.1 multiple sequence alignment.

```
1J8F_A|SIRT2      -GEADMDFLRNLFSQTLSLGSQKERLLDELTLEGVARYMQSERCRRVICL
3GLR_A|SIRT3      --------------------SNASDKGKLSLQDVAELIRARACQRVVVM
244-498|SIRT1     -------------------------------EDAVKLLQ--ECKKIIVL
2B4Y_A|SIRT5      ------------------------GSARPSSSMADFRKFFAKAKHIVII
3PKI_A|SIRT6      GSVNYAAGLSPYADKGKCGLPEIFDPPEELERKVWELARLVWQSSSVVFH
                                                  .              .  ::
1J8F_A|SIRT2      VGAGISTSAGIPDFRS-PSTGLYDNLEKYHLPYPEAIFEISYFKKHPEPF
3GLR_A|SIRT3      VGAGISTPSGIPDFRS-PGSGLYSNLQQYDLPYPEAIFELPFFFHNPKPF
244-498|SIRT1     TGAGVSVSCGIPDFRSRDGIYARLAVDFPDLPDPQAMFDIEYFRKDPRPF
2B4Y_A|SIRT5      SGAGVSAESGVPTFRG--AGGYWRKWQAQDLATPLAFAHNPSRVWEFYHY
3PKI_A|SIRT6      TGAGISTASGIPDFRG--PHGVWTMEERGLAPKFDTTFESAR-------
                    ***:*. .*:* **.                :      :    .
1J8F_A|SIRT2      FALAKELYPGQFKPTICHYFMRLLKDKGLLLRCYTQNIDTLERIAGLEQE
3GLR_A|SIRT3      FTLAKELYPGNYKPNVTHYFLRLLHDKGLLLRLYTQNIDGLERVSGIPAS
244-498|SIRT1     FKFAKEIYPGQFQPSLCHKFIALSDKEGKLLRNYTQNIDTLEQVAGIQR-
2B4Y_A|SIRT5      RREVMGSKEPNAGHRAIAECETRLGKQGRRVVVITQNIDELHRKAGTKN-
3PKI_A|SIRT6      ------------PTQTHMALVQLERVGLLRFLVSQNVDGLHVRSGFPRD
                              *       :**:* *.   :*
1J8F_A|SIRT2      DLVEAHGTFYTSHCVSASCRHEYPLSWMKEKIFSEVTP-----------
3GLR_A|SIRT3      KLVEAHGTFASATCT--VCQRPFPGEDIRADVMADRVP-----------
244-498|SIRT1     -IIQCHGSFATASCL--ICKYKVDCEAVRGDIFNQVVP-----------
2B4Y_A|SIRT5      -LLEIHGSLFKTRCTSCGVVAENYKSPICPALSGKGAPEPGTQDASIPVE
3PKI_A|SIRT6      KLAELHGNMFVEECA--KCKTQYVRDTVVGTMGLKATG----------R
                   :  : **.:     *       .  :    :  .
1J8F_A|SIRT2      KCEDCQS--------LVKPDIVFFGESLPARFFSCMQSDFLKVDLLLVMG
3GLR_A|SIRT3      RCPVCTG--------VVKPDIVFFGEPLPQRFL-LHVVDFPMADLLLILG
|244-498|SIRT1    RCPRCPAD---EPLAIMKPEIVFFGENLPEQFHRAMKYDKDEVDLLIVIG
2B4Y_A|SIRT5      KLPRCEEA---GCGGLLRPHVVWFGENLDPAILEEVDRELAHCDLCLVVG
3PKI_A|SIRT6      LCTVAKARGLRACRGELRDTILDWEDSLPDRDLALADEASRNADLSITLG
                    .              ::   :: : : *          ** : :*
1J8F_A|SIRT2      TSLQVQPFASLISKAPLS-TPRLLINKEKAGQSDPFLGMIMGLGGGMDFD
3GLR_A|SIRT3      TSLEVEPFASLTEAVRSS-VPRLLINRDLVG--------------PLA
244-498|SIRT1     SSLKVRPVALIPSSIPHE-VPQILINREPLP------------------
2B4Y_A|SIRT5      TSSVVYPAAMFAPQVAARGVPVAEFNTETTP------------------
3PKI_A|SIRT6      TSLQIRPSGNLPLATKRRGGRLVIVNLQPTK------------------
                  :*   : * . :            .* :
1J8F_A|SIRT2      SKKAYRDVAWLGECDQGCLALAELLGWKKELEDLVRREHASIDAQS----
3GLR_A|SIRT3      WHPRSRDVAQLGDVVHGVESLVELLGWTEEMRDLVQRETGKLDGPDK---
244-498|SIRT1     --HLHFDVELLGDCDVIINELCHRLGGEYA-------------------
2B4Y_A|SIRT5      -ATNRFRFHFQGPCGTTLPEALA-------------------------
3PKI_A|SIRT6      -HDRHADLRIHGYVDEVMTRLMEHLGLEIPAWDGPRVLERALPPLPRPPT
                       .  *
1J8F_A|SIRT2      -------------------------------------------------
3GLR_A|SIRT3      -------------------------------------------------
244-498|SIRT1     -------------------------------------------------
2B4Y_A|SIRT5      -------------------------------------------------
3PKI_A|SIRT6      PKLEPKEESPTRINGSIPAGPKQEPCAQHNGSEPASPKRERPTSPAPHRP

1J8F_A|SIRT2      -----------
3GLR_A|SIRT3      -----------
244-498|SIRT1     -----------
2B4Y_A|SIRT5      -----------
3PKI_A|SIRT6      PKRVKAKAVPS
```

Phylogenetic tree:

```
                                    ┌── 1J8F_A|SIRT2_46%: 0.10500
                         ┌──────────┤
                         │          └── 3GLR_A|: 0.09500  41%
          ┌──────────────┤
          │              │          ┌──── 2NYR_A|SIRT5_28%: 0.13750
──────────┤              └──────────┤
          │                         └──── 3PKI_A|: 0.14250
          └──────────────────────────── sp: 0.13250
```

Sequence alignment of allosteric site: CLUSTAL 2.1 multiple sequence alignment

```
SIRT1_114-217        -------PPLADNLYDEDDDDEGEEEEEAAAAAIGYRDN-LLFGDEIITNGFHSCESDEE
2E2N_A               MMIIVGVDAGGTKTKAVAYDCEGNFIGEGSSGPGNYHNVGLTRAIENIKEAVKIAAKGEA
Q86WX3|1-136_AROS    MSAALLRRGLELLAASEAPRDPPGQAKPRGAPVKRPRKTKAIQAQKLRNSAKGKVPKSAL
                                           .:       :.      . :  ...       ..

SIRT1_114-217_       DRASHASS-----SDWT---PRPRIGPYTFVQQH--------------------------
2E2N_A               DVVGMGVAGLDSKFDWENFTPLASLIAPKVIIQHDGVIALFAETLGEPGVVVIAGTGSVV
Q86WX3|1-136_AROS    DEYRKRECRDHLRVNLKFLTRTRSTVAESVSQQI--------------------------
                     *       .     :        . .. *

SIRT1_114-217        ----------------------------------LMIGTDPRTILKDLLPETIPPPE
2E2N_A               EGYNGKEFLRVGGRGWLLSDDGSAYWVGRKALRKVLKMMDGLENKTILYNKVLKTINVKD
Q86WX3|1-136_AROS    ---------------------------------LRQNRGRKACDRPVAKTKKKKA
                                                     :        :.      : :*

SIRT1_114-217        LDD---------------------------------------------------------
2E2N_A               LDELVMWSYTSSCQIDLVASIAKAVDEAANEGDTVAMDILKQGAELLASQAVYLARKIGT
Q86WX3|1-136_AROS    EGTVFTEEDFQKFQQEYFGS----------------------------------------
                       .

SIRT1_114-217        ------------------------------------------------------------
2E2N_A               NKVYLKGGMFRSNIYHKFFTLYLEKEGIISDLGKRSPEIGAVILAYKEVGCDIKKLISD
Q86WX3|1-136_AROS    ------------------------------------------------------------
```
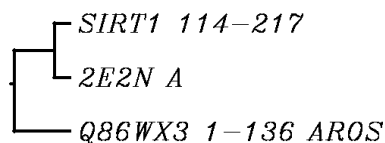
Phylogenetic tree:

```
        ┌─── SIRT1 114-217
   ┌────┤
.  │    └── 2E2N A
   └──────── Q86WX3 1-136 AROS
```

4.2 High-throughput virtual screening:

In search of new scaffold as SIRT1 modulators in treatment of cancer and metabolic disorders, a high throughput virtual screening of~3000 molecules of *in house* database was carried into catalytic domain and allosteric domain of SIRT1 separately. The multi-step Schrödinger's Protein preparation tool (PPrep) has been used for final preparation of homology

models. Hydrogens were added to the model automatically *via* the Maestro interface. The obtained model was minimized using the OPLS 2005 force field to RMSD of $0.3A^{0.}$ The receptor grid (coordinates for catalytic domain were X: 12.91; Y: 27.76; Z: 33.29 and for allosteric site were X: 39.82; Y: 36.31; Z: 28.54) was generated by using receptor grid generation tool of Schrödinger package. All 3000 *in house* molecules were sketched by using Schrödinger's software tools and converted to their 3D representations. LigPrep program (Version 2.4.107) of Schrödinger suite 2010 was used for final preparation of ligand's for docking. High throughput virtual screening was performed followed by SP and XP docking using GLIDE (Version 5.6.109) of Schrödinger suite 2010. Compounds were selected based on docking score, Hbond, interaction pattern.

Chemistry:

All commercially available chemicals and solvents were used without further purification. TLC experiments were performed on alumina backed silica gel 40 F254 plates (Merck, Darmstadt, Germany). Melting points were determined using (Buchi BM530) in open capillary tubes and are uncorrected. Elemental analyses (C, H, and N) were carried out on an automatic Flash EA1112 series, CHN analyzer 9 (Thermo). All ^{1}H and ^{13}C NMR spectra were recorded on a Bruker AM300 (300.12 MHz, 75.12 MHz), Bruker Bio Spin corp., Germany. Molecular weights of unknown compounds were checked by LC-MS 6100B series (Agilent Technologies). Chemical shifts are expressed in δ (ppm) relative to tetramethylsilane (TMS) as an internal reference standard. The signals are designated as follows: s, singlet; d, doublet; dd, doublet of doublets; t, triplet; m, multiplet.

4.3 SYNTHETIC SCHEME
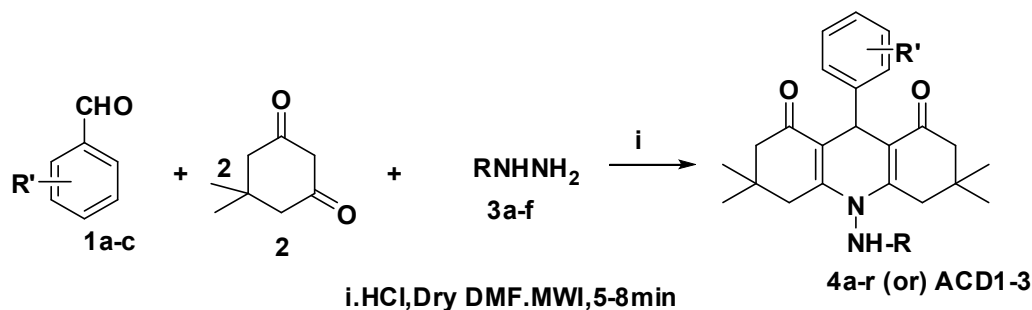
4.3.1 Acridinedione derivatives (ACD):

Fig. 4.1: Synthetic protocol for Acridinedione (ACD) Derivatives

4.3.2 Benzthiazolyl-2-thiosemicarbazone derivatives (B2TS):

a: AcOH/KSCN/Br$_2$/0°C to RT; b: CS$_2$/0-15°C/EtOH/KOH; c:$_2$HN-NH$_2$/EtOH/reflux

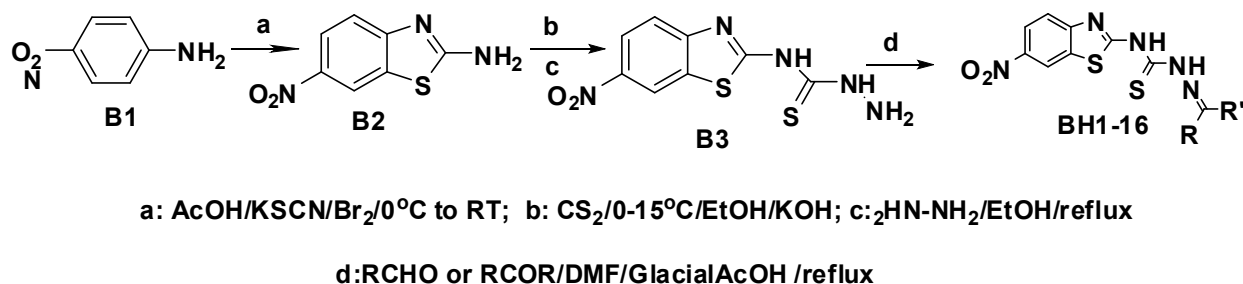**d:RCHO or RCOR/DMF/GlacialAcOH /reflux**

Fig. 4.2: Synthetic protocol for Benzthiazolyl-2-thiosemicarbazone (B2TS) derivatives

4.3.3: Spiro-piperidin-4-one derivatives (SP):

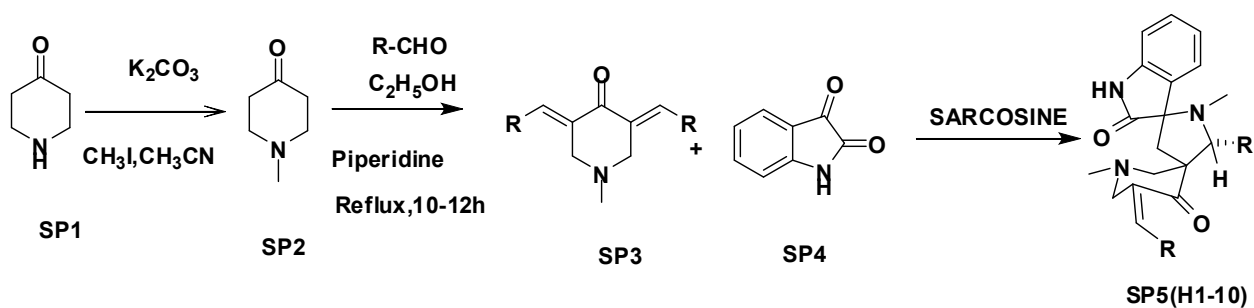**Fig. 4.3:** Synthetic protocol for Spiro-piperidin-4-one (SP) derivatives.
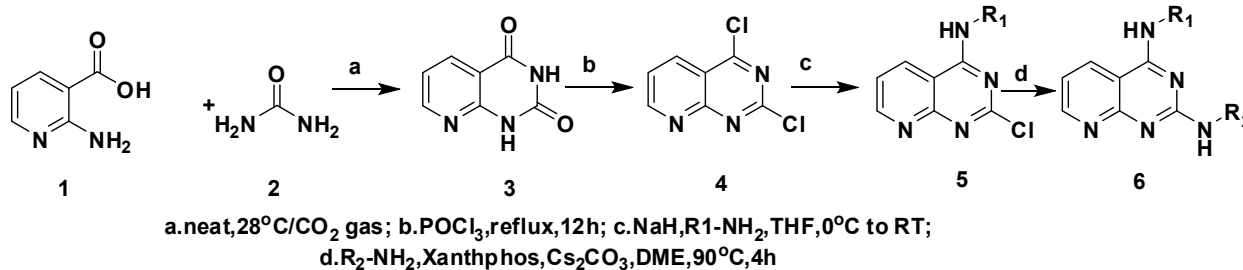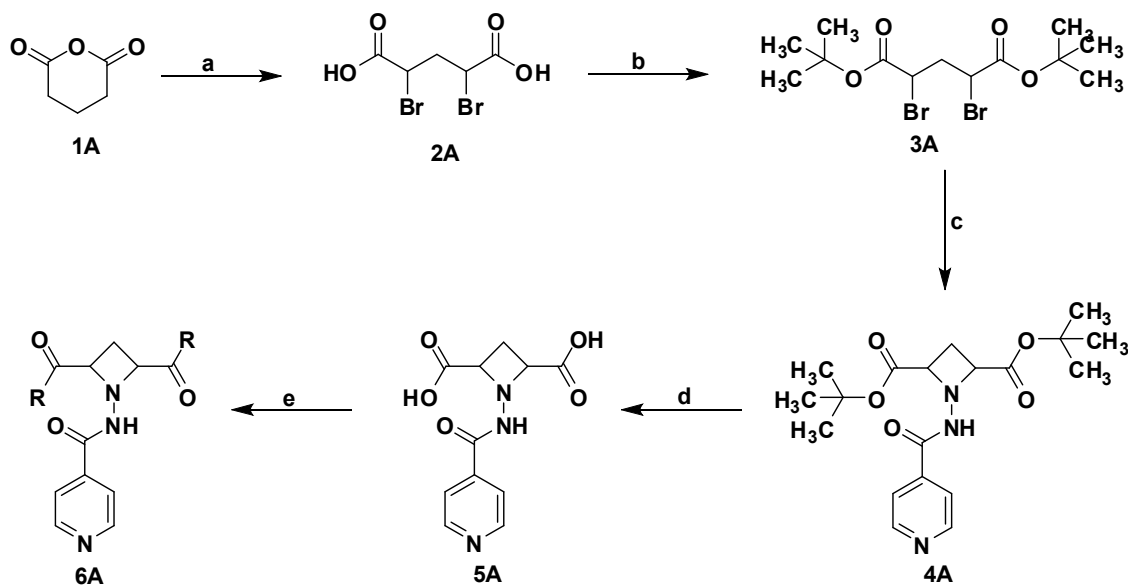
4.3.4: Pyrido pyrimidine series (PP):

a.neat,28°C/CO$_2$ gas; b.POCl$_3$,reflux,12h; c.NaH,R1-NH$_2$,THF,0°C to RT;
d.R$_2$-NH$_2$,Xanthphos,Cs$_2$CO$_3$,DME,90°C,4h

Fig.4.4: Synthetic scheme for pyridopyrimidine (PP) series.

4.3.5: 1-(Isonicotinamido) azetidine-2,4-dicarboxamides series (AZD):

a. Br$_2$/ HCOOH; b. Isobutylene, H$^+$, RT; c.Isoniazid, DMF, 80°C; d. TFA, DCM, RT; e.R-NH$_2$, EDC.HCl, HOBT, TEA, DCM,RT.

Fig. 4.5: Synthetic protocol for Azetidine (AZD) derivatives.

4.4 *In vitro* SIRT1 enzymatic assay:

In vitro SIRT1 assay was based on unique SIRT1 substrate/developer combination. The substrate usually consists of 4 amino acids from 379-382 [(Arg-His-Lys-Lys (Ac)] of human p53, which was tagged with aminomethylcoumarin (AMC). The fluorescence intensity of released AMC from substrate upon addition of developer solution is proportional to the amount of lysine deacetylation in the substrate. The results of virtual screening were validated by *in vitro*

screening of the test compounds against hSIRT1 activity using SIRT1 direct fluorescent screening assay kit by Cayman Chemical Company, USA according to the manufacturer's protocol. Briefly all the compounds were dissolved in DMSO and incubated with enzyme and deacetylation reaction was initiated by addition of 125μM peptide and 3mM NAD$^+$. Reaction was stopped by addition of nicotinamide and deacetylation was measured by recording the fluorescence at 355nm excitation and 460nm emission in Perkin Elmer victor^{TM}3 Multiplate reader.

The fluorescence intensity was calculated by using following formula.

$$\text{Fluorescence intensity} = 100 * \frac{(\text{Sample fluorescence} - \text{Blank fluorescence})}{(\text{Enzyme control fluorescence} - \text{Blank fluorescence})}.$$

Blank consists of all reaction components except the enzyme and enzyme control contains all reaction components except the test compound. Additionally, test compound control also included in order to avoid interference of auto fluorescence. Compounds with a relative percentage less than or equal to 50 were considered as inhibitors and relative percentage over or equal to 150 were considered as SIRT1 activators [Nayagam V.M., *et al*., 2006].

4.5 Detection of acetylated/deacetylated substrate by RP-HPLC:

The SIRT1 reaction (50μl) was carried out with substrate [Arg-His-Lys-Lys (Ac)] under following standard SIRT1 reaction conditions for molecules confirmed as activators from *in vitro* assay: SIRT1 enzyme incubated with activator molecules dissolved in DMSO at desired concentration in assay buffer containing 50 mM Tris/Cl, pH 8.0, 137 mM NaCl, 2.7 mM KCl, 1 mMMgCl2, 1 mg/ml BSA. Reaction was initiated by addition 125 μM substrate and 3mM NAD$^+$. Deacetylation of substrate peak was measured at time points of 0, 15, 30 min at 214nm by using RP-HPLC of Shimadzu class LC-20AD HPLC system, composed by a binary pump,

100 µl injection loop, Photo Diode Array (PDA) detector set. The separation of the acetylated and deacetylated peptide product peaks was achieved using a Luna C18, 150* 4.6 mm (551237-39) column with accompanying guard. Mobile phase A was 100% Water with 0.1% trifluoroacetic acid, whereas mobile phase B was 100%Acetonitrile (HPLC grade from Sigma) with 0.1% trifluoroacetic acid. Gradient program used was 0–35% over 15 min followed by rapid ramp up to 100% B to wash and then 100% A to re-equilibrate the column. Flow rate was kept constant at 1.0 ml/min, column temperature was set at 25 °C, and UV detection was set at 214nm [Pacholec M., *et al*., 2010]. The retention times of the deacetylated peptide and acetylated substrate were ~13.8 and ~14.2 min respectively.

4.6 Cell based assays:

Human chronic myeloid leukemia cells, K562, human metastatic breast cancer cells, MDA-MB 231, human androgen dependent prostate cancer cells, LNCaP, human androgen independent prostate cancer cells, PC3, mouse fibroblast cells, 3T3-L1 and human embryonic kidney cells, HEK293 cells were procured from NCCS, Pune, India. Phosphate buffered saline (PBS), RPMI 1640, DMEM (Dulbecco's Modified Eagle Medium), FCS (Fetal calf serum), FBS (Fetal Bovine Serum), Penicillin, Gentamycin and Streptomycin were purchased from Sigma (St.Louis, USA). Insulin, Dexamethasone and IBMX (3-Isobutyl-1-MethylXanthine) were purchased from Sigma-Aldrich. MTT (3-(4, 5-dimethylthiazol-2-yl)-2, 5-diphenyl tetrazolium bromide), Proteinase K, RNase A, PMSF (Phenylmethylsulfonyl fluoride), Leupeptin, Aprotinin, Pepstatin A, Trypsin, Tween-20, Triton X-100, Ponceau S, Sodium orthovanadate, Sodium Bicarbonate, EDTA and Calcium chloride were purchased from Sigma Chemical Company (St.Louis, USA). Low fat milk powder was purchased from E-Merck. Nitrocellulose membranes and Super Signal West Pico Chemiluminescence substrate were procured from

Thermo fisher scientific, USA. X-ray film and development solutions were from Kodak. Acrylamide, N, N'-Methylene-bis-acrylamide, SDS (Sodium Dodecyl Sulfate), Ammonium per sulfate, β-Mercaptoethanol and Bromophenol blue were purchased from Bio-Rad Laboratories (Richmond, USA). Antibodies againstAc-p53K382 from Upstate, Charlottesville, VA, USA and SIRT1 from Millipore, USA were used.

4.6.1 Cell culture and treatment:

Human chronic myeloid leukemia cells, K562, human metastatic breast cancer cells, MDA-MB 231, human androgen dependent prostate cancer cells, LNCaP, human androgen independent prostate cancer cells, PC3 were grown in RPMI 1640 supplemented with 10% heat inactivated FBS, 100 IU/ml penicillin, 100 μg/ml streptomycin and 2 mM L-glutamine. 3T3-L1 fibroblasts were grown in DMEM (High glucose 4.5g) supplemented with 10% FCS and 100 IU/ml penicillin, 100 μg/ml streptomycin and 2 mM L-glutamine. Cultures were maintained in a humidified atmosphere with 5% CO_2 at 37 $^{\circ}$C. The cultured cells were passed twice each week, seeding at a density of $2x10^5$ cells/ml. For treatment exponentially growing cells were collected and resuspended in fresh culture medium.

3T3-L1 fibroblasts were differentiated into adipocytes by supplementing with IBMX, Insulin, Dexamethasone along with DMEM and Fetal Bovine serum for 8 days by changing media every two days. After differentiation, cells were maintained in maintenance media of containing Insulin for another 2 days. Stock solutions of synthesized compounds (10 mM) and Standard drugs like suramin, Resveratrol, Finasteride and doxorubicin (10 mM) in DMSO were prepared and stored at –20°C. The final concentration of DMSO in all the cultures was 0.1%. Cell viability was determined by the trypan blue dye exclusion method**.**

4.6.2 Cell proliferation assay:

Cell proliferation was assessed using the MTT staining as described by Mossman [Mosmann T., 1983]. The MTT assay was based on the reduction of the tetrazolium salt, MTT, by viable cells. The dehydrogenase using NADH or NADPH as coenzyme can convert the yellow form of the MTT salt to insoluble, purple formazan crystals [Liu K.Z., *et al*., 1997]. Formazan solution was read spectrophotometrically after the crystals were dissolved by organic solvent (DMSO). K562, MDAMB231, PC3, LNCaP and HEK 293 cells ($5x10^3$ cells/well) were incubated in 96-well plates in the presence or absence of test compound and/or doxorubicin for 24 h in a final volume of 100 μl. At the end of the treatment, 20 μl of MTT (5 mg/ml in PBS) was added to each well and incubated for an additional 4 hours at 37 ^{o}C. The purple-blue MTT formazan precipitate was dissolved in 100 μl of DMSO. The activity of the mitochondria, reflecting cellular growth and viability, was evaluated by measuring the optical density at 570 nm on a multi-well plate reader. Each concentration was tested in three different experiments run in four replicates. Means and standard deviations were calculated and reported as the percentage of growth vs. control. The viable cells were counted by the trypan blue exclusion assay with a hemocytometer.

4.6.3 Adipocyte Differentiation Assay:

$1*10^5$3T3-L1 cells were cultured to confluence in DMEM supplemented with 10% FCS. At 2 days post-confluence (designated day 0), cells were incubated with test compounds along with differentiation media (DMEM supplemented with 10% FBS, 1 mg/L Insulin, 0.5 mmol/L IBMX and 0.25 μmol/L Dexamethasone) until differentiation observed in control. During this, media has replaced after every two days. After 8days, the media was replaced with DMEM supplemented with 10% FBS and 1 mg/L insulin. After treatment, dishes were washed in PBS,

and the cells were fixed in 10% formaldehyde for 1 h and stained with Oil O Red staining. In order to check the effect of test compounds on mature adipocytes cells were treated with test compounds dissolved in DMSO and cells not treated with received similar volumes of DMSO. After 24 h treatment, dishes were washed in PBS, and the cells were fixed in 10% formaldehyde for 1 h and stained with Oil O Red staining. [Green H.*, et al*., 1975].

Oil O Red staining: Cells after treatment were stained with Oil O red solution (3mg/ml in 3:2 isopropyl alcohol: water) and then fixed with 10% formalin solution, washed with PBS and incubated at room temperature for 30 min. Microscopic pictures were taken. After that oil was eluted in 150µl of DMSO and absorbance was noted at 510nm.

4.6.4 Measurement of Triglycerides:

$1*10^5$ fully differentiated 3T3-L1 adipocytes were seeded into 6 –well plates and treated with test compounds for 24 h and total triglyceride content was measured by using a commercially available assay kit from Euro diagnostics Ltd., according to the manufacturer's instructions. Briefly, after 24h treatment, cells were washed with PBS then scraped into 200 µl PBS and homogenized by sonication for 1 min. The total triglycerides in the lysates were measured using the assay kit at 546nm using spectrophotometer [Buccolo G., *et al*., 1973].

4.6.5 Quantification of apoptosis by flow cytometry (Annexin V assay):

Apoptosis, or programmed cell death, is an important and active regulatory pathway of cell growth and proliferation. Cells respond to specific induction signals by initiating intracellular processes that result in characteristic physiological changes. Annexin V is a calcium dependent phospholipid binding protein with high affinity for phosphatidyl serine (PS), a membrane component normally localized to the internal face of the cell membrane. Early in the apoptotic pathway, molecules of PS are translocated to the outer surface of the cell membrane

where Annexin V conjugated to phycoerythrin can readily bind them. Late stage apoptotic cells show loss of membrane integrity. The membrane impermeant dye 7-AAD was used to distinguish these late stage apoptotic as well as dead cells from early apoptotic cells. Apoptosis starts with cell shrinkage expressed by changes in light - scatter signals. Briefly 0.2×10^6 LNCaPcells/ml were treated with test compounds and incubated for 24h at 37 °C and 5% CO_2. After harvesting, cells were resuspended in 50 µl complete RPMI medium. A volume of 150 µl staining solution (135 µl 1X apoptosis buffer, 10 µl Annexin V-PE and 5 µl of 7-AAD) was then added to each well, incubated in the dark at RT for 20 min and acquired by using Guava EasyCyte system ($1*10^4$ cells counted/sample, flow rate setting medium). The Nexin intensity gates were set to position the live population in the lower left corner of the dot plot. The angles of the gates were then positioned to divide the dot plot into four quadrants. Each quadrant of the dot plot contains a distinct population of cells that was dependent on the presences and intensity of cellular stains per cell [Ravi *et al*., 2011].

4.6.6 *In situ* caspase -3 activation assay*:*

0.5×10^6 LNCaP cells/ml were seeded in a 6 well plate and incubated overnight to form a monolayer. Next day, Growth medium was replaced with serum free media and cells were treated test compounds and incubated for 72h at 37^oC and 5% CO_2. Subsequently cells were trypsinzed, resuspended in 1 ml serum free media and transferred to microfuge tubes to receive 10 µl of freshly prepared FLICA reagent and incubated for 1 hour at 37 ^{0}C and 5% CO_2 away from light. After extensive washes with wash buffer, samples were adjusted to equal number of cells in PBS, 100 µl of each cell suspension transferred to black 96-well plate in duplicates and Fluorescence read at excitation wavelength of 490 nm and emission wavelength of 520 nm in a plate reader [Wang Z., *et al*., 2005].

4.6.7 Preparation of whole cell extracts and immunoblot analysis:

The protocol was based on Sam brook *et al*. (1989). To prepare the whole cell extract, cells were washed with PBS and suspended in a lysis buffer (20 mM Tris, 1 mM EDTA, 150 mM NaCl, 1% NP-40, 0.5% deoxycholic acid, 1 mM β-glycerophosphate, 1 mM sodium orthovanadate, 1 mM PMSF, 10 µg/ml leupeptin,20 µg/ml aprotinin). After 30 min of shaking at 4 ^{0}C, the mixtures were centrifuged (10,000x g) for 10 min, and the supernatants were collected as the whole-cell extracts. The protein content was determined according to the Bradford method [Bradford M.M., 1996]. An equal amount of total cell lysate was resolved on 8-12 % SDS-PAGE gels along with protein molecular weight standards, and then transferred onto Nitrocellulose membranes. The membranes were blocked with 5% w/v nonfat dry milk and then incubated with the primary antibodies (SIRT1, Ac-p53)in 10 ml of antibody-diluted buffer (1X Tris-buffered saline and 0.05% Tween 20 with 5% milk) with gentle shaking at 4 ^{0}C for 8-12 h and then incubated with peroxidase conjugated secondary antibodies. Signals were detected using an ECL Western blotting detection kit.

4.6.8 Reverse Transcriptase-PCR analysis:

1*106 3T3-L1 adipocytes (or) LNCaP cells (or) prostate tissue samples from rat were treated with various concentrations of test compounds for 24h. Total mRNA was isolated by using TRI reagent (Sigma) according to manufacturer's protocol. Reverse transcription of 5 µg of total RNA isolated was achieved by mixing the RNA with 1 µl (1mM) of deoxynucleotides, 1 µl (2.5µM) of random nonamers, 0.25 µl RNase inhibitor (10 U/µl), and 1 µl of AMV reverse transcriptase (1 U/µl) and 2 µl of 10X buffer in a 20 µl reaction volume and followed by incubation at 42 0C for 60 min. cDNA was quantified and equal amount was taken for further analysis. One micro liter of the RT product was taken and PCR was carried out in Bio-Rad

gradient thermo cycler (Bio-Rad). The primer sequences [Kim S., *et al*., 2011] and the annealing temperatures used are given in Table 2. The PCR product was visualized on 1.5-3 % agarose gels under UV light and relative quantification was done by using Image lab analysis software.

Table 2: Primer sequences and conditions used for the RT-PCR analysis. M-Mouse; R-Rat; H-Human.

A = Annealing Temperature, D = Denaturation Temperature, E = Extension Temperature.

Gene	Sense (5'-3')	Size (bp)	A (^{0}C)	D (^{0}C)	E (^{0}C)	No.of cycles
M_SIRT1	FP:AGCAGGTTGCAGGAATCCAA RP:CACGAACAGCTTCACAATCAACTT	101	59	95	72	45
M_E2F1	FP:CCTCGCAGATCGTCATCATC RP: AGAGCAGCACGTCAGAATCG	102	59	95	72	45
M_PPARγ	FP:TTCGGAATCAGCTCTGTGGA RP: CCATTGGGTCAGCTCTTGTG	148	59	95	72	45
M_C/EBPα	FP:TCGGTGCGTCTAAGATGAGG RP: TCAAGGCACATTTTTGCTCC	187	59	95	72	45
M_FAS	FP:TTGCCCGAGTCAGAGAACC RP: CGTCCACAATAGCTTCATAGC	171	59	95	72	45
M_LPL	FP:TGCCGCTGTTTTGTTTTACC RP: TCACAGTTTCTGCTCCCAGC	172	59	95	72	45
M_LEPTIN	FP:CTCCAAGGTTGTCCAGGGTT RP: AAAACTCCCCACAGAATGGG	143	59	95	72	45
M_GAPDH	FP:AGAACATCATCCCTGCATCC RP: TCCACCACCCTGTTGCTGTA	321	59	95	72	45
R_ SIRT1	FP:CAGAGCAT CACACGCAAGC RP: CAGGAAACAG AAACCCCAG	306	52.1	95	72	40
R_ β actin	FP:GAGAGGGAAATCGTGCGTGAC RP: TAGAGCCACCAATCCACACAGAG	421	52.1	95	72	40
H_SIRT1	FP:TAGAGCCTCACATGCAAGCTCTA RP: GCCAATCATAAGATGTTGCTGAAC	88	59	95	72	40
H_PSA	FP:GGCACAACGCACCAGACACTC RP: AGACCCTCCCTCCTTGGCTCA	111	59	95	72	40
H_GapDH	FP:TGAAGCAGGCGTCGGAGGG RP: AAAGGTGGAGGAGTGGGTGTCG	101	59	95	72	40

4.7 *In vivo* Studies:

Animals:

Swiss albino male mice weighing around 17-20g and Male Wistar albino rats weighing 180–220 g were procured from an Institutional animal facility centre for inducing obesity and prostate cancer studies. They were housed individually in clean and transparent polypropylene cages maintained at room temperature with 12-h light/dark cycle and had free access to food and water. After 3 days of acclimatization, they were randomly distributed into experimental groups. The study was reviewed and preapproved by the Institutional Animal Ethics Committee (IAEC), BITS-Pilani, Hyderabad Campus, Hyderabad (IAEC/RES/2/2 on 04-05-2011). "Principles of laboratory animal care" (NIH publication number 85-23, revised 1985) guidelines were followed

4.7.1 Administration and dosage for prostate cancer study:

Animals were divided into five groups of six each. Group I served as control**.** Group II served as a positive control, received only testosterone propionate at 3 mg/kg dose. Group III-V received standard drug Finasteride (5 mg/kg), Compound 1 and 13 (10 mg/kg) suspended in distilled water by using 5% methyl cellulose and administered by I.P route along with testosterone propionate (3 mg/kg) diluted with distilled water using Tween 80 as emulgent and injected subcutaneously daily for 14 days to induce prostatic hyperplasia (PH) [Arruzabala M.L., *et al*., 2006]. Based on the toxicity studies explained in our previous paper [Yogeeswari P., *et al*., 2005] dosing regimen was fixed.

4.7.2 Histopathological investigations:

The dorsolateral and ventral prostate glands were isolated, placed in cassettes, fixed in 10% neutral buffered formalin, dehydrated in a series of alcohol dilutions, fixed in xylene, embedded in paraffin wax, sliced into 3 micron sections. Sections were stained with hematoxylin

and eosin. Furthermore we have monitored prostate, seminal vesicle weights. The sections were evaluated by Dr. Ponnammal, (Pathologist, Madras Medical College) and blinded to the treatment groups for the incidence and degree of pathology within the tissue samples.

4.7.3 Administration and dosage for obesity study:

Animals were divided into two groups, one group receiving normal chew diet and other with high fat diet of 60% Kcal energy. All animals were maintained at HFD for 3 months. Weight gain, glucose levels were measured every 15 days. After 3 months, HFD animals were divided into test and control groups [Ono *et al*., 2006]. Each group contains 6 animals. Test drug suspended in distilled water by using 5% methyl cellulose at concentration of 30mg/kg was administered by oral gavage for one month. Orlistat at 30 mg/kg was used as standard drug and during treatment animal were maintained at HFD. Glucose levels were measured periodically. After one month treatment serum lipid profile was measured by using commercially available kits from Euro Diagnostics Pvt. Ltd.

Table 3: Composition of HFD for 5Kg

Casein-1kg	L-Cysteine - 0.015 kg
Maltodextran - 0.625 kg	Sucrose- 0.334 kg
Cellulose - 0.25 kg	Soya bean oil - 0.125 kg
Tallow - 1.225 kg	Salt mix - 0.175 kg
Vitamin mix - 0.05 kg	Cholinechloride - 0.045 kg

4.8 Statistical analysis:

Data are expressed as mean $\pm$ SEM for experiments in triplicates. Variances in different groups were calculated by one way ANOVA analysis followed by post Dunnet's test using Graphpad Prism 5.0.*$P < 0.05$, **$P < 0.01$, and ***$P < 0.001$.

CHAPTER 5

DESIGN OF
SIRT1 INHIBITORS

CHAPTER 5
DESIGN OF SIRT1 INHIBITORS

5.1 Design, synthesis, biological interventions of acridinedione derivatives (ACD):

5.1.1 Design of a homology model and active site prediction:

Homology model of hSIRT1 catalytic domain was generated by using comparative homology modeling and active site was predicted according to procedure explained under materials and methods section 4.1 and shown in **Fig.5.1.** This model has 83.7% residues in most favored regions and ProSA Web Z score of -6.37. Active site has site score of 0.84 and Dscore (druggable score) of 0.85with hydrophobic score of 1.55 and hydrophilic score of 0.613.
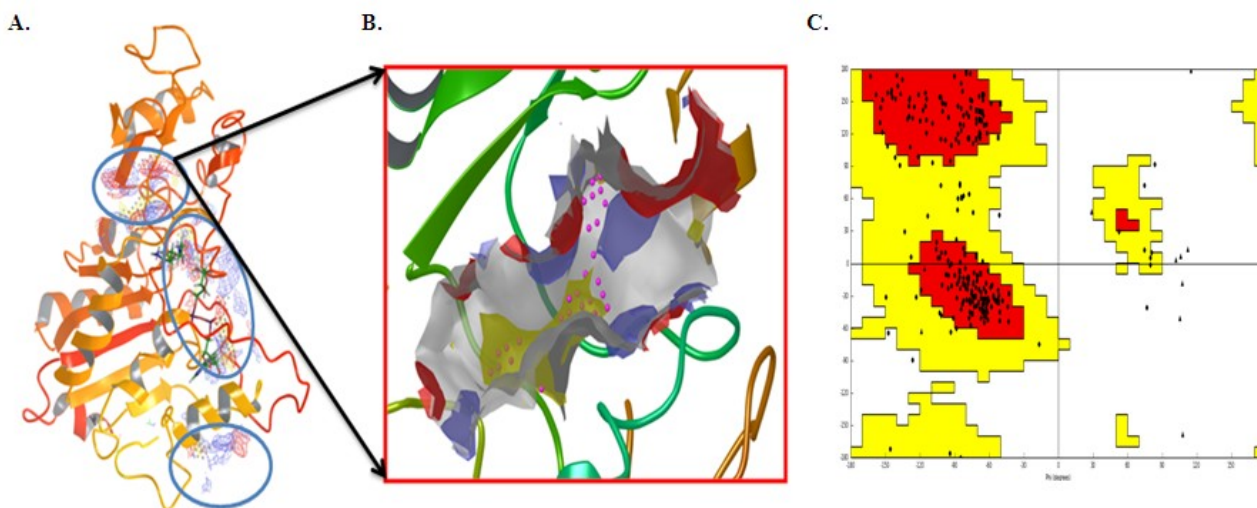
Fig.5.1: A. Homology model of hSIRT1 catalytic domain. Circles denote putative active site pockets. **B.** Surface diagram of active site pocket shown in red box. Red-hydrogen acceptor; Blue-hydrogen donor; Yellow-hydrophobic region. **C.** Ramchandran plot.

5.1.2 High throughput virtual screening of *in house* database and biological activity of hit compounds:

With an aim of identifying novel SIRT1 inhibitors, virtual screening of *in house* database of ~3000 molecules was carried out by using GLIDE (Schrödinger L.L.C., USA), GOLD and AUTODOCK 4.0 software's against catalytic core of SIRT1. As acridinedione derivatives shown good docking score, binding energy and fitness values, compounds **ACD1, ACD2,** and **ACD3** were selected for (**Fig.5.2**) *in vitro* enzymatic assay at 50μM concentration along with reference compound **suramin**. Antiproliferative activities of **ACD1-3** on MDA-MB231, K562 cells at 10 μM concentration were shown in **Fig.5.4.** Binding energy, docking score, fitness and percentage inhibition against SIRT1 values are presented in **Table 4.**
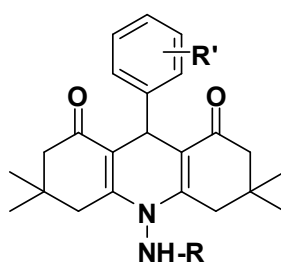

Fig.5.2: *In house* database hit compound.

Table 4: Docking scores, *in vitro* SIRT1 assay and cell proliferation study of **ACD1-3**.

Code	R	R'	Autodock score (Kcal/mol)	Gold Fitness	GLIDE Score	% Inhibition of hSIRT1 at 50μM	MDA-MB231 IC$_{50}$ (μM)	K562 IC$_{50}$ (μM)
ACD1		*o*-Benzyloxy	-6.79	52.50	-4.92	72.63	5	10
ACD2		*m*-Benzyloxy	-7.46	57.84	-3.41	53.67	>50	10
ACD3		*p*-Benzyloxy	-7.68	55.80	-3.76	No inhibition	>50	>50
Suramin			-4.67	45.7	-3.33	82.28	31.19	18.49

Further to explore the structure activity relationship of hit compounds (**ACD1-3**), a series of the six simplified derivatives (**4a–r**) (**Table 5**) were prepared. Docking score, fitness values and binding affinity values of all the designed molecules along with reference compound Suramin were shown in **Table 5**. The designed compounds have shown better docking scores than the initial hit compounds (**ACD1-3)**, hence were synthesized and characterized by a one pot synthetic protocol previously reported [Manjashetty T.H., *et al.*, 2011].

5.1.3 Synthesis and Characterization:

i.HCl,Dry DMF.MWI,5-8min
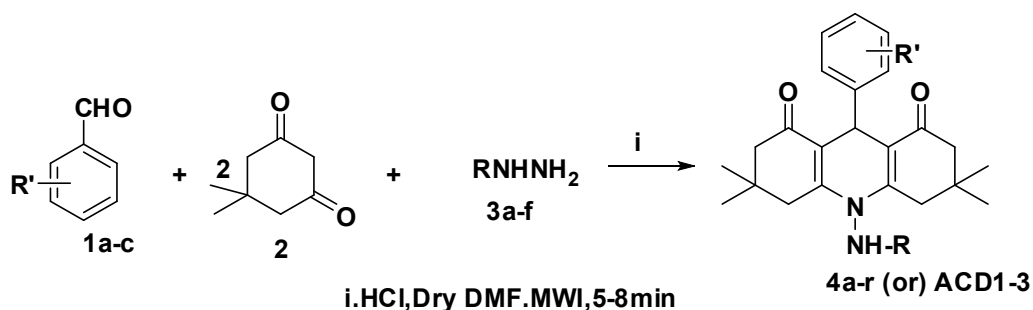
The target molecules (**4a-r**) were synthesized via a microwave assisted one-pot three component reaction of either *ortho, meta* or *para* substituted benzyloxy benzaldehydes (1.0 mmol) (**1a-c**), 5,5-dimethylcyclohexane-1,3-dione (2.0 mmol) (**2**), and corresponding phenyl hydrazine's or aryl/heteroaryl acid hydrazides (1.0 mmol) (**3a-f**) in the ratio 1:2:1 in dry DMF media with catalytic amount of HCl. The reaction mixture was the subjected to microwave irradiation at a constant power for 360W with 3-5min/cycle. The number of cycles in turn depended on the completion of the reaction, which was monitored by TLC. The reaction mixture was then evaporated to dryness, water (10 ml) was added to the residue and extracted with dichloromethane(2*15 ml), the combined organic layer was successively washed with 5% aq. citric acid(2*10 ml), water(1*10 ml), 5% aq.sodium hydrogen carbonate(1*15 ml) and finally washed with brine (1*15 ml), dried over anhydrous Na_2SO_4 and evaporated under reduced

pressure to give the product which was further recrystalized from ethanol to get desired product in quantitative yield. The structure was confirmed by ^{1}H NMR, ^{13}C NMR by Bruker AM-300 (300.12 MHz, 75.12 MHz,) and mass (LCMS6100B). Both analytical and spectral data (^{1}H NMR, ^{13}C NMR, and mass spectra) of all the synthesized compounds were in full agreement with the proposed structures.

To explore the scope and limitations of these conditions a series of the six simplified derivatives, (**4a–r**) (**Table 5**) were prepared by introduction of either unsubstituted Phenyl/Benzoyl derivatives or with various electron withdrawing / donating groups like 2,4-dinitrophenyl or 4-nitrobenzoyl or 2,4-dichlorobenzoyl or 2,6-dimethoxynicotionoyl group at C_9 (R position) and also with either *ortho, meta* or *para* benzyloxy substituent on C_9 phenyl ring of aminoacridine dione [3,4,6,7tetrahydro-3,3,6,6tetramethyl-10amino-9-phenylacridine–1,8(2H, 5H,9H,10H)–dione]. As apparent from the **Table 5**, the compounds were found to react well to give the correspondingaminoacridinedione in excellent yields (64- 84%).

Table 5: Physicochemical properties, docking results of **4a-r** (ACD series).

Code	R	R'	Glide score	Gold Fitness	Auto Dock Score (Kcal/mol)	M.P(^{0}C)	Yield (%)	Molecular Formula	Molecular Weight
4a	Phenyl	*o*-Benzyloxy	-3.53	45.1	-8.85	146-148	83.67	$C_{36}H_{38}N_2O_3$	546.0
4b	Phenyl	*m*-Benzyloxy	-6.09	51.1	-8.95	141-142	75	$C_{36}H_{38}N_2O_3$	546.0
4c	Phenyl	*p*-Benzyloxy	-3.36	48.0	-8.54	150-152	64.24	$C_{36}H_{38}N_2O_3$	546.0
4d	2,4-Dinitro phenyl	*o*-Benzyloxy	-4.28	57.6	-10.84	154-156	85	$C_{37}H_{36}N_4O_8$	665.3
4e	2,4-Dinitro phenyl	*m*-Benzyloxy	-	-	-	163-165	65.34	$C_{37}H_{36}N_4O_8$	665.3
4f	2,4-Dinitro phenyl	*p*-Benzyloxy	-5.19	55.4	-8.52	158-160	74.57	$C_{37}H_{36}N_4O_8$	665.3
4g	Benzoyl	*o*-Benzyloxy	-	-	-	160-162	67.58	$C_{37}H_{38}N_2O_4$	574.7
4h	Benzoyl	*m*-Benzyloxy	-	-	-	155-156	75.2	$C_{37}H_{38}N_2O_4$	574.7
4i	Benzoyl	*p*-Benzyloxy	-5.90	51.9	-7.84	170-172	80.01	$C_{37}H_{38}N_2O_4$	574.7
4j	4-Nitro benzoyl	*o*-Benzyloxy	-	-	-	150-152	77.2	$C_{37}H_{37}N_3O_6$	619.7
4k	4-Nitro benzoyl	*m*-Benzyloxy	-	-	-	154-156	73.25	$C_{37}H_{37}N_3O_6$	619.7
4l	4-Nitro benzoyl	*p*-Benzyloxy	-	-	-	163-165	65.24	$C_{37}H_{37}N_3O_6$	619.7
4m	2,4-Dichloro benzoyl	*o*-Benzyloxy	-	-	-	158-160	71.02	$C_{37}H_{36}Cl_2N_2O_4$	643.5
4n	2,4-Dichloro benzoyl	*m*-Benzyloxy	-	-	-	140-142	70.25	$C_{37}H_{36}Cl_2N_2O_4$	643.5
4o	2,4-Dichlorobenzoyl	*p*-Benzyloxy	-	-	-	156-158	68.9	$C_{37}H_{36}Cl_2N_2O_4$	643.5
4p	2,6-Dimethoxy nicotionoyl	*o*-Benzyloxy	-	-	-	178-180	68.77	$C_{38}H_{41}N_3O_6$	357.4
4q	2,6-Dimethoxy nicotionoyl	*m*-Benzyloxy	-	-	-	180-183	78.6	$C_{38}H_{41}N_3O_6$	357.4
4r	2,6-Dimethoxy nicotionoyl	*p*-Benzyloxy	-3.08	42.8	-9.23	189-192	75.25	$C_{38}H_{41}N_3O_6$	357.4

10-(Aminophenyl)-9-(2-(benzyloxy)phenyl)-3,4,6,7-tetrahydro-3,3,6,6-tetramethylacridine-1,8 (2H,5H,9H,10H)-dione (4a):

Yellowish orange solid; ^{1}H NMR (300 MHz, CDCl$_3$): δ = 0.91 (s, 6H, 2*CH$_3$), 1.1 (s, 6H, 2 *CH$_3$) 1.87 (d, J = 8.7Hz, 2H), 1.97 (d, J = 9.1 Hz, 2H,), 2.73 (dd, J$_{Gem}$= 9.3 Hz,4H,(2*CH$_2$)H$_2$,H$_7$), 4.6 (s, 1H, H$_9$), 5.2 (s, 2H,-O- CH$_2$), 6.7–7.16 (m, 9H, ArH of 2*phenyl), 7.2-7.3(m, 5H, ArH of Benzyl), 4.3 (s, 1H, NH); ^{13}C NMR (75 MHz, CDCl$_3$): δ= 194.3, 159.3, 152.1, 145.9, 140.5, 133.2, 130.8, 129.2, 127.3, 126.8, 123.2, 121.4, 120.1, 115.1, 113.6, 112.3, 73.4, 51.3, 38.1, 33.1, 31.3, 26.9; EI-MS *m/z* 546 (M$^+$);Anal.Calcd for C$_{36}$H$_{38}$N$_2$O$_3$: C, 79.09, H, 7.01, N, 5.12. Found: C, 79.31, H, 6.89, N, 5.25.

10-(Aminophenyl)-9-(3-(benzyloxy)phenyl)-3,4,6,7-tetrahydro-3,3,6,6-tetramethylacridine-1,8 (2H,5H,9H,10H)-dione(4b):

Orange solid; ^{1}H NMR (300 MHz, CDCl$_3$): δ = 0.93 (s, 6H, 2*CH$_3$), 1.05 (s, 6H, 2 *CH$_3$) 1.82 (d, J = 8.3 Hz, 2H), 1.93 (d, J = 9.2 Hz, 2H,), 2.71(dd, J$_{Gem}$= 9.4 Hz, 4H, (2*CH$_2$)H$_2$,H$_7$), 4.51 (s, 1H, H$_9$),), 5.2 (s, 2H,-O- CH$_2$) 6.59–7.16 (m, 9H, ArH of 2*phenyl), 7.2-7.4(m, 5H, ArH of Benzyl), 4.1 (s, 1H, NH); ^{13}C NMR (75 MHz,CDCl$_3$): δ=196.9,165.3,150.9, 145.9,143.8, 140.9, 131.2, 130.1, 129.6, 127.2, 122.1, 120.3, 114.6, 112.7, 111.7, 110.9, 71.1, 51.4, 42.2, 38.1, 32.1,27.2; EI-MS *m/z* 546 (M$^+$); Anal.Calcd for C$_{36}$H$_{38}$N$_2$O$_3$: C, 79.1; H, 7.01; N, 5.1. Found: C, 79.11; H, 7.21; N, 5.65.

10-(Aminophenyl)-9-(4-(benzyloxy)phenyl)-3,4,6,7-tetrahydro-3,3,6,6-tetramethylacridine-1,8(2H,5H,9H,10H)-dione (4c):

Reddish orange solid; ^{1}H NMR (300 MHz, CDCl$_3$): δ = 0.93 (s, 6H, 2*CH$_3$), 1.02 (s, 6H, 2 *CH$_3$) 1.84 (d, J = 8.6 Hz, 2H), 1.93 (d, J = 9.1 Hz, 2H,), 2.7 (dd, J$_{Gem}$= 9.7 Hz, 4H,(2*CH$_2$)H$_2$,H$_7$), 4.49 (s, 1H, H$_9$),), 5.17 (s, 2H,-O- CH$_2$) 6.6–7.2(m, 9H, ArH of 2*phenyl),

7.23-7.4(m, 5H, ArH of Benzyl), 4.5 (s, 1H, NH); ^{13}C NMR (75 MHz,CDCl$_3$): δ= 196.2, 155.3, 151.2, 145.6, 141.3, 133.2, 129.6, 128.9, 128.1,127.2, 126.5, 119.2, 115.1, 113.6, 111.8, 70.9, 51.3, 42.1, 37.6, 31.9, 27.3; EI-MS *m/z* 546 (M$^+$); Anal.Calcd for C$_{36}$H$_{38}$N$_2$O$_3$: C, 79.2; H, 7.01; N, 5.1; Found: C, 79.11; H, 7.71; N, 5.25.

N-(9-(2-(Benzyloxy)phenyl)-1,2,3,4,5,6,7,8-octahydro-3,3,6,6-tetramethyl-1,8-dioxoacridin-10(9H)-yl)-2,4-dinitrobenzamide(4d):

Orange solid; ^{1}H NMR (300 MHz, CDCl$_3$): δ = 0.92 (s, 6H, 2*CH$_3$), 0.99 (s, 6H, 2 *CH$_3$) 1.92 (d, J = 9.1 Hz, 2H), 2.07 (d, J = 9.3 Hz, 2H,), 2.41 (dd, J$_{Gem}$= 8.9 Hz, 4H,(2*CH$_2$)H$_2$,H$_7$), 4.84(s, 1H, H$_9$),), 5.2 (s, 2H,-O- CH$_2$) 6.7–6.96(m, 4H, ArH of phenyl at C$_9$), 7.2–7.4 (m, 5H, ArH of benzyl), 8.4-9.3(m, 3H, ArH of benzoyl), 8.2 (s, 1H, NH); ^{13}C NMR (75 MHz, CDCl$_3$): δ= 195.6, 163.8, 158.5, 153.5, 147.6, 143.2, 141.2, 134.2, 129.8, 128.3, 127.7, 127.0, 126.5, 121.1, 120, 116.4, 112.8, 111, 73.16, 52.3, 38.7, 32, 30.3, 27.1; EI-MS *m/z* 665.3 (M+H)$^+$;Anal.Calcd for C$_{37}$H$_{36}$N$_4$O$_8$: C, 66.86; H, 5.46; N, 8.43. Found: C, 66.91; H, 5.41; N, 8.47.

N-(9-(4-(Benzyloxy)phenyl)-1,2,3,4,5,6,7,8-octahydro-3,3,6,6-tetramethyl-1,8-dioxoacridin-10(9H)-yl)-2,4-dinitrobenzamide (4f):

Reddish orange solid; M.P - 158-160; yield (%) : 74.5; ^{1}H NMR (300 MHz, CDCl$_3$): δ = 0.97 (s, 6H, 2*CH$_3$), 1.05(s, 6H, 2 *CH$_3$) 1.88 (d, J = 8.3 Hz, 2H), 1.93 (d, J = 9.4 Hz, 2H,), 2.7 (dd, J$_{Gem}$= 8.2 Hz, 4H,(2*CH$_2$)H$_2$,H$_7$), 4.44 (s, 1H, H$_9$),), 5.2 (s, 2H,-O- CH$_2$), 6.6–6.95(m, 4H, ArH of phenyl at C$_9$), 7.1–7.3 (m, 5H, ArH of benzyl), 8.5-9.2(m, 3H, ArH of Benzoyl), 8.1 (s, 1H, NH); ^{13}C NMR (75 MHz, CDCl$_3$) δ= 195.2, 163.1, 156.4, 151.3, 147.7, 145.2, 142.1, 136.1, 135.7, 130.3, 129.1, 127, 117.9, 113.9, 111.7, 71.4, 52.4, 40.7, 39.1, 32.1, 28.2; EI-MS *m/z* 665.3 (M+H)$^+$; Anal.Calcd for C$_{37}$H$_{36}$N$_4$O$_8$: C, 66.86; H, 5.46; N, 8.43. Found: C, 66.91; H, 5.51; N, 8.4.

5.1.4 *In vitro* SIRT1 assay:

The synthesized compounds were tested for *in vitro* SIRT1 assay at 50μM concentration according to the protocol explained under materials and methods section 4.4. IC_{50} was calculated using different concentrations (5, 10, 50 μM) for compounds showing more than 50% inhibition and results were shown in **Table 6.**

**Table 6**: *In vitro* SIRT1 assay and IC_{50} values of **4a-r**.

Code	% inhibition of SIRT1 at 50μM	SIRT1_IC_{50} (μM)
4a	82.1	11.08±0.02
4b	51.4	40.06±0.72
4c	55.2	43.14±0.1
4d	83.2	10.13±0.08
4e	33.2	-
4f	54.8	43.29±0.49
4g	39.7	-
4h	21.5	-
4i	52.0	45.97±0.71
4j	39.0	-
4k	33.6	-
4l	35.6	-
4m	-19.7	-
4n	4.7	-
4o	3.6	-
4p	35.2	-
4q	35.6	-
4r	55.1	25.018±0.02
Suramin	53.9	2.8
Doxorubicin	-	-

Binding pose of most active compound **4d** (**Fig.5.3A and B**) clearly demonstrated the orientation of *ortho* benzyloxy group in the hydrophobic groove of the protein

A.
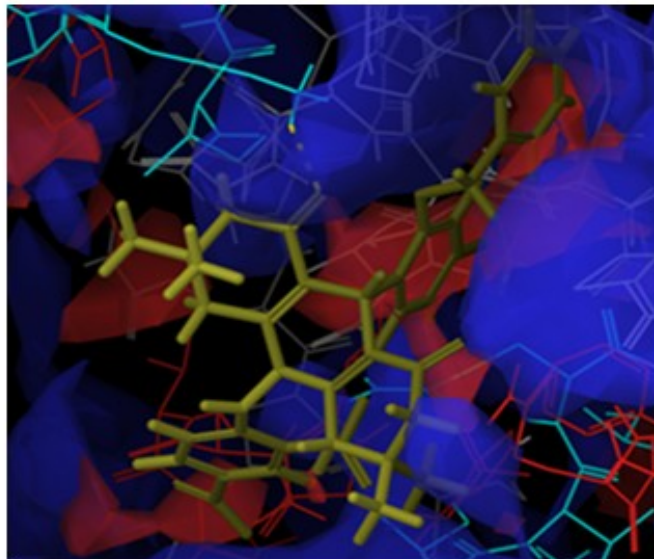
B.
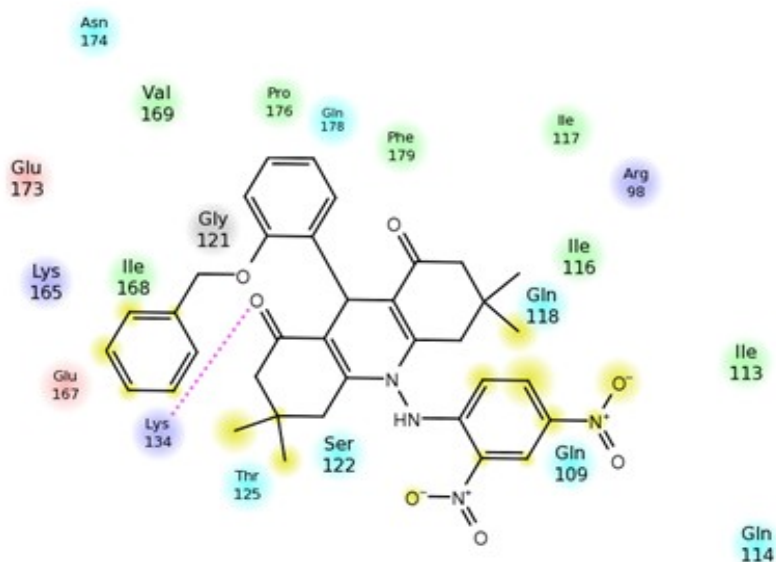
Fig.5.3: **A.** Docking pose of most active compound **4d**.red-hydrophobic; blue-hydrophilic.

B. Ligand interaction diagram showing important amino acids with in 5A^{0}distance. Dotted line represents hydrogen bond to the side chain. Blue-charged positive, green-Hydrophobic group, Yellow-Solvent exposure, Red-acidic group, purple-basic, gray-other groups.

5.1.5 *In vitro* cell proliferation assay:

To investigate the effectiveness of these SIRT1 inhibitors as anticancer agents, compounds **4a, 4b, 4c, 4d, 4f, 4i** and **4r** were evaluated for their ability to inhibit growth of cancer cells at 10 µM concentration by MTT assay according to protocol explained under materials and methods section 4.6.2. Suramin was used as a standard SIRT1 inhibitor and doxorubicin as a standard anticancer drug. K562, MDA-MB231 cells were used as tumor cells and HEK293 as control cells. Percentage inhibition of **4a, 4b, 4c, 4d, 4f, 4i** and **4r** at 10 µM are shown in **Fig.5.4**. IC$_{50}$ values of selected compounds in MDA-MB231 cells were calculated using different concentrations (0.25, 1, 5, 10µM) and results were shown in **Table 7**.
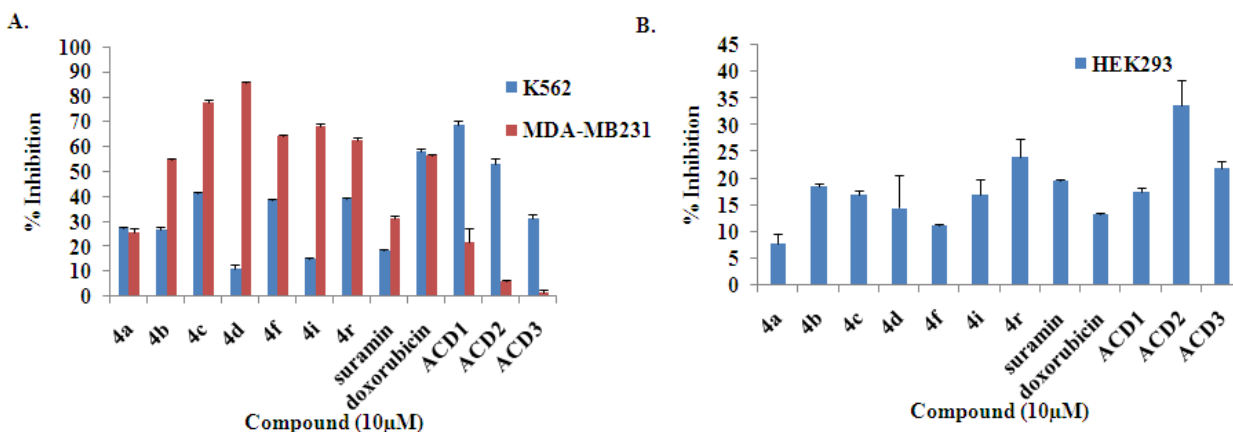

Fig.5.4: *In vitro* cell proliferation assay. **A**. Graph showing % inhibition on K562, MDA-MB231 cells. **B**. Graph showing % growth on HEK293 cells.

Table 7: IC_{50} values of ACD derivatives (**4a-d, 4f, 4i, 4r**) in MDA-MB 231 cells.

Code	MDA -MB231 IC_{50} (µM)
4a	50
4b	0.99
4c	1.38
4d	**0.25**
4f	6.63
4i	3.16
4r	0.31
Doxorubicin	10

5.1.6 Immunoblot analysis:

To investigate further the distinct effects of the compound **4d** as SIRT inhibitor, on cell fate, western blot analysis was performed on MDA-MB231 cells treated with compound **4d** at different concentrations (0,0.1, 0.25 and 0.5 µM) for 24h according to protocol explained under materials and methods section 4.6.7. As shown in **Fig.5.5**, a dose dependent decrease in SIRT1and increase in acetylation status of the SIRT1 target p53K382 levels was observed.
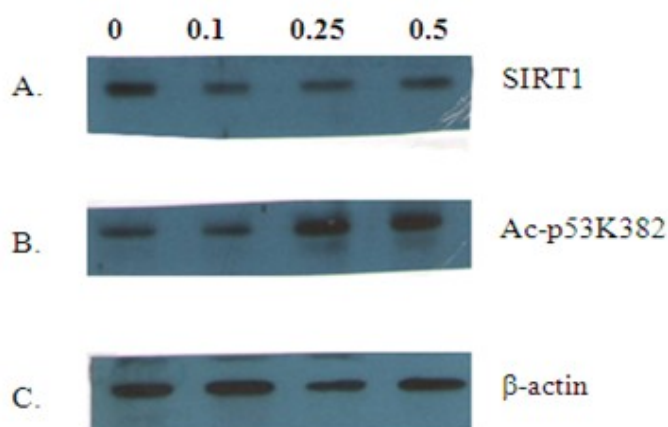

Fig.5.5: Western blot analysis of MDA-MB231 cells treated with compound **4d** at 0, 0.1, 0.25 and 0.5µM concentrations.

5.1.7 Atom based 3D QSAR:

3D QSAR model was developed by Phase module of Schrödinger. All dataset compounds were divided into a training set of 80% and a representative test set of 20%. Individual QSAR model of phase was used for construction of the simplest hypotheses that best correlates the experimental and predicted activities (**Table 8**). Statistically best QSAR model was generated with a R^2 =0.6283, F=20.3, SD=0.1506, RMSE=0.08and Q^2 = 0.6278.For the highly active compound **4d**, the QSAR feature is shown in **Fig.5.6A**. Accumulation of highest positive coefficient $(1.1*10^{-3})$ threshold of cyan colored hydrophobic or non-polar cubes at the *ortho* position of **4d** infers the importance of substitution with hydrophobic moieties at *ortho* position rather than *para* and *meta* positions as shown in **Fig.5.6B**.

Table 8: Aligned compounds for atom based 3D QSAR study and their experimental and predicted biological activity results of ACD derivatives.

Code	pIC$_{50}$ (µM) experimental	pIC$_{50}$ (µM) predicted	Code	pIC$_{50}$ (µM) experimental	pIC$_{50}$ (µM) predicted
4a	4.955	4.783	**4j**	4.301	4.350
4b	4.398	4.560	**4k**	4.301	4.362
4c	4.365	4.549	**4l**	4.301	4.266
4d	4.994	4.738	**4m**	4.301	4.284
4e	4.301	4.352	**4n**	4.355	4.309
4f	4.364	4.313	**4o**	4.301	4.214
4g	4.301	4.335	**4p**	4.301	4.567
4h	4.301	4.289	**4q**	4.301	4.425
4i	4.338	4.221	**4r**	4.602	4.468
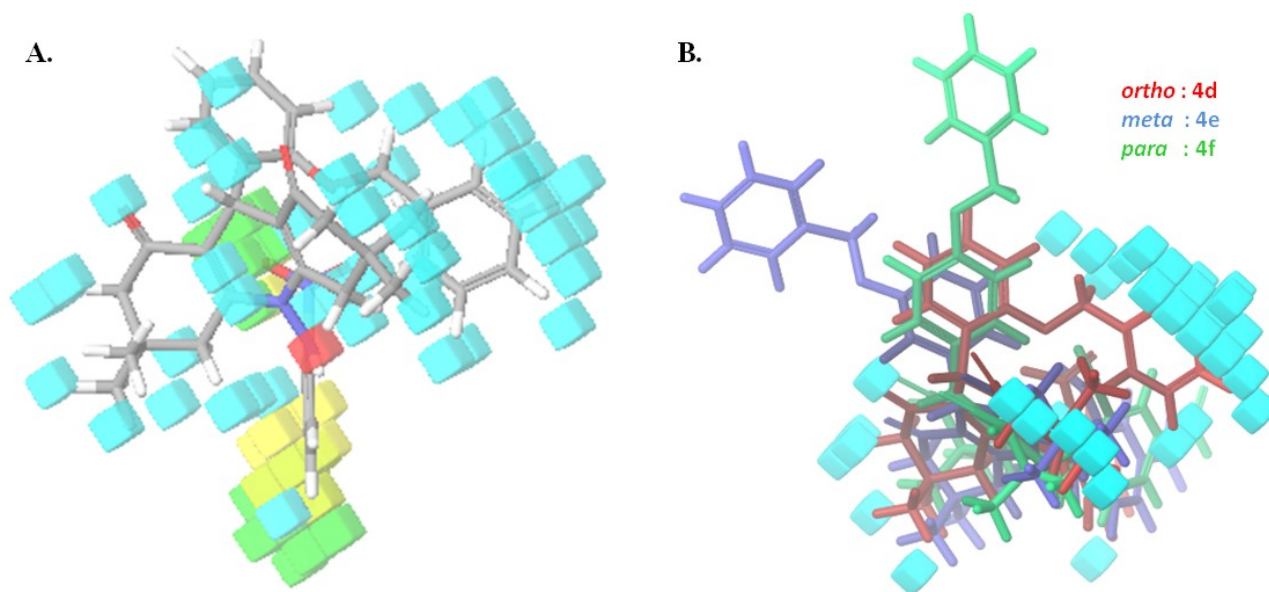
Fig. 5.6: **A.** QSAR visualization of most active compound **4d**. Cubes at that position shows positive threshold effect. Red- Hydrogen bond donor; Cyan-Hydrophobic groups; Green-Negative ionic; Yellow-Positive ionic; Pink-electron withdrawing groups. **B**. QSAR of most active compound **4d** in which benzyloxy is present at *ortho, meta and para* positions (**4d, 4e, 4f**)

5.1.8 Discussion:

Many small molecule inhibitors of SIRT1 have been identified for treatment of various cancers. In the present study we have designed and developed novel small molecule SIRT1 inhibitors. Since crystal structure of hSIRT1 was not available the best model of the catalytic core of hSIRT1 was developed and the fitness of the model was checked by PROCHECK program. This model has 83.7% residues in most favored regions and ProSAWebZ score of -6.37 similar to the template structure scores. Virtual screening of *in house* database of ~3000 molecules using GLIDE (Schrödinger L.L.C., USA), GOLD and AUTODOCK 4.0 software's against catalytic core of hSIRT1 (244-498AA) revealed acridinedione derivatives (ACD) as lead

molecules with good docking score, binding energy and fitness values. In order to validate our docking results, compounds **ACD1, ACD2** and **ACD3** were subjected to *in vitro* enzymatic assay at 50 μM concentration and **ACD1** has shown better inhibition of 72.63% compared to **ACD2** and **ACD3**.

Further to develop a SAR, a series (**4a-r**) of compounds were prepared, screened for *in vitro* SIRT1 assay at 50μM concentration and the compounds **4a, 4b, 4c, 4d, 4f, 4h, 4r** has shown more than 50% inhibition (**Table 5**). Further **4a** and **4d**were found to be the most potent inhibitors compared to reference compound **Suramin** with an IC_{50} of 11±0.02μM and 10±0.08μM respectively. Others like **4b, 4c, 4f, 4i, 4l, and 4n** were found to be better inhibitors than Suramin and the remaining compounds showed no inhibition. The percentage inhibition and IC_{50} values are presented in **Table 5**. The higher inhibitory activity of compounds **4a** and **4d** might be attributed to the presence of benzyloxy phenyl substitution at *ortho* position and the presence of phenyl and 2, 4-dinitrophenyl groups at –R position (**Fig.5.2**). Binding pose of most active compound **4d** (**Fig.5.3A and B**) clearly demonstrated the orientation of *ortho* benzyloxy group in the hydrophobic groove of the protein (red-hydrophobic; blue-hydrophilic).

Further to investigate the effectiveness of these SIRT1 inhibitors as anticancer agents, compounds**4a, 4b, 4c, 4d, 4f, 4i** and **4r** were evaluated for their ability to inhibit growth of K562MDA-MB231 cells. Compound **4d, 4r** has shown significant inhibition in MDA-MB231 with an IC_{50}value of 0.25, 0.99 μM respectively whereas **4b, 4c** has shown IC_{50} value around 1 μM. But compound **4a**, having IC_{50} of 11±0.02μM in *in vitro* assay doesn't show any significant inhibition in cell lines. From this it is clear that substitution of -R with electron withdrawing group (2 4, dinitrophenyl) increases the activity compare to other substitutions.

Western blot analysis of SIRT1 and Ac-p53K382 in MDA-MB231 treated with compound 4d at different concentrations (0, 0.1, 0.25, 0.5µM) showed dose dependent decrease in SIRT1 and increase in Ac-p53K382 protein levels (**Fig.5.5**). Further upon atom based 3D QSAR studies of ACD derivatives (**4a-r**) with respect to IC_{50} values of SIRT1 showed accumulation of highest positive coefficient ($1.1*10^{-3}$) threshold of cyan colored hydrophobic or non-polar cubes at the *ortho* position of **4d** infers the importance of substitution with hydrophobic moieties at *ortho* position rather than *para* and *meta* positions as shown in **Fig.5.6B**.

5.2 Design, synthesis, biological interventions of benzthiazolyl-2-thiosemicarbazone derivatives (B2TS):

**5.2.1 Design of homology model and active site prediction:**

Homology model of hSIRT1 catalytic domain was generated by using comparative homology modeling and active site was predicted according to procedure explained under materials and methods section 4.1 as shown in **Fig.5.1.** This model had 83.7% residues in most favored regions and ProSA Web Z score of -6.37.

5.2.2: High-throughput virtual screening of *in house* database:

With an aim of identifying novel SIRT1 inhibitors, virtual screening of *in house* database of ~3000 molecules was carried out by using GLIDE (Schrödinger L.L.C., USA) and GOLD software against the catalytic core of SIRT1. As benzthiazolyl-2-thiosemicarbazone (B2TS) derivatives showed good docking score and fitness values, these molecules were synthesized. Docking score and fitness values are presented in **Table 9**.

5.2.3 Synthesis and Characterization:

General procedure for the synthesis of substituted benzothiazole derivatives:
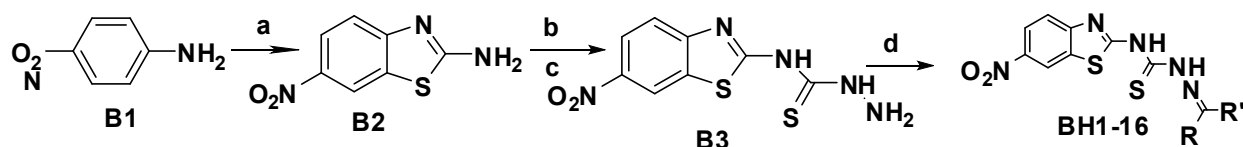
a: AcOH/KSCN/Br$_2$/0°C to RT; b: CS$_2$/0-15°C/EtOH/KOH; c:$_2$HN-NH$_2$/EtOH/reflux
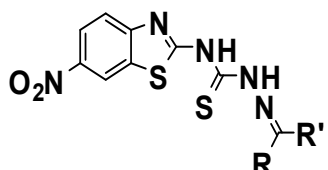
d:RCHO or RCOR/DMF/GlacialAcOH /reflux

The synthesis of the target molecules were achieved by a previously reported procedure [Yogeeswari P., *et al.*, 2005]. In a typical procedure, a solution of potassium thiocyanate in acetic acid was added to a solution of *p*-nitro aniline (**B1**) in acetic acid; the reaction mixture was

stirred at RT for 30 minutes and then cooled to 0°C. A solution of bromine in acetic acid was then added drop wise at 0°C. The reaction mixture was then warmed to RT and stirred at RT for 24 hrs. Cold water was then added to the reaction mixture for precipitation and the precipitate was then suspended in water, neutralized with aq. ammonia and filtered. The solid obtained was then washed with water and dried to get 6-nitro-2-aminobenzothiazole (**B2**) in quantitative yield. Further, 6-nitro-2-aminobenzothiazole (1g) was added to a solution of KOH in ethanol at RT. The reaction mixture was then heated to 150°C and carbon disulphide (0.0068 mmol) was added in small portions to the reaction mixture at this temperature. After the complete addition, heating was continued for another 30 min. The reaction mixture was then cooled to ambient temperature, hydrazine hydrate was then added drop wise and refluxed for 3 hours (monitored by TLC for completion). The reaction mixture was evaporated to dryness. The crude product was then further purified by recrystallisation from ethanol-ethyl acetate mixture (7:3 v/v) to give the desired product (**B3**) in quantitative yield.

Final library was then obtained by preparing Schiff base of above prepared thiosemicarbazide with various aldehydes and ketones in DMF at equimolar concentration with catalytic amount of acetic acid. The structure was further confirmed by NMR (Bruker AM-300 MHz) and mass (LCMS1600B). Both analytical and spectral data (^{1}H NMR, ^{13}C NMR, and mass spectra) of all the synthesized compounds were in full agreement with the proposed structures. As apparent from the **Table 9**, the compounds were found to react well to give the corresponding benzthiazolyl-2-thiosemicarbazone (**BH1-16**) in excellent yields (54- 96%).

Table 9: Physico-chemical properties, docking score of B2TSderivatives (**BH1-16**).

Code	R	R'	Gold Fitness	Glide score	M.P (^{0}C)	Yield (%)	Molecular Formula	Molecular Weight
BH1	H	Phenyl	52.03	-3.75	110-113	95.13	$C_{15}H_{11}N_5O_2S_2$	357.41
BH2	H	Chlorophenyl	ND	-3.35	165-167	60.12	$C_{15}H_{10}ClN_5O_2S_2$	391.06
BH3	H	2-Trifluoromethyl Phenyl	ND	-3.34	140-143	95.24	$C_{16}H_{10}F_3N_5O_2S_2$	425.02
BH4	H	4-Methylphenyl	ND	-3.32	150-152	90.12	$C_{16}H_{13}N_5O_2S_2$	371.44
BH5	H	4-Hydroxy-3-Methoxyphenyl	ND	-4.17	220-222	80.23	$C_{16}H_{13}N_5O_4S_2$	403.04
BH6	H	2-Nitrophenyl	ND	-3.27	185-188	50.10	$C_{15}H_{10}N_6O_4S_2$	402.02
BH7	H	4-Nitrophenyl	ND	-2.78	175-178	50.12	$C_{15}H_{10}N_6O_4S_2$	402.02
BH8	H	4-Methoxyphenyl	ND	-3.61	165-168	90.12	$C_{16}H_{13}N_5O_3S_2$	387.05
BH9	H	2-Hydroxyphenyl	ND	-4.67	220-222	90.12	$C_{15}H_{11}N_5O_3S_2$	373.07
BH10	CH_3	Phenyl	38.43	-3.82	222-224	91.32	$C_{16}H_{13}N_5O_2S_2$	371.05
BH11	CH_3	4-Fluorophenyl	40.45	-3.23	122-124	62.45	$C_{16}H_{12}FN_5O_2S_2$	389.21
BH12	CH_3	4-Bromophenyl	43.61	-3.60	142-144	52.23	$C_{16}H_{12}BrN_5O_2S_2$	450.33
BH13	CH_3	2-Hydroxyphenyl	56.29	-4.40	150-154	62.23	$C_{16}H_{13}N_5O_3S_2$	387.10
BH14	CH_3	4-Nitrophenyl	44.76	-3.80	182-184	96.45	$C_{16}H_{12}N_6O_4S_2$	416.04
BH15	CH_3	4-Methylphenyl	42.72	-3.40	190-192	63.32	$C_{17}H_{15}N_5O_2S_2$	416.04
BH16	CH_3	2-Aminophenyl	40.31	-4.40	120-122	82.23	$C_{16}H_{14}N_6O_2S_2$	386.06
Suramin			45.7	-3.33				

ND: Not determined

2-Amino-6-nitrobenzothiazole (B2):

Yellow solid; M.P 247-249°C; Yield (69%);. ^{1}H NMR (300 MHz, DMSO-d$_6$): δ=7.43 (d, 1H, J= 9.1Hz), 8.13 (dd, 1H, J=9.0, 2.4 Hz), 8.31 (s, 2H NH$_2$), 8.68 (d, 1H, J =2.2 Hz)^{13}CNMR (75MHz, CDCl$_3$): δ=172.3, 158.2, 141.6, 132.1, 122.8, 118.4, 117.6 EI-MS *m/z:* 195.07 (M$^+$).

N-(6-Nitrobenzo[d]thiazol-2-yl)hydrazinecarbothioamide (B3):

Yellow solid; M.P 200-203°C; Yield (93%);. ^{1}H NMR (300 MHz, DMSO-d$_6$): δ=7.45 (d, 1H, J= 9.1Hz), 8.14 (dd, 1H, J=9.1, 2.4 Hz), 8.69 (d, 1H, J =2.1Hz)2.31 (s, 1H NH), 4.21 (s, 1H NH), 5.1 (s, 2H NH$_2$). ^{13}CNMR (75MHz, CDCl$_3$): δ= 184.3, 178.7, 158.7, 141.8 , 132.5, 122.9, 118.7, 117.7 EI-MS *m/z:* 269.03 (M$^+$).

2-Benzylidene-N-(6-nitrobenzo[d]thiazol-2-yl)hydrazinecarbothioamide (BH1):

Yellow solid; ^{1}H NMR (300 MHz, DMSO-d$_6$): δ=7.46 (d, 1H, J= 9.1Hz, Bt-H), 8.17 (dd, 1H, J=9.1, 2.4 Hz, Bt-H), 7.53-7.81(m, 5H, ArH) 8.51 (s, 1H imine), 8.71 (d, 1H, J =2.1Hz, Bt-H),4.51 (s, 1H NH),12.31 (s, 1H, NH), ^{13}CNMR (75MHz, CDCl$_3$): δ= 187.6, 178.4, 158.1, 144.3, 141.8, 134.4, 132.6, 131.3, 129.6, 128.4, 123.0, 118.4, 117.4;EI-MS *m/z:* 357.03 (M$^+$). Anal. Calcd for C$_{15}$H$_{11}$N$_5$O$_2$S$_2$: C, 50.41; H, 3.10; N, 19.59. Found: C, 50.46; H, 3.16; N, 19.61.

2-(4-Hydroxy-3-methoxybenzylidene)-N-(6-nitrobenzo[d]thiazol-2-yl)hydrazinecarbo-thioamide (BH5):

Yellow solid; ^{1}H NMR (300 MHz, DMSO-d$_6$): ^{1}H NMR (300 MHz, DMSO-d$_6$): δ=3.82 (s, 3H, -OCH$_3$), 7.06-7.63 (m, 4H, 3 Ar-H &1 Bt-H), 8.14 (dd, 1H, J=9.1, 2.4 Hz, Bt-H), 8.03 (s, 1H, imine), 8.68 (d, 1H, J =2.7 Hz, Bt-H),3.92 (s, 1H NH), 9.72 (s, 1H, OH),11.43 (s, 1H, NH). ^{13}CNMR (75MHz, CDCl$_3$): δ=187.2, 178.1, 157.9, 150.7, 147.8, 144.2, 142.0, 132.1, 131.4, 124.6, 123.1, 118.7, 117.7, 117.1, 112.0, 56.7; EI-MS *m/z:* 403.04 (M$^+$). Anal. Calcd for C$_{16}$H$_{13}$N$_5$O$_4$S$_2$:C, 47.63; H, 3.25; N, 17.36. Found: C, 47.69; H, 3.24; N, 17.31.

N-(6-Nitrobenzo[d]thiazol-2-yl)-2-(2-nitrobenzylidene)hydrazinecarbothioamide (BH6):

Yellowish orange solid; ^{1}H NMR (300 MHz, DMSO-d$_6$):δ= 7.54-7.89 (m, 5H, 4ArH & 1 Bt-H), 8.12 (dd, 1H, J=9.3, 2.1 Hz, Bt-H), 8.37 (s, 1H imine), 8.69 (d, 1H, J =1.8 Hz, Bt-H), 4.26 (s, 1H NH), 11.91 (s, 1H, NH). ^{13}CNMR (75MHz, CDCl$_3$): δ=187.5, 178.4, 158.0, 146.3, 141.9, 141.4, 135.3, 132.8, 132.2, 131.4, 129.1, 124.7, 123.1, 118.9, 117.6;EI-MS *m/z:* 402.02 (M$^+$).Anal. Calcd for C$_{15}$H$_{10}$N$_6$O$_4$S$_2$: C, 44.79; H, 2.47; N, 20.84. Found: C, 44.74; H, 2.48; N, 20.83.

**2-(2-Hydroxybenzylidene)-N-(6-nitrobenzo[d]thiazol-2-yl)hydrazinecarbothioamide(BH9**):

Yellow solid; ^{1}H NMR (300 MHz, DMSO-d$_6$): δ=7.08-7.62 (m, 5H, 4ArH & 1 Bt-H), 8.12 (dd, 1H, J=9.1, 2.1 Hz), 8.87 (s, 1H imine), 8.71 (d, 1H, J =2.1 Hz, Bt-H), 5.03 (s, 1H NH), 10.54 (s, 1H, NH). ^{13}CNMR (75MHz, CDCl$_3$): δ= 186.9, 178.4, 158.1, 156.4, 143.7, 141.7, 134.7, 132.4, 128.1, 123.6, 123.2, 118.8, 118.2, 117.9, 117.5;EI-MS *m/z:* 373.07 (M$^+$). Anal. Calcd for C$_{15}$H$_{11}$N$_5$O$_3$S$_2$: C, 48.25; H, 2.97; N, 18.76. Found: C, 48.17; H, 3.01; N, 18.69.

2-(1-(2-Hydroxyphenyl)ethylidene)-N-(6-nitrobenzo[d]thiazol-2yl)hydrazinecarbo-thioamide (BH13):

Yellow solid;^{1}H NMR (300 MHz, DMSO-d$_6$):δ=3.36 (s, 3H, -CH$_3$),7.01 -7.57 (m, 5H, 4ArH & 1 Bt-H), 8.14 (dd, 1H, J=9.2, 2.1 Hz, Bt-H), 8.76 (d, 1H, J =1.9 Hz, Bt-H), 5.01 (s, 1H NH), 9.84 (s, 1H, NH).10.3 (s, 1H, NH).^{13}CNMR (75MHz, CDCl$_3$):δ= 181.7, 177.6, 167.2, 162.1, 155.9, 142.0, 134.7, 133.3, 131.9, 124.5, 123.3, 118.6, 118.2,117.5, 116.8, 16.0;EI-MS *m/z:* 387.10(M$^+$). Anal. Calcd for C$_{16}$H$_{13}$N$_5$O$_3$S$_2$:C, 49.60; H, 3.38; N, 18.08. Found: C, 49.31; H, 3.18; N, 17.99.

5.2.4 *In vitro* SIRT1 assay:

The synthesized compounds (**BH1-16**) of B2TS series were tested for *in vitro* SIRT1 assay at 50μM concentration according to protocol explained under materials and methods section 4.4. *In vitro* SIRT1 inhibition at 50μM concentration was shown in **Fig.5.7**and IC_{50} values are illustrated in **Table 10**.

.
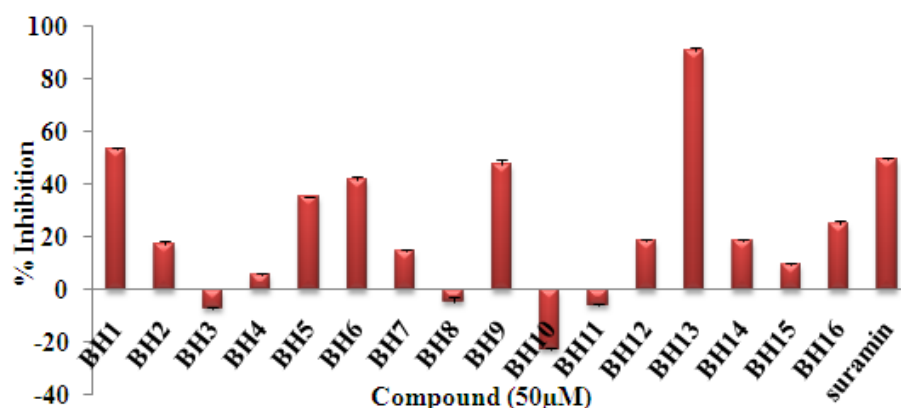
Fig.5.7: *In vitro* SIRT1 assay of B2TS derivatives: %inhibition of hSIRT1 by **BH1-16** at 50μM concentration.

Table 10: IC_{50} of B2TS derivatives (**BH1-16**) againstSIRT1.

| Code	SIRT1_IC_{50} (μM)	Code	SIRT1_IC_{50} (μM)
BH1	46.27±0.7	**BH9**	51.12±0.78
BH2	>100	**BH10**	>100
BH3	>100	**BH11**	>100
BH4	>100	**BH12**	>100
BH5	71.02±0.18	**BH13**	15.3±0.8
BH6	60.8±0.3	**BH14**	>100
BH7	>100	**BH15**	>100
BH8	>100	**BH16**	>100
suramin	50.11±0.5		

5.2.5: Antiproliferative assay:

The antiproliferative activity of **BH1-16** was performed by MTT assay according to protocol explained under materials and methods section 4.6.2. K562, MDA-MB231, PC3, LNCaP and HEK293 cells (5×10^3 cells/well) were incubated in 96-well plates in the presence or absence of test compound or **Doxorubicin** at a concentration of 10 μM for 24 h. The % inhibition was shown in **Fig.5.8A**. IC$_{50}$ values were determined for most active compounds **BH1** and **BH13** in LNCaP cells treated with (0.25, 0.5, 1.0, 5.0, 10 μM) or without the test compound and the results are depicted in **Fig.5.8B**
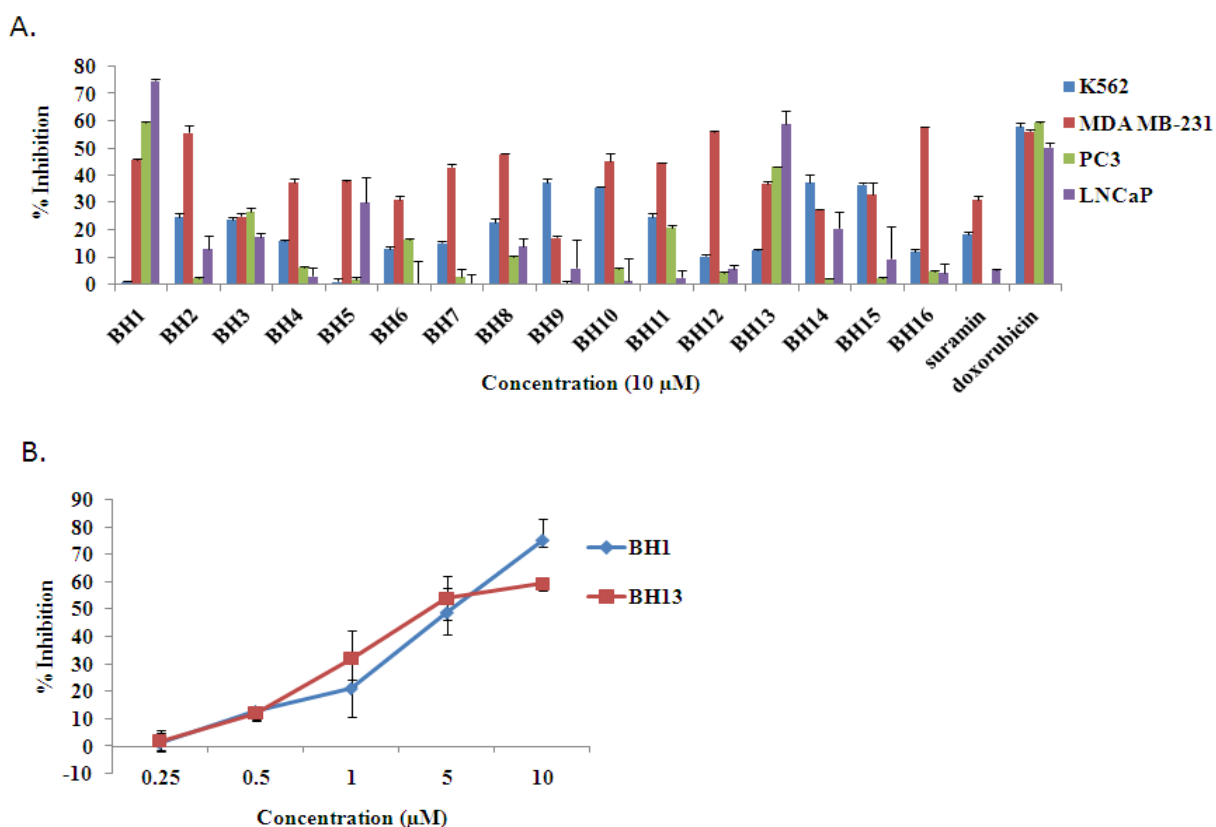
Fig.5.8: A. *In vitro* antiproliferative activity of B2TS derivatives (**BH1-16**) at 10μM concentration on various cell lines. **B**. Dose dependent activity of **BH1** and **BH13** on LNCaP cells

5.2.6 Annexin V assay:

Annexin V, a recombinant phosphatidylserine-binding protein, interacts strongly and specifically with phosphatidylserine residues and can be used for the detection of apoptosis (Arur S., *et al*., 2003).Induction of apoptosis by **BH1** and **BH13** was measured by annexin V assay according to protocol explained under section 4.6.5. Results from Annexin V assay using flow cytometer demonstrated a dose-dependent (0, 5, 10, 50 µM) increase in the Annexin V positive cells indicating induction of apoptosis in LNCaP cells by **BH1** and **BH13** as shown in **Fig.5.9.**
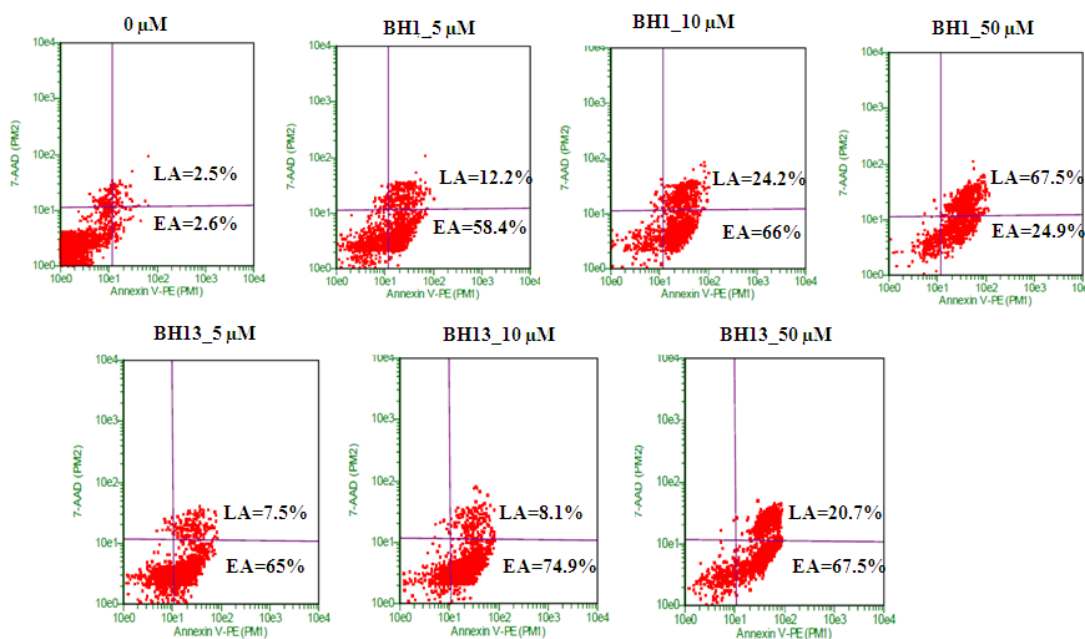
Fig.5.9: Annexin V assay of LNCaP cells treated with **BH1** and **BH13** at 0, 5, 10, 50 µM concentrations. LA: Late apoptotic; EA: Early apoptotic. % of cells in LA, EA are shown.

**5.2.7 *In situ* caspase 3 activation assay:** 0.5×10^{6} cells/ml LNCaP cells were treated with **BH1** and **BH13** at 0, 5, 10, 50 µM concentrations for 24 h and activation of caspases was measured according to protocol explained under materials and methods section 4.6.6. As shown in **Fig.5.10**, a dose dependent increase in caspase 3 active cells was observed in both **BH1** and **BH13** treated cells which indicate induction of apoptosis.
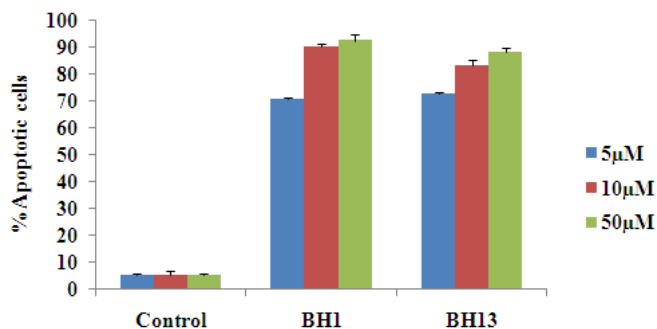
Fig.5.10: In-situ caspase 3 analysis of cells treated with **BH1** and **BH13**.

5.2.8 Immunoblot analysis:

To investigate the distinct effects of **BH1** and **BH13** as SIRT inhibitors, western blot analysis was performed on LNCaP cells treated with **BH1** and **BH13** at different concentrations (0, 5, 10 and 50 µM) for 24h according to protocol mentioned in section 4.6.7.
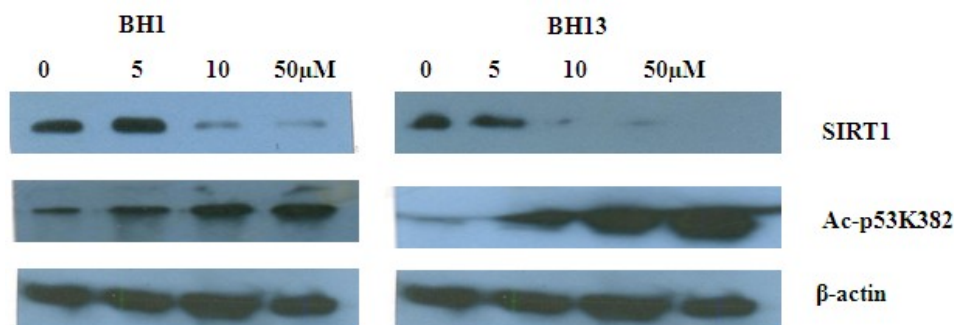

Fig.5.11: Immunoblot analysis of SIRT1 and Ac-p53K382 levels in LNCaP cells treated with compound **BH1** and **BH13**. Equal loading was confirmed by β-actin.

As shown in **Fig.5.11**, a dose dependent decrease in SIRT1and increase in acetylation status of the SIRT1 target Ac-p53K382 levels was observed

5.2.9 Transcript levels of SIRT1 and PSA:

In order to investigate the effect of **BH1** and **BH13** on transcript levels of SIRT1 and PSA, RT-PCR analysis was performed according to protocol mentioned under section 4.6.8 and

a dose dependent decrease in SIRT1 and PSA levels was observed as shown in Fig.5.12**.** Relative

mRNA levels are calculated by using Image lab analysis software (Bio-rad).
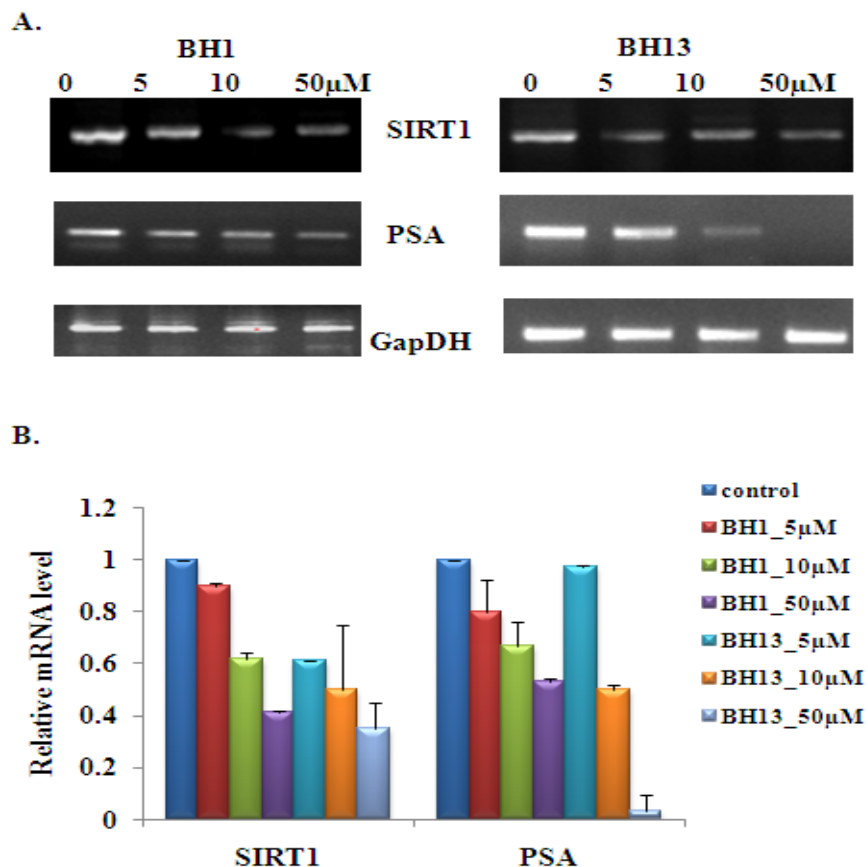

Fig.5.12:A.RT-PCR analysis of SIRT1, PSA levels in LNCaP cells. **B**. Relative levels of SIRT1,

PSA were calculated by image analysis software. Equal loading was confirmed by GapDH.

5.2.10 *In vivo* studies:

Effect of **BH1** and **BH13** were studied on testosterone induced hyperplasia in rats

according to protocol explained under materials and methods section 4.7.1. Animal body weight

was monitored periodically during the study and no significant difference was found among the

groups before and after treatment. Substantial elevation in prostate weights was noticed with

testosterone treatment compared to negative control. As shown in **Fig.5.13A**, significant

reduction in elevation of prostate and seminal vesicle weights was observed in rats treated with **BH13** compare to **BH1**. Further Histopathological study showed decrease in induction of hyperplasia with **BH1** and **BH13** (**Fig.5.13B**) of prostate tissues isolated from animals according to protocol explained under section 4.7.2 of materials and methods. RT-PCR analysis of prostate tissues from animals also shown decrease in SIRT1 levels compare to testosterone induced. (**Fig.5.13C**)
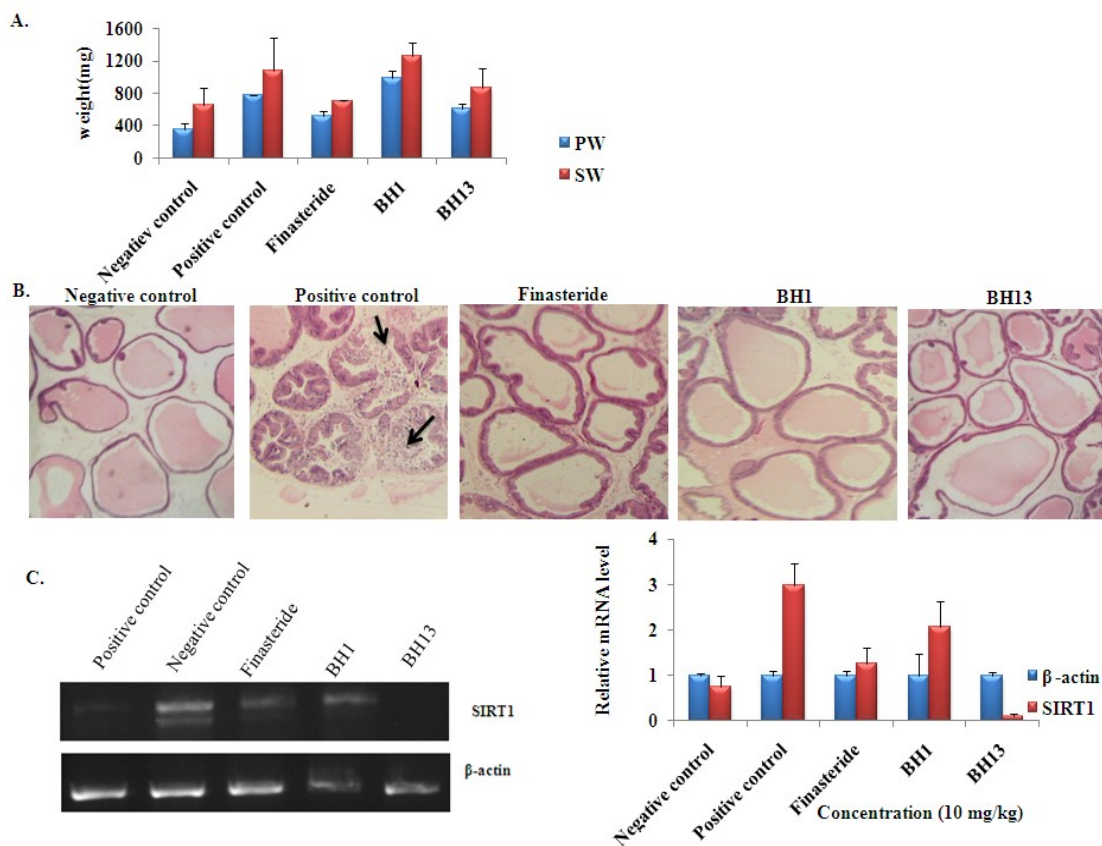
Fig.5.13: Effect of **BH1** and **BH13** (10 mg/kg) on testosterone induced hyperplasia in rat: **A.** Change in body weight before and after treatment**. B**. Histopathology study of prostate tissues of rat treated with **BH1** and **BH13** along with positive, negative controls and standard drug **Finasteride**. Arrows indicate disruption in architecture of cell. **C**. SIRT1 transcript levels in prostate tissues isolated from treated animals**.**

5.2.11 Discussion:

In the present study we have designed and developed small molecule novel SIRT1 inhibitors. Since crystal structure of SIRT1 was not available the best model of the catalytic core of SIRT1 was developed using homology modeling and the fitness of the model was checked by PROCHECK program. This model had 83.7% residues in most favored regions and ProSA Web Z score of -6.37 similar to the template structure scores. Virtual screening of *in house* database of ~3000 molecules was carried out by using GLIDE and GOLD software's against catalytic core of SIRT1 and a series of benzthiozolyl-2-thiosemicarbazone (B2TS) derivatives were identified as lead molecules. Among all, **BH1** and **BH13** showed highest fitness values of 52.03, 56.29 and glide docking score of -4.40, -3.75 respectively. In order to validate our *in silico* results, the compounds **BH1-16** were synthesized and tested for *in vitro* SIRT1 enzymatic inhibition Amongst, **BH1** & **BH13** showed inhibition of 90% and 54% whereas **BH9** & **BH5** showed moderate inhibition of 48% and 35% at 50µM concentration Further **BH1** and **BH13** showed better inhibition with an IC$_{50}$ of 46.27±0.7µM and 15.3±0.8µM respectively compared to Suramin.

It has been reported that SIRT1 is significantly elevated in human prostate cancer [Huffman D.M., *et al* 2007], acute chronic myeloid leukemia [Bradbury C.A., *et al*., 2005], metastatic breast cancer [Lara E., *et al*., 2009] and various other cancers [Stunkel W., *et al*., 2007]. Recently it has also been reported that SIRT1 levels are closely related to the PSA and Bcl2 levels in benign prostate hyperplasia. As the SIRT1 levels increases, PSA levels also increases [Liu Da-qi *et al*., 2011]. To explore the efficacy of our SIRT1 inhibitors as anticancer agents, cell proliferation assay was performed by MTT assay in four different cancer cell lines (K562, PC3, MDAMB-231and LNCaP) at 10µM concentration. None of the tested compounds

(**BH1-16**) showed significant inhibition in K562 cells whereas **BH2, BH12** and **BH16** showed moderate inhibition of above 50% on MDA-MB231 cells, while **BH1** and **BH13** showed 59.2%, 43.1% of growth inhibition of PC3 cells and 75% and 59%in LNCaP cells respectively. Hence IC_{50} values were determined for BH1 and **BH13** in LNCaP cells with different concentrations (0.25, 0.5, 1, 5, 10µM) and found to be 4.09±0.02 µM and 5.07±1.258 µM respectively.

Several SIRT1 inhibitors were reported to induce apoptosis in various cancer cells. Hence to understand the mechanism of inhibition of cell proliferation of LNCaP cells by **BH1** and **BH13**, cell death was quantified in terms of percentage of apoptotic cells. Flow-cytometry analysis of androgen sensitive LNCaP cells treated with **BH1** and **BH13**, demonstrated that apoptotic rate reached more than 70.0% after incubation with 5µM concentration for 24h and increased dose dependently up to 50µM. This dose dependent increase in apoptotic cells by **BH1 & BH13** demonstrates the induction of apoptosis.

Caspases are critical mediators of apoptosis. Amongst, caspase 3 is a frequently activated death protease which catalyzes cleavage of many cellular proteins. Activation of caspase 3 has been identified as a marker to study induction of apoptosis. Upon in-situ caspase 3 assay, significant dose dependent activation of caspase 3 was observed in cells treated with **BH1 & BH13** which clearly demonstrates the induction of apoptosis. Furthermore a dose dependent decrease in mRNA levels of SIRT1 and PSA by **BH1** and **BH13** in LNCaP cells demonstrates the induction of apoptosis through inhibition of SIRT1.

To validate the results of mRNA levels of SIRT1, protein levels were evaluated by western blot analysis. Treatment of LNCaP cells with **BH1** and **BH13** resulted in significant decline in the SIRT1 and increase in Ac-p53K382 protein levels.

In order to explore the efficiency of the **BH1** and **BH13** in treatment of benign prostate hyperplasia, *in vivo* studies were performed on testosterone induced hyperplasia in rats. Compounds **BH1** and **BH13** were administered along with testosterone for 15 days continuously and no significant difference was found in animal body weight among the groups before and after treatment. Substantial elevation in prostate and seminal vesicle weights was noticed with positive (testosterone) control compared to negative control while significant reduction in elevation of prostate and seminal weights was observed in **BH1** and **BH13** treated rats. There was no change in the histoarchitecture of prostate gland in negative control group. The tissues were tightly packed; epithelium was cuboidal and regular in size (**Fig.5.13B**). In positive control there was disruption in the histoarchitecture of the prostate tissue. The amount of connective tissue was well marked with increased oval acini size. Stromal proliferation and glandular hyperplasia with epithelial proliferation and nuclear stratification have been observed. Compound **BH1** and **BH13** treatments showed reduction in the histoarchitecture disruption of prostate (**Fig.5.13B**) and no stromal appearance. Moreover reduced SIRT1 transcript levels observed in **BH13** treated animals compare to testosterone induced prostate.

CHAPTER 6

DESIGN OF
SIRT1 ACTIVATORS

CHAPTER 6
DESIGN OF SIRT1 ACTIVATORS

6.1 Design, synthesis, biological interventions of spiro-piperidine-4-one (SP) derivatives:

6.1.1 Design of homology model of allosteric site and active site prediction:

Homology model of hSIRT1 allosteric site (114-217 AA) was designed according to method explained under materials and methods section 4.1. Homology model of allosteric site and predicted active site pocket was shown in **Fig.6.1**. Active site has site score of 0.79 and Dscore (druggable score) of 0.78 with hydrophobic score of 0.895 and hydrophilic score of 0.73.
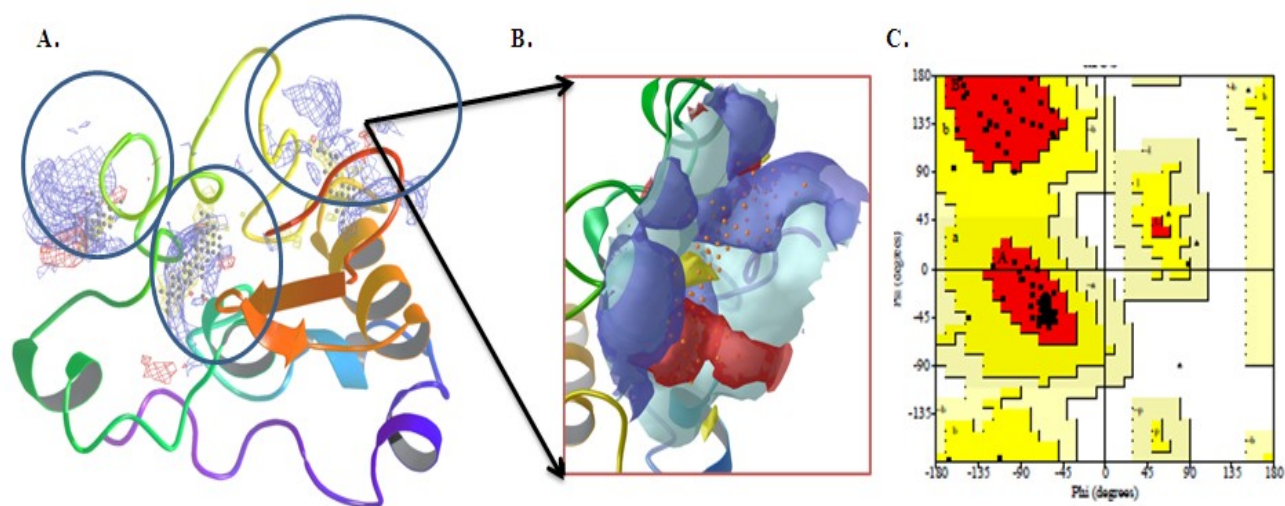

Fig.6.1: **A.** Homology model of hSIRT1 allosteric site. Circles denote putative active site pockets **B.** surface diagram of active site pocket shown in red box. Red-hydrogen acceptor; Blue-hydrogen donor; Yellow-hydrophobic region. **C.** Ramchandran plot.

.

This model showed 92.9% residues in most favored regions and ProSA Web Z score of - 6.38 similar to the template structure scores. Binding site pocket was identified by using SITEMAP and contains ASP166; ARG167; SER169; HIS170; ALA171; SER172; SER173; SER174; ASP175; TRP176; PRO184; TYR185; PHE187; VAL188; HIS191; LEU192 amino acid residues with respect to the full length SIRT1 sequence.

6.1.2 High-throughput virtual screening of *in house* database:

High-throughput virtual screening of *in house* database of ~3000 molecules into allosteric site of hSIRT1 revealed spiro-piperidine-4-one (SP) derivatives as lead molecules with better docking score and hydrogen bonds compare to standard resveratrol were specified in **Table 11**.

6.1.3 Synthesis and characterization:
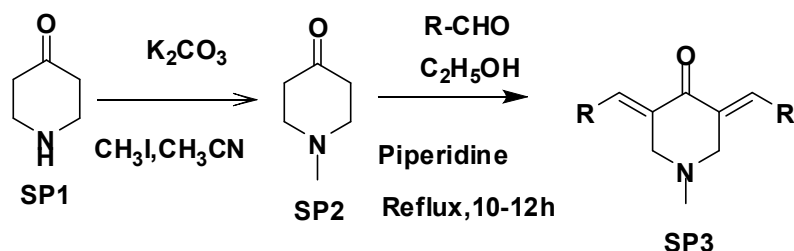
Piperidine-4-one (**SP1**) (1.5 mmol) in acetonitrile, K_2CO_3 (1.5 mmol) followed by methyl iodide (1.2mmol) at RT were stirred for 6h at RT and monitored by TLC. The reaction mixture was quenched with water, extracted with ethyl acetate and purified through column chromatography. To the 1-methylpiperidin-4-one (**SP2**) in ethanol corresponding aldehyde was added followed by piperidine(0.5 mmol) and the reaction was refluxed for 10h.The reaction mixture was then evaporated to dryness, water (10ml) was added to the residue and extracted with dichloromethane(2*15 ml), the combined organic layer was successively washed with 5% aq. citric acid(2*10 ml), water(1*10 ml), 5% aq.sodium hydrogen carbonate(1*15 ml) and finally washed with brine (1*15 ml), dried over anhydrous Na_2SO_4 and evaporated under reduced

pressure to give the product which was further recrystalized from ethanol to get desired product **SP3** in quantitative yield .The structure was further confirmed by NMR (Bruker AM-300 MHz) and Mass (LCMS1160B).
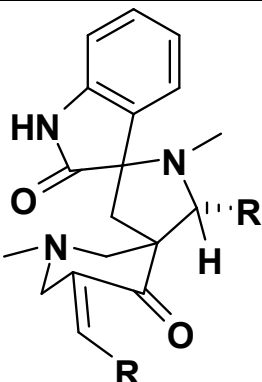
Synthesis of 1-methyl-4-arylpyrrolo-(spiro[2.3″]oxindole)–spiro[3.3′]-1′-methyl-5′-(arylidene)piperidin-4′-ones:
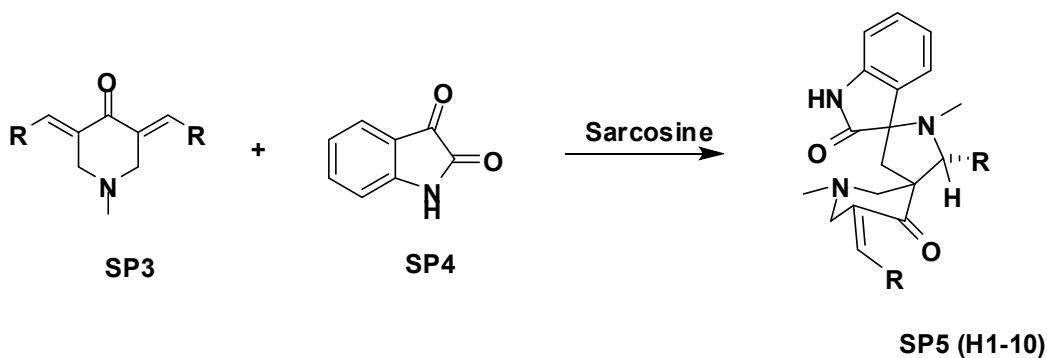
A mixture of **SP3** (1 mmol), isatin (**SP4**) (0.147 g, 1 mmol) and sarcosine (0.089g, 1 mmol) were dissolved in methanol (10 ml) and refluxed for 30 min. After completion of the reaction as evident from TLC, the mixture was poured into water (50 ml). The precipitated solid was filtered and washed with water to obtain pure compounds **SP5 (H1-10)**.

Table 11: Physico-chemical properties, docking score of SP derivatives (**H1-10**).

Code	R	Glide score	Hbond	M.P (^{0}C)	Yield (%)	Molecular Formula	Molecular Weight
H1	C_6H_5	-3.25	0	180-182	56	$C_{30}H_{29}N_3O_2$	449.54
H2	*p*-MeC$_6$H$_4$	-5.27	0	190-192	67	$C_{32}H_{33}N_3O_2$	477.60
H3	*p*-MeOC$_6$H$_4$	-5.51	1	213-214	80	$C_{32}H_{33}N_3O_4$	509.60
H4	*o*-Cl C$_6$H$_4$	-4.25	1	200–202	90	$C_{30}H_{27}C_{l2}N_3O_2$	518.43
H5	*o*-MeC$_6$H$_4$	-3.27	1	180–181	91	$C_{32}H_{33}N_3O2$	477.60
H6	*o*-MeOC$_6$H$_4$	-4.46	1	197–199	96	$C_{32}H_{33}N_3O4$	509.60
H7	*m*-FC$_6$H$_4$	-2.58	0	175–177	94	$C_{29}H_{25}F_2N_3O_2$	485.52
H8	1-Napthyl	-5.01	0	224–225	92	$C_{37}H_{31}N_3O_2$	549.24
H9	*o,p*-Cl$_2$C$_6$H$_4$	-4.78	0	215–217	96	$C_{30}H_{25}C_{l4}N_3O_2$	585.05
H10	2-Furyl	-4.67	0	240-242	98	$C_{25}H_{23}N_3O_4$	249.17
Resveratrol		-3.14	1			$C_{14}H_{12}O_3$	228.24

1-Methyl-4-(2-methoxyphenyl)pyrrolo-(spiro[2.3″]oxindole)-spiro[3.3′]-1′-methyl-5′-(2-methoxyphenylmethylidene)piperidin-4′-one (H3):

yellow solid (0.20 g, 80%,.), ^{1}H NMR (300 MHz, CDCl$_3$): δ = 1.69 (1Hd, d, J ¼ 12.4 Hz), 2.06 (3H, s), 2.15 (3H, s), 2.96 (1Hf, d, J ¼ 12.8 Hz), 3.25–3.49 (3H, m, Hb, He, Hg), 3.86 (3H, s), 3.87 (3H , s), 3.89 (1Hc, dd, J ¼ 10.8, 7.3 Hz,), 4.78 (1Ha, dd, J ¼ 10.8, 9.3 Hz), 6.63–7.33 (ArH,m), 6.62 (1H, s), 8.34 (1H, bs,); ^{13}C NMR (75 MHz, CDCl$_3$): δ = 34.66, 44.63, 44.88,55.20, 55.25, 56.69, 56.93, 57.20, 65.93, 75.85, 108.74, 113.53, 113.71, 121.82, 127.66, 127.80, 128.62, 130.30, 131.41, 131.94, 137.48, 141.92, 158.32, 159.93, 177.70, 198.49. EI-MS m/z: 523 (M^{+}); Anal. Calcd. For C$_{32}$H$_{33}$N$_3$O$_4$: C, 73.42; H, 6.30; N, 8.03. Found: C, 73.72; H, 6.15; N, 7.89.

1-Methyl-4-(2-methylphenyl)pyrrolo-(spiro[2.3″]oxindole)-spiro[3.3′]-1′-methyl-5′-(2-methylphenylmethylidene)piperidin-4′-one (H5):

Obtained as white solid , ^{1}H NMR (300 MHz, CDCl$_3$): δ = 8.85 (1 H, s, NH), 7.51 (1 H, s, C═CH), 6.76–7.85 (12 H,m, Ar), 4.99 (1 H, t, J =9.6 Hz, 4-CH), 4.02 (1 H, t, J =9.6 Hz, 5-CH$_2$), 3.42 (1 H, t, J =8.4 Hz, 5-CH$_2$), 3.28 (1 H, d, J=12.9 Hz, 2′-CH$_2$), 3.18 (1 H, d, J =14.7 Hz, 6′-CH$_2$), 2.89 (1 H, dd, J =14.7,2.4 Hz, 6′-CH$_2$), 2.31 (3 H, s, Ar-CH$_3$), 2.15 (3 H, s, Ar-CH$_3$), 2.14 (3 H, s, 1-N–CH$_3$), 1.96(3 H, s, 1′-N–CH$_3$), 1.68 (1 H, d, J=12.9 Hz, 2′-CH$_2$); ^{13}CNMR(75 MHz, CDCl$_3$): δ = 198.5, 178.0,142.3, 138.0, 137.8, 137.1, 137.0, 134.3, 133.0, 130.2, 130.1, 129.3, 128.6, 128.3, 127.8,127.3, 126.5, 125.7, 125.3, 122.3, 109.1, 76.9, 64.2, 58.4, 57.2, 45.3, 41.6, 34.7, 21.2, 20.1. EI-MS m/z 477.6 (M^{+}); Anal.Calcd for C$_{32}$H$_{33}$N$_3$O$_2$: C, 78.18; H, 6.77; N, 8.55. Found: C, 78.10; H, 6.84; N, 8.64.

1-Methyl-4-(2-methoxyphenyl)pyrrolo-(spiro[2.3″]oxindole)-spiro[3.3′]-1′-methyl-5′-(2-methoxyphenylmethylidene)piperidin-4′-one (H6):

white solid, ^{1}H NMR (300 MHz, CDCl$_3$):δ= 8.79 (1 H, s, NH), 7.69 (1 H, s, C=CH), 6.69–7.62 (12 H,m, Ar), 4.90 (1 H, dd, *J*=10.8, 10.5 Hz, 4-CH), 4.11 (1 H, t, *J*=9.9 Hz, 5-CH$_2$), 3.82 (3 H, s, Ar-OCH$_3$), 3.72 (3 H, s, Ar-OCH$_3$), 3.34 (1 H, t, *J*=8.1 Hz, 5-CH$_2$), 3.22 (1 H, d, *J* =14.4 Hz, 6′-CH$_2$), 3.02 (1 H, d, *J*=12.3 Hz, 2′-CH$_2$), 2.90 (1 H, d, *J*=14.7 Hz, 6′-CH$_2$), 2.14 (3 H, s, 1-N–CH$_3$), 1.93 (3 H, s, 1′-N–CH$_3$), 1.82 (1 H, d, *J*=12.3 Hz, 2′-CH$_2$); ^{13}C NMR (75 MHz, CDCl$_3$):δ= 197.3,178.0, 158.1, 158.0, 142.3, 133.1, 132.6, 130.1, 129.8, 128.5, 128.1, 127.6, 127.4, 127.3,11 124.5, 122.0, 120.3, 119.7, 110.5, 109.8, 108, 7, 77.0, 63.8, 57.0, 56.7, 55.8, 55.3, 54.8, 45.3,39.3, 34.8.EI-MS *m/z* 509.6 (M$^+$); Anal.Calcd for C$_{32}$H$_{33}$N$_3$O$_4$: C, 73.40; H, 6.35; N, 8.02.Found: C, 73.47; H, 6.30; N, 8.09.

1-Methyl-4-(2,4-dichlorophenyl)pyrrolo-(spiro[2.3″]oxindole)-spiro[3.3′]-1′-methyl-5′-(2,4-dichlorophenylmethylidene)piperidin-4′-one (H9):

Obtained as white solid, ^{1}H NMR (300 MHz, CDCl$_3$): δ= 8.63 (1 H, s, NH), 7.50 (1 H, s, C=CH),6.71–8.00 (10 H, m, Ar), 5.05 (1 H, t, *J*=8.4 Hz, 4-CH), 3.86 (1 H, t, *J*=9.0 Hz, 5-CH$_2$), 3.47 (1H, t, *J*=8.4 Hz, 5-CH$_2$), 3.10 (1 H, d, *J* =14.7 Hz, 6′-CH$_2$), 2.89–2.96 (2 H, m, 2′-CH$_2$ and 6′-CH$_2$), 2.10 (3 H, s, 1-N–CH$_3$), 1.94 (3 H, s, 1′-N–CH$_3$), 1.80 (1 H, d, *J*=12.6 Hz, 2′-CH$_2$); ^{13}C NMR (75 MHz, CDCl$_3$): δ= 197.0, 177.8, 142.0, 136.3, 135.6, 135.5, 134.9, 134.4, 133.5, 132.9, 132.0,131.7, 130.5, 129.6, 128.9, 128.7, 127.8, 127.0, 126.6, 126.3, 122.6, 109.0, 77.0, 63.5, 57.8,57.7, 56.9, 45.4, 41.7, 34.7. EI-MS *m/z* 585.05 (M$^+$);Anal.Calcd for C$_{30}$H$_{25}$Cl$_4$N$_3$O$_2$: C,59.92; H, 4.19; N, 6.99.Found: C, 59.82; H, 4.29; N, 6.91.

6.1.4 *In vitro* SIRT1 Assay:

SIRT1 fluorimetric enzyme assay is based on unique SIRT1 substrate/developer combination. The substrate usually consisted of 4 amino acids from 379-382 [(Arg-His-Lys-Lys (Ac)] of human p53, which was tagged with aminomethylcoumarin (AMC). The fluorescence signal is generated in proportional to the amount of deacetylation of lysine in the substrate. SIRT1 activation of synthesized SP derivatives was studied by *in vitro* assay using recombinant SIRT1 and fluorophore-labeled acetylated p53 peptide substrate according to protocol mentioned under section 4.4. As shown in **Fig.6.2**, **H3** and **H6** showed significant increase in the SIRT1 activity compare to standard resveratrol whereas **H2, H5, H8** and **H9** showed moderate activation. Furthermore compounds **H1, H4, H7**, and **H10** don't show any significant activation.
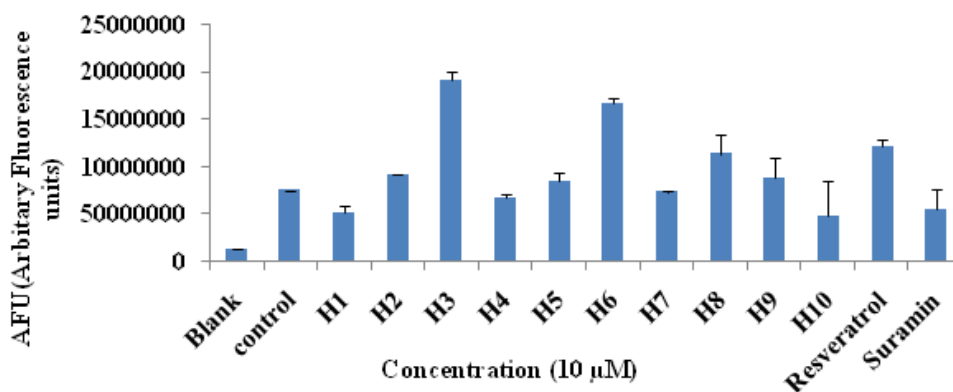

Fig.6.2: *In vitro* SIRT1 activation of SP derivatives (**H1-10**).

6.1.5 Detection of acetylated/deacetylated substrate by RP-HPLC:

SIRT1 activation by **H3** and **H6** was studied in terms of increase in deacetylation of acetylated substrate [(Arg-His-Lys-Lys (Ac)] by using RP-HPLC method according to protocol explained under section 4.5.
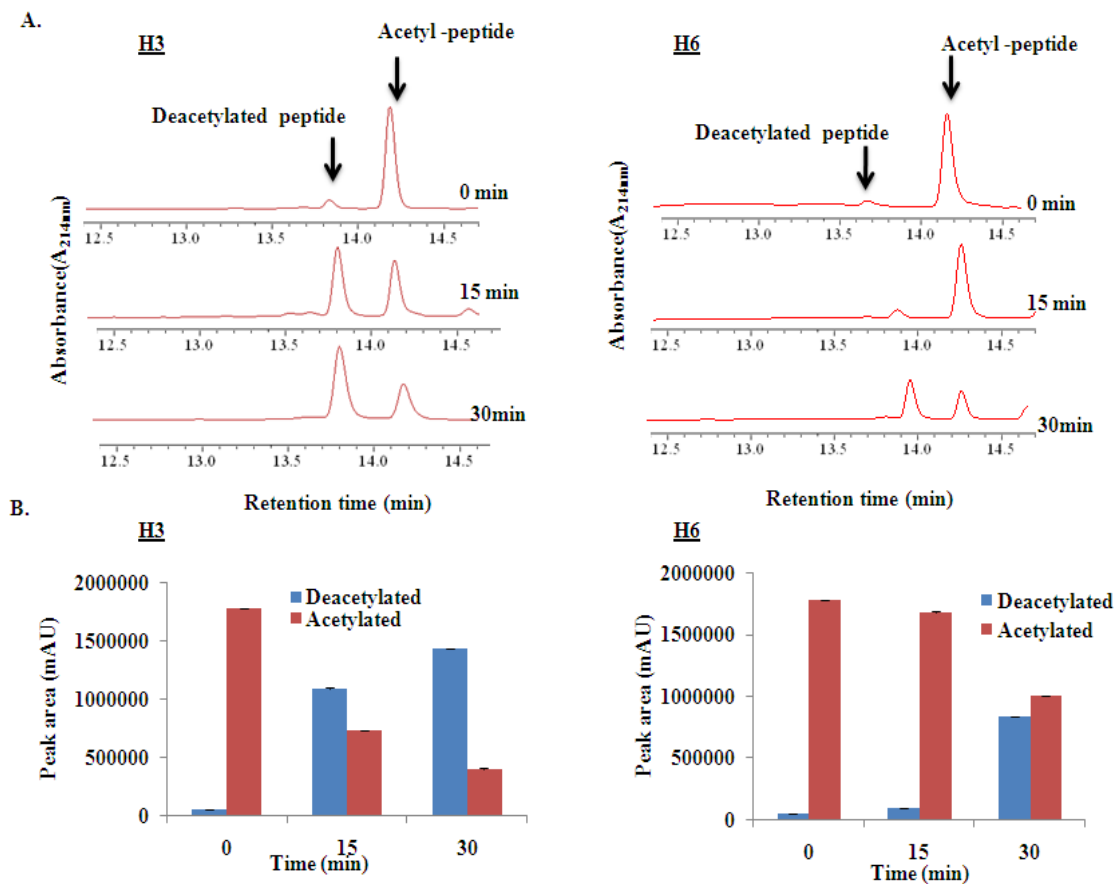
Fig.6.3: A. Detection of acetylated and deacetylated peptide peak treated by **H3 and H6** by HPLC. **B.** Peak areas of acetylated and deacetylated products are represented in bar graph.

As illustrated in **Fig.6.3**, compound **H3**exhibited significant increase in deacetylation of acetylated substrate peak in time dependent manner at 10 µM concentration compare to **H6**. Hence further experiments were continued with **H3.**

6.1.6 Effect of H3 on 3T3-L1 cells:

In order to investigate the antiobesity activity of **H3** in the well-known cell based adipogenesis differentiation assay, $1*10^5$3T3-L1cells were treated with increasing concentrations (0, 10, 50 µM) of **H3** along with differentiation media containing insulin, dexamethasone,

IBMX. Treatment was continued until differentiation was observed in control cells (untreated). Inhibition of differentiation by **H3** was measured by Oil O Red staining. After treatment, plates were washed with PBS, and the cells were fixed in 10% formaldehyde for 1 h and stained with Oil O Red staining according to protocol described under section 4.6.3. As shown in **Fig.6.4**, microscopically the intensity of Oil O Red staining decreased dose dependently during differentiation.
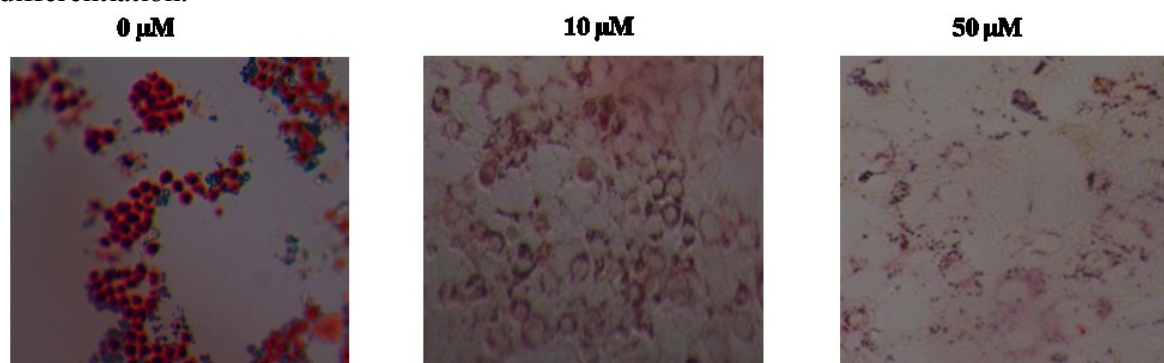
Fig.6.4: Inverted microscopic pictures of 3T3-L1 cells treated with **H3** at different concentrations.

Quantification of the dye extracted from cells treated with **H3** during differentiation as well as in mature adipocytes using a spectrophotometer was described in detail in the materials and methods section 4.6.3 and results are shown in **Fig.6.5**.
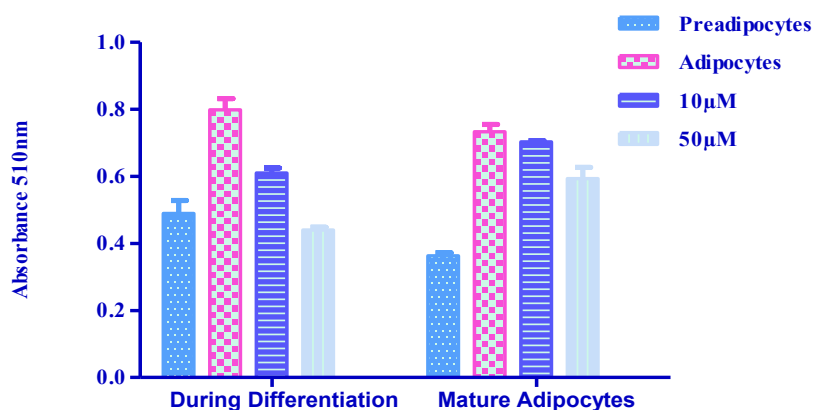
Fig.6.5: Measurement of lipid accumulation in preadipocytes and mature adipocytes treated with **H3**.

Intensity of dye incorporated also decreased in fully differentiated adipocytes treated with **H3**, demonstrating the decrease in amounts of fatty acids and triglycerides produced by the cells. These results suggest that the compound identified with SIRT1 activating properties have a significant effect on fat mobilization in differentiated adipocytes, and thus **H3** is anticipated to have antiobesity properties.

6.1.7 Measurement of Triglycerides:

$1*10^5$ fully differentiated 3T3-L1 adipocytes were treated with different concentrations (0, 10, 50 µM) of **H3** for 24h. Total triglyceride content in cells was measured according to protocol explained in section 4.6.4.
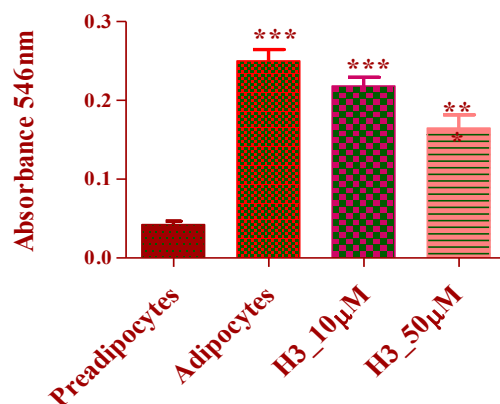
Fig.6.6: Triglyceride accumulation in mature adipocytes treated with various concentrations of **H3**.

As shown in **Fig.6.6**, a dose dependent decrease in triglyceride accumulation was observed with **H3**.

6.1.8 RT- PCR analysis:

$1*10^6$ 3T3-L1 adipocytes treated with **H3** at 0, 10, 50 µM concentrations for 24h and checked for transcript levels of SIRT1, PPARγ, C/EBPα, E2F1, leptin, FAS and LPL according to protocol explained under section 4.6.8 using gene specific primers specified in **Table 2** of material and methods section.
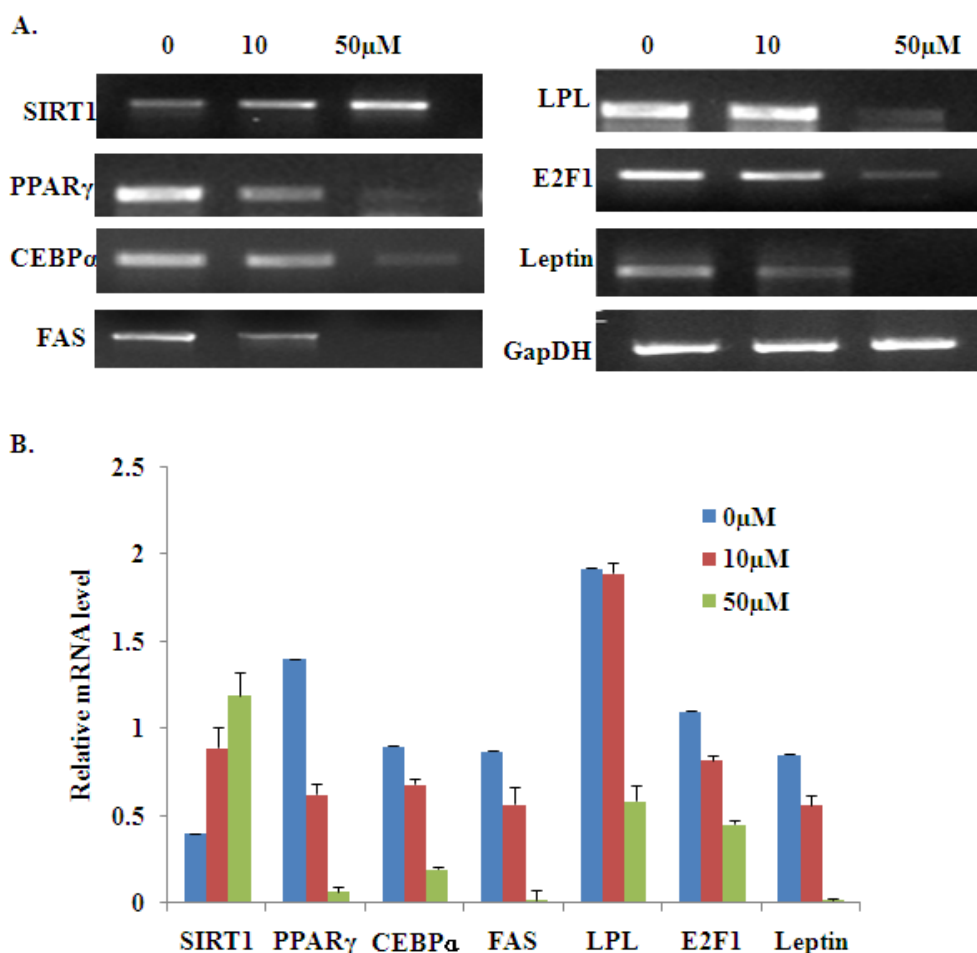
Fig.6.7: **A.** RT-PCR analysis of adipogenic enzymes in fully differentiated adipocytes treated with **H3** at different concentrations. **B**. Quantification of band intensity by using Image lab analysis software.

As shown in **Fig.6.7A**, a dose dependent increase in SIRT1 levels clearly demonstrated the SIRT1-mediated antiadipogenic activity of **H3**. Further, a dose-dependent decrease in expression of transcription factors PPARγ, C/EBPα was observed. Additionally FAS, LPL, E2F1 and leptin gene expression was dose dependently and significantly down regulated by **H3** treatment. Equal loading was confirmed by GapDH. Quantification of band intensity was done by Image lab analysis software and results were shown in **Fig.6.7B**.

6.1.9: *In vivo* studies on HFD induced obese mice:

Obesity was induced by feeding HFD to male albino mice for 3 months and treated with **H3** at a concentration of 30 mg/kg body weight for one month according to procedure explained under materials and methods section 4.7.3. Orlistat was used as a standard antiobesity drug at a concentration of 30mg/kg body weight.
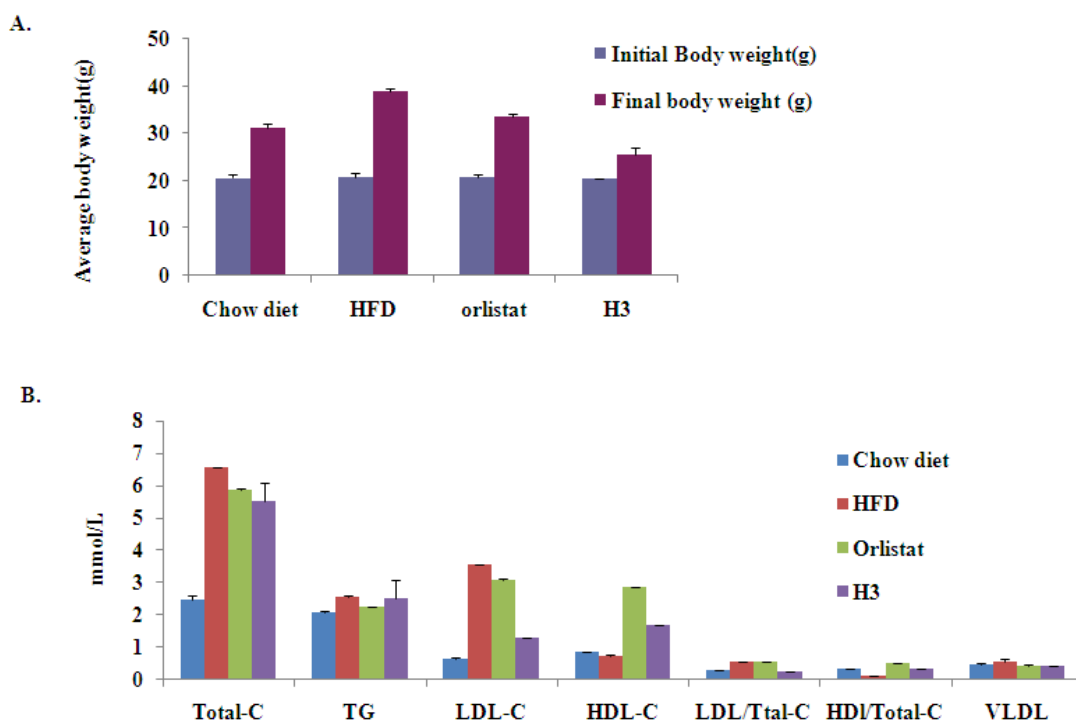
Fig.6.8: A. Average body weight of mice before and after treatment with **H3** along with HFD. **B.** Serum lipid profile after treatment with **H3**.

As shown in **Fig.6.8A**, body weight gain of the HFD group mice was considerably higher than the other groups. The weight gain of Orlistat and **H3** groups were normalized to the chow diet group. Feed intake of all experimental groups was not significantly different. Modulation in serum lipids profile was shown in **Fig.6.8B**.

6.1.10 Discussion:

In recent years, SIRT1 has become an interesting and promising target in terms of its effects on longevity, metabolism, and other aging-related disorders. Several small-molecule activators of SIRT1 have been identified by utilizing a commercially available deacetylase activity assay. In the present study we identified and demonstrated a novel SIRT1 activator 1-Methyl-4-(2-methoxyphenyl)pyrrolo-(spiro[2,3″]oxindole)-spiro[3,3′]-1′-methyl-5′-(2-methoxyphenylmethylidene) piperidin-4′-one (**H3**). Since crystal structure of SIRT1 was not available the best model of the allosteric domain (114-217AA) of SIRT1was developed and the fitness of the model was checked by PROCHECK program. This model showed 92.9% residues in most favored regions and ProSA Web Z score of -6.38 similar to the template structure scores. Binding site pocket was identified using SITEMAP and pocket contains ASP166; ARG167; SER169; HIS170;ALA171; SER172; SER173; SER174; ASP175; TRP176; PRO184; TYR185; PHE187; VAL188; HIS191; LEU192 amino acid residues with respect to full length SIRT1 sequence. Virtual screening of *in house* database of ~3000 molecules was carried out by using GLIDE against allosteric domain of SIRT1 and a series of spiro-piperidin-4-ones (**SP**) derivatives (**H1-10**) were identified as lead molecules. At 10 μM concentration, **H3 and H6** showed 2-3 fold increase in SIRT1 deacetylase activity which is better than the reference compound resveratrol whereas **H2, H5, H8** and **H9** showed moderate to low activation. Remaining compounds demonstrated low or no activation with respect to control.

Further quantification of deacetylation/acetylation of acetylated peptide was performed by RP-HPLC. SIRT1 incubated with 10μM concentration of **H3** and **H6** for different time periods (0, 15, 30min) and reaction was initiated by adding substrate. The conversion was determined by calculating peak areas at retention time ~13.8 min and ~14.2 min for deacetylated and acetylated products respectively. **Fig.6.3** clearly demonstrates that peak area of deacetylated product increased time dependently for SIRT1 incubated with **H3** but no significant increase with **H6**. The significant activation of SIRT1 by **H3** and **H6** was contributed due to the presence of methoxy phenyl ($-OCH_3C_6H_4$) substitution at *para* and *ortho* positions.

In order to validate the above results, the antiobesity activity of **H3** was performed in the well-known cell based adipogenesis differentiation assay. 3T3-L1 cells were treated with varying concentration of **H3** during differentiation of preadipocytes to adipocytes and also in mature adipocytes. Inhibition of differentiation by **H3** was measured by Oil O Red staining. Microscopically the intensity of Oil O Red staining decreased dose dependently. The size and number of intracellular cytosolic fat deposits are reduced in a dose dependant manner (**Fig.6.3**) confirming the inhibition of adipocyte differentiation by **H3**. Thus **H3** is anticipated to have antiobesity and/or antidiabetic properties.

SIRT1 has been shown to regulate transcription of various downstream targets like PPARγ, C/EBPα [Picard F., *et al*., 2004], leptin, LPL [Bordone L., *et al*., 2007] which control the fat metabolism and mobilization. To establish mechanistic insights, mRNA levels of SIRT1 and its downstream targets like PPARγ and C/EBPα were studied in mature adipocytes treated with various concentrations of **H3** by RT-PCR. As shown in **Fig.6.7A,** a dose dependent increase in transcript levels of SIRT1 and decrease in PPARγ and C/EBPα were observed which demonstrates the SIRT1 mediated inhibition of adipogenesis by **H3**.

Under fasting conditions, SIRT1 transcription is regulated by p53 and FOXO3a [Nemoto S., *et al*., 2004] and E2F1 in response to DNA damage. Further it has been reported SIRT1 regulate E2F1 expression in negative feedback mechanism. Thus mRNA levels of E2F1 were also studied and dose dependent decrease in levels of E2F1 was observed. Expression of mRNA levels of lipoprotein lipase, marker of adipocyte differentiation in mature adipocyte indicates lipid accumulation. LPL hydrolyses the triacylglycerides and promotes cellular uptake of chylomicron remnants, cholesterol-rich lipoproteins, and free fatty acids. Decrease in transcript levels of LPL in **Fig.6.7A** corroborates the reduced lipid accumulation in mature adipocytes. Another important adipocyte gene, FAS is the crucial enzyme in de novo lipogenesis, catalyzing the reactions for the synthesis of long-chain fatty acids [Sul H.S., *et al*., 1998] and its expression increases during adipogenesis[Student A.K., *et al*., 1980]. Reduced levels of FAS was also observed in cells treated with **H3** demonstrating the inhibition of denovo lipogenesis. Leptin is an endocrine /paracrine hormone secreted from adipocytes plays a crucial role in food intake and energy balance. Leptin levels increases in mature adipocytes and decreases with increasing expression of SIRT1. **Fig.6.7A** also further confirms the decrease in leptin levels with **H3**. To authenticate the *in vitro* antiobesity properties of **H3**, preliminary *in vivo* studies were performed on HFD induced obese mice. HFD induced mice (n=6) were treated orally with test (**H3**) and standard (**Orlistat**) at a concentration of 30 mg/kg body weight for one month and body weight and lipid profile were measured. As shown in **Fig.6.8A**, **H3** showed reduction in body weight gain significantly lower serum Total-C concentration, TG concentration, LDL-C concentration, and the ratio of LDL-C/ Total-C compared to the HFD group. Supplementation of **Orlistat** and **H3**exhibited a trend towards increased serum HDL-C levels, compared to HFD group, and the ratio of HDL-C/ Total-C exhibited higher values in the **Orlistat** and **H3** treated group than in the

HFD group. These results are in agreement with the previous results reported by Daozong Xia *et al.,* group on HFD induced mice model [Xia D., *et al*., 2010]

6.2 Design, synthesis, biological interventions of Pyrido[2,3-d]pyrimidine (PP) derivatives:

6.2.1 Design of homology model of allosteric site and active site prediction:

Homology model of hSIRT1 allosteric site was generated by using comparative homology modeling procedure explained under materials and methods section 4.1. Ribbon model of allosteric site and active site pocket was shown in **Fig.6.1**. This model showed 92.9% residues in most favored regions and ProSA Web Z score of -6.38 similar to the template structure scores. Binding site pocket was identified by using SITEMAP and contains ASP166; ARG167; SER169; HIS170; ALA171; SER172; SER173; SER174; ASP175; TRP176; PRO184; TYR185; PHE187; VAL188; HIS191; LEU192 amino acid residues with respect to full length SIRT1 sequence.

6.2.2 High-throughput virtual screening of *in house* database:

High-throughput virtual screening of *in house* database of ~3000 molecules into allosteric site of SIRT1 revealed pyrido[2,3-d]pyrimidine pharmacophore as a lead pharmacophore (**PP1-5**) (**Fig.6.8**). Binding energy, docking score were presented in **Table 12**.
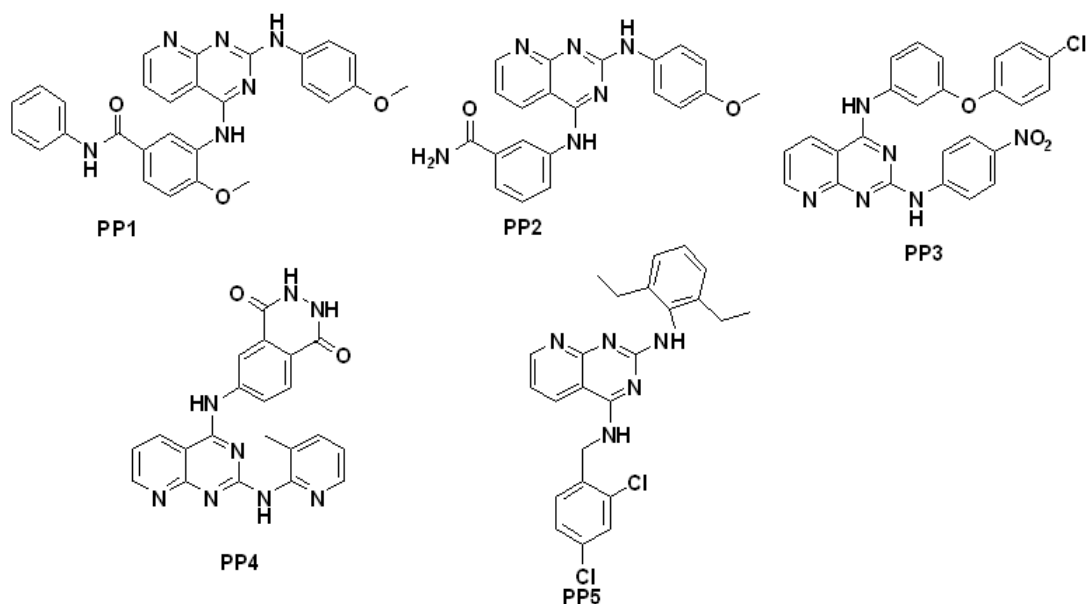
Fig.6.9: Pyrido[2,3-d] pyrimidine hit molecules from virtual screening.

Table 12: SIRT1 activation, docking score, Hbond of Pyrido[2,3-d]pyrimidine hit molecules (**PP1-5**).

Code	% SIRT1 Activation @ 5μM concentration	Docking score	HBond
PP1	203.2	-2.2	2
PP2	176.4	-3.6	3
PP3	159.0	-3.1	1
PP4	168.2	-3.1	3
PP5	129	-2.5	1

Ligand interaction diagram of most active compounds **PP1** and **PP2** among the hit molecules was depicted below.

A.
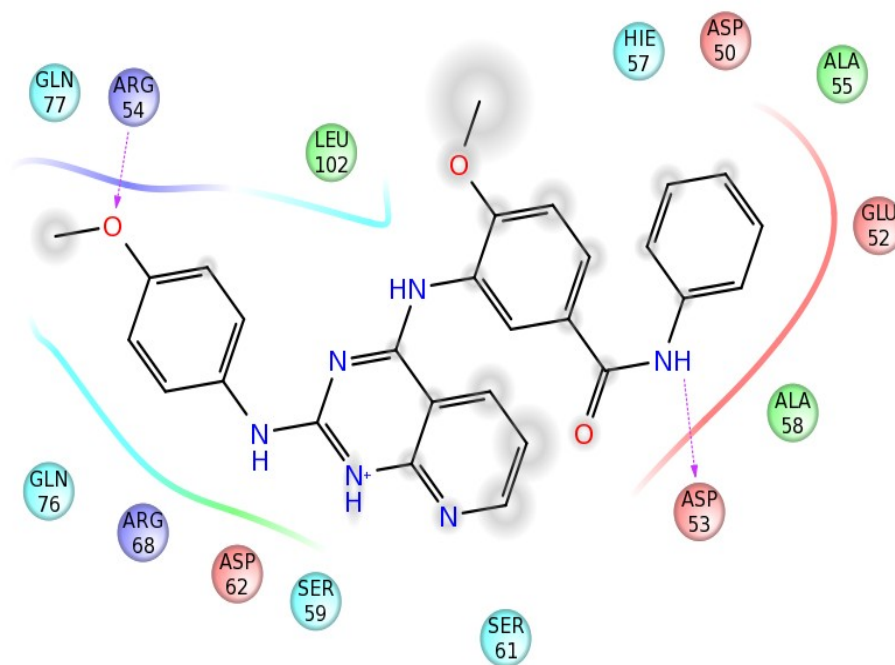
B.
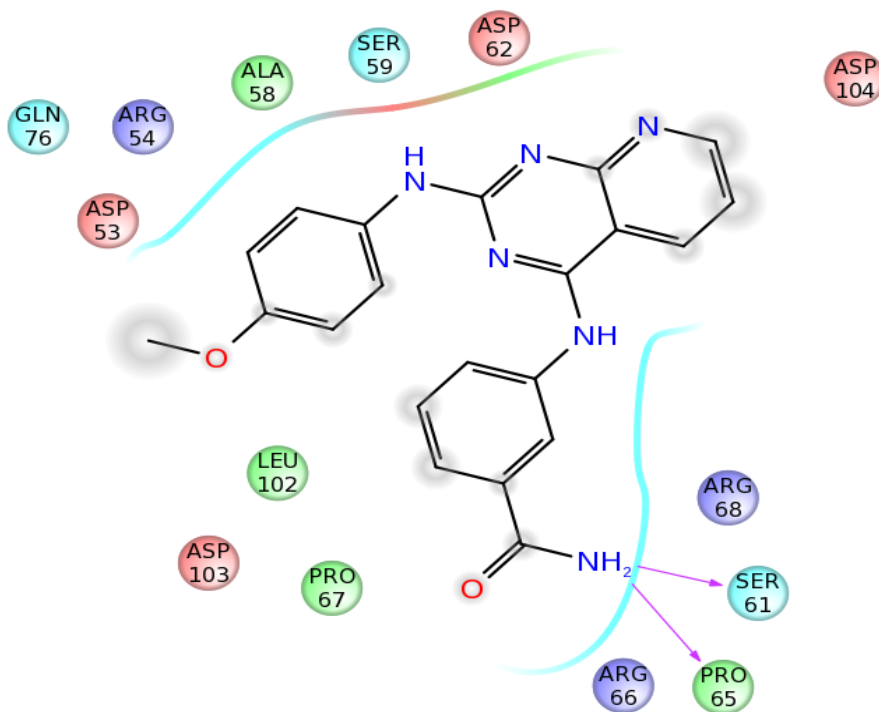
Fig.6.10: Ligand interaction diagram of hit compounds **A**: **PP1** and **B**: **PP2**

In order to construct SAR, various analogues **A1-14** and **B1-14** were designed and synthesized based on hit compounds **PP1** and **PP2**. Docking score, physicochemical properties were tabulated in **Table 13**.

6.2.3 Synthesis and Characterization

a.neat,28°C/CO₂ gas; b.POCl₃,reflux,12h; c.NaH,R1-NH₂,THF,0°C to RT; d.R₂-NH₂,Xanthphos,Cs₂CO₃,DME,90°C,4h
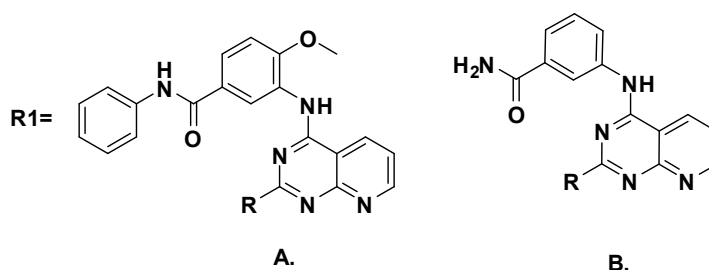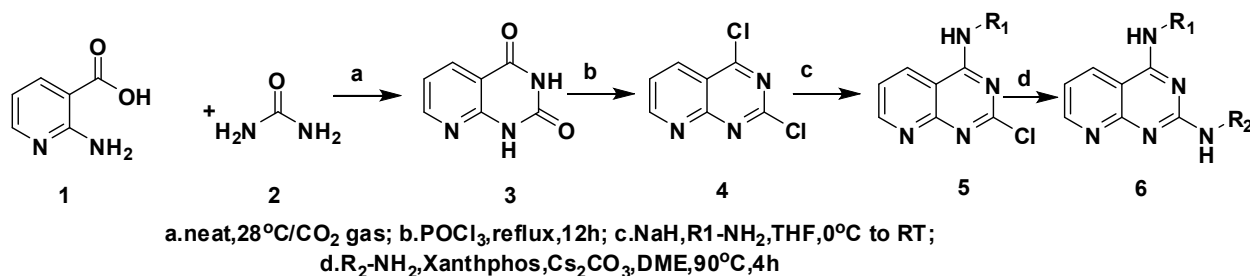
Synthesis of 2,4-dichloropyrido[2,3-d]pyrimidine: Prepared by condensing 2-aminonicotinic acid (**1**) and urea (**2**) at 210 °C to give dihydroxypyrido[2,3-d]pyrimidine (**3**) which was further chlorinated by refluxing it with phosphorous oxychloride to give the dichloro derivative (**4**) as previously reported by Robin and Hitchings [Robins R.K., *et al*., 1954]. To a suspension of sodium hydride (0.4g, 60% in oil, 9.9 mmol) in DMF (10ml) at 0°C was added drop wise a solution of corresponding nucleophile (For 3-aminobenzamide: 0.68g, 4.9 mmol) in DMF (10ml). The reaction was slowly warmed to RT and stirred for 20min at RT. A solution of 2,4-dichloroPyrido[2,3-d]pyrimidine (**4**) (1g, 4.9 mmol) in DMF (10ml) was added drop wise at 0°C and the reaction mixture was stirred at RT for 8 hours. The reaction mixture was quenched with saturated NH₄Cl solution (1*20ml) and extracted with dichloromethane (2*30ml). The combined

organic layer was then washed with brine (1*20ml), dried over anhydrous Na$_2$SO$_4$and evaporated under vacuo. The residue was then purified by column chromatography to give the desired product in quantitative yield **5 (A and B)**.

As 'B' is available commercially, it was purchased and used for library synthesis. In the cases where the corresponding nucleophiles were not commercially available, it was synthesized from the commercially available acid by following procedure.
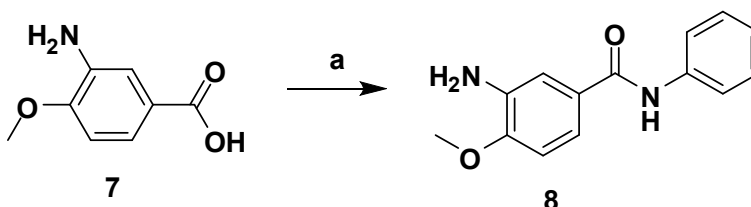
a. i.(COCI)$_2$,DCM, DMF(cat). ii Aniline, (C$_2$H$_5$)$_3$N, DMF

A solution of 3-Amino-4-methoxy benzoyl chloride (**7**) (1g, 5.4mmol, prepared via oxalyl chloride) in dry DMF (10ml) was added to a well stirred mixture of aniline (0.5g, 5.4mmol) and triethylamine (0.82g, 8.1mmol) in DMF (10ml) at 0°C. The reaction mixture was slowly warmed to room temperature (RT) and stirred at RT for 5h.The reaction mixture was poured into water (20ml)and neutralised to pH 8 and extracted with ethyl acetate (2*40ml). The organic layer was washed with water (1*25ml), dried over anhydrous Na$_2$SO$_4$, and evaporated. The resultant residue was purified by column chromatography to give the desired product as yellowish white solid (**8**) (0.98g, 75.4%).
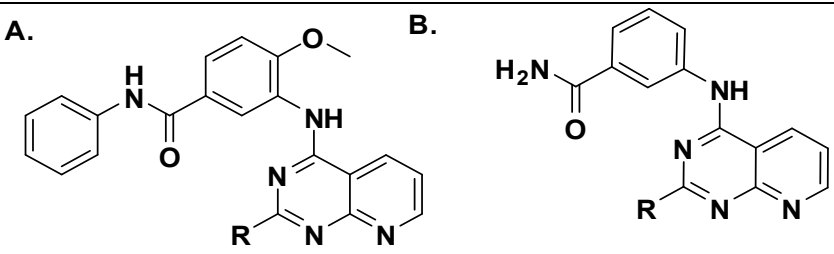
General Procedure for library synthesis:

The Final library was achieved by the Buchwald-Hartwig reaction of amines by the following procedure: To a well stirred and degassed (by argon bubbling) solution of the corresponding 4-chloro-2-substitutedpyrido[2,3-d]pyrimidines (**5**) (For 3-(2-chloropyrido[2,3-

d]pyrimidin-4-ylamino)benzamide: 0.25g, 0.83 mmol) in *tert*-butanol (6ml) was added Pd_2dba_3 (0.15g, 0.17 mmol), 2-dicyclohexylphosphino-2′-4′,6′-triisopropylbiphenyl (0.27g, 0.58 mmol), K_2CO_3 (0.34g, 2.5 mmol) and the corresponding nucleophile (For Aniline (A1) 0.1g, 1.08 mmol) and refluxed for 13 h. The reaction mixture was diluted with ethyl acetate (15ml), washed with 1 N aqueous HCl (1*7ml) and brine (1*10ml), and dried over Na_2SO_4, and evaporated under vacuo. The residue was further purified by flash chromatography to give the desired product in quantitative yield (**6**).

A Library of 28 final compounds were synthesised based on the virtual screening/ SAR inputs and as is evident from the **Table 13**, all the reactions went smoothly giving the desired product in quantitative yield. Both analytical and spectral data (^{1}H NMR, ^{13}C NMR, and Mass spectra) of all the synthesized compounds were in full agreement with the proposed structures.

Table 13: Physico-chemical properties and docking scores of **A1-14** and **B1-14 (PP Series)**.

Code	R	Glide score	M.P(^{0}C)	Yield (%)	Molecular Formula	Molecular Weight
A1	Phenyl	-3.16	190-192	72	$C_{20}H_{16}N_6O$	356.13
A2	3-Chloro-2-methylphenyl	-3.52	116-118	63	$C_{21}H_{17}ClN_6O$	404.12
A 3	4-Nitrophenyl	-4.21	160-162	77	$C_{20}H_{15}N_7O_3$	401.1
A 4	2,4-Dimethoxyphenyl	-4.35	228-230	65	$C_{22}H_{20}N_6O_3$	416.21
A 5	3-Fluoro-6-methylphenyl	-4.32	Brown oil	78	$C_{21}H_{17}FN_6O$	388.14

A 6	2-Pyridyl	-4.06	192-194	70	$C_{19}H_{15}N_7O$	357.20
A 7	3-Methyl-2-pyridyl	-4.03	Brown oil	63	$C_{20}H_{17}N_7O$	371.15
A 8	5-Nitrothiazol-2-yl	-3.40	210-212	67	$C_{17}H_{12}N_8O_3S$	408.08
A 9	6-Nitro2-benzothiazolyl	-2.35	230-232	69	$C_{21}H_{14}N_8O_3S$	458.08
A 10	Benzyl	-2.35	160-162	84	$C_{21}H_{18}N_6O$	370.15
A 11	4-Bromophenyl	-3.03	227-229	79	$C_{20}H_{15}BrN_6O$	434, 436
A 12	4-Chlorophenyl	-4.06	236-238	78	$C_{20}H_{15}ClN_6O$	390.1
A 13	2,6-Diethylphenyl	-3.90	119-121	71	$C_{24}H_{24}N_6O$	412.20
A 14	Pyridin-4-ylamino	-3.56	127-129	69	$C_{19}H_{15}N_7O$	357.13
B1	Phenyl	-3.89	121-123	80	$C_{27}H_{22}N_6O_2$	462.19
B2	3-Chloro-2-methylphenyl	-3.97	110-112	73	$C_{28}H_{23}ClN_6O_2$	510.16
B 3	4-Nitrophenyl	-3.97	122-124	80	$C_{27}H_{21}N_7O_4$	507.17
B 4	2,4-Dimethoxyphenyl	-4.45	305-307	66	$C_{29}H_{26}N_6O_4$	522.20
B 5	3-Fluoro-6-methylphenyl	-4.36	140-142	79	$C_{28}H_{23}FN_6O_2$	494.20
B 6	2-Pyridyl	-4.28	200-202	71	$C_{26}H_{21}N_7O_2$	463.17
B 7	3-Methyl-2-pyridyl	-4.23	110-112	73	$C_{27}H_{23}N_7O_2$	477.23
B 8	5-Nitrothiazol-2-yl	-3.45	218-220	75	$C_{24}H_{18}N_8O_4S$	514.12
B 9	6-Nitro2-benzothiazolyl	-5.67	220-222	69	$C_{28}H_{20}N_8O_4S$	564.14
B 10	Benzyl	-4.50	98-100	84	$C_{28}H_{24}N_6O_2$	476.53
B 11	4-Bromophenyl	-3.91	222-224	76	$C_{27}H_{21}BrN_6O_2$	540.1
B 12	4-Chlorophenyl	-3.94	230-232	80	$C_{27}H_{21}ClN_6O_2$	496.14
B 13	2,6-Diethylphenyl	-4.06	115-117	77	$C_{31}H_{30}N_6O_2$	518.23
B 14	Pyridin-4-ylamino	-5.07	332-334	65	$C_{26}H_{21}N_7O_2$	463.18

3-(2-Chloropyrido[2,3-d]pyrimidin-4-ylamino)-4-methoxy-N-phenylbenzamide (A):

Off-white solid; ^{1}H NMR (300 MHz, CDCl$_3$): δ = 3.82 (s, 3H, -OCH$_3$), 6.96-7.03 (m, 2H, Ar-H), 7.21-7.63 (m, 7H, H$_6$& 6-Ar-H), 8.3 (dd, 1H,H$_5$, J= 1.7Hz, J= 7.6Hz), 8.83 (dd,1H, H$_7$, J = 1.6 Hz, J=4.8Hz). ^{13}C NMR (75MHz, CDCl$_3$): δ = 163.9, 158.3, 156.4, 156.1, 153, 151.2, 138.3, 133, 129.2, 127.8, 127.1, 126.8, 121.8, 119.3, 116.1, 114.3, 113, 106.4, 57.2. EI-MS *m/z*: 405.10 [M$^+$]. Anal.Calcd for C$_{21}$H$_{16}$ClN$_5$O$_2$: C, 62.15; H, 3.97; N, 17.26. Found: C, 62.21; H, 4.01; N, 17.24

4-Methoxy-N-phenyl-3-(2-(phenylamino)pyrido[2,3-d]pyrimidin-4-ylamino)benzamide (A1):

Buff coloured solid; ^{1}H NMR (300 MHz, CDCl$_3$): δ = 3.83 (s, 3H, -OCH$_3$), 6.86-7.01 (m, 3H, Ar-H), 7.16-7.69 (m, 11H, H$_6$ & 10 Ar-H), 8.42 (1H, dd, H$_5$, J = 1.7Hz, J = 7.8Hz), 8.83 (dd, 1H, H$_7$, J = 1.5Hz, J = 4.7Hz).^{13}C NMR (75MHz, CDCl$_3$): δ = 168.5, 164, 156.3, 155.7, 153.2, 151.3, 139.1, 138.3, 132.9, 129.9, 129.2, 128, 127.4, 126.7, 122.7, 121.8, 118.6, 117.8, 116.4, 114.4, 113, 96, 57.4. EI-MS *m/z* 462.19 (M$^+$). Anal.Calcd for C$_{27}$H$_{22}$N$_6$O$_2$: C, 70.12; H, 4.79; N, 18.17: Found: C, 69.98; H, 4.73; N, 18.15.

3-(2-(2,4-Dimethoxyphenylamino)pyrido[2,3-d]pyrimidin-4-ylamino)-4-methoxy-N-phenylbenzamide (A4):

Brown solid;^{1}H NMR (300 MHz, CDCl$_3$): δ = 3.83 (s, 3H, -OCH$_3$), 3.86 (s, 3H, -OCH$_3$), 3.87 (s, 3H, -OCH$_3$), 6.34-6.42 (m, 3H, Ar-H), 6.94-6.98 (m, 2H Ar-H), 7.31-7.67 (m, 7H, H$_6$ & 6Ar-H), 8.31 (dd, H$_5$, J = 1.4Hz, J = 7.8Hz), 8.78 (dd, H$_7$, J = 1.4Hz, J = 4.3Hz). ^{13}C NMR (75MHz, CDCl$_3$): δ = 168.6, 164.3, 163.6, 156.6, 155.4, 153.3, 151.2, 148.7, 138.3, 133, 129, 128.4, 127.8, 126.9, 125.3, 121.7, 118.6, 115.7, 114.3, 113, 107.8, 101.3, 96.2, 57.6, 57.3, 56.9. EI-MS

m/z: 522.20 (M$^+$). Anal.Calcd for $C_{29}H_{26}N_6O_4$: C, 66.66; H, 5.02; N, 16.08; Found: C, 66.65; H, 5.05; N, 16.07.

3-(2-(Pyridin-2-ylamino)pyrido[2,3-d]pyrimidin-4-ylamino)-4-methoxy-N-phenylbenzamide (A6):

Brown solid; ^{1}H NMR (300 MHz, CDCl$_3$): δ = 3.83 (s, 3H, -OCH$_3$), 6.67-6.98 (m, 4H, Ar-H), 7.28-7.63 (m, 8H, H$_6$ & 7 Ar-H). 8.11 (d, 1H, J = 7.8Hz, Ar-H), 8.36 (dd, 1H, H$_5$, J = 1.8Hz, J = 7.6Hz), 8.78 (dd, 1H, H$_7$, J = 1.4Hz, J = 4.8Hz). ^{13}C NMR (75MHz, CDCl$_3$): δ = 168.5, 164.1, 156.3, 155.6, 154.7, 153.1, 151.2, 149.4, 138.5, 138.1, 132.9, 129, 128.1, 127.4, 126.7, 121.7, 118.8, 118, 116.3, 114.2, 113, 108.1, 96.2, 57.4. EI-MS *m/z:* 463.17 (M$^+$). Anal.Calcd for $C_{26}H_{21}N_7O_2$: C, 67.38; H, 4.57; N, 21.15; Found: C, 67.41; H, 4.57; N, 21.35.

4-Methoxy-3-(2-(6-nitrobenzo[d]thiazol-2-ylamino)pyrido[2,3-d]pyrimidin-4-ylamino)-N-phenylbenzamide(A9):

Orange yellow solid; ^{1}H NMR (300 MHz, CDCl$_3$): δ = 3.83 (s, 3H, -OCH$_3$), 6.91-6.97 (m, 2H, Ar-H), 7.21-7.67 (m, 7H, H$_6$, & 6 Ar-H), 8.06 (d, J=6.4Hz, 1-Bt-H), 8.29-8.78 (m, 4H, H$_5$, H$_7$& 2-Bt-H). ^{13}C NMR (75MHz, CDCl$_3$): δ = 174.7, 168.5, 164.1, 159.6, 156.5, 155.4, 153, 151, 144.7, 138, 132.7, 131.4, 129, 128.3, 127.3, 126.8, 121.8, 121.3, 119.3, 118.5, 117.6, 115.9, 114.3, 113, 96.1, 57.3. EI-MS *m/z:* 564.14 (M$^+$). Anal.Calcd for $C_{28}H_{20}N_8O_4S$: C, 59.57; H, 3.57; N, 19.85.Found:C, 59.61; H, 3.54; N, 19.83.

3-(2-Chloropyrido[2,3-d]pyrimidin-4-ylamino) benzamide (B):

Off whitesolid;.^{1}H NMR (300 MHz, CDCl$_3$): δ = 7.12 (d, 1H, J = 7.2Hz), 7.28-7.36 (m, 3H, H$_6$ & 2 Ar H), 7.83 (d , 1H, J = 6.9Hz, 1 Ar H), 8.31 (dd, 1H, H$_5$, J = 1.7Hz, J = 7.5Hz), 8.79 (dd, 1H, H$_7$, J = 1.6Hz, J = 4.7Hz) ^{13}C NMR (75MHz, CDCl$_3$): δ = 169.6, 158.1, 155.9, 153.2, 153,

142.7, 135.3, 133.6, 127.1, 121.8, 117.5, 114.0, 111.8, 103.2 MS *m/z* 299.06 (M$^+$). Anal.Calcd

forC$_{14}$H$_{10}$ClN$_5$O: C, 56.10; H, 3.36; N, 23.37; Found: C, 56.13; H, 3.34; N, 23.33

3-(2-(Phenylamino)pyrido[2,3-d]pyrimidin-4-ylamino)benzamide (B1):

Brown solid; ^{1}H NMR (300 MHz, CDCl$_3$): δ = 7.03-7.41 (m, 7H, H$_6$ & 6 Ar-H), 7.67-7.71 (m,

2H, Ar-H), 7.86 (d, 1H, J = 7.4Hz, Ar-H) 8.43 (dd, 1H, H$_5$, J = 1.8Hz, J = 7.6Hz), 8.87 (dd, 1H,

H$_7$, J=1.6Hz, J=4.9Hz). ^{13}C NMR (75MHz, CDCl$_3$): δ = 171.6, 171.1, 156.8, 155.2, 153.1, 142.7,

137.1, 135.2, 133.8, 129.5, 127.3, 123.3, 122.1, 118.3, 117.8, 113.9, 111.7, 95.6.MS *m/z* 356.13

(M$^+$). Anal.Calcd for C$_{20}$H$_{16}$N$_6$O: C, 67.40; H, 4.53; N, 23.58; Found: C, 67.31; H, 4.51; N,

23.24.

3-(2-(2,4-Dimethoxyphenylamino)pyrido[2,3-d]pyrimidin-4-ylamino)benzamide (B4):

Light brown solid;.^{1}H NMR (300 MHz, CDCl$_3$): δ = 3.79 (s, 3H, -OCH$_3$),3.81 (s, 3H, -OCH$_3$),

6.46-6.57 (m, 3H, H$_6$ & 2 Ar-H),7.12 (s, 1H, Ar-H), 7.32-7.47 (m, 3H, H$_6$ & 2 Ar-H), 7.83 (d,

1H, J= 7.8Hz, Ar-H), 8.46 (1H, dd, H$_5$, J = 1.8Hz, J = 7.3Hz), 8.84 (1H, dd, H$_7$, J = 1.4Hz, J =

4.8Hz).^{13}C NMR (75MHz, CDCl$_3$): δ = 171.5, 170.9, 165.8, 156.5, 155.4, 153.2, 148.3, 142.9,

135.2, 133.9, 127.4, 124.2, 122.9, 118.2, 117.5, 114.1, 111.8, 107.8, 101.6, 96, 56.2, 55.9. EI-MS

m/z 416.21(M$^+$). Anal.Calcd for C$_{22}$H$_{20}$N$_6$O$_3$: C, 63.45; H, 4.84; N, 20.18; Found:C, 63.39; H,

4.86; N, 20.21.

3-(2-(Pyridin-2-ylamino)pyrido[2,3-d]pyrimidin-4-ylamino)benzamide (B6):

Buff colour solid; ^{1}H NMR (300 MHz, CDCl$_3$): δ = 6.67-6.84 (m, 2H, Ar-H), 7.06 (s, 1H, Ar-

H), 7.33-7.42 (m, 3H, H$_6$ & 2 Ar-H), 7.58 (t, 1H, J = 6.9Hz ,Ar-H)7.88-8.03 (m, 2H, Ar-H), 8.41

(dd, 1H, H$_5$, J = 1.8Hz, J = 7.8Hz), 8.87 (dd, 1H, H$_7$, J = 1.4Hz, J = 4.9Hz).^{13}CNMR (75MHz,

CDCl$_3$): δ = 171.3, 170.7, 156.4, 155.1, 154.5, 153, 148.3, 142.7, 138.3, 135.3, 133.9, 127.1,

121.9, 117.9, 117.2, 114.3, 112, 108.3, 96.3.EI-MS *m/z* 357.20 (M$^+$). Anal.Calcd for C$_{19}$H$_{15}$N$_7$O: C, 63.86; H, 4.23; N, 27.44; Found: C, 63.92; H, 4.26; N, 27.39.

3-(2-(6-Nitrobenzo[d]thiazol-2-ylamino)pyrido[2,3-d]pyrimidin-4-ylamino)benzamide (B9):

Yellowish orange solid. ^{1}H NMR (300 MHz, CDCl$_3$): δ = 7.06 (s, 1H, Ar-H), 7.36-7.42 (m, 3H, H$_6$, 2Ar-H), 7.88-8.01 (m, 2H, 1Ar-H & 1Bt-H), 8.36-8.81 (m, 4H, H$_6$, H$_7$ & 2Bt-H).^{13}C NMR (75MHz, CDCl$_3$): δ = 177.1, 171.7, 171, 159.8, 156.4, 155.4, 153, 144.6, 142.5, 135.3, 134, 131.4, 126.9, 121.5, 121.2, 119.3, 117.7, 117.5, 114, 111.7, 96.1. EI-MS *m/z* 458.08 (M$^+$). Anal.Calcd for C$_{21}$H$_{14}$N$_8$O$_3$S: C, 55.02; H, 3.08; N, 24.44; Found: C, 55.01; H, 3.09; N, 24.42.

6.2.4 *In vitro* SIRT1 assay:

Activation of SIRT1 by PP derivatives (**A1-14** and **B1-14**) was studied by *in vitro* assay using recombinant SIRT1 and fluorophore-labeled acetylated p53 peptide substrate according to protocol mentioned under section 4.4.
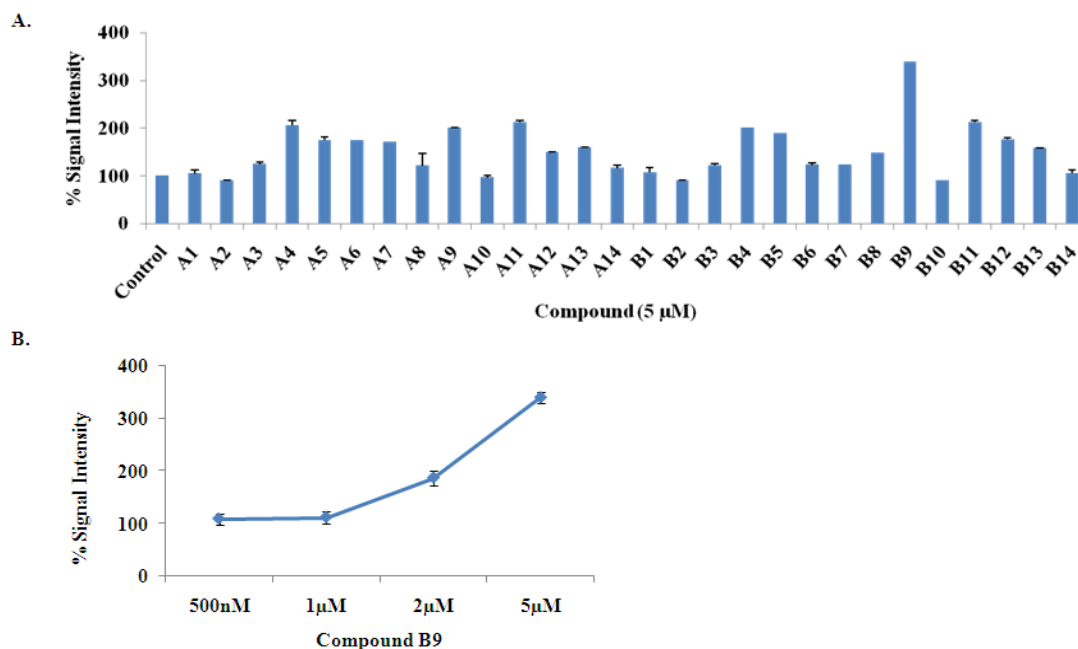
Fig.6.11: A. *In vitro* SIRT1 activation at 5µM concentration by **A1-14** and **B1-14**. **B**. Dose dependent activation of most active compound **B9**.

The result from **Fig.6.11A** clearly demonstrates that the most active compound from the series is **B9** with 2-3 fold activation of SIRT1. A few compounds **A4, B4, A11** and **B11** have moderate activation of SIRT1 and all other compounds have little or no activation. Hence, the experiment is repeated with a various concentrations of **B9** to establish the dose dependent activation of SIRT1 and is depicted in **Fig.6.11B.**

6.2.5 Detection of acetylated/deacetylated substrate by RP-HPLC:

SIRT1 activation by most active compound **B9** was further studied in terms of increase in deacetylation of acetylated substrate in RP-HPLC according to protocol explained under section 4.5. As shown in **Fig.6.12**, Compound **B9** showed significant increase in deacetylation of acetylated substrate in time dependent manner at 5 µM concentration.
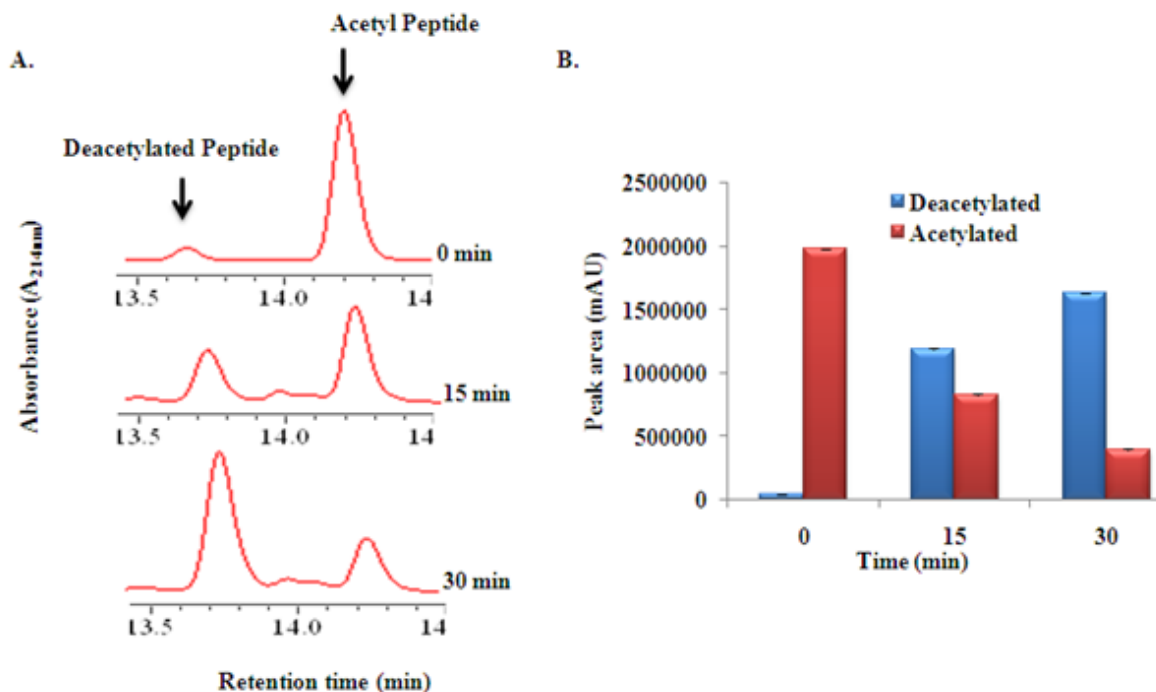
Fig.6.12: A. Detection of acetylated and deacetylated peptide peak treated by **B9** by HPLC. **B.** Peak areas of acetylated and deacetylated products are represented in bar graph.

6.2.6 Effect of B9 on 3T3-L1 cells:

In order to investigate the antiobesity activity of **B9** in the well-known cell based adipogenesis differentiation assay, $1*10^5$ 3T3-L1cells were treated with increasing concentrations (0, 5, 10, 50 µM) of **B9** along with differentiation media containing insulin, dexamethasone, IBMX. Treatment was continued until differentiation was observed in control cells (untreated). Inhibition of differentiation by **B9** was measured by Oil O Red staining. After treatment, plates were washed with PBS, and the cells were fixed in 10% formaldehyde for 1 h and stained with Oil O Red staining according to protocol described under section 4.6.3.As shown in **Fig.6.13**, microscopically the intensity of Oil O Red staining decreased dose dependently during differentiation.
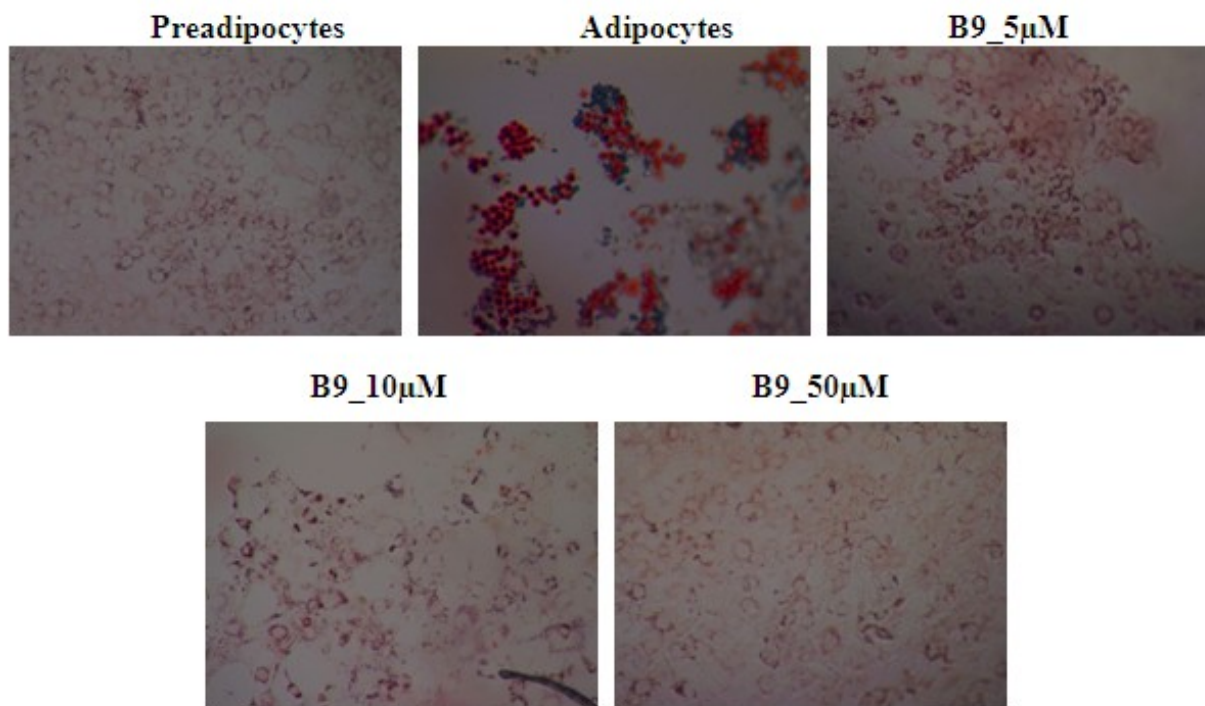
Fig.6.13: Inverted microscopic pictures of 3T3-L1 cells treated with compound **B9** at different concentrations.

Quantification of the dye extracted from cells treated with **B9** during differentiation as well as in mature adipocytes using a spectrophotometer was described in detail in the materials and methods section 4.6.3 and results were shown in **Fig.6.14**. Intensity of dye incorporated also decreased in fully differentiated adipocytes treated with **B9,** demonstrating the decrease in amounts of fatty acids and triglycerides produced by the cells. These results suggest that the compound identified with SIRT1 activating properties have a significant effect on fat mobilization in differentiated adipocytes, and thus **B9** is anticipated to have antiobesity properties.
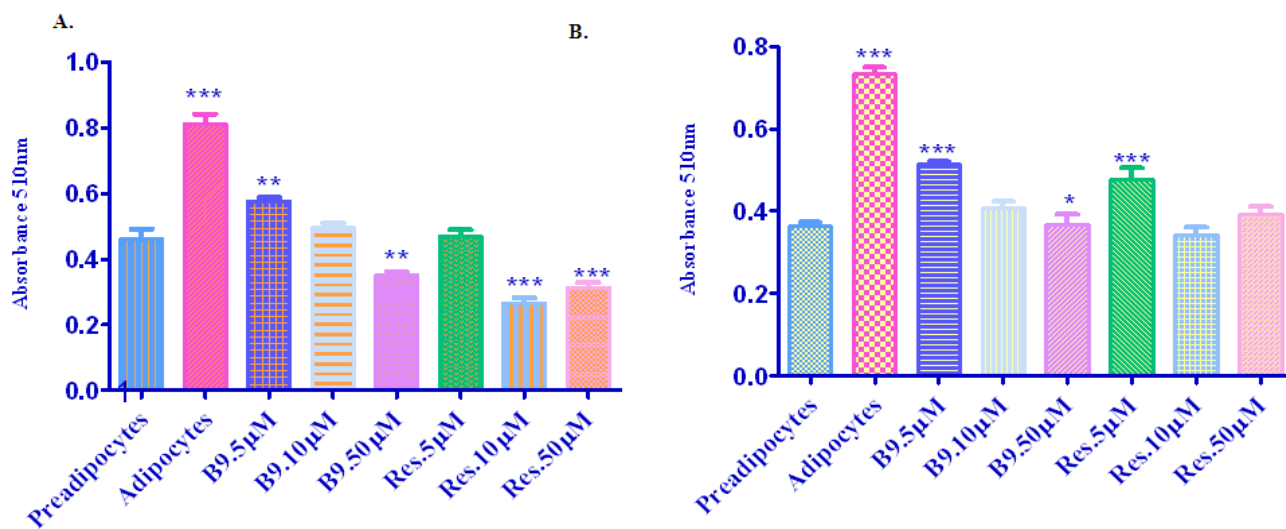
Fig.6.14: Measurement of lipid accumulation in preadipocytes (**A**) and mature adipocytes (**B**) treated with various concentrations of **B9** and quantified by extracting Oil O Red. Resveratrol was used as standard.

6.2.7 Measurement of triglycerides:

$1*10^5$ fully differentiated 3T3-L1 adipocytes were treated with different concentrations (0, 5, 10, 50 μM) of **B9** for 24h. Total triglyceride content in cells was measured according to protocol explained in section 4.6.4 and results were shown in **Fig.6.15**, a dose dependent decrease in triglyceride accumulation was observed with **B9**.
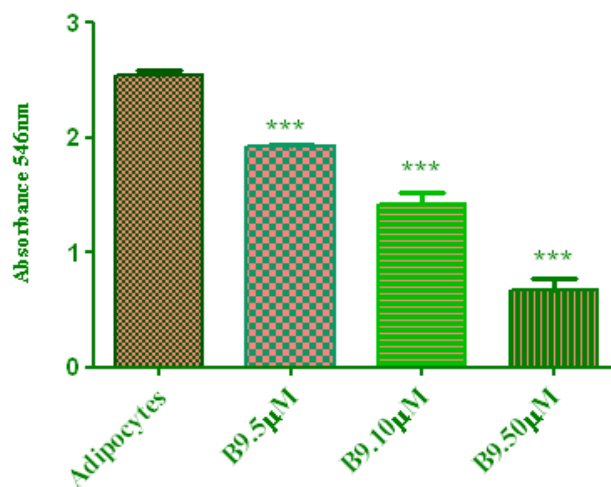
Fig.6.15: Triglyceride accumulation in fully differentiated adipocytes treated with different concentrations of **B9**.

6.2.8 RT-PCR analysis:

$1*10^6$ 3T3-L1 adipocytes treated with **B9** at 0, 5, 10, 50 µM concentrations for 24h and checked for transcript levels of SIRT1, PPARγ, C/EBPα, E2F1, leptin, FAS and LPL according to protocol explained under section 4.6.8 using gene specific primers specified in **Table 2** of material and methods section.

As shown in **Fig.6.16A**, a dose dependent increase in SIRT1 levels clearly demonstrates the SIRT1 mediated antiadipogenic activity of **B9**. Further, a dose dependent decrease in expression of transcription factors PPARγ, C/EBPα was observed. Additionally FAS, LPL, E2F1 and leptin gene expression was dose dependently and significantly down regulated by **B9** treatment. Equal loading was confirmed by GapDH. Quantification of band intensity was done by Image lab analysis software and results were shown in **Fig.6.16B**.
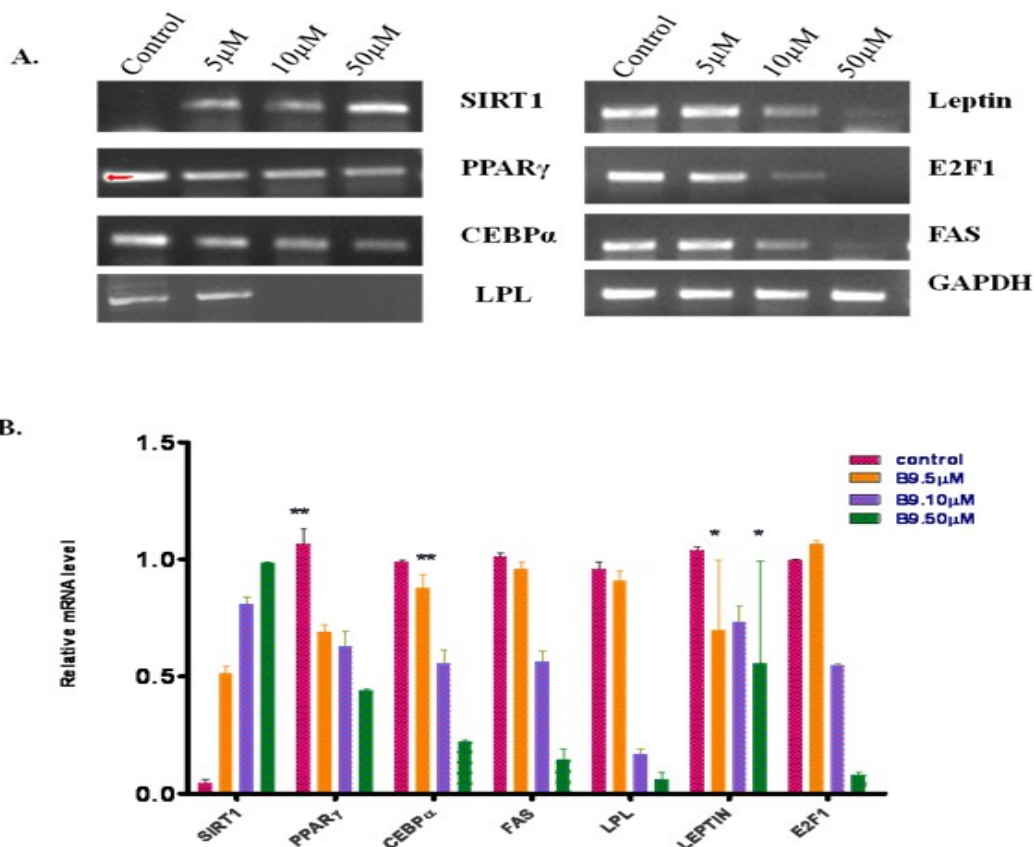
Fig.6.16: A.RT-PCR analysis of adipogenic enzymes in fully differentiated adipocytes treated with **B9** at different concentrations. **B.** Quantification of band intensity by using Image lab analysis software**.**

6.2.9 *In vivo* studies on high fat diet induced obese mice:

Obesity was induced by feeding HFD to male albino mice for 3 months and treated with **B9** at a concentration of 30 mg/kg body weight for one month according to procedure explained under materials and methods section 4.7.3. Orlistat was used as a standard antiobesity drug at a concentration of 30 mg/kg body weight. As shown in **Fig.6.17A**, body weight gain of the HFD group mice was considerably higher than the other groups. The weight gain of Orlistat and **B9** groups were normalized to the chow diet group. Feed intake of all experimental groups was not significantly different. Modulation in serum lipids profile was shown in **Fig.6.17B**.
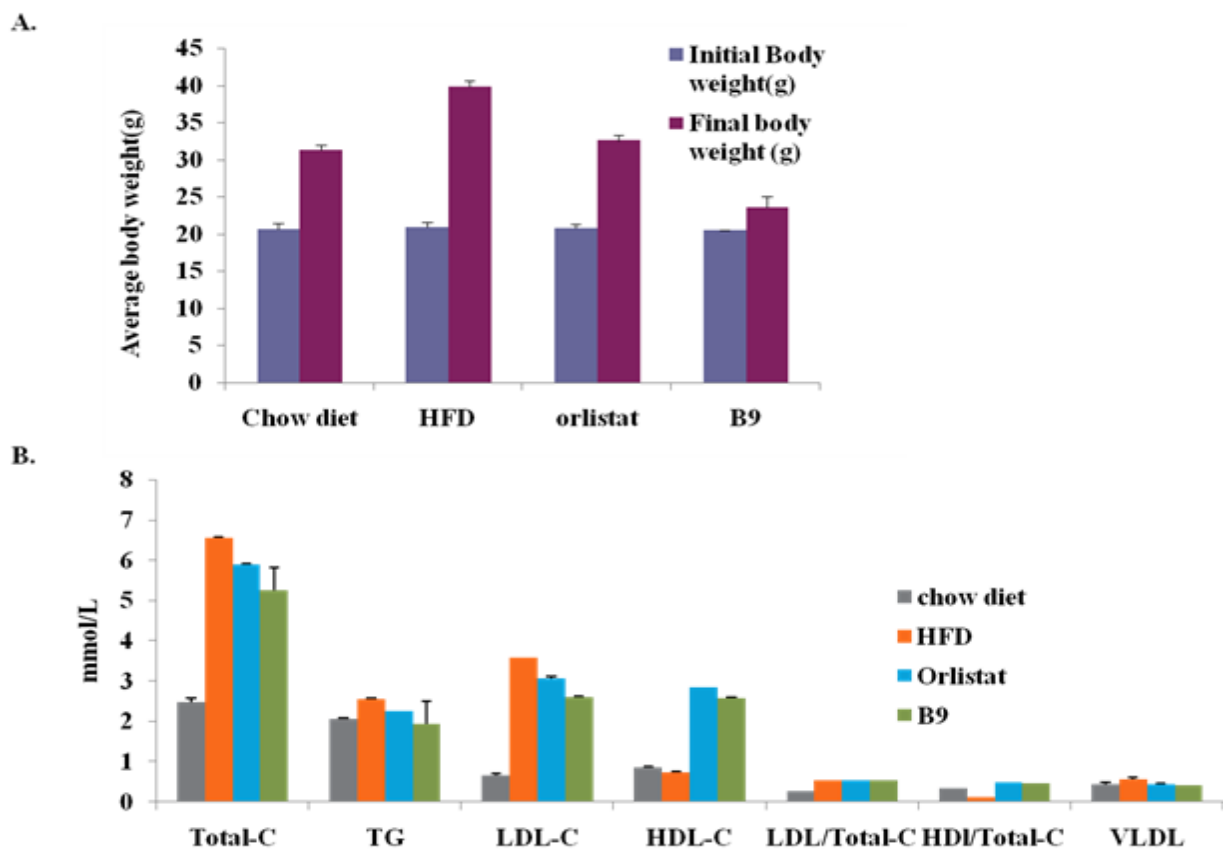
Fig.6.17: A. Average body weight of mice before and after treatment with **B9** along with high fat diet fed. **B**. Serum lipid profile after treatment with **B9**.

Interacting amino acids with in 5A^0 distance of compounds**A9** and **B9** was shown in **Fig.6.18**.
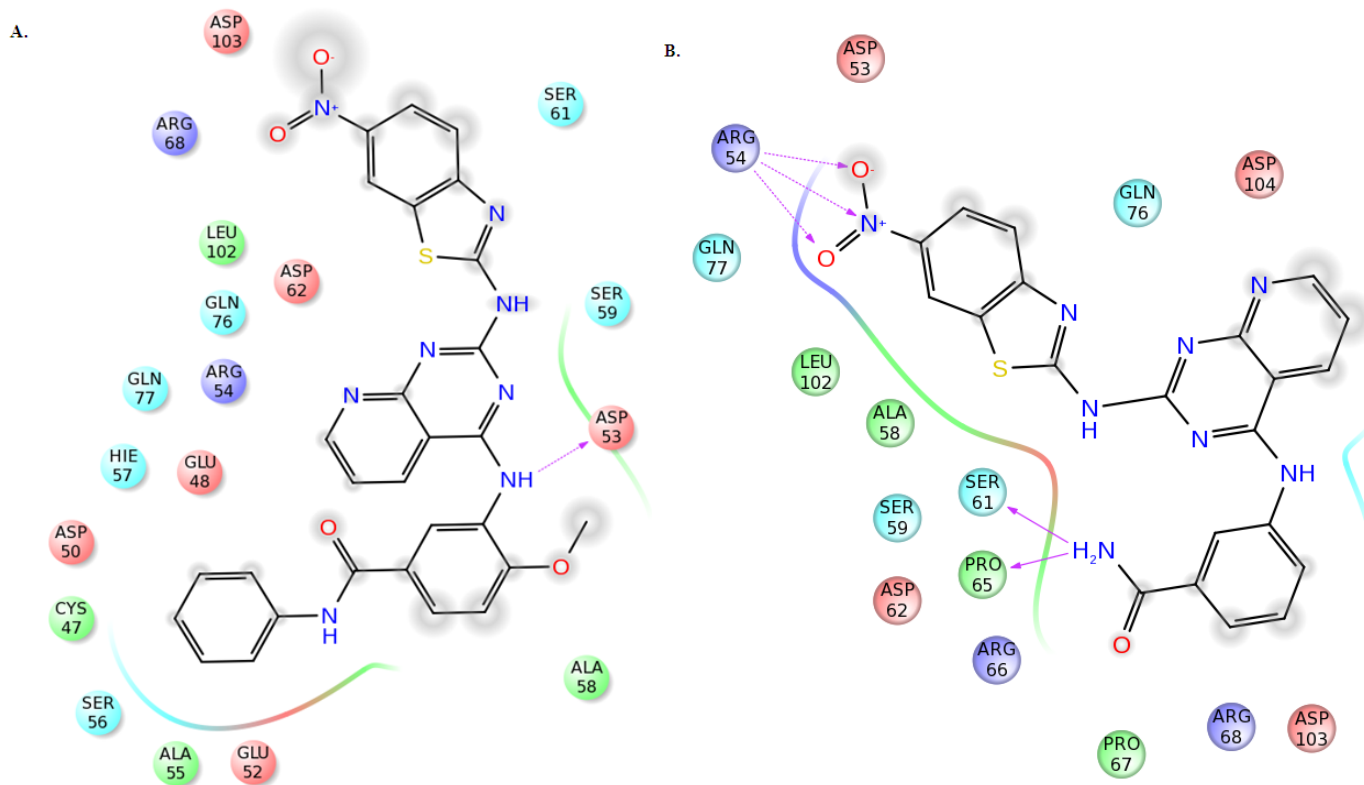
Fig.6.18: Ligand interaction diagram of **A9** (**A**) and **B9** (**B**) within 5A^0 distance. Blue-positively charged; Cyan-polar; Green-Hydrophobic; Red-negatively charged; Circular bubbles-solvent exposure; Solid pink arrows- Hbond with backbone; Dotted pink arrows-Hbond with side chain.

6.2.10 Discussion:

The worldwide widespread of obesity, nurtured by the modern lifestyle by the lack of physical activity and an energy-dense diet, has contributed to create a unique condition where a majority of overfed individuals exceeded the number of malnourished [Tanumihardjo S.A., *et al*., 2007]. Obesity is a heterogeneous condition in which body fat distribution is closely associated with metabolic perturbations consequently leading to cardiovascular disorders [Despres J.P., 2007] and type II diabetes [Hussain A., *et al*., 2010] risk which is a foremost

cause of mortality in westernized societies. Moreover, accumulation of visceral fat is strongly associated with insulin resistance and with a typical atherogenic dyslipidemia state [Despres J.P., 2006]. SIRT1 is reported to be one of the targets for treatment of obesity and related disorder [Pulla V.K., *et al*., 2012]. Obesity plays a crucial role in the development of Type II diabetes mellitus by mobilizing free fatty acids and certain inflammatory cytokines promoting insulin resistance. In recent years, SIRT1 has become an interesting and promising target in terms of its effects on longevity, metabolism, and other aging-related disorders. The compound resveratrol and SRT1720 etc., has been identified as a potent activators of SIRT1 in cell-based models and *in vitro* screens by other groups. In the present study we have identified a SIRT1 activator and elucidated the modified SIRT1 activity in numerous biological systems. Since crystal structure of SIRT1 was not available the best model of the allosteric domain of SIRT1 was developed and the fitness of the model was checked by PROCHECK program. This model showed 92.9% residues in most favored regions and ProSA Web Z score of -6.38 similar to the template structure scores. Binding site pocket was identified using SITEMAP and pocket contains ASP166; ARG167; SER169; HIS170; ALA171; SER172; SER173; SER174; ASP175; TRP176; PRO184; TYR185; PHE187; VAL188; HIS191; LEU192 with respect to full length SIRT1 sequence. Virtual screening of *in house* database of ~3000 molecules was carried out by using GLIDE against allosteric domain of hSIRT1 (114-217AA) and we identified 5 hits of pyrido[2,3-d] pyrimidine pharmacophore as SIRT1 activators. Among all, **PP1** showed most activation whereas **PP2** and **PP4** showed moderate activation. **PP3** and **PP5** showed less or no activation. Further to develop a SAR, series of derivatives of **PP1** (**A1-14**) and **PP2** (**B1-14**) were synthesized and screened for SIRT1 activity. Among all, compound **B9** showed significant increase in SIRT1 activity whereas **A4, B4, B11, A11** showed moderate activation. All the

remaining compounds showed less or no activation. **PP1** showed H-bond interaction with backbone residues of charged amino acids ASP166 and ARG167 whereas **PP2** with SER174 and PRO178 Most active compound among synthesized compounds, **B9** also showed strong Hbond interaction with side chain residues of ARG 167 along with SER174 and PRO178. Correspondingly **A9** has shown one hydrogen bond with ASP166 and didn't show interaction with ARG167 due to change in orientation of core moiety upon 6-nitro2-benzothiazolyl substitution. Recently, it has been proven that aromatic residues and charged residues in the area of active site are very important because they are involved in putative stacking and electrostatic interactions, respectively [Sharma A., *et al*., 2012]. Moreover our docking data reveal that interaction with charged residues especially with ARG167 plays key role in activity.

Further HPLC measurement of deacetylation/acetylation of acetylated peptide incubated with **B9** also studied in order to quantify the substrate with respect to time. A time dependent increase in deacetylation peak with t_R 13.8 min and decrease in acetylated peak with t_R 14.2 min was observed when incubated with 10μM concentration of **B9** for 30 min.

Further studies on 3T3-L1 cells, compound **B9** suppressed triglyceride accumulation and decreased fat droplets during adipocyte differentiation. The microscopic picture confirms this finding, whereby the size and number of intracellular cytosolic fat deposits are reduced in a dose dependant manner (**Fig.6.12**). Intensity of Oil O Red incorporated into the cells also decreased confirming the inhibition of adipocyte differentiation by **B9**. These results suggest that the compounds identified with SIRT1 activating properties have a significant effect on fat mobilization in differentiated adipocytes, and thus **B9** is anticipated to have antiobesity and/or antidiabetic properties.

The antiobesity mechanism works by inhibiting fat accumulation and fatty acid synthesis and by activating fatty acid oxidation. PPARγ, a lipid-activated transcription factor, is present in adipose tissue and regulates genes involved in lipid metabolism including FAS and aP2. Because PPARγ is activated by fatty acids, fat accumulation is associated with PPARγ activation. Thus, modulation of PPARγ activity may be an effective way to regulate obesity. In our study, compound **B9**, significantly suppressed PPARγ mRNA expression. Additionally, the expression of C/EBPα, a key regulator of lipogenesis, decreased markedly following **B9** treatment compared with that in differentiated control cells. PPARγ and C/EBPα play an important role in adipocyte differentiation, because they are transcriptional activators for adipocyte genes including aP2, lipoprotein lipase. SIRT1 has been shown to regulate transcription of various downstream targets like PPARγ, C/EBPα, leptin, LPL which control the fat metabolism and mobilization. An elevated transcript level of SIRT1 was observed in cells treated with **B9** demonstrating the activation of SIRT1 and its substrates PPARγ and C/EBPα by **B9**.

Under fasting conditions, SIRT1 transcription is regulated by p53 and FOXO3a andE2F1 in response to DNA damage. Further it has been reported SIRT1 regulate E2F1 expression in negative feedback mechanism. Thus mRNA levels of E2F1 were also studied and levels of E2F1 were declining with increasing SIRT1 upon B9 treatment.

We observed that compound **B9** also reduced the expression of mRNA levels of LPL which play an important role in lipid metabolism and the level of LPL is related with triglyceride concentration in adipose tissues, up regulation of LPL activity is closely associated with obesity. Another important adipocyte gene, FAS is the crucial enzyme in de novo lipogenesis, catalyzing the reactions for the synthesis of long-chain fatty acids [Sul H.S., *et al*., 1998] and its expression increases during adipogenesis [Student A.K., *et al*., 1980]. Reduced levels of FAS were observed

in cells treated with B9 demonstrating the inhibition of denovo lipogenesis. Lipid metabolism not only necessitates lipid synthesis and degradation, also involves lipid signaling and fatty acid storage in adipose tissue. Leptin is an endocrine /paracrine hormone secreted from adipocytes play a crucial role in food intake and energy balance. Leptin levels increases in mature adipocytes and decreases with increasing expression of SIRT1 [Bordone L., *et al*., 2007]. Reduced levels of leptin with **B9** revealed the effect of **B9** on energy balance.

Preliminary studies on high fat diet induced mice, **B9** has showed decrease in body weight gain and significantly lowered the serum Total-C concentration, TG concentration, LDL-C concentration, and the ratio of LDL-C/ Total-C compared to the HFD group. Supplementation of oral **B9** exhibited a trend towards increased serum HDL-C levels, compared to HFD group, and the ratio of HDL-C/ Total-C exhibited higher values in the **B9** group than in the HFD group.

6.3 Design, synthesis, biological interventions of Azetidine (AZD) derivatives:

6.3.1 Design of homology model of allosteric site and active site prediction:

Homology model of hSIRT1 allosteric site was generated by using comparative homology modeling procedure explained under materials and methods section 4.1. Model and active site was shown in **Fig.6.1**.

6.3.2 High-throughput virtual screening of *in house* database:

High-throughput virtual screening of *in house* database of ~3000 molecules into allosteric site of SIRT1 revealed 1-(isonicotinamido)azetidine-2,4-dicarboxamides pharmacophore as a lead pharmacophore (**A1-12**). Docking scores were represented in **Table 14**.

6.3.3 Synthetic procedure and characterization:

Experimental procedure for synthesis of novel1-(isonicotinamido)azetidine-2,4-dicarboxamides.

Step – I: Synthesis of 2,4-dibromopentanedioic acid (2A):
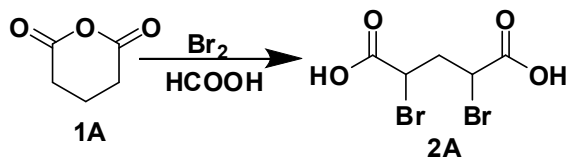
Bromine (44.9 ml, 0.876 mol) was added drop wise to glutaric anhydride **(1A)** (50 g, 0.438 mol) in a three-necked flask fitted with reflux condenser and $CaCl_2$ guard tube at room temp. After the addition of bromine, the reaction mixture was heated to 90 °C for one hour and then at 100 °C for another one hour. The reaction mixture was cooled to room temperature and formic acid (40 ml) was added slowly. The content of the flask was heated to 100°C for one hour. The reaction mixture was quenched with water and extracted with ethyl acetate (4 x 100 ml). The combined organic layer was dried over sodium sulphate and concentrated to give white

gummy solid. The trituration of the gummy solid with diethyl ether gave 27 g (21 % yield) of intermediate **2A**.

B.P=352.3 °C at 760 mmHg; MF: $C_5H_6Br_2O_4$; MW: 289.91; IR (KBr) cm^{-1}: 3000-2850, 1710, 1300, 665; ^{1}H NMR (CDCl$_3$) δ=11(s, 2H, COOH), 4.2 (t, 2H, CH), 2.75 (t, 2H, CH$_2$).

Step – II: Synthesis of di-tert-butyl 2, 4-dibromopentanedioate (3A):
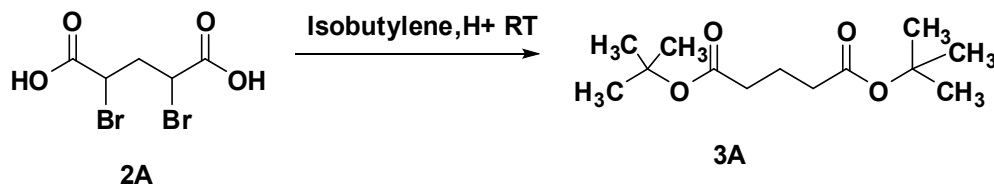
To a solution of intermediate **2A** (10 g) in dry dichloromethane (100 ml), isobutylene and 2-3 drops of concentrated sulfuric acid was added. The reaction mixture was stirred in an autoclave overnight. The reaction mixture was washed with water, saturated aq. NaHCO$_3$ solution, brine and dried over Na$_2$SO$_4$. After evaporation of the solvent, the crude product was purified by column chromatography to give 6.93 g (50 %) of intermediate **3A** as colorless oil. B.P: 282.3 °C at 760 mmHg; MF: $C_{13}H_{22}Br_2O_4$; MW: 399.99; IR (KBr) cm^{-1}: 1735, 1250, 665; ^{1}H NMR (CDCl$_3$) δ= 4.2 (t, 2H, CH), 2.85 (t, 2H, CH$_2$), 1.4(s, 18H).

Step–III: Synthesis of (2R,4R)-di-tert-butyl-1-(isonicotinamido)azetidine-2,4-dicarboxylate (4A):
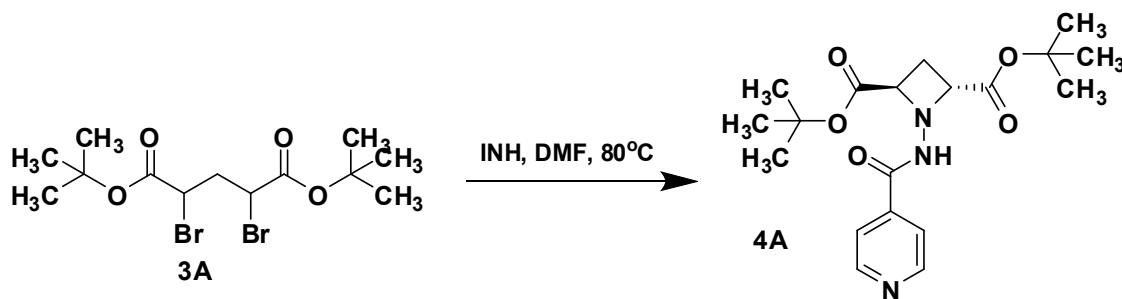
To a solution of intermediate **3A** (500 mg, 1.24 mmol) in dry DMF (10 ml), Isoniazid (511.53 mg, 3.73 mmol) was added and heated to 80° C for 2 hrs. The reaction mixture was concentrated to remove DMF and the residue was dissolved in dichloromethane. The organic layer was washed with saturated aq. $NaHCO_3$ solution, water, brine, dried over Na_2SO_4 and concentrated. The crude product was purified by column chromatography to afford the ester **4A** as pale yellow thick oil(200 mg, 47%).MF: $C_{19}H_{27}N_3O_5$; MW: 377.20; IR (KBr) cm^{-1}: 3315, 3081-3011, 1735, 1644-1430, 1640-1620, 1550, 1250; ^{1}H NMR (CDCl$_3$) δ= 4.4-4.2 (t, 2H, CH), 2.85-3 (t, 2H, CH$_2$), 1.4(s, 18H), 8.99(d, 2H), 7.8(d, 2H), 8(s, 1H).
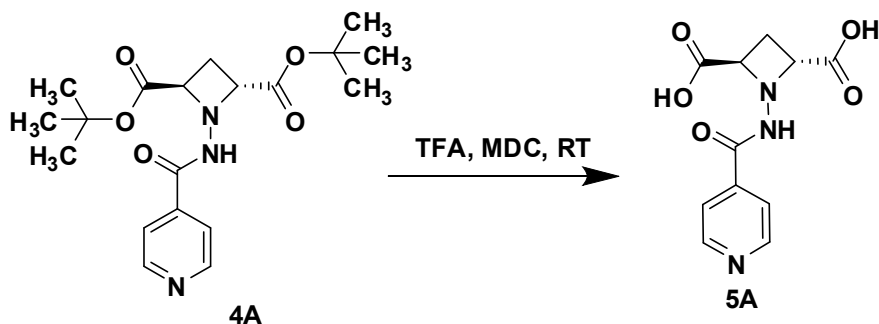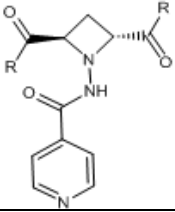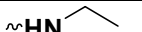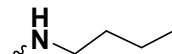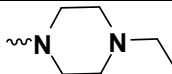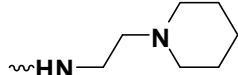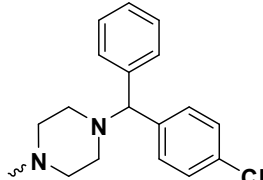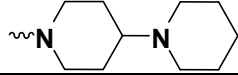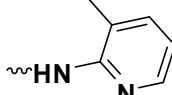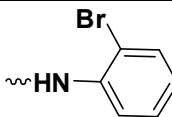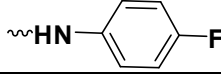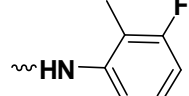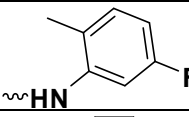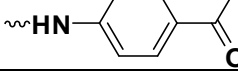
The ester **4A** (3.3 g, 9.72 mmol) was dissolved in dry dichloromethane (20 ml) and trifluoro acetic acid (20 ml) was added. The reaction mixture was stirred at room temperature for 48hrs and concentrated under high vacuum. The crude product was purified by column chromatography to afford the scaffold **5A** as thick oil (1.7g, 77% by LC-MS). MF: $C_{11}H_{11}N_3O_5$; MW: 265.07; IR (KBr) cm^{-1}: 3400-2800, 3315, 3081-3011, 1710, 1644-1430, 1640-1620, 1550,1250; ^{1}H NMR (CDCl$_3$) δ= 4.4-4.2 (t, 2H, CH), 2.85-3 (t, 2H, CH$_2$), 8.99(d, 2H), 7.8(d, 2H), 8(s, 1H), 11(s,2H).

Step–IV: General procedure for the synthesis of final compounds:
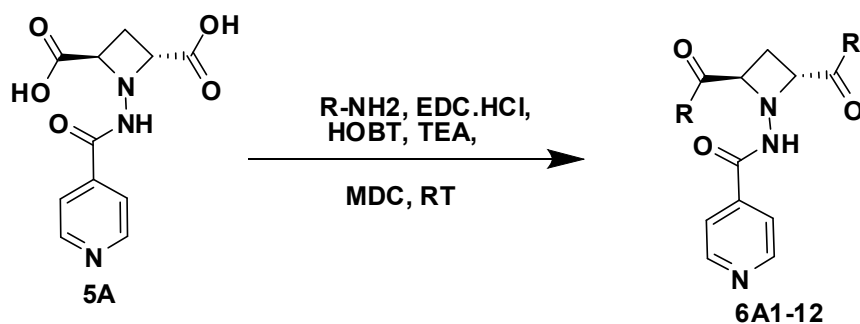
To a solution of the dicarboxylic acid **5A** (100 mg, 0.44 mmol) in dry dichloromethane (10 ml), various amines (**6A1-12**) (0.969 mmol) was added at 0° C and stirred under nitrogen atmosphere. EDC.HCl (253 mg, 1.32 mmol), HOBt (202 mg, 1.32 mmol) and triethylamine (267 mg, 2.64 mmol) were added at 0 °C and stirred at RT for 16hrs. The reaction mixture was quenched with water and extracted with dichloromethane. The combined organic layers were washed with brine, dried over sodium sulphate and concentrated. The crude products were purified by column chromatography to get the titled compounds with physicochemical properties as presented in the following **Table 14**.

Table 14: Physicochemical properties, docking score of 1-(isonicotinamido)azetidine-2,4-dicarboxamides derivatives (**A1-12**)

Code	R	GLIDE score	M.P/B.P(^{0}C)	Yield (%)	Molecular Formula	Molecular Weight
6A1	~HN (ethyl)	-3.892	122-124	88	$C_{15}H_{21}N_5O$	319.16
6A2	HN (propyl)	-2.365	159-160*	89	$C_{19}H_{29}N_5O_3$	375.47
6A3	N-piperazine-N-ethyl	-6.043	166-168*	82	$C_{23}H_{35}N_7O_3$	457.57
6A4	HN-ethyl-N-piperidine	-4.165	156-159*	87	$C_{25}H_{39}N_7O_3$	485.62
6A5	piperazine-CH(phenyl)(4-Cl-phenyl)	-4.493	165-167	79	$C_{45}H_{45}Cl_2N_7O_3$	802.79
6A6	N-piperidine-N-piperidine	-4.893	180-183*	79	$C_{31}H_{47}N_7O_3$	565.75
6A7	HN-(3-methylpyridin-2-yl)	-1.380	153-155	61	$C_{23}H_{23}N_7O_3$	445.19
6A8	HN-(2-bromophenyl)	-2.297	147-148	68	$C_{23}H_{19}Br_2N_5O_3$	573.24
6A9	HN-(4-fluorophenyl)	-1.801	147-148	67	$C_{23}H_{19}F_2N_5O_3$	451.15
6A10	HN-(3-fluoro-2-methylphenyl)	-2.297	163-165	67	$C_{25}H_{23}F_2N_5O_3$	479.18
6A11	HN-(5-fluoro-2-methylphenyl)	-1.842	157-160	73	$C_{25}H_{23}F_2N_5O_3$	479.48
6A12	HN-(4-acetylphenyl)	-3.021	152-154	64	$C_{27}H_{25}N_5O_5$	499.52
*: Indicates Boiling point						

N^2, N^4-Diethyl-1-(isonicotinamido)azetidine-2, 4-dicarboxamide (6A1):

Brown solid; ^{1}H NMR (300 MHz, CDCl$_3$): δ = 1.07-1.10 (m, 6H, -CH$_3$), 2.63-2.65 (m, 1H, -CH), 2.87-2.89 (m, 1H, -CH), 3.32-3.38 (m, 4H, -CH$_2$), 4.48- 4.53 (m, 2H, -CH), 7.73(d, 2H, J = 7.3Hz, -ArH), 8.79 (d, 2H, J = 7.5 Hz, -ArH). ^{13}C NMR (75MHz, CDCl$_3$): δ= 170.9, 166.3, 149.7, 140.8, 121.3, 67.3, 67.1, 32.7, 18.1, 17.9, 14.7, 14.5. EI-MS *m/z* 319.16 (M$^+$). Anal. Calcd for C$_{15}$H$_{21}$N$_5$O$_3$: C, 56.41; H, 6.63; N,21.93; Found: C, 56.39; H, 6.64; N, 21.89.

N^2,N^4-Bis(4-ethylpiperazin-1-yl)-1-(isonicotinamido)azetidine-2,4-dicarboxamide (6A3):

Yellowish brown liquid; ^{1}H NMR (300 MHz, CDCl$_3$): δ = 1.06-1.08 (m, 6H, -CH$_3$), 2.34-2.41(m, 12H), 2.67-2.88 (m, 10H), 4.49-4.53(m, 2H, -CH), 7.77 (d, 2H, J = 7.4Hz,-ArH), 8.83(d, 2H, J = 7.9Hz, -ArH). ^{13}C NMR (75MHz, CDCl$_3$): δ = 170, 166.3, 149.4, 140.8, 121.6, 67.5, 67.4, 54.7, 54.5, 49.7, 49.5, 18.4, 18.2, 12.9. EI-MS *m/z* 487.30 (M$^+$). Anal. Calcd for C$_{23}$H$_{37}$N$_9$O$_3$: C, 56.65; H, 7.65; N, 25.85; Found: C, 56.67; H, 7.64; N, 25.85.

N^2,N^4-Bis(4-(bis(4-chlorophenyl)methyl)piperazin-1-yl)-1-(isonicotinamido)azetidine-2,4-dicarboxamide (6A5):

Tann solid; ^{1}H NMR (300 MHz, CDCl$_3$): δ = 2.36-2.38 (m, 8H), 2.65-2.86 (m, 10H), 4.47-4.51(m, 2H, -CH), 5.14 (s, 2H, -CH), 7.21-7.41(m, 16H, Ar-H), 7.79 (d, 2H, J = 7.3Hz, Ar-H), 8.87(d, 2H, J = 7.9Hz, Ar-H). ^{13}C NMR (75MHz, CDCl$_3$): δ = 169.9, 166.2, 149.6, 141, 140.8, 131.6, 129.7, 129.5, 129.4, 121.6, 74.4, 67.4, 67.2, 56.9, 56.7, 47, 18.1, 17.9. EI-MS *m/z* 899.24 (M$^+$). Anal. Calcd for C$_{45}$H$_{45}$Cl$_4$N$_9$O$_3$: C, 59.94; H, 5.03; N, 13.98; Found: C, 59.91; H, 5.01; N, 14.

N^2,N^4-Bis(3-fluoro-2-methylphenyl)-1-(isonicotinamido)azetidine-2,4-dicarboxamide (6A10):

Yellow solid; ^{1}H NMR (300 MHz, CDCl$_3$): δ = 2.31 (s, 6H, 2*CH$_3$), 2.84-2.87 (m, 1H,-CH), 3.04-3.07 (m, 1H, -CH), 4.46- 4.49 (m, 2H, -CH), 7.09-7.23 (m, 6H, Ar-H), 7.78 (d, 2H, J = 7.5Hz,-ArH), 8.81 (d, 2H, J = 7.9Hz, -ArH).^{13}C NMR (75MHz, CDCl$_3$): δ = 171.6, 166.7, 161.7, 161.5, 149.7, 140.7, 138.7, 138.6, 127.5, 127.3, 121.7, 117, 116.9, 113.9, 113.7, 110, 109.3, 66.9, 66.7, 17.9, 17.8, 8.9, 9.1. EI-MS *m/z* 479.18 (M$^+$). Anal. Calcd for C$_{25}$H$_{23}$F$_2$N$_5$O$_3$: C, 62.62; H, 4.83; N, 14.61; Found: C, 62.59; H, 4.83; N, 14.63.

N2,N4-bis(5-fluoro-2-methylphenyl)-1-(isonicotinamido)azetidine-2,4-dicarboxamide (6A11):

Buff colour solid; ^{1}H NMR (300 MHz, CDCl$_3$): δ = 2.09 (s, 6H, 2*CH$_3$), 2.78-2.82 (m, 1H,-CH), 3.01-3.04 (m, 1H, -CH), 4.47- 4.53 (m, 2H, -CH), 6.83 - 7.17 (m, 4H, Ar-H), 7.61 (s, 2H), 7.8 (d, 2H, J = 7.4Hz, -ArH), 8.83 (d, 2H, J = 7.8Hz, -ArH).^{13}C NMR (75MHz, CDCl$_3$): δ = 171.4, 166.6, 160.3, 160, 149.6, 140.5, 138.9, 138.7, 130.6, 130.3, 127.3, 127.1, 121.6, 111, 110.9, 110.3, 110.1, 67.2, 67, 17.9, 17.8, 17.5, 17.3. EI-MS *m/z* 479.18 (M$^+$). Anal. Calcd for C$_{25}$H$_{23}$F$_2$N$_5$O$_3$: C, 62.62; H, 4.83; N, 14.61; Found: C, 62.64; H, 4.79; N, 14.59.

6.3.4 *In vitro* SIRT1 assay:

Activation of SIRT1 by AZD derivatives (**6A1-12)** was studied by *in vitro* assay using recombinant SIRT1 and fluorophore-labeled acetylated p53 peptide substrate according to protocol mentioned under section 4.4. The result from **Fig.6.19A** clearly demonstrates that the most active compound from the series is **6A11** with 6-7 fold activation of SIRT1. A few compounds **6A1, 6A2, 6A3** and **6A5** have moderate activation of SIRT1 and all other compounds have little or no activation. Hence, the experiment is repeated with a various

concentrations of **6A1, 6A2, 6A3, 6A5** and 6A11 to establish the dose dependent activation of SIRT1 and is depicted in **Fig.6.19B.**
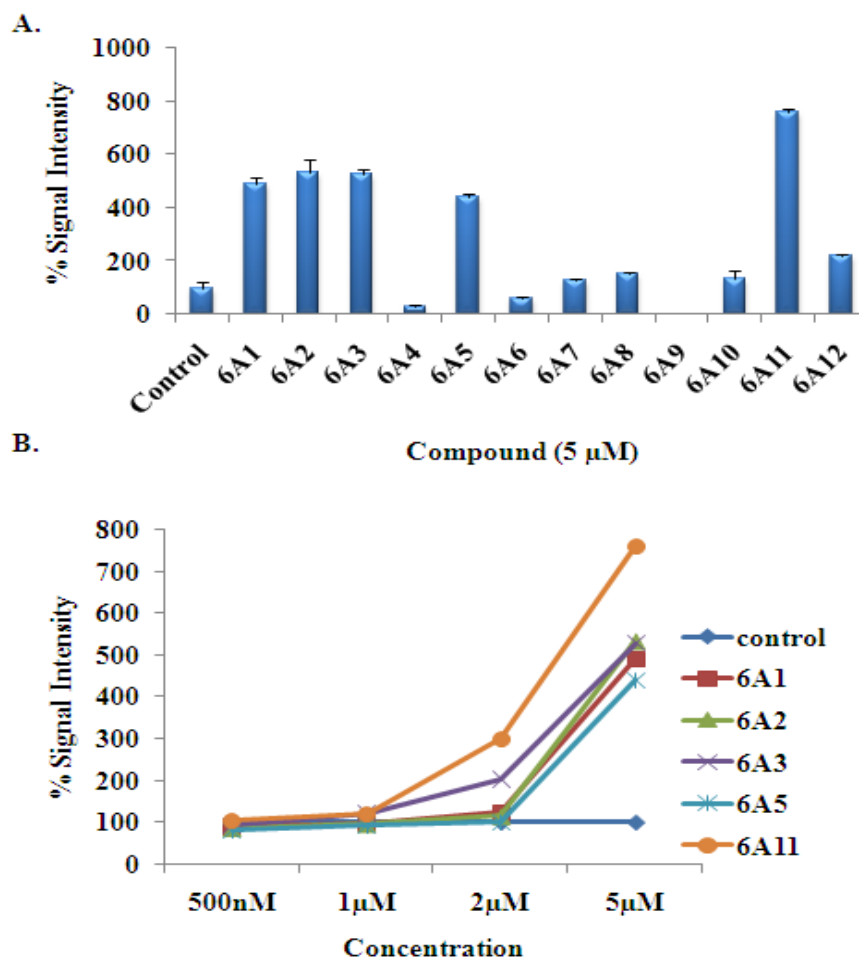
Fig.6.19:A. *In vitro* SIRT1 activation at 5μM concentration by **6A1-12. B**. Dose dependent activation of SIRT1 by most active compounds.

6.3.5 HPLC assay:

SIRT1 activation by most active compound among series **6A11** was studied in terms of increase in deacetylation of acetylated substrate by using HPLC method according to protocol explained under section 4.5. As shown in **Fig.6.20**, Compound **6A11** showed significant increase in deacetylation of acetylated substrate in time dependent manner at 5 μM concentration suggesting that the compound directly activating SIRT1.
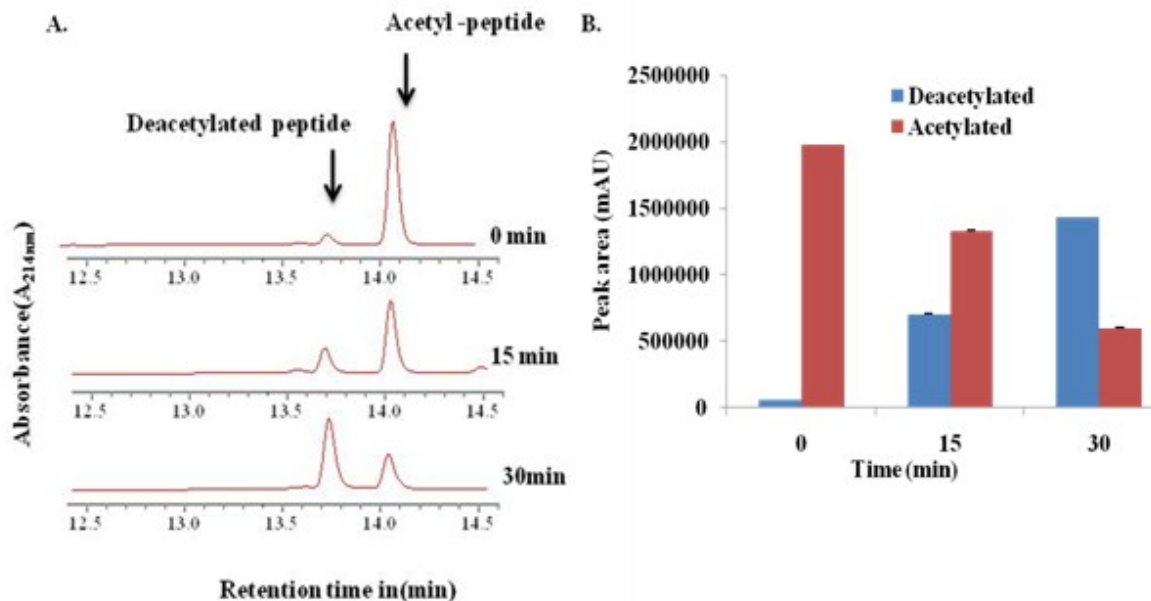
Fig.6.20: A. Detection of acetylated and deacetylated peptide peak treated by **6A11** by HPLC. **B**. Peak areas of acetylated and deacetylated products are represented in bar graph.

6.3.6 Effect on 3T3-L1 cells:

In order to investigate the antiobesity activity of **6A11**, $1*10^5$ 3T3-L1cells were treated with increasing concentrations (0, 5, 10, 50 µM) of **6A11** along with differentiation media containing insulin, dexamethasone, IBMX. Treatment was continued until differentiation was observed in control cells (untreated). Inhibition of differentiation by **6A11** was measured by Oil O Red staining according to protocol described under materials and methods section 4.6.3. As shown in **Fig.6.21**, a dose dependent decrease in Oil O Red accumulation was observed in cells treated with **6A11**.
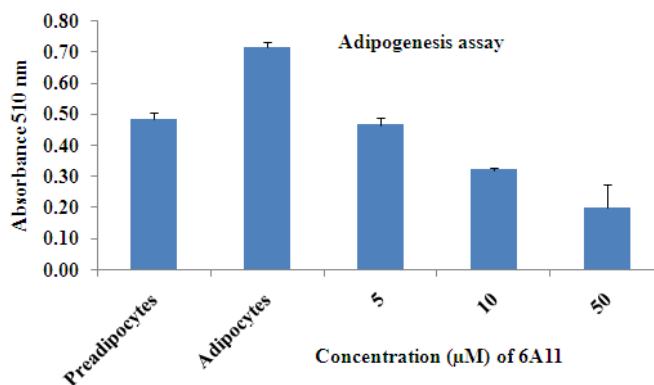
Fig.6.21: Measurement of lipid accumulation in preadipocytes treated with various concentrations of **6A11** and quantified by extracting Oil O Red.

6.3.7 Measurement of triglycerides:

$1*10^5$ fully differentiated 3T3-L1 adipocytes were treated with different concentrations of **6A11** (0, 5, 10, 50 µM) for 24h. Total triglyceride content in cells was measured according to protocol explained in section 4.6.4. As shown in **Fig.6.22**, a dose dependent decrease in triglyceride accumulation was observed with **6A11**.
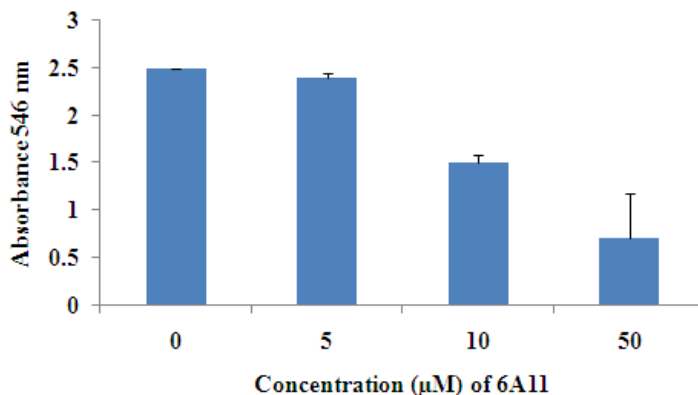
Fig.6.22: Measurement of triglyceride accumulation in adipocytes treated with various concentrations of **6A11**.

6.3.8 RT-PCR studies:

$1*10^6$ 3T3-L1 adipocytes treated with different concentrations of **6A11** (0, 5, 10, 50 µM) for 24h and checked for transcript levels of SIRT1, PPARγ2, C/EBPα, E2F1, leptin, FAS and LPL according to protocol explained under section 4.6.8 using gene specific primers shown in **Table 2** of materials and methods section.
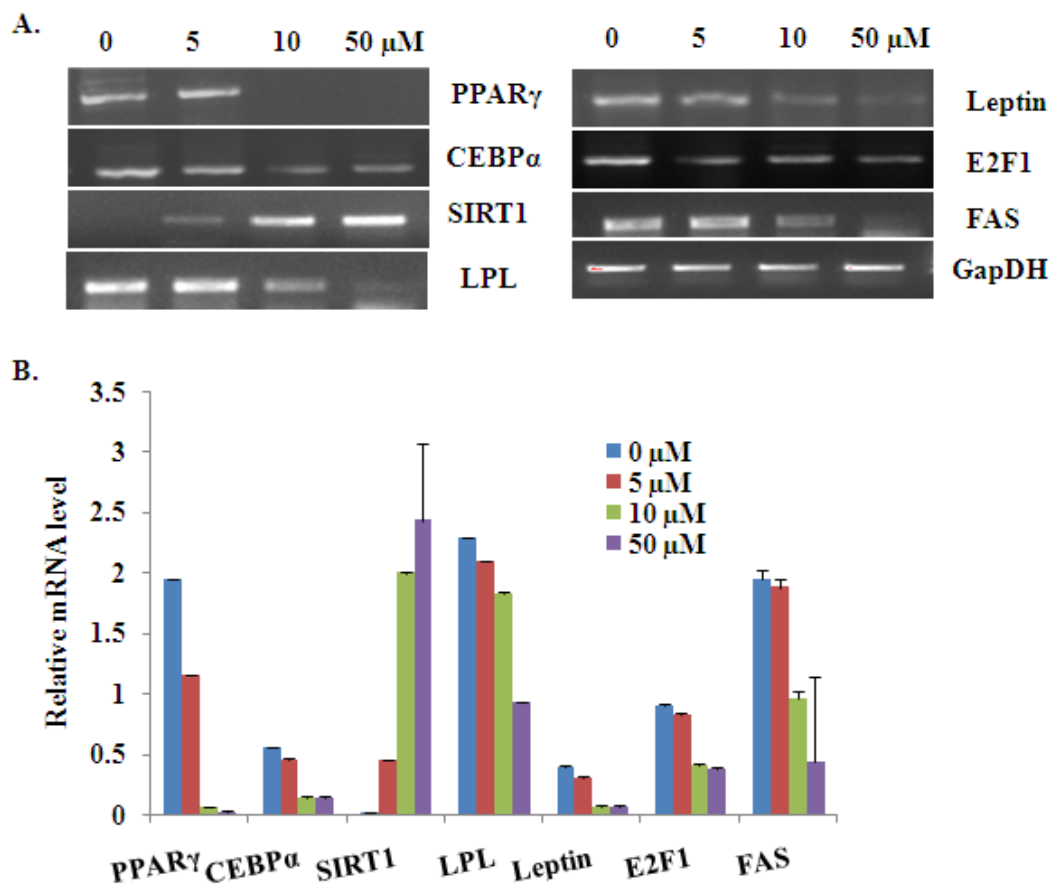
Fig.6.23: **A**.RT-PCR analysis of adipogenic enzymes in fully differentiated adipocytes treated with **6A11** at different concentrations. **B**. Quantification of band intensity by using Image lab analysis software**.**

As shown in **Fig.6.23A**, a dose dependent increase in SIRT1 levels clearly demonstrates the SIRT1 mediated antiadipogenic activity of **6A11**. Further, a dose dependent decrease in expression of transcription factors PPARγ, C/EBPα was observed. Additionally FAS, LPL, E2F1 and leptin gene expression was dose dependently and significantly down regulated by **6A11** treatment. Equal loading was confirmed by GapDH. Quantification of band intensity was done by Image lab analysis software and results were shown in **Fig.6.23B**

6.3.9 Discussion:

In recent years, SIRT1 has become an interesting and promising target in terms of its effects on longevity, metabolism, and other aging-related disorders. Several small-molecule activators of SIRT1 have been identified by utilizing a commercially available deacetylase activity assay. In present study was we identified and developed novel SIRT1 activators. Since crystal structure of SIRT1 was not available the best model of the allosteric domain of SIRT1 was developed and the fitness of the model was checked by PROCHECK program. This model showed 92.9% residues in most favored regions and ProSA Web Z score of -6.38 similar to the template structure scores. Binding site pocket was identified using SITEMAP and pocket contains ASP166; ARG167; SER169; HIS170; ALA171; SER172; SER173; SER174; ASP175; TRP176; PRO184; TYR185; PHE187; VAL188; HIS191; LEU192 with respect to full length SIRT1 sequence. Virtual screening of *in house* database of ~3000 molecules was carried out by using GLIDE against allosteric domain of SIRT1 (114-217AA) and a series of 1-(isonicotinamido)azetidine-2,4-dicarboxamides derivatives were identified as lead molecules. Among all, **6A11** showed significant activation of SIRT1 activity. In order to investigate the antiobesity activity of **6A11** in the well-known cell based adipogenesis differentiation assay, 3T3-L1 cells were treated with varying concentration of **6A11** during differentiation of preadipocytes to adipocytes and also in mature adipocytes. Inhibition of differentiation by **6A11**

146

was measured by Oil O Red staining. A dose dependent decrease in intensity of red o oil in the cells confirms the inhibition of adipocyte differentiation by **6A11**. These results suggest that the compounds identified with SIRT1 activating properties have a significant effect on fat mobilization in differentiated adipocytes, and thus **6A11** is anticipated to have antiobesity and/or antidiabetic properties.

The prime most transcription factors, PPARγ and C/EBPα have been shown to activate adipocyte-specific genes and are involved in the growth arrest that is required for adipocyte differentiation. During adipocyte differentiation levels of PPARγ and C/EBPα will elevate and declines when it inhibited. To test this hypothesis transcript levels of PPARγ and C/EBPα were analyzed in cells treated with **6A11**. Interestingly, levels of PPARγ and C/EBPα were decreased in dose dependent manner compare to fully differentiated adipocytes as control. SIRT1 has been shown to regulate transcription of various downstream targets like PPARγ, C/EBPα, leptin, LPL which control the fat metabolism and mobilization. An elevated transcript level of SIRT1 was observed in cells treated with **6A11** demonstrating the activation of SIRT1 and its substrates PPARγ and C/EBPα by **6A11**.

Under fasting conditions, SIRT1 transcription is regulated by p53 and FOXO3a and E2F1 in response to DNA damage. Further it has been reported SIRT1 regulate E2F1 expression in negative feedback mechanism. Thus mRNA levels of E2F1 were also studied and levels of E2F1 were declining with increasing SIRT1. Expression of mRNA levels of lipoprotein lipase, marker of adipocyte differentiation in mature adipocyte indicates lipid accumulation. LPL hydrolyses the triacylglycerides and promotes cellular uptake of chylomicron remnants, cholesterol-rich lipoproteins, and free fatty acids. Decrease in transcript levels of LPL observed with increasing concentration **6A11** signifying the reduced lipid accumulation. Another important adipocyte

gene, FAS is the crucial enzyme in de novolipogenesis, catalyzing the reactions for the synthesis of long-chain fatty acids [Sul H.S., *et al.*,1998] and its expression increases during adipogenesis[Student A.K., *et al.*, 1980]. Reduced levels of FAS were observed in cells treated with **6A11** demonstrating the inhibition of denovo lipogenesis. Lipid metabolism not only necessitates lipid synthesis and degradation, also involves lipid signaling and fatty acid storage in adipose tissue. Leptin is an endocrine /paracrine hormone secreted from adipocytes play a crucial role in food intake and energy balance. Leptin levels increases in mature adipocytes and decreases with increasing expression of SIRT1. Reduced levels of leptin with **6A11** revealed the effect of **6A11** on energy balance.

CHAPTER 7

SUMMARY
AND
CONCLUSION

CHAPTER 7
SUMMARY AND CONCLUSION

Given the spread of cancer and obesity related complications among the current global population, development of new treatment strategies is of main importance. Based on initial biological investigations, clinical and literature data, the SIRT1 appear to be an important biological target for the treatment of various disorders. From the literature, it has proven that SIRT1 inhibitors and activators have prime importance in treatment of various cancers and obesity related metabolic disorders. Hence the present study focused on the design of novel inhibitors and activators of SIRT1.

In summary, in an high throughput virtual screening campaign against human recombinant SIRT1 using a library comprising ~3000 compounds, we successfully identified two novel scaffolds viz., Acridinedione (ACD), Benzthiazolyl-2-thiosemicarbazone (B2TS) as SIRT1 inhibitors and three scaffolds viz., Spiro-piperidine-4-one (SP), Pyrido [2,3-d] pyrimidine (PP), 1-(isonicotinamido) azetidine-2, 4-dicarboxamides (AZD) as SIRT1 activators. In total, **91 compounds** [ACD (21); B2TS (16); SP (10); PP (32); AZD (12)] have been synthesized and characterized.

Compound **4d** from ACD series and **BH1, BH13** from B2TS series has shown potent SIRT1 inhibition and also suppressed the growth of breast cancer MDA-MB231 and prostate cancer LNCaP cells with IC_{50} of 0.25 µM and 46.27±0.7, 15.3±0.8 µM respectively by decreasing SIRT1 protein levels. Further **BH1** and **BH13** at 10 mg/Kg dosage showed significant reduction in hyperplasia induced by testosterone upon *in vivo* studies.

SIRT1, an NAD$^+$-dependent deacetylase that acts on proteins involved in cellular regulation, has been implicated in longevity and as a mediator of the beneficial effects of calorie restriction. In present study we identified a series of small-molecule SIRT1 activators (compound **H3** from SP series, **B9** fromPP series, **6A11** from AZD series) that are structurally unlike, and 2-3 fold more potent than, Resveratrol, the well-known SIRT1 activator found in red wine. Studies on 3T3-L1 fibroblasts **H3, B9, 6A11** suppressed the adipocyte differentiation and triglyceride accumulation by up regulation of SIRT1 followed by decline in the adipogenic markers PPARγ, C/EBPα along with FAS, E2F1, Leptin and LPL.

Preliminary *in vivo* studies on high fat diet induced obese mice compound **H3** and **B9** showed significant reduction in body weight gain as well as decrease in bad cholesterol and increase in good cholesterol levels suggesting the beneficial effects of **H3** and **B9** to ameliorate, treat, or prevent diseases and disorders associated with adipose physiology, e.g., obesity, an obesity-related disease, or a fat-related metabolic disorder.

However, representatives of these compound families need to be further optimized in hit-to-lead programs comprising medicinal chemistry efforts to address important issues such as toxicity and specificity.

FUTURE PERSPECTIVES

Recent studies demonstrated that SIRT1 plays an important role in various metabolic and inflammatory pathways which involve in cancer and metabolic disorders like obesity, type II diabetes and aging.

The present study can be extended to resolve the X-ray crystal structure of SIRT1. Although the synthesized compounds have been found to possess significant *in vitro* and *in vivo* activity, studies are still required to confirm the pharmacodynamic and pharmacokinetic profile of the active molecules including safety profile. The advancement of any of the candidate compounds presented in this thesis along a drug development path will require a significant investment in medicinal chemistry, preclinical and clinical studies.

REFERENCES

REFERENCES

Abdelmohsen K., Pullmann R. Jr., Lal A., Kim H.H., Galban S., Yang X., Phosphorylation of HuR by Chk2 regulates SIRT1 expression. *Mol Cell*. 2007, 25(4): 543-57.

Akbas F., Gasteyger C., Sjodin A., Astrup A., Larsen T.M., A critical review of the cannabinoid receptor as a drug target for obesity management. *Obes Rev*. 2009, 10(1): 58-67.

Allfrey V.G., Faulkner R., Mirsky A.E., Acetylation and Methylation of Histones and Their Possible Role in the Regulation of Rna Synthesis. *Proc Natl Acad Sci* U S A. 1964, 51:786-94.

American chemical society 2012. *Cancer facts and figures* 2012.

Aparicio O.M., Billington B.L., Gottschling D.E., Modifiers of position effect are shared between telomeric and silent mating-type loci in S. cerevisiae. *Cell*. 1991, 66(6): 1279-87.

Arduini A., Serviddio G., Escobar J., Tormos A.M., Bellanti F., Vina J., Monsalve M., Sastre J., Mitochondrial biogenesis fails in secondary biliary cirrhosis in rats leading to mitochondrial DNA depletion and deletions. *Am J Physiol Gastrointest Liver Physiol*. 2011, 301(1): G119-27.

Arruzabala M.L., Molina V., Mas R., Carbajal D., Marrero D., Gonzalez V., Rodriguez E., Effect of coconut oil on testosterone-induced prostatic hyperplasia in Sprague-Dawley rats. *J. Pharm. Pharmacol*. 2006, 59: 995-99.

Arur S., Uche U.E., Rezaul K., Fong M., Scranton V., Cowan A.E., Mohler W., Han D.K., Annexin I is an endogenous ligand that mediates apoptotic cell engulfment. *Developmental Cell*. 2003, 4: 587–598.

Autiero I., Costantini S., Colonna G., Human sirt-1: molecular modeling and structure-function relationships of an unordered protein. *PLoS One*. 2009, 4(10): p. e7350.

Bae N.S., Swanson M.J., Vassilev A., Howard B.H., Human histone deacetylase SIRT2 interacts with the homeobox transcription factor HOXA10. *J Biochem*. 2004, 135(6): 695-700.

Barzilai N., Banerjee S., Hawkins M., Chen W., Rossetti L., Caloric restriction reverses hepatic insulin resistance in aging rats by decreasing visceral fat. *J Clin Invest*. 1998, 101(7): 1353-61.

Bedalov A., Gatbonton T., Irvine W.P., Gottschling D.E., Simon J.A., Identification of a small molecule inhibitor of Sir2p. *Proc Natl Acad Sci* U S A. 2001, 98(26): p. 15113-8.

Bemis J.E., Vu C.B., Xie R., Nunes J.J., Ng P.Y., Disch J.S., Discovery of oxazolo[4,5-b]pyridines and related heterocyclic analogs as novel SIRT1 activators. *Bioorg Med Chem Lett*. 2009, 19(8): 2350-3.

Berg A.H., Scherer P.E., Adipose tissue, inflammation, and cardiovascular disease. *Circ Res*. 2005, 96(9): 939-49.

Bitterman K.J., Anderson R.M., Cohen H.Y., Latorre-Esteves M., Sinclair D.A., Inhibition of silencing and accelerated aging by nicotinamide, a putative negative regulator of yeast sir2 and human SIRT1. *J Biol Chem*. 2002, 277(47): 45099-107.

Blander G., Guarente L., The Sir2 family of protein deacetylases. *Annu Rev Biochem*. 2004, 73: 417-35.

Blander G., Olejnik J., Krzymanska-Olejnik E., McDonagh T., Haigis M., Yaffe M.B., Guarente L., SIRT1 shows no substrate specificity in vitro. *J Biol Chem*. 2005, 280(11): 9780-5.

Blum C.A., Ellis J.L., Loh C., Ng P.Y., Perni R.B., Stein R.L., SIRT1 modulation as a novel approach to the treatment of diseases of aging. *J Med Chem*. 2011, 54(2): 417-32.

Bordone L., Cohen D., Robinson A., Motta M.C., van Veen E., Czopik A., Steele A.D., Crowe H., Marmor S., Luo J., Gu W., Guarente L., SIRT1 transgenic mice show phenotypes resembling calorie restriction. *Aging Cell*. 2007, 6(6): 759-67.

Bordone L., Guarente L., Calorie restriction, SIRT1 and metabolism: understanding longevity. *Nat Rev Mol Cell Biol*. 2005, 6(4): 298-305.

Bordone L., Motta M.C., Picard F., Robinson A., Jhala U.S., Apfeld J., McDonagh T., Lemieux M., McBurney M., Szilvasi A., Easlon E.J., Lin S.J., Guarente L., Sirt1 regulates insulin secretion by repressing UCP2 in pancreatic beta cells. *PLoS Biol.* 2006, 4(2): e31.

Bradbury C.A., Khanim F.L., Hayden R., Bunce C.M., White D.A., Drayson M.T., Craddock C., Turner B.M., Histone deacetylases in acute myeloid leukaemia show a distinctive pattern of expression that changes selectively in response to deacetylase inhibitors. *Leukemi*. 2005, 19(10): 1751-9.

Bradford M.M., A rapid and sensitive method for the quantitation of microgram quantities of protein utilizing the principle of protein-dye binding. *Anal Biochem.* 1976, 72: 248-54.

Braunstein M., Rose A.B., Holmes S.G., Allis C.D., Broach JRTranscriptional silencing in yeast is associated with reduced nucleosome acetylation. *Genes Dev*. 1993, 7(4): 592-604.

Brunet, A., Sweeney L.B., Sturgill J.F., Chua K.F., Greer P.L., Lin Y., Tran H., Ross S.E., Mostoslavsky R., Cohen H. Y., Hu L. S., Cheng H. L., Jedrychowski M. P., Gygi S. P., Sinclair D. A., Alt F. W., Greenberg M. E., Stress-dependent regulation of FOXO transcription factors by the SIRT1 deacetylase. *Science*. 2004, 303(5666): 2011-5.

Buccolo G., David H., Quantitative determination of serum triglycerides by the use of enzymes. *Clin Chem*. 1973, 19: 476

Bush E.W., McKinsey T.A., Targeting histone deacetylases for heart failure. *Expert Opin Ther Targets.* 2009, 13(7): 767-84.

Cahill D.P., Kinzler K.W., Vogelstein B., Lengauer C., Genetic instability and darwinian selection in tumours. *Trends Cell Biol*. 1999, 9(12): M57-60.

Canto C., Auwerx J., PGC-1alpha, SIRT1 and AMPK, an energy sensing network that controls energy expenditure. *Curr Opin Lipidol*. 2009, 20(2): 98-105.

Canto C., Gerhart-Hines Z., Feige J.N., Lagouge M., Noriega L., Milne J.C., Elliott P.J., Puigserver P., Auwerx J., AMPK regulates energy expenditure by modulating NAD+ metabolism and SIRT1 activity. *Nature*. 2009, 458(7241): 1056-60.

Chaput J.P., St-Pierre S., Tremblay A., Currently available drugs for the treatment of obesity: Sibutramine and orlistat. *Mini Rev Med Chem*. 2007, 7(1): 3-10.

Chen D., Bruno J., Easlon E., Lin S.J., Cheng H.L., Alt F.W., Guarente L., Tissue-specific regulation of SIRT1 by calorie restriction. *Genes Dev*. 2008, 22(13): p. 1753-7.

Chen W.Y., Wang D.H., Yen R.C., Luo J., Gu W., Baylin S.B., Tumor suppressor HIC1 directly regulates SIRT1 to modulate p53-dependent DNA-damage responses. *Cell.* 2005, 123(3): 437-48.

Choudhary C., Kumar C., Gnad F., Nielsen M.L., Rehman M., Walther T.C., Olsen J. V., Mann M., Lysine acetylation targets protein complexes and co-regulates major cellular functions. *Science*. 2009, 325(5942): 834-40.

Chua K.F., Mostoslavsky R., Lombard D.B., Pang W.W., Saito S., Franco S., Kaushal D, Cheng H.L., Fischer M.R., Stokes N., Murphy M.M., Appella E., Alt F.W., Mammalian SIRT1 limits replicative life span in response to chronic genotoxic stress. *Cell Metab*. 2005. 2(1): 67-76.

Cohen H.Y., Miller C., Bitterman K.J., Wall N.R., Hekking B., Kessler B., Howitz K.T., Gorospe M., de Cabo R., Sinclair D., A.Calorie restriction promotes mammalian cell survival by inducing the SIRT1 deacetylase. *Science.* 2004, 305(5682):390-2.

Comings D.E., A general theory of carcinogenesis. *Proc Natl Acad Sci U S A*. 1973, 70(12): 3324-8.

Cooke D., Bloom S., The obesity pipeline: current strategies in the development of anti-obesity drugs. *Nat Rev Drug Discov*. 2006, 5(11): 919-31.

Cooper G.M., Cellular transforming genes. *Science*. 1982,217(4562): 801-6.

Dai J.M., Wang Z.Y., Sun D.C., Lin R.X., Wang S.Q., SIRT1 interacts with p73 and suppresses p73-dependent transcriptional activity. *J Cell Physiol*. 2007, 210(1): 161-6.

Dalton J.A., Jackson R.M., An evaluation of automated homology modelling methods at low target template sequence similarity. *Bioinformatics*. 2007, 23(15): 1901-8.

De Simone G., D'Addeo G., Sibutramine: balancing weight loss benefit and possible cardiovascular risk. *Nutr Metab Cardiovasc Dis*. 2008, 18(5): 337-41.

Denu J.M., Linking chromatin function with metabolic networks: Sir2 family of NAD(+)-dependent deacetylases. *Trends Biochem Sci*. 2003, 28(1):41-8.

Despres J.P., Cardiovascular disease under the influence of excess visceral fat. *Crit Pathw Cardiol*. 2007, 6(2): 51-9.

Despres J.P., Intra-abdominal obesity: an untreated risk factor for Type 2 diabetes and cardiovascular disease. *J Endocrinol Invest*. 2006, 29(3): 77-82.

Dominy J.E. Jr., Lee Y., Gerhart-Hines Z., Puigserver P., Nutrient-dependent regulation of PGC-1alpha's acetylation state and metabolic function through the enzymatic activities of Sirt1/GCN5. *Biochim Biophys Acta*. 2010, 1804(8): 1676-83.

Elchebly M., Payette P., Michaliszyn E., Cromlish W., Collins S., Loy A.L., Normandin D., Cheng A., Himms-Hagen J., Chan C.C., Ramachandran C., Gresser M.J., Tremblay M.L., Kennedy B.P., Increased insulin sensitivity and obesity resistance in mice lacking the protein tyrosine phosphatase-1B gene. *Science*. 1999, 283(5407): 1544-8.

Espinosa J.M., Emerson B.M., Transcriptional regulation by p53 through intrinsic DNA/chromatin binding and site-directed cofactor recruitment. *Mol Cell.* 2001, 8(1): 57-69.

Feige J.N., Lagouge M., Canto C., Strehle A., Houten S.M., Milne J.C., Lambert P.D., Mataki C., Elliott P.J., Auwerx J., Specific SIRT1 activation mimics low energy levels and protects against diet-induced metabolic disorders by enhancing fat oxidation. *Cell Metab.* 2008, 8(5): 347-58.

Feinberg A.P., Cancer epigenetics takes center stage. *Proc Natl Acad Sci U S A*, 2001. 98(2): 392-4.

Feinberg A.P., Cui H., Ohlsson R., DNA methylation and genomic imprinting: insights from cancer into epigenetic mechanisms. *Semin Cancer Biol*. 2002, 12(5): 389-98.

Feinberg A.P., Tycko B., The history of cancer epigenetics. *Nat Rev Cancer*. 2004, 4(2): 143-53.

Fernstrom J.D., Choi S., The development of tolerance to drugs that suppress food intake. *Pharmacol Ther*. 2008, 117(1): 105-22.

Finnin M.S., Donigian J.R., Pavletich N.P., Structure of the histone deacetylase SIRT2. *Nat Struct Biol.* 2001, 8(7): 621-5.

Fire A., Xu S., Montgomery M.K., Kostas S.A., Driver S.E., Mello C.C., Potent and specific genetic interference by double-stranded RNA in Caenorhabditis elegans. *Nature*. 1998, 391(6669): 806-11.

Firestein R., Blander G., Michan S., Oberdoerffer P., Ogino S., Campbell J., Bhimavarapu A., Luikenhuis S., de Cabo R., Fuchs C., Hahn W.C., Guarente L.P., Sinclair D.A., The SIRT1 deacetylase suppresses intestinal tumorigenesis and colon cancer growth. *PLoS One.* 2008, 3(4): e2020.

Fischle W., Emiliani S., Hendzel M.J., Nagase T., Nomura N., Voelter W., Verdin E., A new family of human histone deacetylases related to *Saccharomyces cerevisiae* HDA1p. *J Biol Chem.* 1999, 274(17): 11713-20.

Fisher J.S., Gao J., Han D.H., Holloszy J.O., Nolte LAActivation of AMP kinase enhances sensitivity of muscle glucose transport to insulin. *Am J Physiol Endocrinol Metab.* 2002, 282(1): E18-23.

Fontana L., Meyer T.E., Klein S., Holloszy J.O., Long-term calorie restriction is highly effective in reducing the risk for atherosclerosis in humans. *Proc Natl Acad Sci U S A.* 2004, 101(17): 6659-63.

Ford E., Voit R., Liszt G., Magin C., Grummt I., Guarente L., Mammalian Sir2 homolog SIRT7 is an activator of RNA polymerase I transcription. *Genes Dev.* 2006, 20(9): 1075-80.

Ford J., Jiang M., Milner J., Cancer-specific functions of SIRT1 enable human epithelial cancer cell growth and survival. *Cancer Res.* 2005, 65(22): 10457-63.

Frye R.A., Characterization of five human cDNAs with homology to the yeast SIR2 gene: Sir2-like proteins (sirtuins) metabolize NAD and may have protein ADP-ribosyltransferase activity. *Biochem Biophys Res Commun.* 1999, 260(1): 273-9.

Frye R.A., Phylogenetic classification of prokaryotic and eukaryotic Sir2-like proteins. *Biochem Biophys Res Commun.* 2000, 273(2): 793-8.

Fulco M., Cen Y., Zhao P., Hoffman E.P., McBurney M.W., Sauve A.A., Sartorelli V., Glucose restriction inhibits skeletal myoblast differentiation by activating SIRT1 through AMPK-mediated regulation of Nampt. *Dev Cell.* 2008, 14(5): 661-73.

Fulco M., Schiltz R.L., Iezzi S., King M.T., Zhao P., Kashiwaya Y., Hoffman E., Veech R.L., Sartorelli V., Sir2 regulates skeletal muscle differentiation as a potential sensor of the redox state. *Mol Cell.* 2003, 12(1): 51-62.

Furler S.M., Poynten A.M., Kriketos A.D., Lowy A.J., Ellis B.A., Maclean E.L., Courtenay B.G., Kraegen E.W., Campbell L.V., Chisholm D.J., Independent influences of central fat and skeletal muscle lipids on insulin sensitivity. *Obes Res*. 2001, 9(9): 535-43.

Gatbonton T., Schuler A.D., Posakony J., Li H., Goehle S., Kollipara R., Depinho R.A., Gu Y., Simon J.A., Bedalov A., Antitumor activity of a small-molecule inhibitor of human silent information regulator 2 enzymes. *Cancer Res.* 2006, 66(8): 4368-77.

Gerhart-Hines Z., Rodgers J.T., Bare O., Lerin C., Kim S.H., Mostoslavsky R., Alt F.W., Wu Z., Puigserver P., Metabolic control of muscle mitochondrial function and fatty acid oxidation through SIRT1/PGC-1alpha. *EMBO J.* 2007, 26(7): 1913-23.

Gey C., Kyrylenko S., Hennig L., Nguyen L.H., Buttner A., Pham H.D., Giannis A., Phloroglucinol derivatives guttiferone G, aristoforin, and hyperforin: inhibitors of human sirtuins SIRT1 and SIRT2. *Angew Chem Int Ed Engl*. 2007, 46(27): 5219-22.

Glass D.J., A signaling role for dystrophin: inhibiting skeletal muscle atrophy pathways. *Cancer Cell.* 2005, 8(5): 351-2.

Gottlieb S., Esposito R.E., A new role for a yeast transcriptional silencer gene, SIR2, in regulation of recombination in ribosomal DNA. *Cell.* 1989, 56(5): 771-6.

Grant P.A., A tale of histone modifications. *Genome Biol*. 2001, 2(4): REVIEWS0003.

Green H., Kehinde O., An established preadipose cell line and its differentiation in culture. II. Factors affecting the adipose conversion. *Cell.* 1975, 5:19-27.

Gu F., Dube N., Kim J.W., Cheng A., Ibarra-Sanchez Mde J., Tremblay M.L., Boisclair Y.R., Protein tyrosine phosphatase 1B attenuates growth hormone-mediated JAK2-STAT signaling. *Mol Cell Biol*. 2003, 23(11): 3753-62.

Guarente L., Sir2 links chromatin silencing, metabolism, and aging. *Genes Dev*. 2000, 14(9): 1021-6.

Guerrero R.F., Garcia-Parrilla M.C., Puertas B., Cantos-Villar E., Wine, resveratrol and health: a review. *Nat Prod Commun*. 2009, 4(5): 635-58.

Haber M., Stewart B.W., Oncogenes. A possible role for cancer genes in human malignant disease. *Med J Aust*. 1985, 142(7): 402-6.

Haigis M.C., Mostoslavsky R., Haigis K.M., Fahie K., Christodoulou D.C., Murphy A.J., Valenzuela, D. M., Yancopoulos, G. D., Karow M., Blander G., Wolberger C., Prolla T. A., Weindruch R., Alt F.W., Guarente L., SIRT4 inhibits glutamate dehydrogenase and opposes the effects of calorie restriction in pancreatic beta cells. *Cell*. 2006, 126(5): 941-54.

Halgren T.A., Identifying and characterizing binding sites and assessing druggability. *J Chem Inf Model*. 2009, 49(2): 377-89.

Halili M.A., Andrews M.R., Sweet M.J., Fairlie D.P., Histone deacetylase inhibitors in inflammatory disease. *Curr Top Med Chem*. 2009, 9(3): 309-19.

Hallows W.C., Lee S., Denu J.M., Sirtuins deacetylate and activate mammalian acetyl-CoA synthetases. *Proc Natl Acad Sci U S A*. 2006, 103(27): 10230-5.

Hanahan D., Weinberg R.A., The hallmarks of cancer. *Cell*. 2000, 100 (1): p. 57-70.

Haslam D.W., James W.P., Obesity. *Lancet*. 2005, 366(9492): 1197-209.

Hernick M., Fierke C.A., Zinc hydrolases: the mechanisms of zinc-dependent deacetylases. *Arch Biochem Biophys*. 2005, 433(1): 71-84.

Holmes B.F., Sparling D.P., Olson A.L., Winder W.W., Dohm G.L., Regulation of muscle GLUT4 enhancer factor and myocyte enhancer factor 2 by AMP-activated protein kinase. *Am J Physiol Endocrinol Metab*. 2005, 289(6): E1071-6.

Hou X., Xu S., Maitland-Toolan K.A., Sato K., Jiang B., Ido Y., Lan F., Walsh K., Wierzbicki M., Verbeuren T.J., Cohen R.A., Zang M., SIRT1 regulates hepatocyte lipid metabolism through activating AMP-activated protein kinase. *J Biol Chem*. 2008, 283(29): 20015-26.

Howitz K.T., Bitterman K.J., Cohen H.Y., Lamming D.W., Lavu S., Wood J.G., Zipkin R.E., Chung P., Kisielewski A., Zhang L.L., Scherer B., Sinclair D.A., Small molecule activators of sirtuins extend *Saccharomyces cerevisiae* lifespan. *Nature*. 2003, 425(6954): 191-6.

http://clinicaltrials.gov/ct2/show/study/NCT01485965?term=Huntington%27s+Disease.

http://string-db.org/newstring_cgi/show_network_section.pl

http://www.clinicaltrials.gov/ct2/results?term=NCT01018628&Search=Search.

http://www.clinicaltrials.gov/ct2/results?term=NCT01412645&Search=Search.

http://www.clinicaltrials.gov/ct2/show/NCT00020579?term=histone+deacetylase&rank=39.

http://www.clinicaltrials.gov/ct2/show/NCT00383565?term=histone+deacetylase&rank=6.

http://www.clinicaltrials.gov/ct2/show/NCT00603902?term=Lorcaserin&rank=1.

http://www.clinicaltrials.gov/ct2/show/NCT00603902?term=Lorcaserin&rank=1

http://www.clinicaltrials.gov/ct2/show/NCT00686218?term=histone+deacetylase&rank=4.

http://www.clinicaltrials.gov/ct2/show/NCT00697879?term=histone+deacetylase&rank=1.

http://www.clinicaltrials.gov/ct2/show/NCT01018017.

http://www.clinicaltrials.gov/ct2/show/NCT01038089?term=NCT01038089&rank=1.

http://www.clinicaltrials.gov/ct2/show/NCT01158417?term=NCT01158417&rank=1.

http://www.clinicaltrials.gov/ct2/show/NCT01344707?term=histone+deacetylase&rank=3.

http://www.clinicaltrials.gov/ct2/show/NCT01464112?term=histone+deacetylase&rank=13.

http://www.clinicaltrials.gov/ct2/show/study/NCT00792467?term=histone+deacetylase&rank=1
9.

Huffman D.M., Grizzle W.E., Bamman M.M., Kim J.S., Eltoum I.A., Elgavish A., Nagy T.R., SIRT1 is significantly elevated in mouse and human prostate cancer. *Cancer Res.* 2007, 67(14): 6612-8.

Huhtiniemi, T., Wittekindt C., Laitinen T., Leppanen J., Salminen A., Poso A., Comparative and pharmacophore model for deacetylase SIRT1. *J Comput Aided Mol Des.* 2006, 20(9): 589-99.

Hussain A., Hydrie M.Z.I., Claussen B., Asghar S., Type 2 Diabetes and obesity: A review. *Journal of Diabetology*. 2010, 2.

Ide T., Shimano H., Yahagi N., Matsuzaka T., Nakakuki M., Yamamoto T., Nakagawa Y., Takahashi A., Suzuki H., Sone H., Toyoshima H., Fukamizu A., Yamada N., SREBPs suppress IRS-2-mediated insulin signalling in the liver. *Nat Cell Biol*. 2004, 6(4): 351-7.

Imai S., Armstrong C.M., Kaeberlein M., Guarente L., Transcriptional silencing and longevity protein Sir2 is an NAD-dependent histone deacetylase. *Nature*. 2000, 403(6771): 795-800.

Ivy J.M., Hicks J.B., Klar A.J., Map positions of yeast genes SIR1, SIR3 and SIR4. *Genetics*. 1985, 111(4): 735-44.

Jackson M.D., Schmidt M.T., Oppenheimer N.J., Denu J.M., Mechanism of nicotinamide inhibition and transglycosidation by Sir2 histone/protein deacetylases. *J Biol Chem.* 2003, 278(51): 50985-98.

Jacobson M.P., Pincus D.L., Rapp C.S., Day T.J., Honig B., Shaw D.E., Friesner R.A., A hierarchical approach to all-atom protein loop prediction. *Proteins*. 2004, 55(2): 351-67.

Jaenisch R., Bird A., Epigenetic regulation of gene expression: how the genome integrates intrinsic and environmental signals. *Nat Genet.* 200, 33 Suppl: 245-54.

Jager S., Handschin C., St-Pierre J., Spiegelman B.M., AMP-activated protein kinase (AMPK) action in skeletal muscle via direct phosphorylation of PGC-1alpha. *Proc Natl Acad Sci U S A.* 2007, 104(29): 12017-22.

Jeong J., Juhn K., Lee H., Kim S.H., Min B.H., Lee K.M., Cho M.H., Park G.H., Lee K.H., SIRT1 promotes DNA repair activity and deacetylation of Ku70. *Exp Mol Med.* 2007, 39(1):8-13.

Jessen N., Pold R., Buhl E.S., Jensen L.S., Schmitz O., Lund S., Effects of AICAR and exercise on insulin-stimulated glucose uptake, signaling, and GLUT-4 content in rat muscles. *J Appl Physiol.* 2003, 94(4): 1373-9.

Jin L., Wei W., Jiang Y., Peng H., Cai J., Mao C., Dai H., Choy W., Bemis J.E., Jirousek M.R., Milne J.C., Westphal C.H., Perni R.B., Crystal structures of human SIRT3 displaying substrate-induced conformational changes. *J Biol Chem*. 2009, 284(36): 24394-405.

Kadowaki T., Yamauchi T., Adiponectin and adiponectin receptors. *Endocr Rev*. 2005, 26(3): 439-51.

Kalle A.M., Mallika A., Badiger J., Alinakhi., Talukdar P., Sachchidanand. Inhibition of SIRT1 by a small molecule induces apoptosis in breast cancer cells. *Biochem Biophys Res Commun*. 2010, 401(1): 13-9.

Karamadoukis L., Shivashankar G.H., Ludeman L., Williams A.J., An unusual complication of treatment with orlistat. *Clin Nephro*. 2009, 71(4): 430-2.

Kim E.J., Kho J.H., Kang M.R., Um S.J., Active regulator of SIRT1 cooperates with SIRT1 and facilitates suppression of p53 activity. *Mol Cell*. 2007, 28(2): 277-90.

Kim S., Jin Y., Choi Y., Park T., Resveratrol exerts anti-obesity effects via mechanisms involving down-regulation of adipogenic and inflammatory processes in mice. *Biochem Pharmacology.* 2011, 81:1343–51.

Kitamura Y.I., Kitamura T., Kruse J.P., Raum J.C., Stein R., Gu W., Accili D., FoxO1 protects against pancreatic beta cell failure through NeuroD and MafA induction. *Cell Metab*. 2005, 2(3): 153-63.

Klar A.J., Fogel S., Macleod K., MAR1-a Regulator of the HMa and HMalpha Loci in *Saccharomyces cerevisiae. Genetics*. 1979, 93(1): 37-50.

Knudson A.G., Mutation and cancer: statistical study of retinoblastoma. *Proc Natl Acad Sci U S A.* 1971, 68(4): 820-3.

Kobayashi Y., Furukawa-Hibi Y., Chen C., Horio Y., Isobe K., Ikeda K., Motoyama N., SIRT1 is critical regulator of FOXO-mediated transcription in response to oxidative stress. *Int J Mol Med*. 2005, 16(2): 237-43.

Koves T.R., Li P., An J., Akimoto T., Slentz D., Ilkayeva O., Dohm G.L., Yan Z., Newgard C.B., Muoio D.M., Peroxisome proliferator-activated receptor-gamma co-activator 1alpha-mediated metabolic remodeling of skeletal myocytes mimics exercise training and reverses lipid-induced mitochondrial inefficiency. *J Biol Chem*. 2005, 280(39): 33588-98.

Kuzmichev A., Margueron R., Vaquero A., Preissner T.S., Scher M., Kirmizis A., Ouyang X., Brockdorff N., Abate-Shen C., Farnham P., Reinberg D., Composition and histone substrates of polycomb repressive group complexes change during cellular differentiation. *Proc Natl Acad Sci U S A*. 2005, 102(6): 1859-64.

Lan F., Cacicedo J.M., Ruderman N., Ido Y., SIRT1 modulation of the acetylation status, cytosolic localization, and activity of LKB1. Possible role in AMP-activated protein kinase activation. *J Biol Chem*. 2008, 283(41): 27628-35.

Landry J., Slama J.T., Sternglanz R., Role of NAD(+) in the deacetylase activity of the SIR2-like proteins. *Biochem Biophys Res Commun*. 2000, 278(3): 685-90.

Landry J., Sutton A., Tafrov S.T., Heller R.C., Stebbins J., Pillus L., The silencing protein SIR2 and its homologs are NAD-dependent protein deacetylases. *Proc Natl Acad Sci U S A*. 2000, 97(11):5807-11.

Langley E., Pearson M., Faretta M., Bauer U.M., Frye R.A., Minucci S., Pelicci P. G., Kouzarides T., Human SIR2 deacetylates p53 and antagonizes PML/p53-induced cellular senescence. *EMBO J*. 2002, 21(10): 2383-96.

Lara E., Mai A., Calvanese V., Altucci L., Lopez-Nieva P., Martinez-Chantar M.L., Varela-Rey M., Rotili D., Nebbioso A., Ropero S., Montoya G., Oyarzabal J., Velasco S., Serrano M., Witt M., Villar-Garea A., Imhof A., Mato J.M., Esteller M., Fraga M.F., Salermide, a Sirtuin inhibitor with a strong cancer-specific proapoptotic effect. *Oncogene*. 2009, 28(6): 781-91.

Laskowski R.A., MacArthur M.W., Moss D.S., Thornton J.M., PROCHECK: a program to check the stereochemical quality of protein structures. *J Appl Cryst*. 1993, 26: 283-291.

Legube G., Trouche D., Regulating histone acetyltransferases and deacetylases. *EMBO Rep*. 2003, 4(10): 944-7.

Leibiger I.B., Berggren P.O., Sirt1: a metabolic master switch that modulates lifespan. *Nat Med*. 2006, 12(1): 34-6; discussion 36.

Li X., Zhang S., Blander G., Tse J.G., Krieger M., Guarente L., SIRT1 deacetylates and positively regulates the nuclear receptor LXR. *Mol Cell*. 2007, 28(1): 91-106.

Li Z., Maglione M., Tu W., Mojica W., Arterburn D., Shugarman L.R., Meta-analysis: pharmacologic treatment of obesity. *Ann Intern Med*. 2005, 142(7): 532-46.

Librizzi M., Longo A., Chiarelli R., Amin J., Spencer J., Luparello C., Cytotoxic Effects of Jay Amin Hydroxamic Acid (JAHA), a Ferrocene-Based Class I Histone Deacetylase Inhibitor, on Triple-Negative MDA-MB231 Breast Cancer Cells. *Chem Res Toxico*. 2012, 25(11):2608-16

Lill N.L., Grossman S.R., Ginsberg D., DeCaprio J., Livingston D.M., Binding and modulation of p53 by p300/CBP coactivators. *Nature*. 1997, 387(6635): 823-7.

Lillycrop K.A., Burdge G.C., Epigenetic changes in early life and future risk of obesity. *Int J Obes (Lond)*. 2011, 35(1): 72-83.

Lim C.S., SIRT1: tumor promoter or tumor suppressor? *Med Hypotheses*. 2006, 67(2): 341-4.

Lin S.J., Defossez P.A., Guarente L., Requirement of NAD and SIR2 for life-span extension by calorie restriction in Saccharomyces cerevisiae. *Science*. 2000, 289(5487): 2126-8.

Lin S.J., Ford E., Haigis M., Liszt G., Guarente L., Calorie restriction extends yeast life span by lowering the level of NADH. *Genes Dev*. 2004, 18(1): 12-6.

Lin, S.J., Kaeberlein M., Andalis A.A., Sturtz L.A., Defossez P.A., Culotta V.C., Fink G. R., Guarente L., Calorie restriction extends *Saccharomyces cerevisiae* lifespan by increasing respiration. *Nature.* 2002, 418(6895): 344-8.

Liszt G., Ford E., Kurtev M., Guarente L., Mouse Sir2 homolog SIRT6 is a nuclear ADP-ribosyltransferase. *J Biol Chem*. 2005, 280(22):21313-20.

Liu da-qi., yang b., guo., zhang., Yan N.A., Association study of SIRT1 expression with benign prostatic hyperplasia. *Chinese Journal of Clinicians*. 2011, 5:22.

Liu K.Z., Schultz C.P., Johnston J.B., Lee K., Mantsch H.H., Comparison of infrared spectra of CLL cells with their ex vivo sensitivity (MTT assay) to chlorambucil and cladribine. *Leuk Res*. 1997, 21(11-12): 1125-33.

Lovaas J.D., Zhu L., Chiao C.Y., Byles V., Faller D.V., Dai Y., SIRT1 enhances matrix metalloproteinase-2 expression and tumor cell invasion in prostate cancer cells. *Prostate*. 2012, doi: 10.1002/pros.22592. [Epub ahead of print]

Luo J., Nikolaev A.Y., Imai S., Chen D., Su F., Shiloh A., Guarente L.,Gu W., Negative control of p53 by Sir2alpha promotes cell survival under stress. *Cell*. 2001, 107(2): 137-48.

Mai A., Massa S., Lavu S., Pezzi R., Simeoni S., Ragno R., Mariotti F.R., Chiani F., Camilloni G., Sinclair D.A., Design, synthesis, and biological evaluation of sirtinol analogues as class III histone/protein deacetylase (Sirtuin) inhibitors. *J Med Chem*. 2005, 48(24): 7789-95.

Mai A., Massa S., Rotili D.,Cerbara I.,Valente S.,Pezzi R.,Simeoni S.,Ragno R., Histone deacetylation in epigenetics: an attractive target for anticancer therapy. *Med Res Rev*. 2005, 25(3): 261-309.

Mai A., Valente S., Meade S., Carafa V., Tardugno M., Nebbioso A., Galmozzi A., Mitro N., De Fabiani E., Altucci L., Kazantsev A., Study of 1,4-dihydropyridine structural scaffold: discovery of novel sirtuin activators and inhibitors. *J Med Chem*. 2009, 52(17): 5496-504.

Malik H.S., Henikoff S., Phylogenomics of the nucleosome. *Nat Struct Biol*. 2003, 10(11): 882-91.

Manjashetty T.H., Yogeeswari P., Sriram D., Microwave assisted one-pot synthesis of highly potent novel isoniazid analogues. *Bioorg Med Chem Lett*. 2011, 21(7): 2125-8.

Manjulatha K., Srinivas S., Mulakayala N., Rambabu D., Prabhakar M., Arunasree K.M., Alvala M., Basaveswara Rao M.V., Pal M., Ethylenediamine diacetate (EDDA) mediated synthesis of

aurones under ultrasound: their evaluation as inhibitors of SIRT1. *Bioorg Med Chem Lett*. 2012, 22(19): 6160-5.

Marmorstein R., Roth S.Y., Histone acetyltransferases: function, structure, and catalysis. *Curr Opin Genet Dev*. 2001, 11(2): 155-61.

McBurney M.W., Yang X., Jardine K., Hixon M., Boekelheide K., Webb J.R., Lansdorp P.M., Lemieux M., The mammalian SIR2alpha protein has a role in embryogenesis and gametogenesis. *Mol Cell Biol*. 2003, 23(1): 38-54.

McKinsey T.A., Targeting inflammation in heart failure with histone deacetylase inhibitors. *Mol Med*. 2011, 17(5-6): 434-41.

Michael L.F., Wu Z., Cheatham R.B., Puigserver P., Adelmant G., Lehman J.J., Kelly D.P., Spiegelman B.M., Restoration of insulin-sensitive glucose transporter (GLUT4) gene expression in muscle cells by the transcriptional coactivator PGC-1. *Proc Natl Acad Sci U S A*. 2001, 98(7): 3820-5.

Michishita E., Park J.Y., Burneskis J.M., Barrett J.C., Horikawa I., Evolutionarily conserved and nonconserved cellular localizations and functions of human SIRT proteins. *Mol Biol Cell*. 2005, 16(10): 4623-35.

Milne J.C., Lambert P.D., Schenk S., Carney D.P., Smith J.J., Gagne D.J., Small molecule activators of SIRT1 as therapeutics for the treatment of type 2 diabetes. *Nature*. 2007, 450(7170): 712-6.

Monteiro J.P., Cano M.I., SIRT1 deacetylase activity and the maintenance of protein homeostasis in response to stress: an overview. *Protein Pept Lett*. 2011, 18(2): 167-73.

Mootha V.K., Bunkenborg J., Olsen J.V., Hjerrild M., Wisniewski J.R., Stahl E., Bolouri M.S., Ray H.N., Sihag S., Kamal M., Patterson N., Lander E.S., Mann M., Integrated analysis of

protein composition, tissue diversity, and gene regulation in mouse mitochondria. *Cell*. 2003, 115(5): 629-40.

Mootha V.K., Handschin C., Arlow D., Xie X., St Pierre J., Sihag S., Yang W., Altshuler D., Puigserver P., Patterson N., Willy P.J., Schulman I.G., Heyman R.A., Lander E.S., Spiegelman B.M., Erralpha and Gabpa/b specify PGC-1alpha-dependent oxidative phosphorylation gene expression that is altered in diabetic muscle. *Proc Natl Acad Sci U S A*. 2004, 101(17): 6570-5.

Mosmann T., Rapid colorimetric assay for cellular growth and survival: application to proliferation and cytotoxicity assays. *J Immunol Methods*. 1983, 65(1-2): 55-63.

Mostoslavsky R., Chua K.F., Lombard D.B., Pang W.W., Fischer M.R., Gellon L., Liu P., Mostoslavsky G., Franco S., Murphy M.M., Mills K.D., Patel P., Hsu J.T., Hong A.L., Ford E., Cheng H.L., Kennedy C., Nunez N., Bronson R., Frendewey D., Auerbach W., Valenzuela D., Karow M., Hottiger M.O., Hursting S., Barrett J.C., Guarente L., Mulligan R., Demple B., Yancopoulos G.D., Alt F.W., Genomic instability and aging-like phenotype in the absence of mammalian SIRT6. *Cell*. 2006, 124(2): 315-29.

Motta, M.C., Divecha N., Lemieux M., Kamel C., Chen D., Gu W., Bultsma Y., McBurney M., Guarente L., Mammalian SIRT1 represses forkhead transcription factors. *Cell*. 2004, 116(4): 551-63.

Moynihan K.A., Grimm A.A., Plueger M.M., Bernal-Mizrachi E., Ford E., Cras-Meneur C., Permutt M. A., Imai S., Increased dosage of mammalian Sir2 in pancreatic beta cells enhances glucose-stimulated insulin secretion in mice. *Cell Metab*. 2005, 2(2): 105-17.

Napper A.D., Hixon J., McDonagh T., Keavey K., Pons J.F., Barker J., Yau W.T., Amouzegh P., Flegg A., Hamelin E., Thomas R.J., Kates M., Jones S., Navia M.A., Saunders J.O., DiStefano

P.S., Curtis R., Discovery of indoles as potent and selective inhibitors of the deacetylase SIRT1. *J Med Chem*. 2005, 48(25): 8045-54.

Nayagam V.M., Wang X., Tan Y.C., Poulsen A., Goh K.C., Ng T., Wang H., Song H.Y., Ni B., Entzeroth M., Stunkel W., SIRT1 modulating compounds from high-throughput screening as anti-inflammatory and insulin-sensitizing agents. *J Biomol Screen*. 2006, 11(8): 959-67.

Nemoto S., Fergusson M.M., Finkel T., Nutrient availability regulates SIRT1 through a forkhead-dependent pathway. *Science*. 2004, 306(5704): 2105-8.

Nishimasu H., Fushinobu S., Shoun H., Wakagi T., Crystal structures of an ATP-dependent hexokinase with broad substrate specificity from the hyperthermophilic archaeon Sulfolobus tokodaii. *J Biol Chem*. 2007, 282(13): 9923-31.

North B.J., Marshall B.L., Borra M.T., Denu J.M., Verdin E., The human Sir2 ortholog, SIRT2, is an NAD+-dependent tubulin deacetylase. *Mol Cell*. 2003, 11(2): 437-44.

Norvell A., McMahon S.B, Cell biology. Rise of the rival. *Science*. 2010, 327(5968): 964-5.

Ohsawa S., Miura M., Caspase-mediated changes in Sir2alpha during apoptosis. *FEBS Lett*. 2006, 580(25): 5875-9.

Olsson A., Manzl C., Strasser A., Villunger A., How important are post-translational modifications in p53 for selectivity in target-gene transcription and tumour suppression? *Cell Death Differ*. 2007, 14(9): 1561-75.

Ono Y,, Hattori E,, Fukaya Y,, Imai S,, Ohizumi Y., Anti-obesity effect of Nelumbo nucifera leaves extract in mice and rats. *J Ethnopharmacol*. 2006,106:238-244.

Pacholec M., Bleasdale J.E., Chrunyk B., Cunningham D., Flynn D., Garofalo R.S., Griffith D., Griffor M., Loulakis P., Pabst B., Qiu X., Stockman B., Thanabal V., Varghese A., Ward J.,

Withka J., Ahn K., SRT1720, SRT2183, SRT1460, and resveratrol are not direct activators of SIRT1. *J Biol Chem*. 2010, 285(11): 8340-51.

Pan P.W., Feldman J.L., Devries M.K., Dong A., Edwards A.M., Denu J.M., Structure and biochemical functions of SIRT6. *J Biol Chem*. 2011, 286(16): 14575-87.

Patti M.E., Butte A.J., Crunkhorn S., Cusi K., Berria R., Kashyap S., Miyazaki Y., Kohane I., Costello M., Saccone R., Landaker E.J., Goldfine A.B., Mun E., DeFronzo R., Finlayson J., Kahn C.R., Mandarino L.J., Coordinated reduction of genes of oxidative metabolism in humans with insulin resistance and diabetes: Potential role of PGC1 and NRF1. *Proc Natl Acad Sci U S A*. 2003, 100(14): 8466-71.

Peck B., Chen C.Y., Ho K.K., Di Fruscia P., Myatt S.S., Coombes R.C., Fuchter M.J., Hsiao C.D., Lam E.W., SIRT inhibitors induce cell death and p53 acetylation through targeting both SIRT1 and SIRT2. *Mol can ther.* 2010,9(4):844-855.

Pfluger P.T., Herranz D., Velasco-Miguel S., Serrano M., Tschop M.H., Sirt1 protects against high-fat diet-induced metabolic damage. *Proc Natl Acad Sci U S A*. 2008, 105(28): 9793-8.

Picard F., Kurtev M., Chung N., Topark-Ngarm A., Senawong T, Machado De Oliveira R., Leid M., McBurney M.W., Guarente L., Sirt1 promotes fat mobilization in white adipocytes by repressing PPAR-gamma. *Nature*. 2004, 429(6993): 771-6.

Pillarisetti S., A review of Sirt1 and Sirt1 modulators in cardiovascular and metabolic diseases. Recent Pat Cardiovasc *Drug Discov*. 2008, 3(3): 156-64.

Pitot H.C., Dragan Y.P., Facts and theories concerning the mechanisms of carcinogenesis. *FASEB J*. 1991, 5(9): 2280-6.

Posakony J., Hirao M., Stevens S., Simon J.A., Bedalov A., Inhibitors of Sir2: evaluation of splitomicin analogues. *J Med Chem*. 2004, 47(10): 2635-44.

Puigserver P., Rhee J., Donovan J., Walkey C.J., Yoon J.C., Oriente F., Kitamura Y., Altomonte J., Dong H., Accili D., Spiegelman B.M. Insulin-regulated hepatic gluconeogenesis through FOXO1-PGC-1alpha interaction. *Nature*. 2003, 423(6939): 550-5.

Pulla V.K., Battu M.B., Alvala M., Sriram D., Yogeeswari P., Can targeting SIRT-1 to treat type 2 diabetes be a good strategy? A review. *Expert Opin Ther Targets*. 2012, 16(8): 819-32.

Purushotham A., Schug T.T., Xu Q., Surapureddi S., Guo X., Li X., Hepatocyte-specific deletion of SIRT1 alters fatty acid metabolism and results in hepatic steatosis and inflammation. *Cell Metab*. 2009, 9(4): 327-38.

Qiao L., Shao J., SIRT1 regulates adiponectin gene expression through Foxo1-C/enhancer-binding protein alpha transcriptional complex. *J Biol Chem*. 2006, 281(52): 39915-24.

Rajala M.W., Scherer P.E., Minireview: The adipocyte--at the crossroads of energy homeostasis, inflammation, and atherosclerosis. *Endocrinology*. 2003, 144(9): 3765-73.

Randle P.J., Garland P.B., Hales C.N., Newsholme EA.The glucose fatty-acid cycle. Its role in insulin sensitivity and the metabolic disturbances of diabetes mellitus. *Lancet*. 1963, 1(7285): 785-9.

Ravi A., Mallika A., Venkatesh S., Sajeli B., Rukaiyya S.K., Madhava R.B., Antiproliferative activity and standardization of Tecomella undulata bark extract on K562 cells. *J Ethnopharmacol.* 2011, 137:1353-1359.

Revollo J.R., Grimm A.A., Imai S., The NAD biosynthesis pathway mediated by nicotinamide phophoribosyltransferase regulates Sir2 activity in mammalian cells. *J Biol Chem*. 2004, 279(49): 50754-63.

Rhee J., Inoue Y., Yoon J.C., Puigserver P., Fan M., Gonzalez F.J., Spiegelman B.M., Regulation of hepatic fasting response by PPARgamma coactivator-1alpha (PGC-1):

requirement for hepatocyte nuclear factor 4alpha in gluconeogenesis. *Proc Natl Acad Sci U S A*. 2003, 100(7): 4012-7.

Robins R. K., Hitchings G. H., Studies on Condensed Pyrimidine Systems. XII. Synthesis of Some 4- and 2,4-Substituted Pyrido[2,3-d]pyrimidines *J. Am. Chem. Soc.* 1954,77(8): 2256–60.

Rodgers J.T., Lerin C., Haas W., Gygi S.P., Spiegelman B.M., Puigserver P., Nutrient control of glucose homeostasis through a complex of PGC-1alpha and SIRT1. *Nature*. 2005, 434(7029): 113-8.

Sakaguchi K., Herrera J.E., Saito S., Miki T., Bustin M., Vassilev A., Anderson C.W., Appella E., DNA damage activates p53 through a phosphorylation-acetylation cascade. *Genes Dev*. 1998, 12(18): 2831-41.

Sakamoto J., Miura T., Shimamoto K., Horio Y., Predominant expression of Sir2alpha, an NAD-dependent histone deacetylase, in the embryonic mouse heart and brain. *FEBS Lett*. 2004, 556(1-3): 281-6.

Sakao Y., Kato A., Tsuji T., Yasuda H., Togawa A., Fujigaki Y., Kahyo T., Setou M., Hishida A., Cisplatin induces Sirt1 in association with histone deacetylation and increased Werner syndrome protein in the kidney. *Clin Exp Nephrol*. 2011, 15(3): 363-72.

Sasaki T., Maier B., Bartke A., Scrable H.,Progressive loss of SIRT1 with cell cycle withdrawal. *Aging Cell*. 2006, 5(5): 413-22.

Sasaki T., Maier B., Koclega K.D., Chruszcz M., Gluba W., Stukenberg P.T., Minor W., Scrable H., Phosphorylation regulates SIRT1 function. *PLoS One*. 2008, 3(12): e4020.

Sauve A.A., Schramm V.L., Sir2 regulation by nicotinamide results from switching between base exchange and deacetylation chemistry. *Biochemistry*. 2003, 42(31): 9249-56.

Schreiber S.N., Emter R., Hock M.B., Knutti D., Cardenas J., Podvinec M., Oakeley E.J., Kralli A., The estrogen-related receptor alpha (ERRalpha) functions in PPARgamma coactivator 1alpha (PGC-1alpha)-induced mitochondrial biogenesis. *Proc Natl Acad Sci U S A*. 2004, 101(17): 6472-7.

Schuetz A., Min J., Antoshenko T., Wang C.L., Allali-Hassani A., Dong A., Loppnau P., Vedadi M., Bochkarev A., Sternglanz R., Plotnikov A.N., Structural basis of inhibition of the human NAD+-dependent deacetylase SIRT5 by suramin. *Structure*. 2007, 15(3): 377-89.

Senawong T., Peterson V. J., Leid M., BCL11A-dependent recruitment of SIRT1 to a promoter template in mammalian cells results in histone deacetylation and transcriptional repression. *Arch Biochem Biophys*.2005, 434(2): 316-25.

Shakespear M.R., Halili M.A., Irvine K.M., Fairlie D.P., Sweet M.J., Histone deacetylases as regulators of inflammation and immunity. *Trends Immunol*. 2011, 32(7): 335-43.

Sharma A., Gautam V., Costantini S., Paladino A., Colonna G., Interactomic and pharmacological insights on human sirt-1. *Front Pharmacol*. 2012, 3: 40.

Sherr C.J., Principles of tumor suppression. Cell. 2004, 116(2):235-46.

Shi T., Wang F., Stieren E., Tong Q., SIRT3, a mitochondrial sirtuin deacetylase, regulates mitochondrial function and thermogenesis in brown adipocytes. *J Biol Chem*. 2005, 280(14): 13560-7.

Shore D., Squire M., Nasmyth K.A., Characterization of two genes required for the position-effect control of yeast mating-type genes. *EMBO J*. 1984, 3(12): 2817-23.

Slovacek L., Pavlik V., Slovackova B., The effect of sibutramine therapy on occurrence of depression symptoms among obese patients. *Nutr Metab Cardiovasc Dis*. 2008, 18(8): e43-4.

Smith J., Human Sir2 and the 'silencing' of p53 activity. *Trends Cell Biol*. 2002, 12(9): 404-6.

Smith J.S., Brachmann C.B., Celic I., Kenna M.A., Muhammad S., Starai V.J., A phylogenetically conserved NAD+-dependent protein deacetylase activity in the Sir2 protein family. *Proc Natl Acad Sci U S A*. 2000, 97(12): 6658-63.

Steppel J.H., Horton E.S., Beta-cell failure in the pathogenesis of type 2 diabetes mellitus. *Curr Diab Rep*. 2004, 4(3): 169-75.

Student A.K., Hsu R.Y., Lane M.D., Induction of fatty acid synthetase synthesis in differentiating 3T3-L1 preadipocytes. *J Biol Chem*. 1980. 255(10): 4745-50.

Stunkel W., Peh B.K., Tan Y.C., Nayagam V.M., Wang X., Salto-Tellez M., Ni B., Entzeroth M., Wood J., Function of the SIRT1 protein deacetylase in cancer. *Biotechnol J*. 2007, 2(11): 1360-8.

Sul H.S., Wang D., Nutritional and hormonal regulation of enzymes in fat synthesis: studies of fatty acid synthase and mitochondrial glycerol-3-phosphate acyltransferase gene transcription. *Annu Rev Nutr*. 1998, 18: 331-51.

Suwa M., Egashira T., Nakano H., Sasaki H., Kumagai S., Metformin increases the PGC-1alpha protein and oxidative enzyme activities possibly via AMPK phosphorylation in skeletal muscle in vivo. *J Appl Physiol*. 2006, 101(6): 1685-92.

Suzuki T., Imai K., Nakagawa H., Miyata N., 2-Anilinobenzamides as SIRT inhibitors. *ChemMedChem*. 2006, 1(10): 1059-62.

Tadokoro Y., Ema H., Okano M., Li E., Nakauchi H., De novo DNA methyltransferase is essential for self-renewal, but not for differentiation, in hematopoietic stem cells. *J Exp Med*. 2007, 204(4): 715-22.

Takahashi A., Motomura K., Kato T., Yoshikawa T., Nakagawa Y., Yahagi N., Sone H., Suzuki H., Toyoshima H., Yamada N., Shimano H., Transgenic mice overexpressing nuclear SREBP-1c in pancreatic beta-cells. *Diabetes*. 2005, 54(2): 492-9.

Takata T., Ishikawa F., Human Sir2-related protein SIRT1 associates with the bHLH repressors HES1 and HEY2 and is involved in HES1- and HEY2-mediated transcriptional repression. *Biochem Biophys Res Commun*. 2003, 301(1): 250-7.

Tanikawa M., Wada-Hiraike O., Nakagawa S., Shirane A., Hiraike H., Koyama S., Multifunctional transcription factor TFII-I is an activator of BRCA1 function. *Br J Cancer*. 2011, 104(8): 1349-55.

Tanno M., Sakamoto J., Miura T., Shimamoto K., Horio Y., Nucleocytoplasmic shuttling of the NAD+-dependent histone deacetylase SIRT1. *J Biol Chem*. 2007, 282(9): 6823-32.

Tanny J.C., Dowd G.J., Huang J., Hilz H., Moazed D., An enzymatic activity in the yeast Sir2 protein that is essential for gene silencing. *Cell*. 1999, 99(7): 735-45.

Tanumihardjo S.A., Anderson C., Kaufer-Horwitz M., Bode L., Emenaker N.J., Haqq A.M., Satia J.A., Silver H.J., Stadler D.D., Poverty, obesity, and malnutrition: an international perspective recognizing the paradox. *J Am Diet Assoc*. 2007, 107(11): 1966-72.

Taunton J., Hassig C.A., Schreiber S.L., A mammalian histone deacetylase related to the yeast transcriptional regulator Rpd3p. *Science*. 1996, 272(5260): 408-11.

Thiagalingam S., Cheng K.H., Lee H.J., Mineva N., Thiagalingam A., Ponte JF Histone deacetylases: unique players in shaping the epigenetic histone code. *Ann N Y Acad Sci*. 2003, 983: 84-100.

Thompson J.D., Higgins D.G., Gibson T.J., CLUSTAL W: improving the sensitivity of progressive multiple sequence alignment through sequence weighting, position-specific gap penalties and weight matrix choice. *Nucleic Acids Res.* 1994, 22(22): 4673-80.

van den Berghe G., The role of the liver in metabolic homeostasis: implications for inborn errors of metabolism. *J Inherit Metab Dis*. 1991, 14(4): 407-20.

Van der Horst A., Tertoolen L.G., de Vries-Smits L.M., Frye R.A., Medema R.H., Burgering BM. FOXO4 is acetylated upon peroxide stress and deacetylated by the longevity protein hSir2(SIRT1). *J Biol Chem.* 2004, 279(28): 28873-9.

Vaquero A., Scher M., Lee D., Erdjument-Bromage H., Tempst P., Reinberg D., Human SirT1 interacts with histone H1 and promotes formation of facultative heterochromatin. *Mol Cell.* 2004, 16(1): 93-105.

Vaziri H., Dessain S.K., Ng Eaton E., Imai S.I., Frye R.A., Pandita T.K., hSIR2(SIRT1) functions as an NAD-dependent p53 deacetylase. *Cell.* 2001, 107(2): 149-59.

Vu C.B., Bemis J.E., Disch J.S., Ng P.Y., Nunes J.J., Milne J.C., Discovery of imidazo[1,2-b]thiazole derivatives as novel SIRT1 activators. *J Med Chem.* 2009, 52(5): 1275-83.

Wang C., Chen L., Hou X., Li Z., Kabra N., Ma Y., Nemoto S., Finkel T., Gu W., Cress W. D., Chen J., Interactions between E2F1 and SirT1 regulate apoptotic response to DNA damage. *Nat Cell Biol*. 2006, 8(9): 1025-31.

Wang H., Kouri G., Wollheim C.B., ER stress and SREBP-1 activation are implicated in beta-cell glucolipotoxicity. *J Cell Sci*. 2005, 118(Pt 17): 3905-15.

Wang R.H., Sengupta K., Li C., Kim H.S., Cao L., Xiao C., Kim S., Xu X., Zheng Y., Chilton B., Jia R., Zheng Z.M., Appella E., Wang X.W., Ried T., Deng C.X., Impaired DNA damage

response, genome instability, and tumorigenesis in SIRT1 mutant mice. *Cancer cell*. 2008, 14(4): 312-23.

Wang Z., Liao J., Diwu Z., N-DEVD-N'-morpholinecarbonyl-rhodamine 110: Novel caspase-3 fluorogenic substrates for cell-based apoptosis assay. *Bioorg Med Chem Lett. 2005,* **15**: 2335-38.

Waterland R.A., Garza C., Potential mechanisms of metabolic imprinting that lead to chronic disease. *Am J Clin Nutr*. 1999, 69(2): 179-97.

Waterland R.A., Does nutrition during infancy and early childhood contribute to later obesity via metabolic imprinting of epigenetic gene regulatory mechanisms? *Nestle Nutr Workshop Ser Pediatr Program*. 2005, 56: 157-71; discussion 171-4.

Waterland R.A., Jirtle R.L., Early nutrition, epigenetic changes at transposons and imprinted genes, and enhanced susceptibility to adult chronic diseases. *Nutrition*. 2004, 20(1): 63-8.

Weinert B.T., Wagner S.A., Horn H., Henriksen P., Liu W.R., Olsen J.V., Jensen L. J., Choudhary C., Proteome-wide mapping of the Drosophila acetylome demonstrates a high degree of conservation of lysine acetylation. *Sci Signal.* 2011, 4(183): ra48.

Wende A.R., Huss J.M., Schaeffer P.J., Giguere V., Kelly D.P., PGC-1alpha coactivates PDK4 gene expression via the orphan nuclear receptor ERRalpha: a mechanism for transcriptional control of muscle glucose metabolism. *Mol Cell Biol*. 2005, 25(24): 10684-94.

Withers D.J., Gutierrez J.S., Towery H., Burks D.J., Ren J.M., Previs S., Zhang Y., Bernal D., Pons S., Shulman G.I., Bonner-Weir S., White M.F., Disruption of IRS-2 causes type 2 diabetes in mice. *Nature*. 1998, 391(6670): 900-4.

Wood J.G., Rogina B., Lavu S., Howitz K., Helfand S.L., Tatar M., Sinclair D., Sirtuin activators mimic caloric restriction and delay ageing in metazoans. *Nature*. 2004, 430(7000): 686-9.

Wu Z., Puigserver P., Andersson U., Zhang C., Adelmant G., Mootha V., Troy A., Cinti S., Lowell B., Scarpulla R.C., Spiegelman B.M., Mechanisms controlling mitochondrial biogenesis and respiration through the thermogenic coactivator PGC-1. *Cell*. 1999, 98(1): 115-24.

Xia D., Wu X., Yang Q., Gong J., Zhang Y., Anti-obesity and hypolipidemic effects of a functional formula containing Prumus mume in mice fed high-fat diet. *African J of Biotech*. 2010,9:2463-67.

Yamashita T., Eto K., Okazaki Y., Yamashita S., Yamauchi T., Sekine N., Nagai R., Noda M., Kadowaki T., Role of uncoupling protein-2 up-regulation and triglyceride accumulation in impaired glucose-stimulated insulin secretion in a beta-cell lipotoxicity model overexpressing sterol regulatory element-binding protein-1c. *Endocrinology*. 2004, 145(8): 3566-77.

Yang S.R., Wright J., Bauter M., Seweryniak K., Kode A., Rahman I., Sirtuin regulates cigarette smoke-induced proinflammatory mediator release via RelA/p65 NF-kappaB in macrophages in vitro and in rat lungs in vivo: implications for chronic inflammation and aging. *Am J Physiol Lung Cell Mol Physiol.* 2007, 292(2): L567-76.

Yang, Y., Fu W., Chen J., Olashaw N., Zhang X., Nicosia S.V., Bhalla K.,Bai W., SIRT1 sumoylation regulates its deacetylase activity and cellular response to genotoxic stress. *Nat Cell Biol.* 2007, 9(11): 1253-62.

Yeung F., Hoberg J.E., Ramsey C.S., Keller M.D., Jones D.R., Frye R.A., Mayo M.W., Modulation of NF-kappaB-dependent transcription and cell survival by the SIRT1 deacetylase. *EMBO J.* 2004, 23(12): 2369-80.

Yogeeswari P., Sriram D., Mehta S., Nigam D., Kumar M.M., Murugesan S., Stables J.P., Anticonvulsant and neurotoxicity evaluation of some 6-substituted benzothiazolyl-2-thiosemicarbazones. *Farmaco.* 2005, 60(1): 1-5.

Yoon J.C., Puigserver P., Chen G., Donovan J., Wu Z., Rhee J., Adelmant G., Stafford J., Kahn C.R., Granner D.K., Newgard C.B., Spiegelman B.M., Control of hepatic gluconeogenesis through the transcriptional coactivator PGC-1. *Nature.* 2001, 413(6852): 131-8.

Yun J.W., Possible anti-obesity therapeutics from nature--a review. *Phytochemistry.* 2010, 71(14-15): 1625-41.

Zhao W., Kruse J.P., Tang Y., Jung S.Y., Qin J., Gu W., Negative regulation of the deacetylase SIRT1 by DBC1. *Nature.* 2008, 451(7178): 587-90.

Zhao X., Sternsdorf T., Bolger T.A., Evans R.M., Yao T.P., Regulation of MEF2 by histone deacetylase 4- and SIRT1 deacetylase-mediated lysine modifications. *Mol Cell Biol.* 2005, 25(19): 8456-64.

Zinker B.A., Rondinone C.M., Trevillyan J.M., Gum R.J., Clampit J.E., Waring J.F., Xie N., Wilcox D., Jacobson P., Frost L., Kroeger P.E., Reilly R.M., Koterski S., Opgenorth T.J., Ulrich R.G., Crosby S., Butler M., Murray S.F., McKay R.A., Bhanot S., Monia B.P., Jirousek M.R., PTP1B antisense oligonucleotide lowers PTP1B protein, normalizes blood glucose, and improves insulin sensitivity in diabetic mice. *Proc Natl Acad Sci U S A*. 2002, 99(17): 11357-62.

APPENDIX

APPENDIX

LIST OF PUBLICATIONS

FROM THESIS WORK

1. **Mallika Alvala**, Shubhmita Bhatnagar, Alvala Ravi, Variam Ullas Jeankumar, Thimmappa H Manjashetty, Perumal Yogeeswari, Dharmarajan Sriram, Novel acridinedione derivatives: Design, synthesis, SIRT1 enzyme and tumor cell growth inhibition studies. *Bioorganic & Medicinal Chemistry Letters* 22 (2012) 3256–3260.

2. Venkat Koushik Pulla, Madhu Babu Battu, **Mallika Alvala**, Dharmarajan Sriram, Perumal Yogeeswari, Can Targeting Sirt-1 to Treat Type II Diabetes be a Good Strategy? - A Review: *Expert Opin Ther Targets*. 2012 Aug; 16(8):819-32. Epub 2012 Jul 5.

3. **Mallika Alvala,** Alvala Ravi, Variam Ullas Jeankumar, Venkat Koushik Pulla, Perumal Yogeeswari, Dharmarajan Sriram, Small molecule sirt1 inhibitors: design, *in vitro* and *in vivo* studies. Communicated to *Biochemical and Biophysical Research Communications.*

4. **Mallika Alvala,** Alvala Ravi, Variam Ullas Jeankumar, Venkat Koushik Pulla, Saket Sriram, Perumal Yogeeswari, Dharmarajan Sriram, Spiropiperidine derivatives as sirt1 activators: design, *in vitro* and *in vivo* studies. Communicated to *Bioorganic & Medicinal Chemistry Letters.*

OTHER PUBLICATIONS

1. Ravi A, **Alvala M**, Venkatesh Sama, Arunasree.M.Kalle, Vamshi.K.irlapati, B. Madhava Reddy. Anticancer activity of Pupalia lappacea on chronic myeloid leukemia K562 cells: Accepted in DARU journal of Pharmaceutical sciences- Biomed central.

2. Jeankumar Variam, Manoj Chandran, Ganesh Samala, **Mallika Alvala,** Koushik V Pulla, Yogeeswari Perumal, Elena G Salina, D.Sriram. Development of 5-nitrothiazole derivatives: Identification of leads against both replicative and latent M. tuberculosis. Communicated to *Bioorganic and medicinal chemistry* Letters.

3. Dharmaraja AT, **Alvala M,** Sriram D, Yogeeswari P, Chakrapani H. Design, synthesis and evaluation of small molecule reactive oxygen species generators as selective Mycobacterium tuberculosis inhibitors. Chem Commun (Camb). 2012 Sep 24;48(83):10325-7.

4. Khanapur Manjulatha, S. Srinivas, Naveen Mulakayala, D. Rambabu, M. Prabahkar, Kalle M. Arunasree, **Mallika Alvala**, M.V. Basaveswara Rao, Manojit Pal, Ethylenediaminediacetate (EDDA) mediated synthesis of aurones under ultrasound: Their evaluation as inhibitors of SIRT1. Bioorganic & Medicinal Chemistry Letters, Epub 2012 Aug 9.

5. Lingappa Mallesha, Kikkeri N. Mohana , Bantal Veeresh, Ravi Alvala, and **Alvala Mallika**., Synthesis and In Vitro Antiproliferative Activity of 2-Methyl-3-(2-piperazin-1-yl-ethyl)-pyrido[1,2-a]pyrimidin-4-one Derivatives Against Human Cancer Cell Lines, Arch Pharm Res Vol 35, No 1, 51-57, 2012 Springer.

6. Alvala Ravi, **A. Mallika**, Venkatesh Sama, A. Sajeli Begum, Rukaiyya S. Khan, B. Madhava Reddy., Antiproliferative activity and standardization of Tecomella undulata

bark extract on K562 cells, Journal of Ethnopharmacology, Elsevier, 137, 1353-1359 oct 2011.

7. Dharmarajan Sriram , Perumal Yogeeswari, Swetha Methuku, Devambatla Ravi Kumar Vyas, Palaniappan Senthilkumar, **Mallika Alvala**, Variam Ullas Jeankumar., Synthesis of various 3-nitropropionamides as Mycobacterium tuberculosis isocitrate lyase inhibitor, Bioorganic & Medicinal Chemistry Letters, Elsevier 21, 5149–5154, July 2011**.**

8. Rao RM, Reddy Ch U, Alinakhi, Mulakayala N, **Alvala M**, Arunasree MK, Poondra RR, Iqbal J, Pal M., Sequential coupling/desilylation-coupling/cyclization in a single pot under Pd/C-Cu catalysis: Synthesis of 2-(hetero)aryl indoles, Org Biomol Chem, RSC, 9,3808-16,May 2011.

9. Mohosin Layek, Appi Reddy M., A. V. Dhanunjaya Rao, **Mallika Alvala**, M. K. Arunasree, Aminul Islam,a K. Mukkanti, Javed Iqbal and Manojit Pal, Transition metal mediated construction of pyrrole ring on 2,3-dihydroquinolin-4(1H)-one: synthesis and pharmacological evaluation of novel tricyclic heteroarenes, Organic & Biomolecular Chemistry,RSC,9,1004-1007, Dec2010.

10. Arunasree M. Kalle, **A. Mallika**, Jayasree Badiger, Alinakhi, Pinaki Talukdar, Sachchidanand, Inhibition of SIRT1 by a small molecule induces apoptosis in breast cancer cells, Biochemical and Biophysical Research Communications, ELESVIER, 401, 13-19, Sep 2010.

PAPERS PRESENTED AT NATIONAL/INTERNATIONAL CONFERENCES

1. **Mallika Alvala**, Alvala Ravi, P. Yogeeswari, D. Sriram, Antiobesity effect of novel SIRT1 activator: *In vitro* and *In-vivo* studies. 2nd national symposium on Current Trends in Pharmaceutical Sciences, 17th Nov, 2012 at BITS-Pilani, Hyderabad Campus, Hyderabad.

2. P. Brindha Devi, **Mallika Alvala**, P. Yogeeswari, D. Sriram, Development of pantothenate synthetase inhibitors for Mycobacterium tuberculosis infection: design and enzyme inhibition studies. 3rd World Congress on Biotechnology, Sep13-15th, 2012 at Hyderabad, India.

3. A.Mallika, A.RaviKiran, P. Yogeeswari, D. Sriram, Novel acridinedione derivatives: Design, synthesis, SIRT1 enzyme and tumor growth inhibition studies. 3rd World Congress on Biotechnology, Sep13-15th, 2012 at Hyderabad, India.

4. Jean Kumar. V.U, Manoj C, Vijay Sonia, Patrisha. J. T, **Mallika Alvala**, Yogeeswari P Vinay K. Nandicoorib, Sriram D, Discovery of novel Mycobacterium tuberculosis GlmU inhibitors.16th Annual Conference of the Swedish Structural Biology Network, June 15th - 18th, 2012 at Åkerblads Hotel in Tällberg, Dalecarlia.

5. Rukaiyya S. Khan, **A. Mallika**, S. Mahibalan, D. Sriram and A. Sajeli Begum.*, In vitro* anticancer activity of *Abutilon indicum* leaves on Human breast carcinoma cell line (MDA-MB-231), 4th International Conference on Drug Discovery and Therapy to be held from 12th February - 15th February, 2012, at Dubai Women's College.

6. Rukaiyya S. Khan, **A. Mallika**, Mahibalan S, D. Sriram, Sajeli Begum A., *In vitro* anticancer activity of *Abutilon indicum* leaves on U-87 MG, a brain tumor cell line.

XXXXIV Annual Conference of Indian Pharmacological Society, IPS, INDIA.19th Dec 2011.

7. M.Siddharth Sai, **A.Mallika**, V.U.Jean Kumar, P.Yogeeswari, D.Sriram, Insilico design and synthesis of small molecule inhibitors of human SIRT1 63rd Indian Pharmaceutical Congress, Bangalore, 18th Dec 2011.

8. Mahibalan S , **Mallika A**, Rukaiyya S Khan, Sriram D, Sajeli Begum A, *In Vitro* Anticancer Activity of Safflower Petals on Osteosarcoma (U-87MG) Cell Line., current trends in pharmaceutical biology, BITS-Pilani, Hyderabad campus., Hyderabad, 12th Nov 2011.

9. Alvala Ravi, **A.Mallika**, Venkatesh Sama, B.Madhava Reddy, Anti cancer activity of methanolic extract of Cassia absus seeds in K562 cells, National Conference on Natural Product Research: for Health and Bio pharma Industry, Kumara guru College of Technology, Coimbatore, 25th Mar 2011

10. Alvala Ravi, **A.Mallika**, Venkatesh Sama, B.Madhava Reddy, Anti-proliferative activity of Tecomella undulata Bark extract, APTI CONVENTION-2010, Hyderabad, 2nd Oct 2010.

11. **Mallika A**, Ravi Kiran A, P. Yogeeswari, D. Sriram, Development of homology model and docking studies of Mycobacterium tuberculosis sirtuin protein (Rv1151c) , Med Chem 2011 Congress, IICT, Hyderabad, 26th Feb 2011.

12. Kalle M. Arunasree, **Mallika A**, Alinakhi, Pinaki T, Sachchidanand, A small molecule SIRT1 inhibitor shows potent antitumor effects against metastatic breast cancer cells. 33rd Annual meeting of Indian Society of Cell Biology, held at University of Hyderabad, Hyderabad, India, during December 10-13, 2009.

13. **M. Mallika**, P. Yogeeswari, D. Sriram, Design and synthesis of gold (III) and platinum (III) complexes of aryl-substituted semicarbazones as anti tumour agents, National Symposium on Challenges in Drug Discovery Research: Networking Opportunities between Academia & Industries, Pilani, 7-8th April, 2006.

BIOGRAPHY OF M.MALLIKA

Mrs. M. Mallika completed her Bachelor of Pharmacy from The Nalanda College of Pharmacy, Osmania University in the Year 2003 and Master of Pharmacy from BITS Pilani, Rajasthan in 2006. She has about 3 years of experience in drug discovery field at Institute of Life sciences, University of Hyderabad, Hyderabad from 2007-2010. She has been appointed as a Research Associate at Birla Institute of Technology and Science, Pilani, Hyderabad campus from 2010-2012 under the supervision of Dr. D. Sriram. She has published twelve scientific publications in well-renowned international journals. She had presented papers at various national and international conferences. She has been awarded as "Best Research Scholar of the year 2012", Pharmacy Department, BITS-Pilani, Hyderabad and award has been sponsored by Bharat Biotech Ltd., Hyderabad.

BIOGRAPHY OF Dr. D. SRIRAM

Dr. D. Sriram is presently working in the capacity of Associate Chair Professor at Pharmacy Group, Birla Institute of Technology and Science, Pilani, Rajasthan. He received his Ph. D. in 2000 from Banaras Hindu University, Varanasi. He has been involved in teaching and research for last 9 years. He has 175 peer-reviewed research publications to his credit. He is a life member of Association of Pharmacy Teachers of India, and Association of Microbiologists of India and member of Canadian Society of Pharmaceutical Sciences. He has collaborations with various national and international organizations such as Karolinska institute, Sweden; the Indian Institute of Science, Bangalore; National Institute of Immunology, New Delhi; AstraZeneca, India. He was awarded the Young Pharmacy Teacher of the year award of 2006 by the Association of Pharmacy Teachers of India. He received ICMR Centenary year award 2011. As a result of his academic and research accomplishment, his biographical profile has been included in the prestigious registry of the 6th edition of "Marquis Who's Who in Science and Engineering". He has guided 5 Ph. D. students and 11 students are pursuing Ph.D currently and his research was funded by agencies like the UGC, CSIR, ICMR, IBSA, DBT, ABG and ST.